NO_3^- and N_2O at the Strawberry Creek Catchment: tracing sources and processes using stable isotopes

by

Marlin Rempel

A thesis
presented to the University of Waterloo
in fulfillment of the
thesis requirement for the degree of
Master of Science
in
Earth Sciences

Waterloo, Ontario, Canada, 2008

I hereby declare that I am the sole author of this project. This is a true copy of the thesis, including any required final revisions, as accepted by my examiners.

I understand that my thesis may be made electronically available to the public.

Marlin Rempel

Abstract

Nitrate (NO_3) contamination in agricultural watersheds is a widespread problem that threatens local drinking supplies and downstream ecology. Dual isotopes of NO_3^- ($\delta^{15}N$ and $\delta^{18}O$) have been successfully used to identify sources of NO_3 contamination and nitrogen (N)-cycle processes in agricultural settings. From 1998 to 2000, tile drainage and stream waters at the Strawberry Creek Catchment were sampled for NO_3^- concentration and isotopes. The results suggest that tile NO_3 were mainly derived from soil organic matter and manure fertilizers, and that they were not extensively altered by denitrification. NO_3^- concentrations and isotopes in the stream oscillated between the influence of tile inputs, during periods of higher basin discharge, and groundwater inputs, during low basin discharge. The affect of denitrification was evident in stream NO_3^- samples.

Sources and processes of dissolved NO_3^- and N_2O were explored using concentrations and stable isotopes during the 2007 Springmelt and 2008 mid-winter thaw events. Tiles are a source of NO_3^- to the stream during both events and concentrations at the outflow are above the 10 mg N/L drinking water limit during the 2008 mid-winter thaw. The stream was a source of N_2O to the atmosphere during both events. $\delta^{15}N$ and $\delta^{18}O$ of N_2O reveal that N_2O is produced from denitrification during both events. $\delta^{18}O$:$\delta^{15}N$ slopes measured in N_2O were due to the influence of substrate consumption (tiles) and gas exchange (stream).

The stable isotopes of dissolved NO_3^- and N_2O were also characterized during non-melt conditions (October 2006 to June 2007 and Fall 2007) at the Strawberry Creek catchment. Again, the purpose was to determine the sources and processes responsible for the measured concentrations and isotopic signatures. The isotope data suggests that N_2O was produced by denitrification. Furthermore, NO_3^- consumption and gas exchange altered the original N_2O signature. Isotopic distinction between soil gas N_2O and dissolved N_2O is suggestive of different production mechanisms between the unsaturated and saturated zones. Since the range of dissolved N_2O isotopes from the Strawberry Creek catchment

are relatively constraned, definition of the local isotopic signature of secondary, agricultural N_2O sources was possible.

Acknowledgements

I would like to thank my supervisor, Sherry Schiff, for sharing her insights into this subject and her guidance in learning the scientific process. My co-supervisor, John Spoelstra, was also very available for technical advice in field and lab methods and with respect to writing. I am also grateful to Michael English for his leadership in the overall project and knowledge of hydrochemical processes at Strawberry Creek. Richard Elgood also provided extensive assistance with sampling, analysis, editing and good humor.

Additionally, I would like to acknowledge Simon Thuss for his technical developments in N_2O analysis. Dave Snider also provided useful feedback for me on several early drafts and had good jokes. Many other students also aided me at various times in field sampling and lab analysis. I would also like to acknowledge the financial support of the Ontario Graduate Scholarship and the President's Scholarship (University of Waterloo). NSERC provided funding for the larger Strawberry Creek project.

Thanks to all my pals here in Waterloo who, through antics and discourse, provided necessary distraction through many evenings. Finally, I wish to thank my family for their support throughout this degree.

Table of Contents

List of Tables

List of Figures

Chapter 1: Introduction to Nitrogen Cycling in Agroecosystems, Study Site, and Objectives of Study

1.1 Introduction

1.1.1 Agriculture and the Nitrogen Cycle

The nitrogen (N) cycle is complex and multi-faceted, driven by biotic and abiotic processes that are ubiquitous in oceanic, terrestrial, and atmospheric environments. N is an important element for plant productivity and biochemical regulation, playing a key role in species diversity, composition, dynamics, and ecosystem function.

Major alterations to the N cycle have occurred because of agriculture, combustion of fossil fuels, and other human activities increasing its availability and mobility (Vitousek et al., 1997). Though combustion of fossil fuels has caused significant change in atmospheric conditions, agriculture itself appears to have had the most widespread impact on the N cycle. The production of fertilizer and proliferation of N fixing crops have increased the rate of N fixation and the amount of reactive N in the environment (Galloway et al., 1995). N mobilization is not exclusively associated with agriculture though some practices such as biomass burning, land clearing and conversion, and wetland drainage are commonly associated with it (Vitousek and Matson, 1993).

Natural geochemical cycling typically does not provide sufficient biologically available forms of N to support desired productivity in agroecosystems. Reactive forms of N such as nitrate (NO_3^-) and ammonium (NH_4^+) are the most important forms of N for plant growth and are used as fertilizers to augment available crop nutrients. The industrial use of N fertilizers increased dramatically due to development of the Haber-Bosch method which combines atmospheric N_2 and water (H_2O) at high temperatures to form NH_4^+. The use of organic fertilizers has also increased dramatically with the onset of industrial agriculture. The growth of N fertilizer use was originally constrained to developed countries where applications have stabilized since the late 1970's (Jenkinson, 2001;

Vitousek et al., 1997). On the other hand, half of industrially fixed N fertilizer use between 1980 and 1990 was in developing nations (Kates et al, 1990).

Another strategy to promote reactive N formation is the cultivation of leguminous crops such as soybeans, peas, alfalfa, and non-leguminous crops like rice. Through microbial associations with root nodules, these crops promote N fixation. Galloway et al. (1995) estimates that leguminous N fixation is about half (43 Tg N yr^{-1}) that of fertilizer production (78 Tg N yr^{-1}) globally.

A major result of increased N fixation and application of N-fertilizers has been the contamination of surface water and groundwater located directly within agricultural catchments and waters in the surrounding environments. Although agriculture is not the only source of N to surface waters, Havens and Steinman (1995) and Gianessi et al. (1986) suggest agriculture is a major non-point contributor. Their results suggest that, in the United States, croplands alone are responsible for 39% of the N found in surface waters and, combined with inputs from pastures and rangelands, the contribution increases to 52%. Howarth et al. (1996) also adds that anthropogenic N inputs are dominated by fertilizer in the North Atlantic and surrounding areas. In northeastern United States, the Saint Lawrence River, and Great Lakes basin, N loading from anthropogenic sources is dominated by atmospheric deposition of N-oxides (Fisher and Oppenheimer, 1991).

In addition to atmospheric deposition of N, increases of N gas species in the atmosphere is of immediate concern. The greenhouse gas nitrous oxide (N_2O) is perhaps the most well known, though ammonia (NH_3) gas is another relevant species. Both of these gases are produced naturally but emissions are enhanced through N fertilization in agroecosystems and through other anthropogenic activities including biomass burning and nylon production (Rahn and Wahlen, 1997).

N_2O has 310 times the radiative forcing capacity of carbon dioxide (CO_2) and the atmospheric concentration is increasing at a rate of 0.2-0.3%/yr (Prinn et al., 1990). Since the onset of the industrial revolution in the early 1800's, the atmospheric concentration of N_2O has increased from 270 to 319 nmol/mol with the greatest increases of 0.6

nmol/mol/yr occurring in the last several decades (Figure 1-1). This has prompted considerable concern in the scientific community with respect to the implications for climate change.

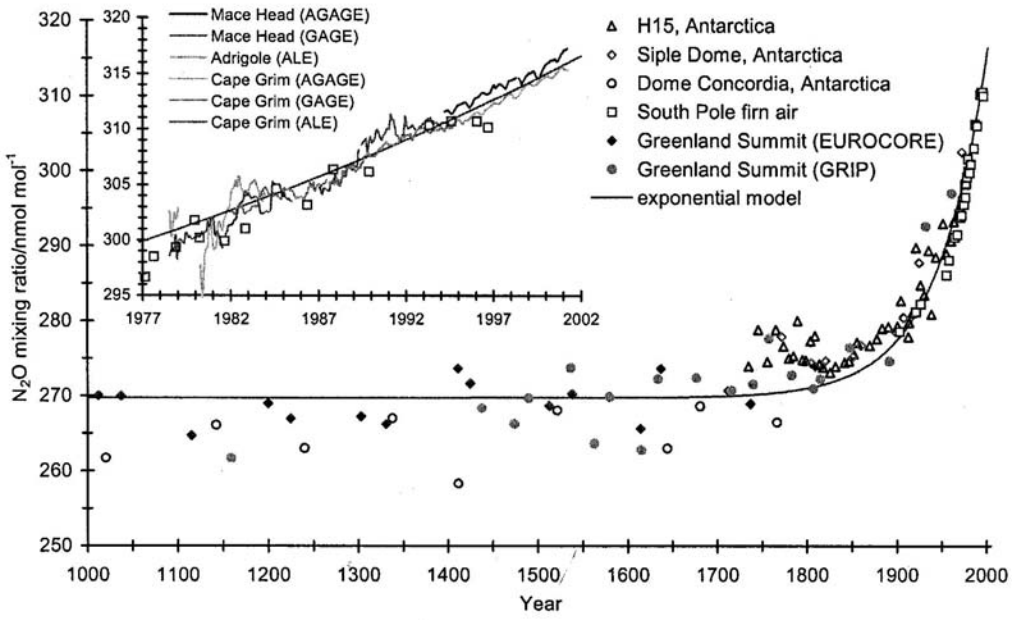

Figure 1-1: Changes in atmospheric N_2O mixing ratio since 1000AD as determined from air trapped in ice cores, firn air and whole air samples. Calculations of increase in global mixing ratios (270 to 319 nmol/mol) and a maximum growth rate of 0.6 nmol/mol/yr in 2000 are derived from the exponential model. After Kaiser (2002).

Increases in atmospheric N_2O concentrations are correlated with the onset of industrialization but must be considered in the context of the global N_2O budget, which includes natural generation of the gas. Table 1-1 provides a general survey of the global N_2O budget and the magnitude of its components showing that natural sources (9.6 Tg/yr in 1994) actually outweigh anthropogenic sources (8.1 Tg/yr in 1994). Of the natural sources, oceans (3.0 Tg/yr) and tropical soils (4.0 Tg/yr) are the most significant with temperate soils (2.0 Tg/yr) and NH_3 oxidation (0.6 Tg/yr) making a lesser contribution. Of the anthropogenic sources, agricultural soils are responsible for the majority of N_2O production and this has made them a key focus area for research. With projected increases of global N fertilizer production of 60% by the year 2020, addressing the issue becomes

more imperative (Food and Agriculture Organization (FAO), 1999). Much of this fertilizer is expected to be used in developing countries that are often tropical and sub-tropical regions and where 41% of global urea fertilization already takes place (FAO).

Table 1-1: Sources of N_2O (Tg/yr). Adapted from Stein and Yung (2003).

Source	1994	1990
Agricultural soils	4.2	3.6
Biomass Burning	0.5	0.5
Industrial Sources	1.3	0.7
Cattle and feedlots	2.1	1
Anthropogenic subtotal	**8.1**	**4.1**
Ocean	3.0	3.6
NH_3 oxidation	0.6	0.6
Tropical soils	4.0	NA
Temperate soils	2.0	NA
All Soils		6.6
Natural subtotal	**9.6**	**10.8**
Total sources	**17.7**	**14.9**
Stratospheric sink	**12.3**	**NA**

*NA = data not available

1.1.2 The Nitrogen Cycle

1.1.2.1 Overview and Leaky Pipe Model

This section introduces key processes in the N cycle. A special emphasis is placed on those that produce and consume NO_3^- and N_2O, the central N species of this thesis research. The following discussion focuses on the microbially-mediated reactions of nitrification and denitrification though attention is also given to other important processes such as N-fixation and ammonification.

Figure 1-2 shows the major processes of the N cycle in the context of Firestone and Davidson's (1989) Leaky Pipe model that explains the regulation of trace N gas production through nitrification and denitrification. According to the model these processes are controlled by three levels of regulation; (1) Flow of N through the pipe, or

availability of NH_4^+ and NO_3^-, which is controlled by the overall rate of the reaction, (2) the ability of the gas to move out of the cell, which is controlled by factors that partition the N species to a more oxidized or reduced form, and (3) the ability of the gas to move from the soil to the atmosphere without reduction. Though the model deals specifically with N_2O and NO, it can be expanded to explain the availability of NO_3^-, particularly the first level of regulation. It is obvious that both cellular (e.g. presence of enzymes and their inhibitors) and environmental (e.g. reactant availability) controls will govern these regulators. This will be discussed further in the following sections.

1.1.2.2 Microbial N fixation

Microbial N fixation is the conversion of atmospheric N_2 (gas) to NH_3 (Equation 1-1).

$$N_2 + 8H^+ + 16ATP + 8e^- \Rightarrow 2NH_3 + H_2 + 16ADP \qquad \textbf{Equation 1-1}$$

Species of the genus *Azotobacter* are the best known aerobic nitrogen fixers and can do so relatively well in ambient atmosphere (Postgate, 1987). The N fixing capability of a sub-group of aerobic microbes (microaerophiles) are agriculturally important because of their symbiotic relationship with leguminous plants. *Rhizobium* and *Bradyrhizobium* are the best known for their associations with clover, alfalfa, peas and beans.

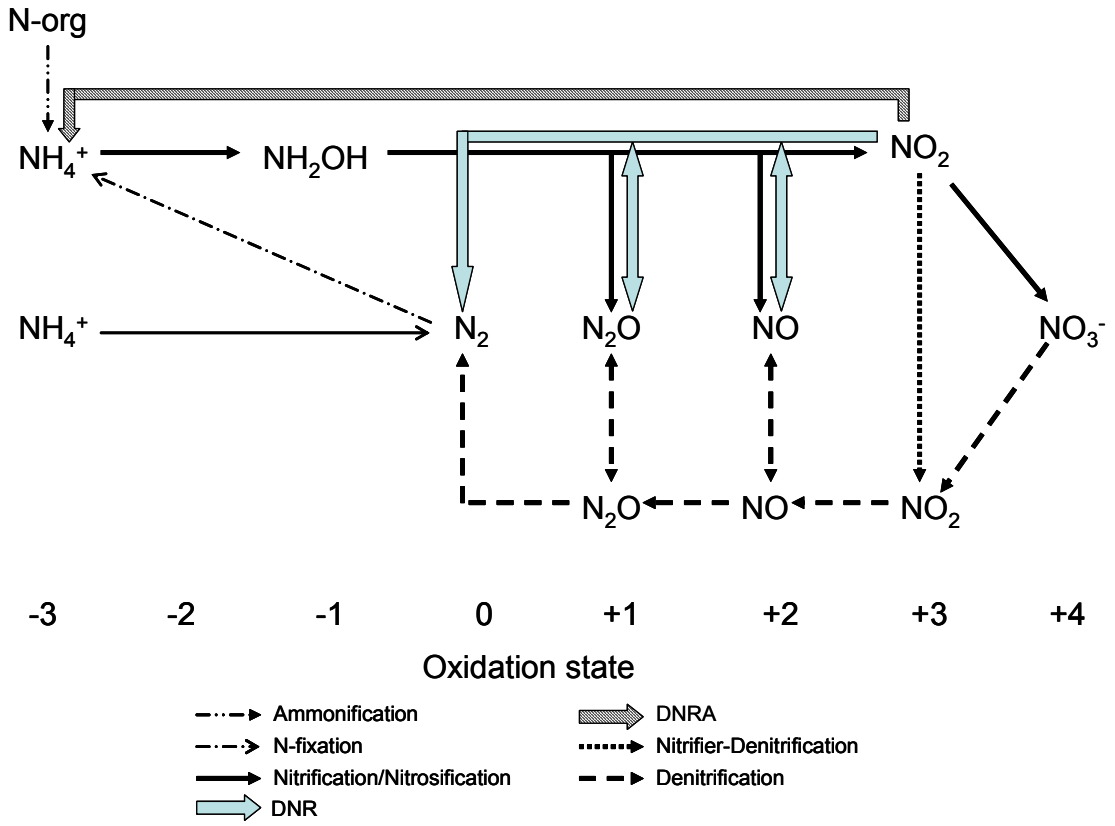

Figure 1-2: The nitrogen cycle modeled after Firestone and Davidson's (1989) Leaky Pipe Concept. The specific transformations are indicated by the labeled arrows. DNRA and DNR are the abbreviated forms of Dissimilatory Nitrate Reduction to Ammonium and Dissimilatory Nitrite Reduction, respectively. Gases in the middle of the diagram (N_2, N_2O, and NO) are those that have escaped the cell to the environment according to the model. Other N species on the periphery of the diagram can be taken from the external environment and moved into the cell for further transformation.

1.1.2.3 Ammonification

Ammonification is the digestion of complex proteins and N compounds found in soil organic matter (organic N) where NH_3 or NH_4^+ is formed (Jansson and Persson, 1982) (Equation 1-2).

$$Org - N \Rightarrow NH_3 + H^+ \qquad \textbf{Equation 1-2}$$

It is performed by heterotrophic microorganisms that use organic N substances as an energy source (Bartholomew, 1965; Jansson, 1971). Factors affecting ammonification

rates include soil temperature-moisture interactions, soil pH, concentrations of other nutrients, organic matter concentration and quality, soil structure (Cassman and Munns, 1980; Stanford and Smith, 1972; Bremner, 1965; Herlihy, 1979).

1.1.2.4 Ammonia volatilization

Gaseous losses of N from different environments, including agroecosystems, can occur by ammonia volatilization. NH_3 loss can be significant in and around areas with high concentrations of plant and animal residues, such as manure piles and feedlots. NH_3 volatilization also occurs in agricultural fields and adjacent forests (Lemon and Van Houtte, 1980). Schlesinger and Hartley (1992) estimate global losses of NH_3-N from fertilized fields, domestic animal waste, and biomass burning at 10, 32, and 5 Tg/yr, respectively.

The process of ammonia volatilization is controlled by the difference between the partial pressure of NH_3 in equilibrium with solution and the partial pressure of NH_3 in the atmosphere. This is summarized in Equation 1-3.

$$\frac{[NH_3]_{aq}}{[NH_3]_g} = H(5.4*10^{1} - 7.8*10^{1}) \text{ (Sander, 1999)} \qquad \textbf{Equation 1-3}$$

where H is Henry's constant and $[NH_3]_{aq}$ and $[NH_3]_g$ are NH_3 concentration in dissolved and gas phases, respectively. Partitioning of NH_3 between the two phases varies with pH and temperature (Hales and Drewes, 1979).

Furthermore, the concentration of free NH_3 species in solution is directly controlled by the equilibrium reaction with NH_4^+ summarized in Equation 1-4.

$$\frac{[NH_3][H^+]}{[NH_4^+]} = Ka \qquad \textbf{(5.89*10}^{\textbf{-10}}\textbf{ at 25}^{\textbf{o}}\textbf{C)} \qquad \textbf{Equation 1-4}$$

also showing the effect of pH. This indicates greater potential for NH_3 volatilization at higher pH. As such, a soil's buffering capacity has a direct affect on NH_3 volatilization. Soils with a high buffering capacity result in increased volatilization because of the neutralization of the acid produced in the dissociation of ammonium ions.

Sorbtion of NH_3 on soil minerals and organic matter occurs through physical adsorption and hydrogen bonding with water, thereby reducing volatilization (Young, 1964; Broadbent and Stevenson, 1966). Chemical reactions create much stronger bonds to the soil surface than physical adsorption where the reaction of NH_3 acids and other groups can form salts and non-exchangeable products. The net result is that NH_3/NH_4^+ tends to be bound and therefore has low mobility.

1.1.2.5 Nitrification

The overall process of nitrification is the microbial oxidation of NH_4^+ to NO_3^-, which can be broken down into two steps consisting of several energy yielding, acid producing reactions. The first step, termed ammonium oxidation or nitrosification, is the conversion of NH_4^+ to nitrite (NO_2) by the *Nitroso* genera of bacteria, including the common *Nitrosomonas* spp. and *Nitrococcus* spp. Within nitrosification, there are two reactions that complete the transformation to NO_2. The first, catalyzed by the enzyme ammonium monooxygenase and with Copper (Cu) as a co-factor, is summarized by Equation 1-5.

$$NH_3 + O_2 + 2H^+ + 2e^- \Rightarrow NH_2OH + H_2O \qquad \textbf{Equation 1-5}$$

The second step of nitrosification oxidizes NH_2OH to NO_2 in the hydroxylamine dehydration reaction shown in Equation 1-6.

$$NH_2OH + H_2O \Rightarrow NO_2^- + 5H^+ + 4e^- \qquad \textbf{Equation 1-6}$$

which is catalyzed by hydroxyl-amine dehydrogenase with the help of molybdenum (Mo) and iron (Fe) co-factors.

A small amount of N_2O can be produced through this reaction though the exact pathway is presently unknown (Yoshida, 1988). Hyponitrous acid (HNO) may be an important intermediate in this reaction. In their medical experiments Sha et al. (2006) found that HNO is highly reactive toward nucleophiles such as thiols and rapidly forms $H_2N_2O_2$ in its presence. $H_2N_2O_2$ then dehydrates to form N_2O. Firestone and Davidson (1989) also suggest that HNO is formed followed by $H_2N_2O_3$ or NO and consequent oxidation to NO_2. NO as an intermediate between HNO and NO_2 is another potential pathway to N_2O

production, though Andersson et al. (1982) state this is unlikely to be completed by one organism. Delwiche (1981) also states that N_2O production is energetically favorable over NO_2 production at higher pH, which may be more important in marine environments (pH ~ 8.3) than in agricultural areas that tend to be on the acidic side.

The second step of nitrification, termed nitrite oxidation, is performed by *Nitro* bacteria (e.g. *Nitrobacteria* spp.) and is summarized in Equation 1-7.

$$NO_2^- + H_2O \Rightarrow NO_3^- + 2H^+ + 2e^- \qquad \textbf{Equation 1-7}$$

1.1.2.6 Nitrifier Denitrification

Nitrifier denitrification is a pathway that combines nitrosification to a partial denitrification series through NO_2^- by which N_2O and N_2 can be produced (Figure 1-2) (Poth and Focht, 1985; Poth, 1986). The enzymes required are believed to be analogous to those required for the same reactions in the other pathways. Several species of Nitrosospira and Nitrosomonas are able to complete this pathway, which differs from coupled nitrification-denitrification where the different species in close proximity are required to produce N_2O and N_2 (Schmidt et al 2004; Wrage et al., 2001). When oxygen becomes limiting, NO_2 can be used as an electron acceptor by ammonium oxidizing bacteria through activation of nitrite reductase (Poth and Focht, 1985). However, oxygen limitation may be more important to this pathway in the lab than in the field where Wrage et al. (2004) suggest NO_2 availability is the limiting agent. NO_2 concentrations in natural systems are often very low as it quickly oxidized to NO_3^- or reduced to N_2O or N_2. No NO_3^- is produced by nitrifier denitrification.

Up to 40% of N_2O produced can be through nitrifier denitrification though it can also be a neglible percent of the N_2O produced (Wrage et al., 2005; Robertson and Tiedge, 1987).

1.1.2.7 Denitrification

Denitrification is the reduction of nitrate to a gaseous N product, resulting in the loss of fixed nitrogen from the environment (Payne, 1973; Firestone and Davidson; 1989). Under anaerobic conditions NO_3^- can serve as an electron acceptor and be consequently

consumed in the production of N_2. N_2O is an obligatory intermediate in the reaction series shown in Equations 1-8 to 1-11.

(1) $NO_3^- + 2H^+ + 2e^- \Rightarrow NO_2^- + H_2O$ **Equation 1-8**

(2) $NO_2^- + 2H^+ + e^- \Rightarrow NO + H_2O$ **Equation 1-9**

(3) $2NO + 2H^+ + 2e^- \Rightarrow N_2O + H_2O$ **Equation 1-10**

(4) $N_2O + 2H^+ + 2e^- \Rightarrow N_2 + H_2O$ **Equation 1-11**

The overall reaction where organic carbon is the electron donor is summarized by Equation 1-12. Sulfide can also be the electron donor when organic carbon is low (ie: deep groundwater).

$4NO_3^- + 5CH_2O + 4H^+ \Rightarrow 2N_2 + 7H_2O + 5CO_2$ **Equation 1-12**

A diverse group of microorganisms that generate metabolic energy in the form of ATP from electron transport phosphorylation are capable to complete these reactions. These microbes are free living without association to other organisms and are capable of anaerobic respiration (Payne 1973, 1976). Bacteria capable of completing the complete denitrification reaction series should have the most environmental importance in terms of their effect on geochemical cycling (Ingraham, 1981; Firestone and Davidson, 1989). *Pseudomonas* and *Alcaligenes* species are the largest populations of denitrifiers found in all environments (Tiedje, 1988).

Ingraham (1981) states that "partial denitrifiers" cannot complete the reaction series for several genetic or physiological reasons that include the absence of reactants, environmental conditions, and absence of crucial enzymes. Most partial denitrifiers are a wide variety of genera only capable of reducing NO_3^- to NO_2^-. Another group are those that lack nitrous oxide reductase and thus do not produce N_2. Several species including *Aquaspirillium itersoni*, *Pseudomonas fluorescens,* and *Achromobacter nephridii* belong to this group.

Though denitrification is generally inhibited by the presence of oxygen there are certain instances where oxygen has a variable effect on enzyme synthesis. For example, there are two species of *Pseudomonas* and one of *Alcaligenes* that can synthesize nitrate reductase (NAR) in the presence of oxygen and NO_3^- (Krul, 1976; Krul and Veeningen, 1977).

1.1.3 Controls on NO_3^- and N_2O availability in agroecosystems

Controls on the availability of NO_3^- and N_2O in agrosystems should be considered in terms of pathways producing and consuming these constituents.

Numerous factors can control the rate of nitrification through which NO_3^- and N_2O are produced though NH_4^+ availability and O_2 appears to be the most important (Firestone and Davidson, 1989; Strauss et al., 2002; Kemp and Dodds, 2002). Factors that can affect NH_4^+ availability include rates of mineralization, which is affected by soil organic matter, water availability, and temperature. Water content itself controls the diffusion of NH_4^+ and O_2, which also affects nitrification rates. Plant uptake of NH_4^+ and physical adsorbtion to soil also limits its availability (Robertson, 1989). In agriculture settings, the amount of ammonium-based fertilizer added will also obviously affect the size of the NH_4^+ pool. Deposition of NO_x's can also influence NH_4^+ availability though this is often masked by fertilization rates in agricultural settings. N_2O production through nitrification appears to be negatively related to organic carbon and C:N ratio (Kemp and Dodds, 2002; Bernhardt and Likens, 2002).

While reducing NO_3^- concentrations denitrification also acts as an additional pathway for N_2O production. Additional NO_3^- attenuation occurs through plant uptake and dissimilatory nitrate reduction (DNRA). The most important controls on denitrification appear to be NO_3^-, O_2, and carbon as an electron donor (Firestone and Davidson, 1989; Robertson, 1989). As reactants, NO_3^- and organic carbon have a positive correlation to denitrification while O_2 inhibits this process. Diffusion of these constituents is largely controlled by water and temperature. Availability of NO_3^- in agroecosystems is also affected by fertilization practices, which have been directly correlated with N_2O production. Soil type and moisture content also control the diffusion of N_2O through the

soil and sediments. The speed of transport and length of transport pathway for N_2O diffusion also determines the likelihood of re-entrance into the denitrication reaction (Perez et al., 2000)

1.1.4 The use of stable isotopes in the Nitrogen cycle

This section provides a background in both general isotope geochemistry and how the theory has generally been applied for understanding the N cycle. As with the previous section, discussion here will focus on isotopic processes related to NO_3^- and N_2O production and consumption.

1.1.4.1 Fundamentals of stable isotope geochemistry

The stable isotopes of an element are those atoms which differ in the number of neutrons present in the nucleus. The difference in neutron counts gives rise to different masses of those isotopes. The two main stable isotopes of N are nitrogen-14 and nitrogen-15. Both isotopes have 7 protons in their nucleus, making them nitrogen atoms, but nitrogen-14 and nitrogen-15 have 7 and 8 neutrons in their nucleus, respectively. The two most abundant oxygen isotopes are oxygen-16 and oxygen-18, which have 8 and 10 neutrons, respectively, along with 8 protons. The sum of protons and neutrons in the isotope is called the mass number while the number of protons is denoted by the proton number. Stable isotopes are therefore ussually distinguished by their mass number.

a) $^{14}_{7}N$ b) $^{15}_{7}N$ c) $^{16}_{8}O$ d) $^{18}_{8}O$

Figure 1-3: Major stable isotopes mentioned in text and used in this study with mass number (superscripted) and proton number (subscripted): *a)* Nitrogen-14, *b)* Nitrogen-15, *c)* Oxygen-16, and *d)* Oxygen-18

Although the abundance of stable isotopes may be quantified and reported in different ways it is always a variation on the ratio of heavy to light isotopes. The stable isotope composition of substances is usually reported in delta (δ) notation in units of permil (‰), according to Equation 1-13.

$$\delta = \frac{R_x}{R_s} - 1$$ **Equation 1-13**

where R_x and R_s are the ratios of the heavy to light isotopes of the sample and standard, respectively. The primary reference material for N is atmospheric air (N_2) and the mole fractions of ^{14}N and ^{15}N in air are 0.996337 and 0.003663, respectively. The recommended reference material for oxygen is Vienna Standard Mean Oceanic Water (VSMOW) which has mole fractions of 0.9976206 and 0.0020004 for ^{16}O and ^{18}O, respectively (Coplen et al., 2002)

1.1.4.1.1 Isotopic Effects

Changes, or fractionation, in isotopic ratios is caused by isotopic discrimination through physical, chemical, or biological processes (Kendall and Caldwell, 1998). The two types of fractionation are equilibrium and kinetic fractionation.

Fractionation (α) is defined and quantified by Equation 1-14,

$$\alpha = \frac{R_{products}}{R_{substrates}}$$ **Equation 1-14**

where R is the ratio of heavy to light isotopes ($^{15}N/^{14}N$ in the case of N). This leads to the enrichment factor (ε) as shown by Equation 1-15.

$$\varepsilon = (\alpha - 1) * 1000$$ **Equation 1-15**

Furthermore, when substrate concentrations are large and enrichment factors are small, the difference in isotopic composition between products and substrates (Δ) is the approximate enrichment factor (ε) of the reaction. This is shown in Equation 1-16.

$$\varepsilon_{products-substrates} \cong \Delta \cong \delta_{products} - \delta_{substrates}$$ **Equation 1-16**

Additionally the Rayleigh equations can be used to describe isotopic fractionation between chemical species with at least two stable isotopes if the reacting species is continuously removed and the fractionation (α) does not change. This is described by Equation 1-17.

$$\frac{R_{products}}{R_{substrates}} = \left(\frac{X_{products}}{X_{substrates}} \right)^{\alpha - 1}$$ **Equation 1-17**

where R is the ratio of the heavy to light isotopes and X is concentration.

Equilibrium fractionation is the result of reversible reactions where the isotopic exchange reaches steady state equilibrium and constant isotopic composition is achieved between products and substrates. For equilibrium reactions, the species with the higher oxidation state will usually have a higher percentage of the heavier isotope. During phase changes of the same compound (e.g. liquid water to water vapor) the denser material will usually contain more of the heavier isotope (Kendall and Caldwell, 1998).

Irreversible kinetic reactions with variable reaction rates result in kinetic isotopic fractionation. Variation in reaction rates is due to the different masses of the isotopes and their vibrational energies (Kendall and Caldwell, 1998). Reaction pathway, reaction rate, and the energy required to break and/or form bonds in a reaction determine the extent of kinetic fractionation. Most of the reactions of the N cycle discussed in this thesis, except for ammonium volatilization, are biologically mediated chemical reactions, thus resulting in kinetic fractionation. With biological processes fractionation is highly dependant on reaction rates, concentrations of reactants and products, environmental conditions, and species of the organism.

1.1.4.2 N cycle isotope systematics

This section serves as a brief review of the known isotopic effects within the N cycle. This section is also meant to highlight the current understanding of the isotopic compositions NO_3^- and N_2O that are observed in nature. The isotopic dynamics of other N species will also be discussed in the context of NO_3^- and N_2O.

1.1.4.2.1 N fixation, N uptake, Ammonification, and Volatilization

Fogel and Cifuentes (1993) report a range of fractionation for N fixation from -3 to +1‰ ($\varepsilon_{p\text{-}r}$), which often produces organic material having $\delta^{15}N$ values close to 0‰ (Kendall, 1998). Mariotti et al. (1980) report ^{15}N fractionation for N assimilation by vascular plants

to be from -2.2 to +0.5‰ (ε_{p-r}). Plant assimilation of NH_4^+ and NO_3^- is reported as to have no noticeable isotopic effect on soil organic matter signatures (Kendall, 1998). N assimilation by soil microbes also produces small fractionations (ε_{p-r} = -1.6 to +1‰) while assimilation by aquatic algae can have a large range of isotopic fractionation (ε_{p-r} = -27 to 0‰), depending on N, enzyme, and diffusion limiting conditions (Hubner, 1986; Fogel and Cifuentes, 1993).

The range of ^{15}N fractionation for ammonification is reported to range from 0 to ±1‰ (ε_{p-r}) (Kendall, 1998; Hogberg; 1997) and therefore it is expected that $\delta^{15}N$ values for NH_4^+ produced from soil organic N will be similar to the isotopic composition of the soil organic N. $\delta^{15}N$ of organic matter varies from +5 to +12.3‰ for agricultural soils across the U.S.A. and +8.6 ± 1.9‰ for Saskatchewan agricultural soils (Shearer et al., 1978; Karamanos et al., 1981).

There are several fractionating steps associated with ammonium volatilization, and this can result in significant changes in isotopic composition of the remaining NH_4^+ and the NH_3 released to the atmosphere. The equilibrium reaction between aqueous NH_4^+ and gaseous NH_3 has an associated enrichment factor of -19‰ (ε_{p-r}), leaving the remaining NH_4^+ enriched in ^{15}N (Fogel and Cifuentes, 1993). The preferential volatilization of $^{14}NH_3$ is a unidirectional reaction that results in an enrichment factor of approximately -34‰ (ε_{p-r}) (Kirshenbaum et al., 1947). Environmental factors such as pH, temperature, and windspeed are known to affect these reported fractionation factors (Kendall, 1998).

1.1.4.2.2 Nitrification

From single organism lab cultures Yoshida (1988) calculated a range of ^{15}N fractionation from -24.6 to -32% (ε_{r-p}) during nitrosification (NH_4^+ to NO_2) while Mariotti et al. (1981) observed a range from -32 to -37‰ (ε_{r-p}). Shearer and Kohl (1986) and Kendall (1998) also reported complete nitrification (NH_4^+ to NO_3^-) fractionation as a range from -12 to -29‰ (ε_{r-p}) for field studies showing that less fractionation may occur in natural systems. See Appendix A for a complete list of enrichment factors and references.

Hollocher et al. (1981) and Andersson and Hooper (1983) show that the oxygen in the first step of nitrosification (NH_4^+ to NH_2OH) comes from atmospheric O_2 ($\delta^{18}O\text{-}O_2$ = +23.5‰). Andersson and Hooper (1983) showed the second oxygen required to form NO_2 came from H_2O. Kumar et al. (1983) and Hollocher (1984) show that the final oxygen used to form NO_3^- also comes from H_2O. In summary, equation 1-18 formulates the most accepted theory of $\delta^{18}O\text{-}NO_3^-$ signature mechanisms from chemolithoautotrophic denitrification (Kendall, 1998; Mayer et al., 2001; Spoelstra et al. 2007). Anderson et al. (1982) challenge this theory by showing that the two oxygen atoms on NO_2 come from rapid exchange with water.

$$1/3 * \delta^{18}O - O_2 + 2/3 * \delta^{18}O - H_2O = \delta^{18}O - NO_3^- \qquad \textbf{Equation 1-18}$$

N_2O is also produced by nitrification and has associated nitrogen-15 fractionation factors. Though it has been shown that a small amount of N_2O can be produced directly from NH_2OH oxidation the two step production of N_2O through nitrifier-denitrification is likely more environmentally relevant (Yoshida, 1988; Sutka et al., 2003). For the second step (NO_2-N_2O) Yoshida (1988) and Sutka et al. (2003) report very similar fractionation factors of -34.9 to -36.2‰ for *Nitrosomonas europaea* culture experiments. Nitrogen-15 fractionation for the complete nitrification-denitrification reaction (NH_4^+ to N_2O) ranges from -45 to -68.2‰ (Ueda et al., 1999; Yoshida, 1988) and from -59.5 to -68.2‰ (Yoshida, 1988). Sutka et al. (2003) also report a nitrogen-15 enrichment factor of -26‰ for hydroxylamine oxidation by *Nitrosomonas europaea* through autotrophic nitrification and +2.3‰ for hydroxylamine oxidation by *Methlycoccus capsulatus* through methanotropic nitrification (Appendix A).

Though little experimental work has been done to explain $^{18}O\text{-}N_2O$ composition formed from NO_2 (during nitrifier-dentrification) two studies show that it has a composition near mean atmospheric O_2 (+23.5‰) (Whalen and Yoshinari, 1985; Perez et al., 2001).

1.1.4.2.3 Denitrification

The isotope systematics of denitrification are as equally complicated as nitrification though it is arguable that more work has been done in this area. It has been reported that the residual NO_3^- pool exhibits an enrichment of 1:2 when measured as $\delta^{18}O$:$\delta^{15}N$ ratio (Mengis et al., 1999, Aravena and Robertson, 1998; Wassenaar, 1995). This has been used as evidence of NO_3^- removal via denitrification. The fractionation most likely occurs during uptake of nitrate into the cell and subsequent reduction. However, fractionation would only occur if NO_3^- within the cell is less limiting than limitations caused by reduction potential or available enzymes. If NO_3^- within the cell is limiting and the reduction potential and/or amount of available enzymes is high, all the NO_3^- in the cell would be consumed and little fractionation would occur. It has also been shown that the reduction of NO_2^- to NO can be rate limiting, suggesting that fractionation can occur at this step (Baumgärtner and Conrad, 1992; Santoro et al. 2006). However, build up of nitrite in the cell is unlikely as it is toxic and would also likely inhibit the uptake of nitrate, which is a stronger oxidizing agent (Firestone and Davidson, 1989). The same theoretical arguments also limit the likelihood of fractionation during the reduction of NO to N_2O.

A large range of apparent fractionation factors are observed between NO_3^- and N_2O (ε = -13.5 to -33‰), likely due to the different scenarios controlling nitrate reduction. These are deemed as apparent fractionations as it is the net isotopic effect of multiple fractionations. For complete reduction of NO_3^- to N_2, Kendall (1998) reports a range of apparent fractionation factors of -5 to -40‰ for nitrogen isotopes. Examples in Appendix A show that this is remarkably consistent between both incubations and field studies.

Enrichment of ^{18}O-NO_3^- shows that NO_3^- containing ^{16}O is preferentially reduced during NO_3^- reduction. As shown in Equations 1-7 to 1-10 water is formed from the loss of oxygen atoms during reduction of NO_3^- to NO_2 and then to NO. Fractionation kinetics suggest that N-^{16}O would be preferentially cleaved during these progressive reductions, resulting in enrichment of the products. A range of ^{18}O enrichment factors (ε = -10 to +32‰) reported in the literature (Appendix A) for the reduction of NO_3^- to N_2O show positive ^{18}O-N_2O enrichment is sometimes, but not always, observed. Alternate isotopic

effects such as oxygen exchange with water show that other processes likely complicate the expected results.

Exchange of O-H_2O with N-species during denitrification has been shown and this can have a significant effect on δ^{18}O-N_2O (Casciotti et al. 2002, Ye et al. 1991, Shearer and Kohl 1988). It appears that the presence of nitrite reductase (NiR) enzymes with either copper (Cu-NiR) or heme cd_1 chromatophores (cd_1-NiR) are a prerequisite for oxygen exchange during NO_2 to NO reduction (Kim and Hollocher, 1984; Hochstein and Tomlinson, 1988; Averill, 1996; Ye et al., 1994). The heme cd_1-NiR is found in 66% of examined denitrifying species (Averill, 1996; Ye et al., 1994). Exchange during NO reduction is also possible. For this reaction, Ye et al. (1991) observed that different rates of exchange were correlated with the different NiR, and suggested that nitric acid reductase (NOR) has similar chromatophores. It is speculated that the amount of oxygen exchange during either reaction may be controlled by the diversity of the functional enzymes present (Kool et al., 2007). Oxygen exchange with NO_3^- and N_2O is less likely though it cannot be excluded as a possibility (Kool et al., 2007).

As δ^{18}O-H_2O in water often ranges from -26 to -2‰ (IAEA, 2001) this can cause a significant masking of the fractionation associated with oxygen cleavage in the progressive reductions of NO_3^- to N_2O. This may be the reason for either negative or small positive enrichment factors for ^{18}O during denitrification (Appendix A). The significance of oxygen exchange on δ^{18}O-N_2O in different environments has not been adequately explored and is addressed further in Chapters 3 and 4.

The reduction of N_2O to N_2, by which microbes gain significant energy, results in ^{18}O enrichment factors of -4.9 to -42‰ (Appendix A). ^{15}N fractionations of -1 to -39‰ have been reported though a range of -2 to -10‰ is more common (Appendix A). It is commonly observed that the ratio of ^{15}N:^{18}O fractionation factors ranges from 0.36 to 0.49 (Mandernack et al., 2000; Schmidt and Voerkelius, 1989; Vieten et al., 2007; Menyailo and Hungate, 2006). This relationship possibly results from the consumption of N_2O following production.

1.2 Study Site description

1.2.1 Introduction and Land Use

The Strawberry Creek Catchment is located near the village of Maryhill, ON, situated 15km from the city of Waterloo, ON. This first-order agricultural catchment is approximately 2.7km^2 (270 hectares, 667.2 acres) with a drainage creek as the dominant hydrologic feature. With its headwaters in a deciduous swamp, the creek runs for 2km through farmland until it reaches Hopewell creek, a tributary of the Grand River. Upper portions of the creek have been channelized to enhance drainage while lower portions likely represent the original geomorphic structure of the creek.

The catchment was chosen as a study site because it is considered to have representative land-use practices, geology, climate, and hydrology of the region. It has been monitored intensively since 1997 through numerous studies giving it one of the longest records of hydrology and meteorology of an agriculture catchment in Southern Ontario.

Figure 1-4: Location of the Strawberry Creek catchment near the city of Waterloo, Ontario, Canada. Rural industry in the Grand River watershed (black outline) is dominated by agriculture, which plays a large role in surface and groundwater quality within the region.

Land-use in the catchment is dominated by agricultural fields for crop cultivation, making up approximately 70% of the land base. Commonly cultivated crops include corn, soybeans, and winter wheat, while less common crops include alfalfa (hay), strawberries, and rhubarb. The practice of summer fallowing is observed sporadically, presumably for water and nutrient management and conservation. In the lowland areas such as the deciduous headwaters and the swamp south of the upper road, the dominant tree species is red maple (Acer rubrum) interspersed with a small presence of red ash (Fraxinus pennsylvanica) and eastern white cedar (Thuja occindentalis). Highland areas such as the two main deciduous swamp areas in the southern portion of the watershed are again dominanted by red maple (Acer rubrum) with American beech (Fagus grandifolia),

Trembling Aspen (Populus tremuloides), white ash (Fraxinus americana), and American basswood (Tilia americana) lightly distributed throughout. One woodland area in the lower portion of the catchment is connected to the creek by ephemeral flow that contributes only during high flow and high water table conditions (typically during the spring).

Another distinct zone in the catchment is the riparian zone that flanks either side of the creek by 3 to 10 meters. Grasses, sedges, and several isolated trees (Salix *spp*. and Acer negundo) are found in this zone. The several riparian zone transects used in this study were the Harris (1999) transect 3 and the Cabrera (2000) A-A' transect (Figure 1-5). Detailed description of the sub-surface geology and other physical characteristics at these transects can be found in Harris (1999) and Cabrera (2000).

1.2.2 Geology and Soils

Late Wisconsinan ice sheet advances and retreats formed the region's complex till sheet stratigraphy and define Strawberry Creek's quaternary geology (Karrow, 1974). Low, broad features of the Guelph drumlin field give the region a gently undulating topography. Slopes in the catchment are variable but always modest and the gradient of the stream is low (Harris, 1999). The low-lying poorly drained swamps and portions of the fields are found near the stream where there is little topographic gradient.

The dominant soils in the catchment are part of the Guelph soil catena, which are the well-drained Orthic gray brown Luvisols (Guelph series) and the Gleyed Orthic Melanic Brunisols (London series). Beneath this soil, three till layers define the stratigraphy of the catchment. The predominant surface layer is the Port Stanley Till which, in this area, is generally loose, sandy, sometimes stony, and pinkish buff. The Port Stanley Till was deposited during the Port Bruce Stade, an important glacial re-advance by the Ontario-Erie ice lobe. The underlying Maryhill Till was deposited earlier (14000 to 15000 YBP) by the same glacial re-advance. This deeper till is finely textured, highly consolidated clay which often has beds of laminated or varved clay and silt, probably resulting from the incorporation of lacustrine sediments (Karrow, 1993). Cabrera (2000) encountered what

he presumed to be the Maryhill Till during peizometer installation and recorded its depth as 1-5m throughout the catchment. Cabrera (2000) also noted that this dense layer possibly acts as an aquiclude to the deeper regional aquifer and forms a superficial aquifer for the stratigraphy above it. Beneath the Maryhill Till lies the sandy Catfish Creek Till of the older (17000 to 20000 YBP) Nissouri stadial, corresponding to the maximum extent of Late Wisconsinan ice (Dreimanis, 1958). It is a stony till with a matrix of sand and silt but very little clay. It is yellow to buff or olive in its oxidized form, which is common due to the seepage of groundwater through this relatively permeable layer.

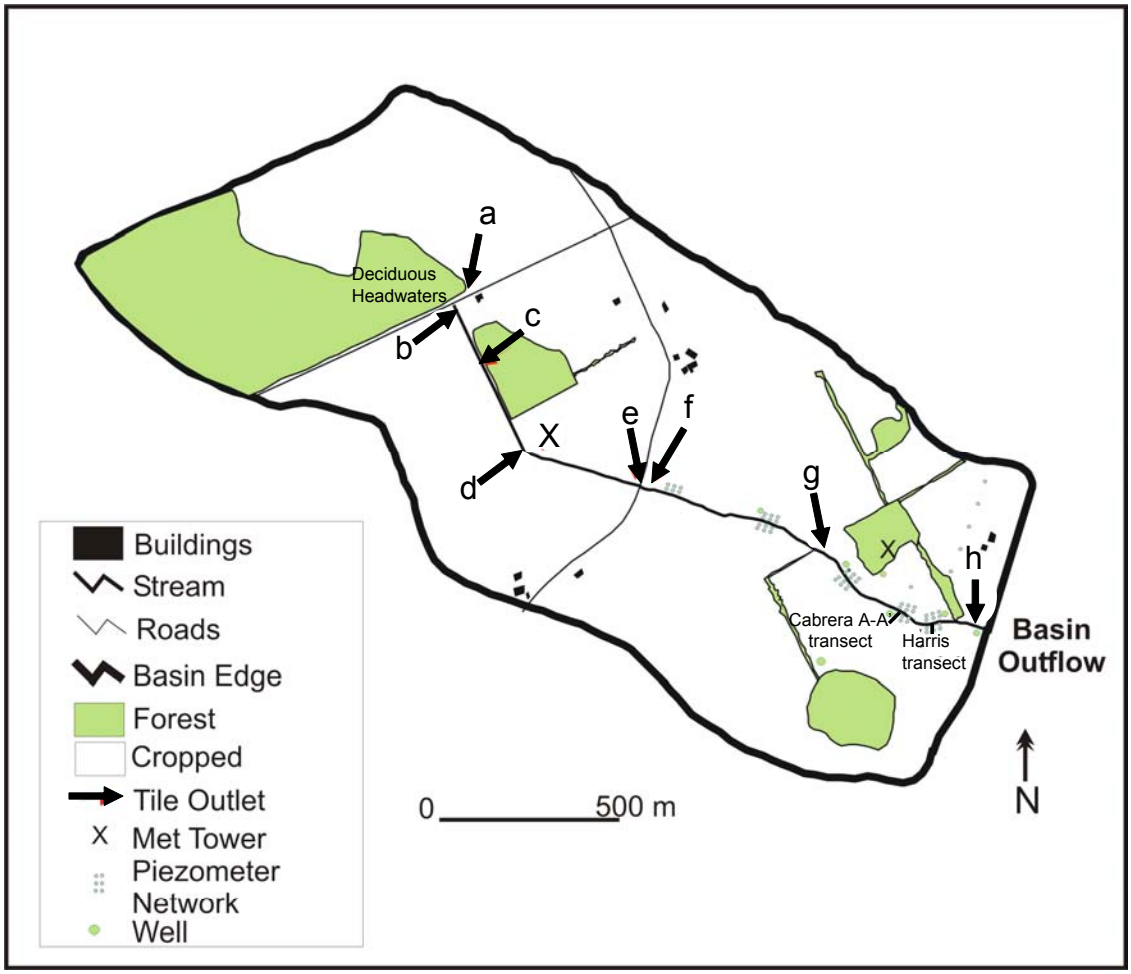

Figure 1-5: Instrumentation at the Strawberry Creek catchment. Tiles monitored in this thesis are shown in the diagram: *a)* Upper road tile, *b)* Shantz tile, *c)* Forest tile, *d)* Bend tile, *e)* AMR tile, *f)* BMR tile, *g)* Fencerow tile and *h)* Harris tile. Locations of groundwater transects used in this study (Cabrera A-A' and Harris) are also indicated on the map

1.2.3 Tile drain networks

The extent of fine textured soils in the Strawberry Creek catchment has necessitated the installation of tile-drain networks to improve sub-surface drainage and soil aeration (Gentry et al., 2000; Deutsch et al., 2005). This is a common practice in the region due to low permeable stratigraphic layers and modest precipitation in the region. The tiles are pipes, made of clay or plastic, which are laid 0.5 to 1m below the soil surface in a variable pattern throughout the field connected to a header pipe that collects the drainage waters and discharges them to surface water ways. The tiles sampled in the different studies that

constitute this thesis are (from headwaters to downstream locations): Upper road tile, Shantz tile, Forest tile, Bend tile, Halfway tile, Above middle road (AMR) tile, Below middle road (BMR) tile, Fencerow tile, and Harris tile (Figure 1-5).

1.3 Objectives

The overall objectives of this thesis are to investigate NO_3^- and N_2O sources and cycling at the Strawberry Creek Catchment using stable isotope geochemistry.

Chapter 1 introduces nitrogen cycling in agroecosystems with respect to NO_3^- and N_2O. Processes and isotopic effects are described.

Chapter 2 explores the effects of seasonal hydrology on NO_3^- isotopes using a data set from 1998 to 2000. Here the influence of denitrification in the tiles versus stream locations under various hydrologic regimes is investigated.

Chapter 3 investigates dissolved N_2O dynamics during two major melt events at the catchment using dual isotopes of N_2O. The 2007 Springmelt and January 2008 melt are compared in this section. Dual N_2O isotopes of soil gas and dual NO_3^- isotopes are also employed.

Chapter 4 describes dissolved N_2O dynamics during baseline conditions from October 2006 to Fall 2007 mainly using stable isotopes of this gas. Streams, tiles, and groundwaters are compared seasonally to investigate mechanisms responsible for N_2O cycling. Dual N_2O isotopes of soil gas and dual NO_3^- isotopes are also employed. A conceptual model for N_2O isotope cycling at the Strawberry Creek catchment is proposed as a summary to the findings in this and the previous chapter.

Chapter 2: NO_3^- Isotopes at the Strawberry Creek Catchment (1998-2000): A reflection of Sources or Processes?

Overview

Nitrate (NO_3) contamination in agricultural watersheds is a widespread problem that threatens local drinking supplies and downstream ecology. Management of NO_3^- is essential. Dual isotopic analysis of NO_3^- ($\delta^{15}N$ and $\delta^{18}O$) has successfully been used to identify sources of NO_3 contamination and nitrogen (N)-cycle processes in agricultural settings. The Strawberry Creek Watershed is a first-order catchment in southern Ontario, typical of regional agriculture practices including the use of tile drain networks to improve drainage. Tile drainage and stream water was sampled for NO_3^- concentration and isotopes to identify whether the isotopic signatures represented the sources of NO_3^- from the fields or whether they were altered by biogeochemical transformations occurring in the soil, water, or sediment. NO_3^- concentrations between tiles are variable and linked to season, hydrology, and N application. NO_3^- isotopes suggest the effects of denitrification were not extensive and could be corrected using expected $\delta^{18}O$ values of unaltered NO_3^-. Our results suggest that tile NO_3 were mainly derived from soil organic matter and manure fertilizers. NO_3^- concentrations in the stream are dominated by the influence of tile inputs once discharge reaches a certain threshold. At very low discharge stream NO_3^- concentrations are controlled by groundwater inputs which also show evidence of denitrification. NO_3^- isotope samples affected by denitrification can also be corrected so that source identification is possible. Corrected stream NO_3^- generally reflects the combination of sources identified at various tiles in the catchment.

2.1 Introduction

The widespread practice of nitrogen (N)-based fertilizer application contributes to nitrate (NO_3^-) contamination of surface-water and groundwater in agricultural watersheds. N is often a limiting nutrient for crop growth and N amendments, through fertilizer application, are often overused to offset this limitation. The necessity for management of this ubiquitous nutrient is driven by the reliance of many rural and urban populations on shallow groundwater wells for drinking water supply in regions where NO_3^- concentrations exceed the human drinking water limit of 10 mg N/L. In addition to human health concerns, agricultural NO_3^- loading leads to eutrophication of surface and groundwaters, both within and outside local agroecosystems (Carpenter, et al., 1998). The increased atmospheric concentration of nitrous oxide (N_2O) has also, in part, been due

to the increased use of organic and inorganic fertilizers in agriculture and has created another impetus for nutrient management to reduce production and emissions of this powerful greenhouse gas (Robertson et al., 2000).

The dominant N inputs to agricultural watersheds are organic and inorganic fertilizers, crop residue, soil organic matter, residential septic systems, and animal feedlots (Carpenter et al., 1998; Wassenaar, 1995; Aravena and Robertson, 1998). Overland run-off and groundwater inputs from fields result in non-point NO_3^- pollution to streams while certain practices, such as tile-drainage systems, contribute to point NO_3^- contamination. It is often difficult to determine the main source of the NO_3^- contamination in agricultural areas due to the number of point and non-point contributions. A further complication in source identification arises from the naturally occurring transformations of nitrification and denitrification. These processes produce and consume NO_3^-, thereby altering its concentrations in surface and ground waters.

The dual NO_3^- isotope method has become a useful tool for fingerprinting different sources of this contaminant. Expected ranges for $\delta^{15}N$ from literature sources are shown in Figure 2-1. The widely accepted theory that one third of nitrate oxygen is from atmospheric O_2 (+23.5‰) and two thirds are from water's oxygen can be used to calculate expected $\delta^{18}O\text{-}NO_3^-$ (Andersson and Hooper, 1983; Kumar et al., 1983; Hollocher, 1984). This is summarized in Equation 2-1.

$$1/3 * \delta^{18}O - O_2 + 2/3 * \delta^{18}O - H_2O = \delta^{18}O - NO_3^- \qquad \textbf{Equation 2-1}$$

The mean monthly weighted average $\delta^{18}O\text{-}H_2O$ from Simcoe, ON ranges from -17.1 to -5.5‰. This means that $\delta^{18}O\text{-}NO_3^-$ should range from -3.5 to +4.0‰. If some allowance is given for evaporative enrichment of $\delta^{18}O\text{-}H_2O$, the upper range at Strawberry Creek could extend to +6‰ as in Mengis et al. (1999).

Isotopic signatures of NO_3^- are retained through various influences such as dilution and plant uptake, though they can be altered by denitrification. Denitrification is an anaerobic reaction series where NO_3^- is ultimately reduced to atmospheric nitrogen (N_2). It is

commonly observed that in a closed system $\delta^{15}N$ values of the residual nitrate pool become enriched 1.5 to 2.0 times more than $\delta^{18}O$ values, producing a slope of 1:2 when $\delta^{18}O\text{-}NO_3^-$ values are plotted versus $\delta^{15}N\text{-}NO_3^-$ (Mariotti et al., 1988, Bottcher et al., 1990, Aravena and Robertson, 1998; Cey et al., 1999). The characteristic isotopic enrichment of nitrate has been used as an indication of denitrification in surface water and groundwater field studies.

The range of ^{15}N fractionation for the conversion of soil organic matter to NH_4^+ (ammonification) is reported to range from 0 to ±1‰ (εp-r) (Kendall, 1998; Hogberg; 1997) and therefore it is expected that $\delta^{15}N$ values for NH_4^+ produced from soil organic N will be similar to the isotopic composition of the soil organic N. Shearer and Kohl (1986) and Kendall (1998) report that ^{15}N fractionation during nitrification (NH_4^+ to NO_3^-) ranges from -12 to -29‰ (εr-p) though less fractionation will occur in agricultural systems. Since NH_4^+ is bound to negatively charged soil particles it can actually be limiting within nitrification and cause there to be no observed fractionation in the NO_3^- produced. Therefore the ^{15}N of NO_3^- should equal that of NH_4^+ in these systems.

Strawberry Creek is a typical first-order catchment in terms of size and land-use practices in Southwestern Ontario, Canada. The main hydrologic feature of the catchment is a small stream that is fed by tile drain and groundwater inputs. With respect to tile drains, the objectives of this paper are: 1) to reveal the dynamics of NO_3^- concentrations from different tiles 2) to identify the source of NO_3^- in relation to N application; 3) to identify if there is alteration of the original NO_3^- source signature. With respect to stream samples, the objectives are: 1) to reveal the influence of NO_3^- inputs from tiles and groundwater; 2) to identify sources of NO_3^-; and 3) to identify if N-cycle processes are affecting NO_3^- concentrations in the stream.

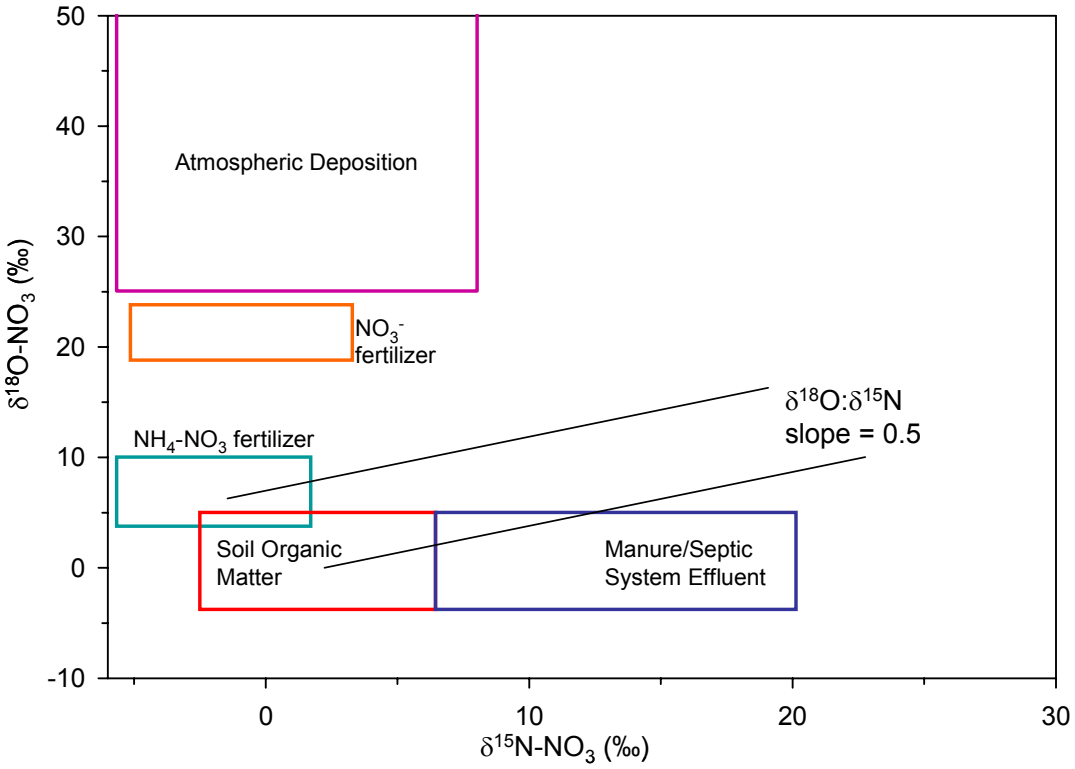

Figure 2-1: Expected $\delta^{15}N$ and $\delta^{18}O$ (NO_3^-) ranges expected for Strawberry Creek. $\delta^{15}N$ ranges are based on literature values reported in Aravena et al. (1993); Wassenaar (1995); Aravena and Robertson, (1998); Kendall (1998); and Spoelstra et al. (2001). $\delta^{18}O$ ranges for NO_3^- from atmospheric deposition, NO_3^- fertilizers, and NH_4^+-NO_3^- fertilizers are based on literature values reported in Kendall (1998); Mayer et al. (2001); Spoelstra et al. (2001); and Wassenaar (1995). The upper range for $\delta^{18}O$-NO_3^- from atmospheric deposition extends to +80‰. $\delta^{18}O$ ranges for NO_3^- from soil organic matter and manure/septic system effluent were calculated based on the range of mean monthly weighted average $\delta^{18}O$ of precipitation (IAEA, 2001) and the $\delta^{18}O$ of atmospheric O_2 (+23.5‰).

2.2 Study Site

For detailed site description see Section 1.2.

2.3 Methods

Stream and tile drain water samples were collected periodically from the Strawberry Creek watershed from late October 1998 to mid-August 2000 for NO_3^- concentration and

isotopic analysis. Stream stage was recorded continuously by pressure transducer except for the period of June 31, 1999 through February 16, 2000 due to equipment failure. Stage was converted to discharge by the established stage-discharge curve. Manual measurements of stage and velocity were taken during sampling occasions in the period of automated equipment failure. During summer months and in periods of low precipitation, tile drains were not flowing.

Samples for NO_3^- isotopic analysis were stored at 4°C and filtered through a 0.45 μm cellulose acetate filter within a day of collection. Sub-samples were taken for NO_3^--N, SO_4^{2-} and $\delta^{18}O$-H_2O analysis. Isotope samples were prepared following an ion exchange method as described by Chang et al. (1999) and Silva et al. (2000) with modifications as in Spoelstra et al. (2004). In brief, 2-5 mg NO_3^--N was passed through anion exchange resin columns (BioRad AG 1-X8 (Cl-) 100-200 mesh resin). The isolated NO_3^- was eluted using HCl and subsequently neutralized through the gradual addition of Ag_2O. The solution was then filtered from the precipitate, frozen and freeze dried to obtain $AgNO_3$ salt.

To isolate the nitrogen component for isotopic analysis, the $AgNO_3$ was combusted with CuO, CaO and Cu° in evacuated 6 mm OD quartz breakseal tubes. The $N_2(g)$ which was produced during the combustion process was then analyzed on a mass spectrometer for $^{15}N/^{14}N$ at the Environmental Isotope Laboratory (EIL) at the University of Waterloo.

For ^{18}O-NO_3^- analysis, the $AgNO_3$ was placed in 6 mm OD breakseal tubes with baked carbon. The breakseal was subsequently evacuated overnight, sealed and combusted. The resulting $CO_{2(g)}$ was analyzed using a VG Prism isotope ratio mass spectrometer at the EIL at the University of Waterloo.

Results for the $^{15}N/^{14}N$ and $^{18}O/^{16}O$ analysis are reported using δ-notation relative to atmospheric nitrogen (air) for $^{15}N/^{14}N$ and Vienna Standard Mean Ocean Water (VSMOW) for $^{18}O/^{16}O$. The $\delta^{15}N$ and $\delta^{18}O$ values of the samples were calibrated against internal NO_3^- isotope standards: EIL-61 ($\delta^{15}N$ = +1.0‰, $\delta^{18}O$ = +11.0‰), EIL-62

($AgNO_3$), and Cambs 35-4. The precision of $\delta^{15}N$ and $\delta^{18}O$ analysis are ± 0.2‰ and ± 0.5‰, respectively.

2.4 Results

2.4.1 Tiles

2.4.1.1 NO_3^- concentration

Dissolved NO_3^- concentration varies considerably among the drainage tiles with average concentration ranging from 5.5 mg N/L to 32.4 mg N/L (Table 2-1). Tiles with lower average NO_3^- concentrations, Forest tile (7.8 mg N/L), Fencerow tile (5.5 mg N/L), Shantz tile (5.6 mg N/L), and Halfway tile (8.3 mg N/L), also have relatively small standard errors and the number of samples is small. AMR tile is an exception with a low average NO_3^- concentration (6.7 mg N/L) but a much larger range (23.6 mg/L) and standard error (2.2) indicating significant variation around this average. Tiles with higher average NO_3^- concentration, Harris tile (16.7mg N/L), BMR tile (18.1 mg N/L), and Bend tile (32.4 mg N/L), had standard errors of 1.1, 3.1, and 6.5 respectively. This indicates that the Harris tile likely has the most consistently high concentrations in contrast to Bend tile which has a large range and few samples giving a large standard error.

Table 2-1: Average, range, and standard error of the mean for NO_3^- concentrations from Strawberry Creek tile drains

Tile	Number of samples	Average NO_3^- (mg N/L)	Max. NO_3^- (mg N/L)	Min. NO_3^- (mg N/L)	Standard Error of the Mean NO3- (mg N/L)
Shantz	4	5.6	7.0	2.8	1.0
Forest	9	7.8	10.3	4.1	0.8
Bend	3	32.4	43.3	20.7	6.5
Halfway	2	8.3	9.0	7.5	0.7
AMR	15	6.8	23.7	0.1	2.2
BMR	10	18.1	32.2	3.4	3.1
Fencerow	4	5.5	7.0	2.9	0.9
Harris	20	16.7	23.7	6.6	1.1

NO_3^- concentrations exhibit seasonal variability though the highest concentrations are measured during periods of high flow (Figure 2-2 and Figure 2-3). Harris and BMR tiles have consistently high concentrations while Shantz tile remains low through a wide range of discharge in most seasons. Temporally, AMR had low NO_3^- concentrations in 1999 and higher concentration in 2000, each measured at discharge less than or greater than 20L/s, respectively (Figure 2-3). Low average NO_3^- concentration measured at Forest and Fencerow tiles were sampled during low flow in the summer of 2000 (Figure 2-2 and Figure 2-3).

2.4.1.2 $\delta^{15}N\text{-}NO_3^-$ and $\delta^{18}O\text{-}NO_3^-$

$\delta^{15}N\text{-}NO_3^-$ values ranged from 0.9 to 18.2‰ (Figure 2-4). Several of the tiles (Forest, Bend, BMR, and Harris tiles) exhibit a small range in values while others (Shantz and AMR tiles) show a large range in $\delta^{15}N\text{-}NO_3^-$ values. Forest, BMR, and Harris tiles were sampled most frequently. AMR tile has two distinct groupings of data, one from 1999 and one from 2000. Maximum values for Shantz, Forest, AMR, and Fencerow tiles were actually collected on August 16, 2000.

$^{18}O\text{-}NO_3^-$ values from Strawberry Creek tiles are much more constrained than $^{15}N\text{-}NO_3^-$ (Figure 2-4). The range of $\delta^{18}O$ values is -1.5 to 7.2‰. Accordingly, individual tiles also vary less, ranging between 1.1‰ (Bend tile) to 5.5‰ (Harris).

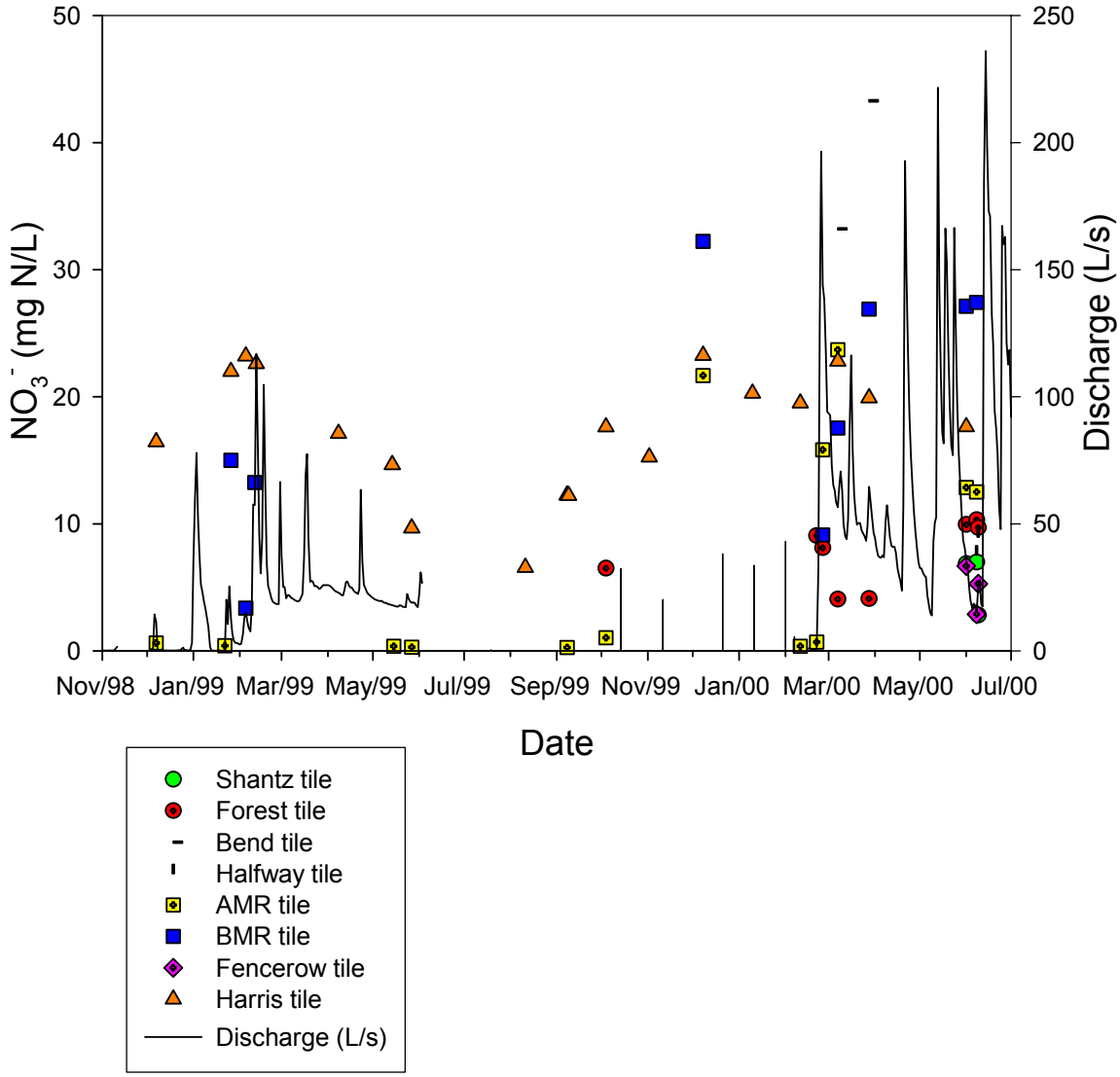

Figure 2-2: Tile NO_3^- concentrations and basin discharge for the sampling period

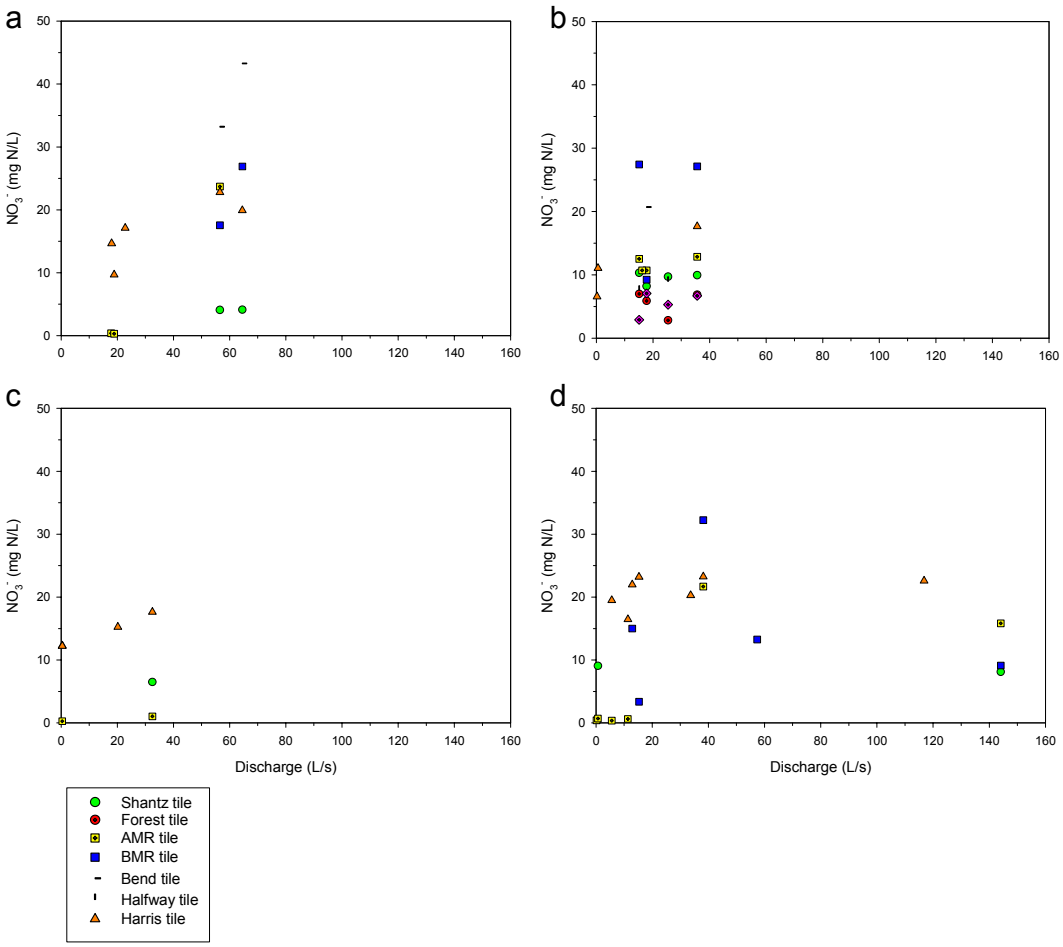

Figure 2-3: The relationship between Outlet discharge and NO_3^- concentration at Strawberry Creek tiles for (a) Spring, (b) Summer, (c) Fall, and (d) Winter seasons.

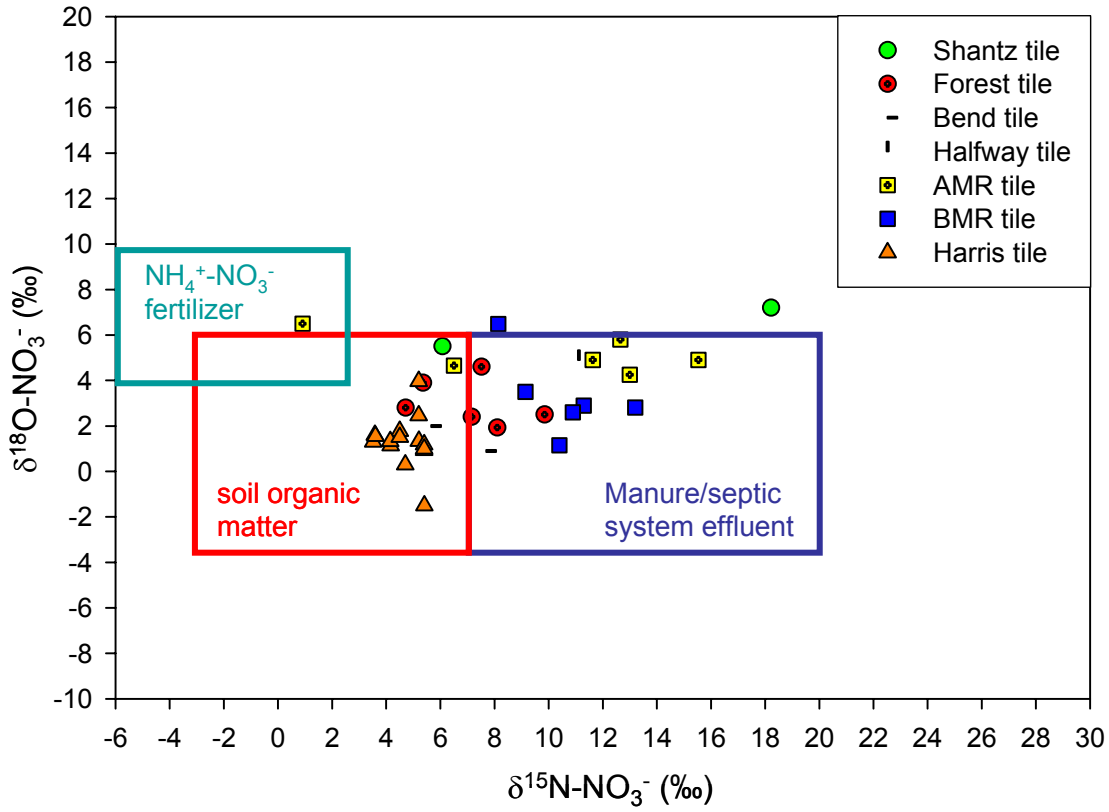

Figure 2-4: $\delta^{18}O$ (VSMOW) and $\delta^{15}N$ (air) of NO_3 for Strawberry Creek tiles. Determination of expected ranges of NO_3^- sources are described in Section 2.1.

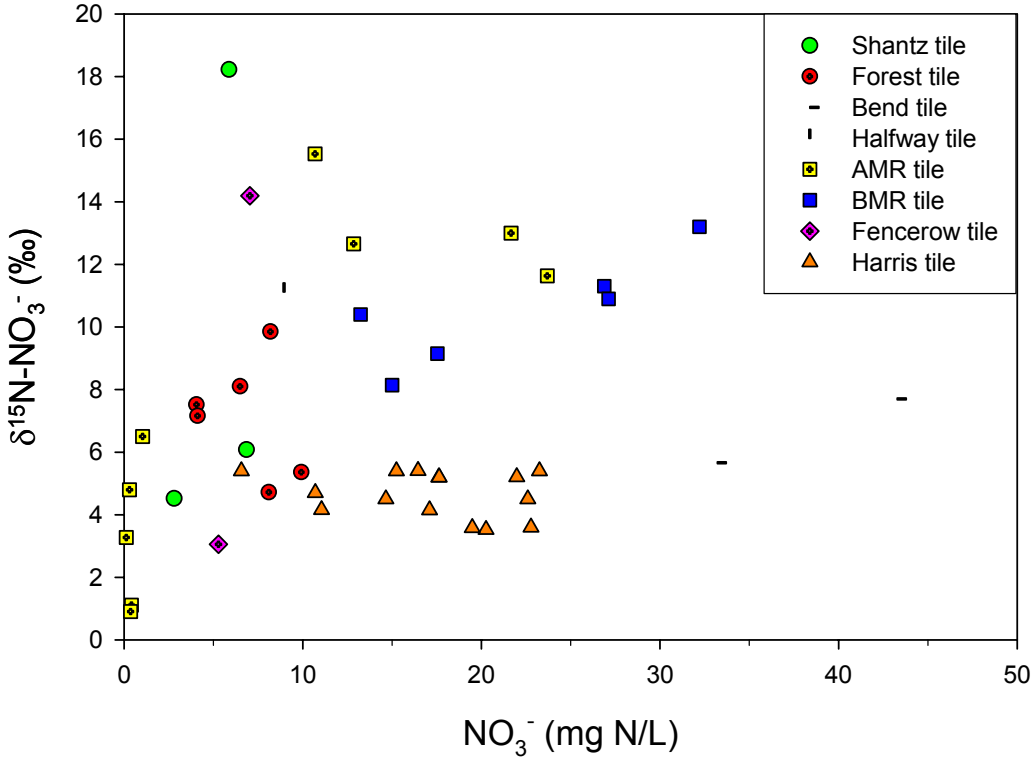

Figure 2-5: The relationship between NO_3^- concentration and $\delta^{15}N\text{-}NO_3^-$ for Strawberry Creek tiles.

2.4.1.3 $\delta^{15}N\text{-}NO_3^-$ and NO_3^-

No significant relationships exist between NO_3^- concentration and $\delta^{15}N\text{-}NO_3^-$ isotopes for individual tiles at Strawberry Creek (Figure 2-5) except for BMR tile ($y = 0.19x + 6.34$, $R^2 = 0.70$). Despite the general absence of trends, the behavior of some individual tiles is reasonably distinct. In the case of Harris tile, NO_3^- concentration is quite variable yet $\delta^{15}N\text{-}NO_3^-$ values are consistent. Others tiles (Forest, Shantz, Fencerow, and AMR-1999) display greater variation in $\delta^{15}N\text{-}NO_3^-$ and less variation in NO_3^- concentration. For example, AMR (1999) shows low NO_3^- concentrations of 0.12 to 1.04 mg N/L that vary in $\delta^{15}N\text{-}NO_3^-$ values from +0.9 to +6.5‰. Variability in both NO_3^- concentration and $\delta^{15}N\text{-}NO_3^-$ is also observed at Bend, BMR, and AMR (2000) tiles. For example, AMR tile

(2000) has a 10 to 25 mg N/L range in NO_3^- concentration and a 12 to 16‰ range in $\delta^{15}N$-NO_3^- values.

2.4.2 Streams

2.4.2.1 NO_3^- concentrations

NO_3^- concentrations in the stream are low in November 1998, April to November 1999, and before the 2000 springmelt when there is little or no tile flow. Stream NO_3^- concentrations are generally higher during periods of higher outlet discharge. Variability in stream NO_3^- concentrations along the stream length is obvious. Where tile NO_3^- concentrations are high the effect on stream NO_3^- concentrations is obvious. This is observed between the Outflow and Lower road tile and between the stream at Middle road and AMR tile (Figure 2-6). On the other hand, Upper road, at Z, and above Harris tile stream locations are not immediately downstream of a tile and do not display influence of tiles in their NO_3^- concentrations.

Table 2-2: Average, range, and standard error of the mean for NO_3^- concentrations from Strawberry Creek stream locations.

Location	Number of samples	Average NO_3^- (mg N/L)	Max. NO_3^- (mg N/L)	Min. NO_3^- (mg N/L)	Standard Error of the Mean NO_3^- (mg N/L)
Upper road	12.0	5.2	11.4	1.3	1.2
Middle road	10.0	5.1	18.5	0.0	2.1
at Z	2.0	1.8	2.5	1.1	0.7
above Harris tile	15.0	5.8	15.8	0.4	1.2
Outflow	33.0	4.8	15.3	0.1	0.8

NO_3^- concentrations in the stream remain low at low outlet discharge and generally increase with increasing discharge (Figure 2-7). Stream NO_3^- concentration tends to "break through" to high concentrations when critical outlet discharge is met. In spring, NO_3^- concentrations remain low until 25 L/s while in summer and fall concentrations are low until 35 L/s of discharge is measured. In winter, NO_3^- concentrations become significant after 10L/s of outlet discharge.

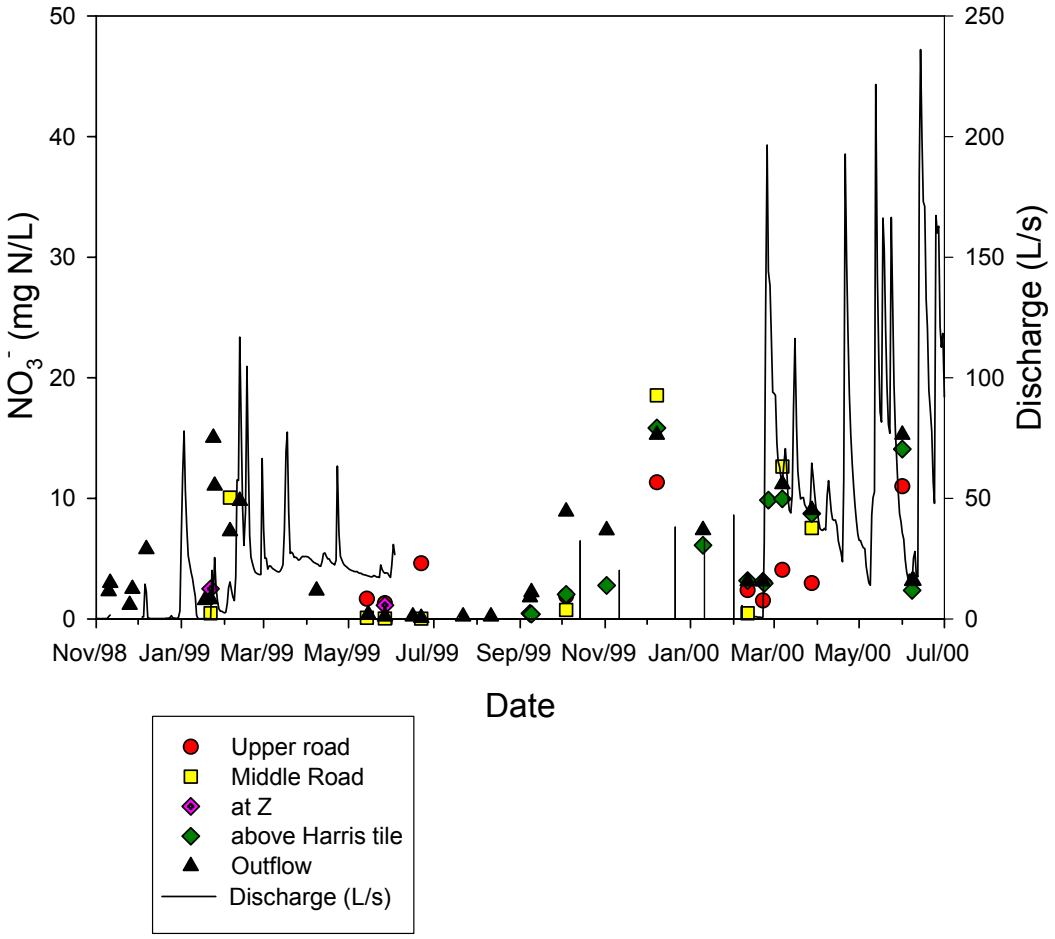

Figure 2-6: Stream NO_3^- concentrations and basin discharge for the sampling period

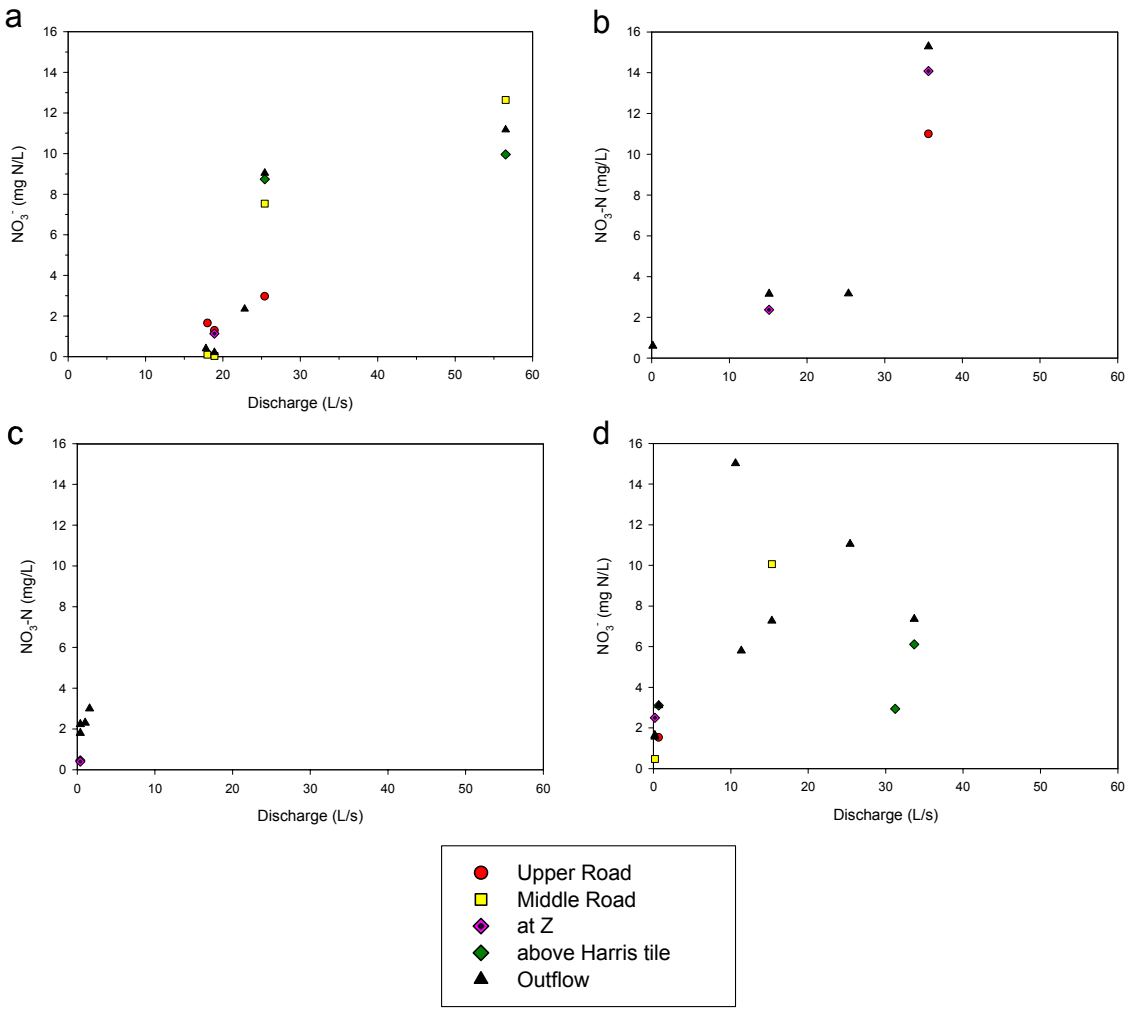

Figure 2-7: The relationship between basin discharge and NO_3^- concentration for stream locations during (a) spring, (b) summer, (c) fall, and (d) winter seasons.

2.4.2.2 $\delta^{15}N$-NO_3^- and ^{18}O-NO_3^-

$\delta^{15}N$-NO_3 values of the stream (Figure 2-8) display a considerably larger range ($\delta^{15}N$ = +2.67 to +17.15‰) than from the tiles (Figure 2-4). Stream sampling locations exhibiting a considerable range of values are Outflow ($\delta^{15}N$ = +5.25 to 14.62‰), above Harris tile ($\delta^{15}N$ = +7.32 to +17.15‰), and Middle Road ($\delta^{15}N$ = +2.67 to +11.88‰) sampling locations (Table B-4). Values between +7.59 and +13.8‰ ($\delta^{15}N$) were measured from the stream at the Upper road.

$\delta^{18}O\text{-}NO_3^-$ values from the streams range from +2.2 to +11.1‰ (Table B-4). Individual stream locations show variable ranges of +3.66 to +10.87‰ (Upper road), +3.53 to +9.86‰ (Middle Road), +2.33 to +6.76‰ (above Harris tile), and +2.2 to +10.5‰ (Outflow).

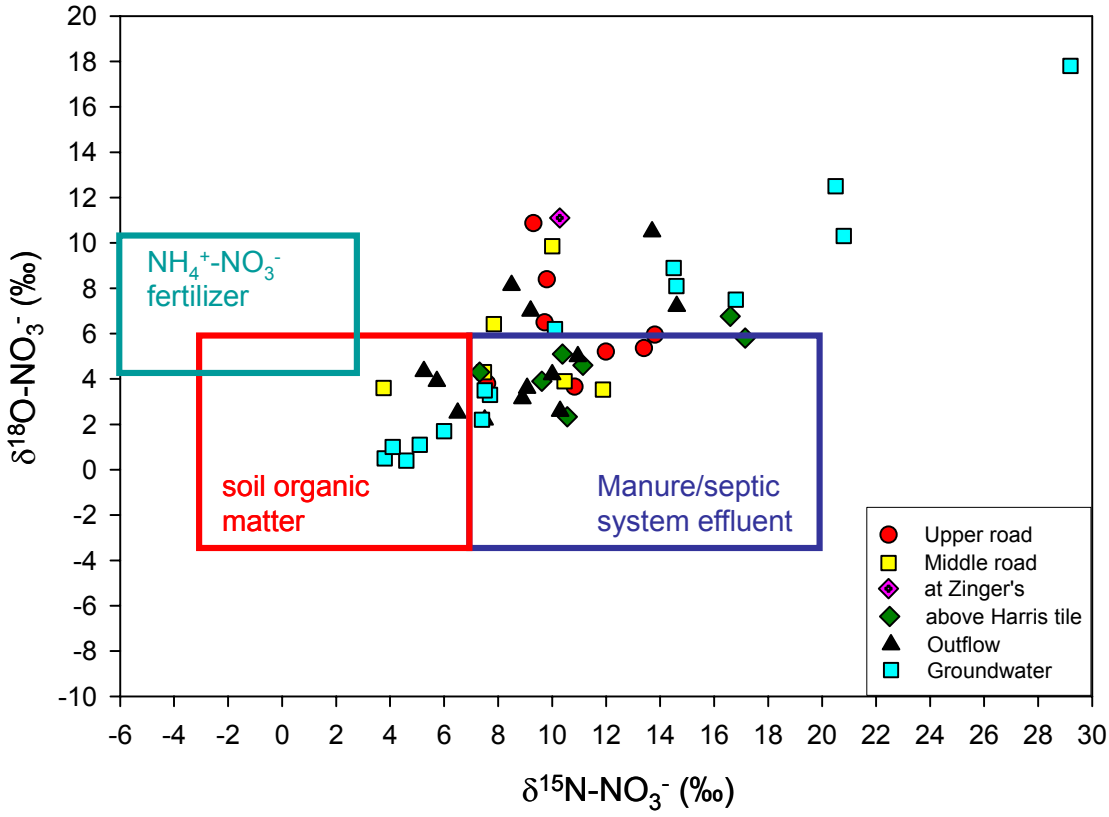

Figure 2-8: $\delta^{18}O$ (VSMOW) and $\delta^{15}N$ (air) of NO_3 for Strawberry Creek stream locations. Also included is groundwater nitrate data from Mengis et al. (1999) showing potential signatures of partially denitrified groundwater inputs. Ranges of NO_3^- sources reported from the literature are indicated.

2.4.2.3 Temporal trend in $\delta^{15}N\text{-}NO_3^-$ values

$\delta^{15}N\text{-}NO_3^-$ values are lower and less variable during the late winter and early spring (Figure 2-9) whereas values become higher and more variable in the summer and fall. $\delta^{15}N\text{-}NO_3^-$ values show an increasing trend from late winter and spring to summer after which values plateau until early fall when they again begin to decrease.

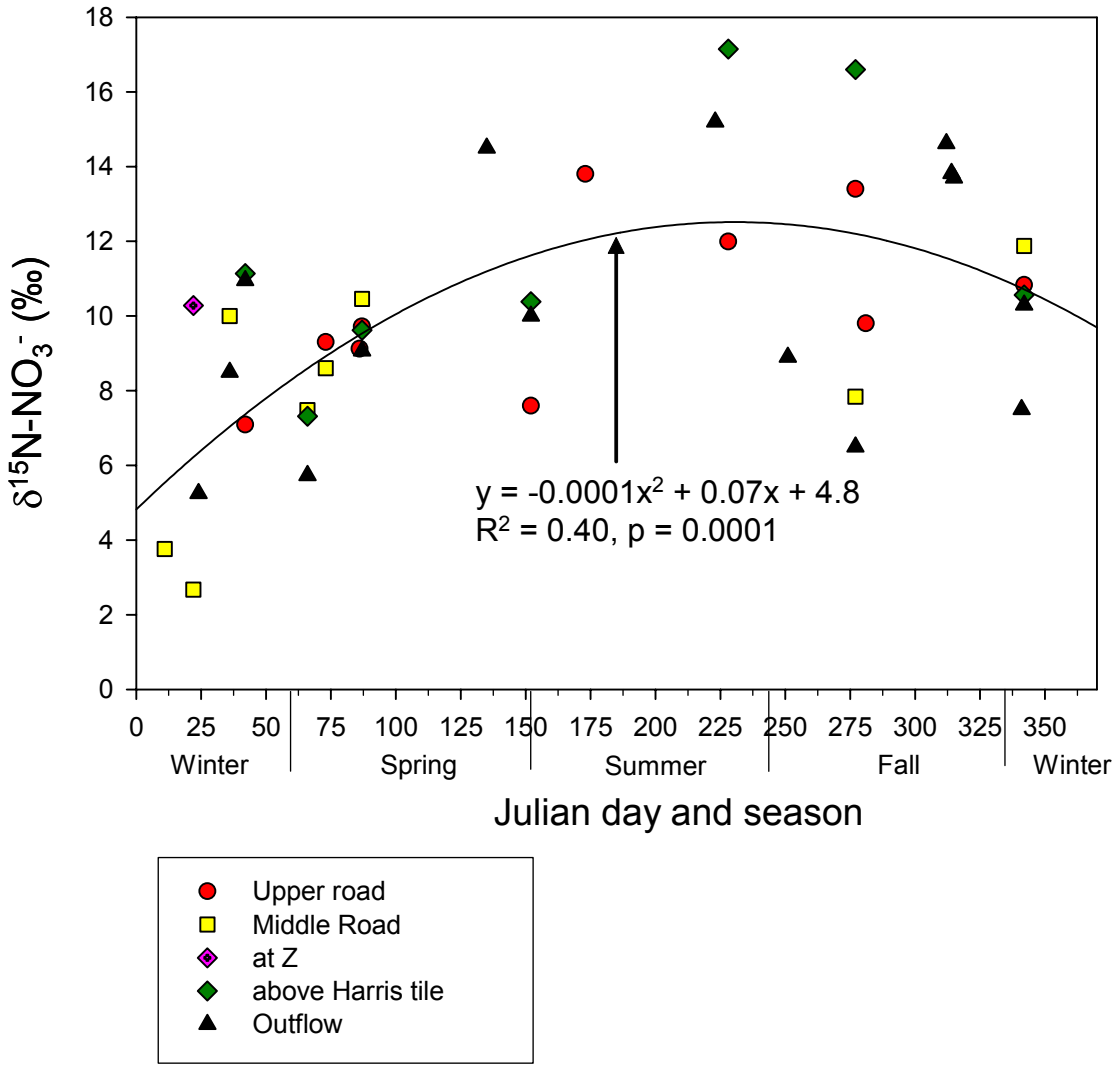

Figure 2-9: Stream $\delta^{15}N\text{-}NO_3^-$ by Julian day and season with the best fit 2nd order polynomial for the compiled dataset

2.4.2.4 $\delta^{15}N\text{-}NO_3^-$ and NO_3^- concentration

$\delta^{15}N\text{-}NO_3^-$ values above +10‰ were observed in all seasons though they were found most consistently during the summer and fall (Figure 2-10). The winter has $\delta^{15}N\text{-}NO_3^-$ values between +10 and +12‰ through NO_3^- concentrations of 0 to 20 mg N/L. The relationship between NO_3^- concentration and $\delta^{15}N\text{-}NO_3^-$ is not strong except during the summer season (Figure 2-10).

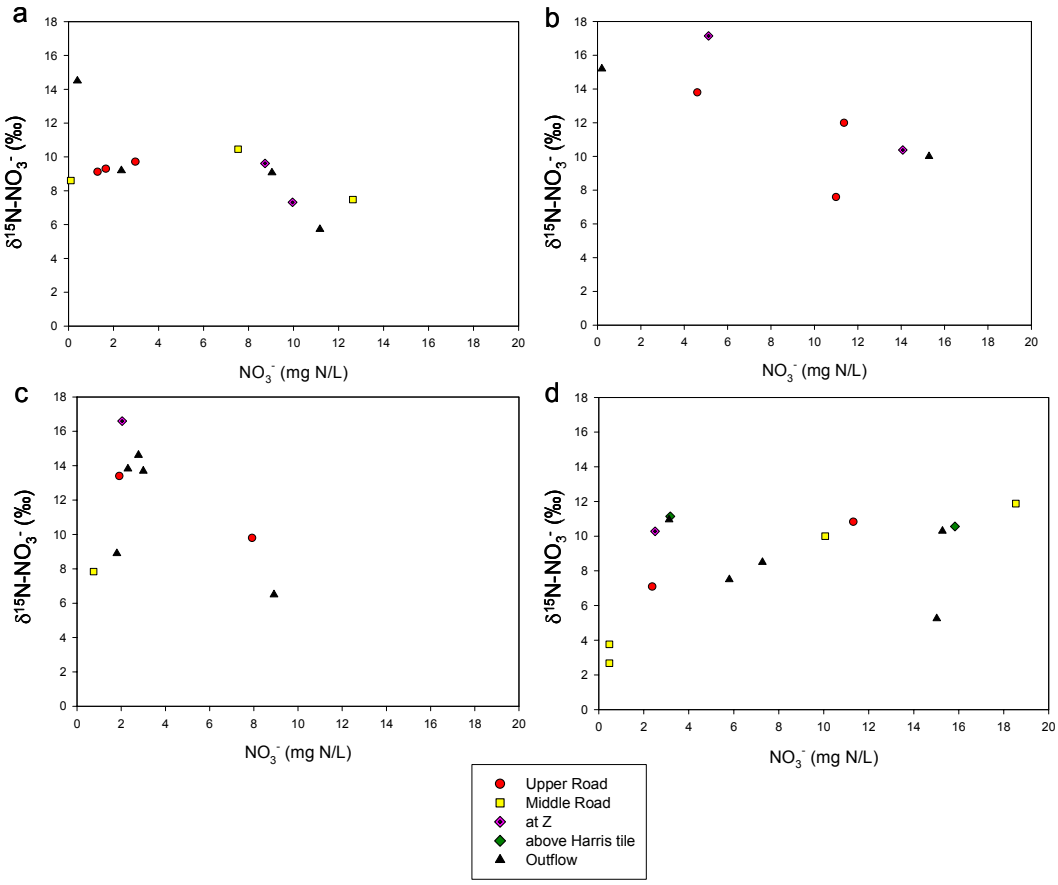

Figure 2-10: The relationship between NO_3^- concentration and $\delta^{15}N\text{-}NO_3^-$ for stream locations during (a) spring, (b) summer, (c) fall, and (d) winter seasons.

2.4.2.5 $\delta^{18}O\text{-}NO_3^-$ and NO_3^- concentration

High $\delta^{18}O\text{-}NO_3^-$ values (greater than +6‰) are measured in the Spring when concentrations are less than 5 mg N/L. During the fall and winter high $\delta^{18}O\text{-}NO_3^-$ (greater than +6‰) is measured when NO_3^- concentrations are less than 10 mg N/L but $\delta^{18}O\text{-}NO_3^-$ is also variable (+2 to +6‰) at these concentrations. $\delta^{18}O\text{-}NO_3^-$ values between +4 and +6‰ are measured in the summer (Figure 2-11).

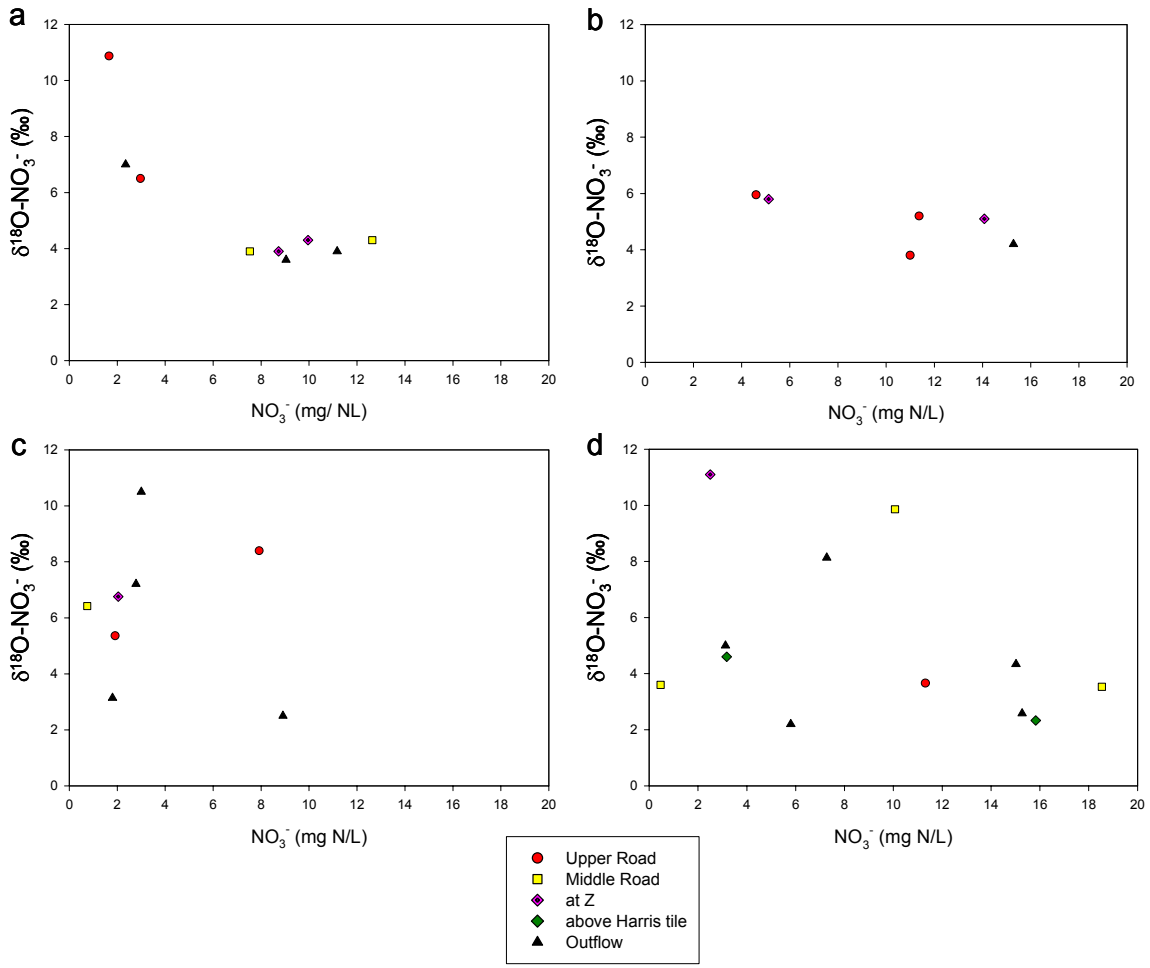

Figure 2-11: The relationship between NO_3^- concentration and $\delta^{18}O\text{-}NO_3^-$ for stream locations during (a) spring, (b) summer, (c) fall, and (d) winter seasons.

2.5 Discussion

2.5.1 Sources and Processes of NO_3^- in Tiles

NO_3^- concentrations vary significantly among individual tiles in the Strawberry Creek catchment. Some of the variability in NO_3^- concentrations at individual tiles is likely due to fertilizer type and application rates (Randall and Gross, 2001; Haygarth, 1997; Gentry et al., 2000) though other factors such as tillage and crop type can also be influential (Dinnes et al., 2002). Differences in chemical export can also be the result of drainage anomalies caused by differences in soil type, soil moisture properties, and the influence of

preferential flowpaths including drainage tiles (Beauchemin et al., 1998; Stamm et al., 1998; Welsch et al., 2001). Denitrification could also influence tile NO_3^- concentrations and must be accounted for before discussing NO_3^- sources which will ultimately be integrated with land-use practices (ie: fertilizer type, application rates, crop type) in addition to influences of seasonality, and hydrology.

A large range of $\delta^{15}N\text{-}NO_3^-$ values is observed from Strawberry Creek tiles creates some uncertainty about the use of this tool for source identification due to possible influence from denitrification. Caution must also be used in predicting source identities from isotope values found in the literature as opposed to direct measurement. For example, in a study of agricultural tile drainage in the St. Lawrence Lowlands of Quebec, tile water $^{15}N\text{-}NO_3$ was consistently enriched compared to source values (Kellman, 2005). However, $\delta^{15}N\text{-}NO_3^-$ differed enough between fields that determination of the type of fertilizer applied was possible. Other studies of tile drain nitrate reveal that tile drain isotope data is often sensitive to denitrification both seasonally and with respect to the amount of time between precipitation events (Deutsch et al., 2005; Kellman and Hillaire-Marcel, 2003). This study is not as detailed with respect to specific events, instead the data provide insight into NO_3^- sources and export under a wide range of flow conditions.

$\delta^{18}O\text{-}NO_3^-$ on the other hand has a much smaller range and, by establishing the $\delta^{18}O$ values for the different NO_3^- sources it is possible to identify the influence of denitrification and correct for it. As in presented in Section 2.1, the range of $\delta^{18}O\text{-}NO_3^-$ (-3.5 to +4.0‰) expected at Strawberry Creek based on mean monthly weighted $\delta^{18}O\text{-}H_2O$ can be extended to +6‰ if evaporative enrichment of ^{18}O occurs in the catchment (Mengis et al., 1999). A $\delta^{18}O\text{-}NO_3^-$ value of +6‰ should therefore be considered the maximum allowable value for non-denitrified sources, unless indicated below.

Mengis et al. (1999) report that groundwater $\delta^{18}O\text{-}NO_3^-$ beneath the field drained by Harris tile was between +0.5 and +6.2‰ while a value of +1‰ was assumed as the true source signature. Since $\delta^{18}O$ values measured at Harris tile usually do not exceed +2‰, this value should be considered the maximum and should also be appropriate for the Bend

tile. Most samples from Forest and BMR tiles have $\delta^{18}O$ values less than +3‰ so this should be the highest value of source NO_3^- for these tiles. AMR, Shantz, and Halfway tiles have a slightly higher average of +5.5‰ so the maximum allowable value for (non-denitrified) NO_3^- from these tiles is +6‰.

Data points corrected to the maximum non-denitrified $\delta^{18}O$-NO_3^- values of the respective sites using a $\delta^{18}O$:$\delta^{15}N$ ratio of 0.67 (Mengis et al., 1999) are presented in Figure 2-12. There are no major changes in source identification compared to uncorrected $\delta^{15}N$ and $\delta^{18}O$. The most noteworthy changes occur at Forest, BMR, and Harris tiles where $\delta^{15}N$ values are reduced by 2.4, 5.2, and 2.96‰, respectively. This places the NO_3^- data points from BMR and Harris tile near the range of NH_4^+-NO_3^- fertilizer which is lower in $\delta^{15}N$ than usual for these sites though still greater than +2‰ making it reasonable. Most of the $\delta^{15}N$ reductions are less than 1‰ and no greater than 1.8‰. As a whole this suggests that significant denitrification has not occurred meaning low NO_3^- concentrations measured in tiles are not a product of this process. However, if local denitrification went to completion there would be no enriched residual NO_3^- left behind, thereby erasing the signal of this process. Back calculation of original $\delta^{18}O$-NO_3^- source values also assumes that $\delta^{18}O$ values higher than the assigned values are not a result of mixing of multiple sources. For example, high $\delta^{18}O$ values could increase with a contribution of atmospheric NO_3^-. Since there is no evidence of high ^{18}O-NO_3^- sources in tile waters, this effect is believed to be minimal but should always be considered in this type of analysis.

After using this correction $\delta^{15}N$ can be used for source identification. Nitrate isotope samples collected from Strawberry Creek tiles generally fall into the ranges of soil organic matter or manure/septic system effluent (Figure 2-12). $\delta^{15}N$ of soil organic matter N at Strawberry Creek ranges from 6.45 to 8.78‰ with an average of 7.32‰ (Sherry Schiff, unpublished data) which should represent $\delta^{15}N$-NH_4^+ values (Kendall, 1998). This should also represent $\delta^{15}N$-NO_3^- values as little fractionation will occur during nitrification because of the large NH_4^+ pool and open system in agricultural settings.

$\delta^{15}N$ values from Harris tile are tightly grouped around the source groundwater $\delta^{15}N$ value (+4‰) reported by Mengis et al. (1999) and fall within literature values for nitrate derived from soil organic matter. It is possible that the NO_3 is derived from the mixing of mineralized NH_4-NO_3 fertilizer and soil organic matter as the farmer has indicated that only inorganic fertilizers have been used on this field (Table 2-3). Though NO_3^- concentrations are fairly consistent season appears to have some influence them. Harris tile shows a range of 6 to 23 mg N/L throughout the year, with the highest concentrations measured in the winter (at low flow), which could be due to reduced plant uptake and microbial activity. The Harris tile also often flows consistently throughout the year, indicating that the tile drain network consistently intersects the watertable. This could be because the watertable is relatively higher than in other fields or the tile drain network is buried relatively deeper than the other tile networks. The combination of fertilizer additions, the Strawberry crop's nutrient retention strategies, and the position of the tile drainage network in relation to the watertable likely plays a role in the higher NO_3^- concentrations observed at the Harris tile (Table 2-3).

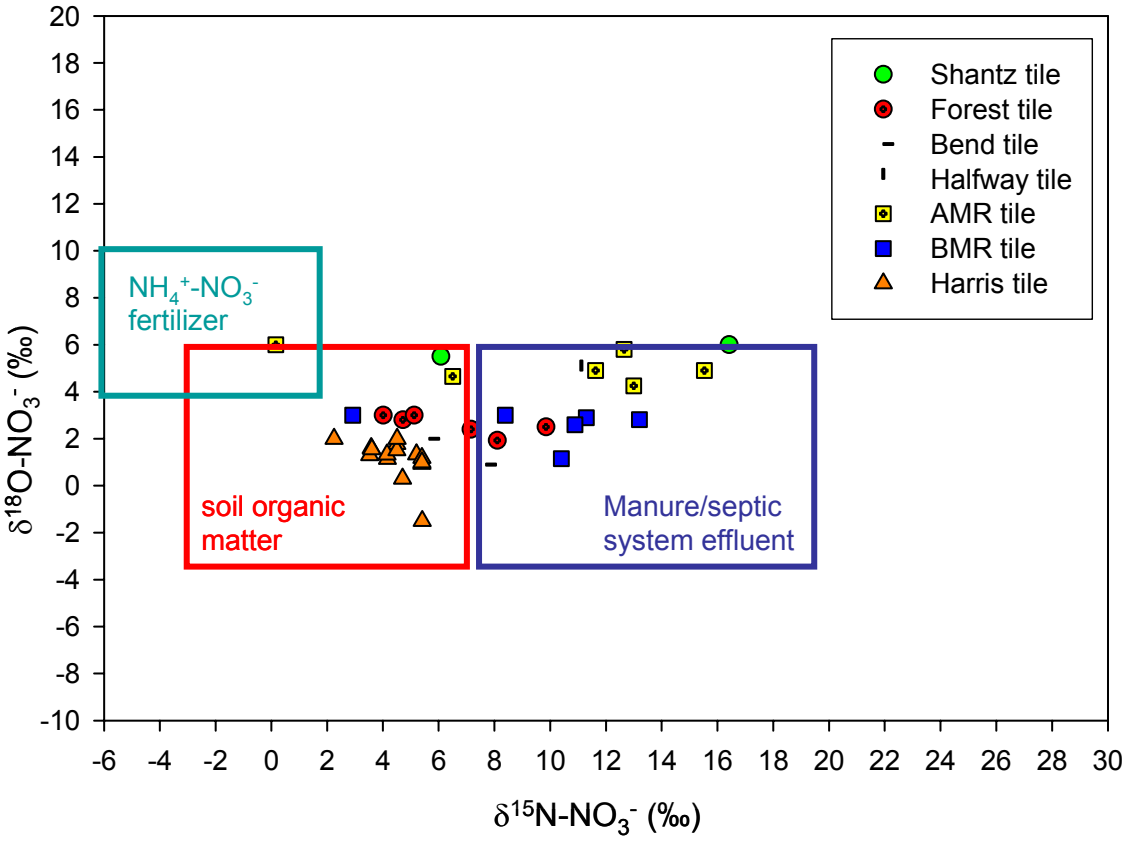

Figure 2-12: $\delta^{15}N$ and $\delta^{18}O$ of NO_3^- of tiles corrected to maximum expected $\delta^{18}O$ values for each site (specified in text).

NO_3^- from the AMR and BMR tiles is generally consistent with the range of values for manure/septic system effluent. This is expected since chicken manure is the only fertilizer that has been used on both these fields (Mike English, pers. comm.). Wassenaar (1995) found similar isotope values in nitrate derived from poultry manure in the Abbottsford aquifer, which are enriched in ^{15}N isotopes due to ammonium volatilization. High NO_3^- concentrations at BMR tile are observed in all seasons and are similar to those of AMR tile from 2000. The low NO_3^- concentrations at AMR tile in 1999 are observed at discharge lower than 20 L/s whereas higher concentrations are observed around discharge of 20 L/s and higher. The distinct temporal separation of $\delta^{15}N$-NO_3^- values from AMR tile suggests NO_3^- was derived from soil organic matter in 1999 but from manure/septic

system effluent in 2000 and that the source of NO_3^- is linked to high concentrations at this tile. This would also explain the consistently high NO_3^- concentrations at BMR tile since the sources (manure) are similar to AMR (2000). Furthermore, access to manure sources of high NO_3^- concentration may be increased through increased pore connectivity at the AMR tile when catchment discharge is high.

Table 2-3: Land-use practices on fields drained by specific tile drains

Tile	Fertilizer Applied	Crop (2000)
Shantz	manure (2000, 2001)	corn
Forest	unknown	corn
Bend	manure	corn
Halfway	manure	corn
AMR	manure	corn
BMR	manure	soybeans
Fencerow	inorganic (2000,2001)	soybeans
Harris	inorganic	strawberries

Several NO_3^- isotope values from Forest tile fall within the range of NO_3^- derived from soil organic matter while others lie further in the range for septic system/manure, likely indicating source mixing. Despite not directly knowing the fertilizer used this is indicative that manure was at least historically used on this field. Consistent NO_3^- concentrations are measured during the summer over a range of outlet discharges (15-35L/s), which means the tiles would have been flowing and drainage significant. High plant uptake from the corn crop planted that year may have moderated NO_3^- concentrations. N fixing soybeans were planted above the Fencerow tile drainage system and lower NO_3^- concentrations measured could also have been a result of plant uptake. Fencerow tile had the same sampling dates and discharges as Forest tile.

Bend tile and Shantz tile drain different fields that are managed by the same farmer though a portion of a deciduous swamp is also drained by Shantz tile. Isotope values suggest NO_3^- is derived from a combination of soil organic matter and manure sources. The constant NO_3^- concentrations from Shantz tile are observed throughout the different seasons over a wide range of outlet discharge may reflect drainage conditions of this tile network. Differences between this tile and BMR tile for example may be due to the type of fertilizer additions as this field receives additions of cow manure (Mike English, pers. com.) and the land is managed by a different farmer who may use a different application rate.

2.5.2 Sources and processes of NO_3^- in streams

The seasonal hydrologic conditions in the catchment are a major factor affecting stream NO_3^- concentrations and isotopes. As explained in the Section 2.4.2.1, high stream NO_3^- concentrations were observed when a critical discharge was met (Figure 2-7). Tile concentrations also show a similar pattern where the highest concentrations coincide with a similar threshold discharge for each season. This shows the influence of tile chemistry on that of the stream during these periods. On the other hand, very low stream NO_3^- concentrations are observed at low discharge ($\leq$ 2.5L/s) during summer, fall, and winter. Macrae et al. (2007) found that when basin discharge was 0-40L/s tiles contributed minimally to basin discharge but when basin discharge was greater than 40L/s tiles could contribute from 0-90% of basin discharge. However, our results show that, in terms of chemical inputs, the critical threshold of tile inputs could be lower than 40 L/s. Furthermore, this suggests that high NO_3^- tile inputs are the dominant influence on stream chemistry when basin discharge is high, though this is variable between seasons, and that low NO_3^- inputs from groundwater dominate when basin discharge is low.

When basin discharge was low, stream samples with low NO_3^- concentrations often have considerably higher $\delta^{15}N\text{-}NO_3^-$ and $\delta^{18}O\text{-}NO_3^-$ values as discussed in the results (Figure 2-10 and Figure 2-11). For $\delta^{15}N$ this was observed in the spring, summer, and fall while for $\delta^{18}O$ it was observed in the spring, fall and winter. This observation has been

shown to be a product of groundwater riparian denitrification at Strawberry Creek and in other studies (Mengis et al., 1999, Aravena and Robertson, 1998; Cey et al., 1998). Mengis et al. (1999) indicate that groundwater from the riparian zone can have $\delta^{15}N$ values of 15.9‰ due to partial denitrification which is similar to high $\delta^{15}N$ values measured in this study. For example, in the summer and fall eight $\delta^{15}N$ values between 13.4‰ and 17.15‰ were measured and one value is found in this range in the spring. In addition, denitrification could occur in the streambed, which would also more likely occur during periods of low flow though this hasn't been fully explored in the Strawberry Creek (Cabrera, 1998).

The changes in stream $\delta^{15}N\text{-}NO_3^-$ with respect to Julian Day (Figure 2-9) indicate that stream NO_3^- is more strongly influenced by denitrification in the summer and fall. This would be expected at Strawberry creek since low flow conditions and warm temperatures would promote higher rates of denitrification in riparian and hyporheic zones (Harris, 2000; Mengis 1999; Cabrera, 2001). A 2nd order polynomial equation confirms this observation, though using Julian day to predict $\delta^{15}N$ is unreliable since the relationship between the variables is not strong ($R^2 = 0.40$, $p = 0.0001$) (Figure 2-9). However, the relationship is considerably strong given the range of hydrologic conditions in the summer and fall seasons and the potential inputs of non-denitrified sources with low $\delta^{15}N\text{-}NO_3^-$ values.

As with the tiles, NO_3^- isotopes in streams can be used for source identification if corrected for denitrification. This again assumes that higher $\delta^{18}O\text{-}NO_3^-$ values are not because of mixing with a high $\delta^{18}O\text{-}NO_3^-$ source, such as NO_3^- from atmospheric deposition. Also, a maximum value for $\delta^{18}O\text{-}NO_3^-$ must again be assigned. Although NO_3^- isotopes of the stream would be influenced by NO_3^- inputs from the nearest tile, they would also be influenced by all upstream inputs including other tiles and groundwater from various fields. For example, the Outflow would be strongly influenced by the Harris tile, where a source $\delta^{18}O\text{-}NO_3^-$ value of +1‰ was assumed, but could also be influenced by denitrified groundwater inputs from the field drained by AMR and Shantz tile, where a

source $\delta^{18}O\text{-}NO_3^-$ value of +6‰ was assumed. To be conservative, a maximum value of +6‰ should be assumed for non-denitrified stream sources.

Several data points near a $\delta^{18}O$ value of +6‰ and $\delta^{15}N$ value of +9‰ are likely the result of partially denitrified groundwater since they are very near groundwater values measured by Mengis et al. (1999) (Figure 2-8). The same is for the two data points near +7‰ ($\delta^{18}O$) and +15‰ ($\delta^{15}N$). When these points are corrected using a $\delta^{18}O$:$\delta^{15}N$ slope of 0.67 they fall in the range expected for manure sources. The other data points that are mostly between +8 and +11 for $\delta^{18}O$ and +9‰ for $\delta^{15}N$ fall in the upper range for soil organic matter when they are corrected.

According to the range of values calculated for strawberry creek and values reported in the literature most NO_3^- in the stream originates from soil organic matter and manure/septic system effluent, as was found for tile drain waters (Figure 2-13). Middle road stream isotope data are consistently distributed in the manure range of isotope values which is consistent with data from AMR and BMR tiles and do not indicate denitrification. The immediate influence of the tiles on this sampling location is apparent.

NO_3^- isotopes reveal that water collected from the stream above Harris tile is generally reflective of manure/septic system sources though evidence of denitrification is indicated by several points that lie in line with a 0.5 slope. Several samples collected from the Outflow generally fall in the range similar to those collected directly from the Harris tile which is indicative of the influence of the tile on the stream (Figure 2-12 and Figure 2-13). However, like at the stream above Harris tile, some NO_3^- isotope samples also show evidence of denitrification. Therefore, NO_3^- isotopes collected from both locations represent the sum of all tile, groundwater inputs, and in-stream processes upstream of these respective points.

Kellman and Hillaire-Marcel (2003) note that a variety of fields with different manure applications and multiple water travel pathways creates difficulties in using isotopes to identify NO_3^- sources and patterns of denitrification in stream locations. This is also true for our study though establishing expected $\delta^{18}O\text{-}NO_3^-$ permits correction for the isotopic

effects of denitrification. In addition, the groundwater study by Mengis et al. (1999) established an isotopic signal for partial denitrification that allows for interpretation of stream data. In-stream denitrification could have the same effect and future studies should investigate where the process is taking place.

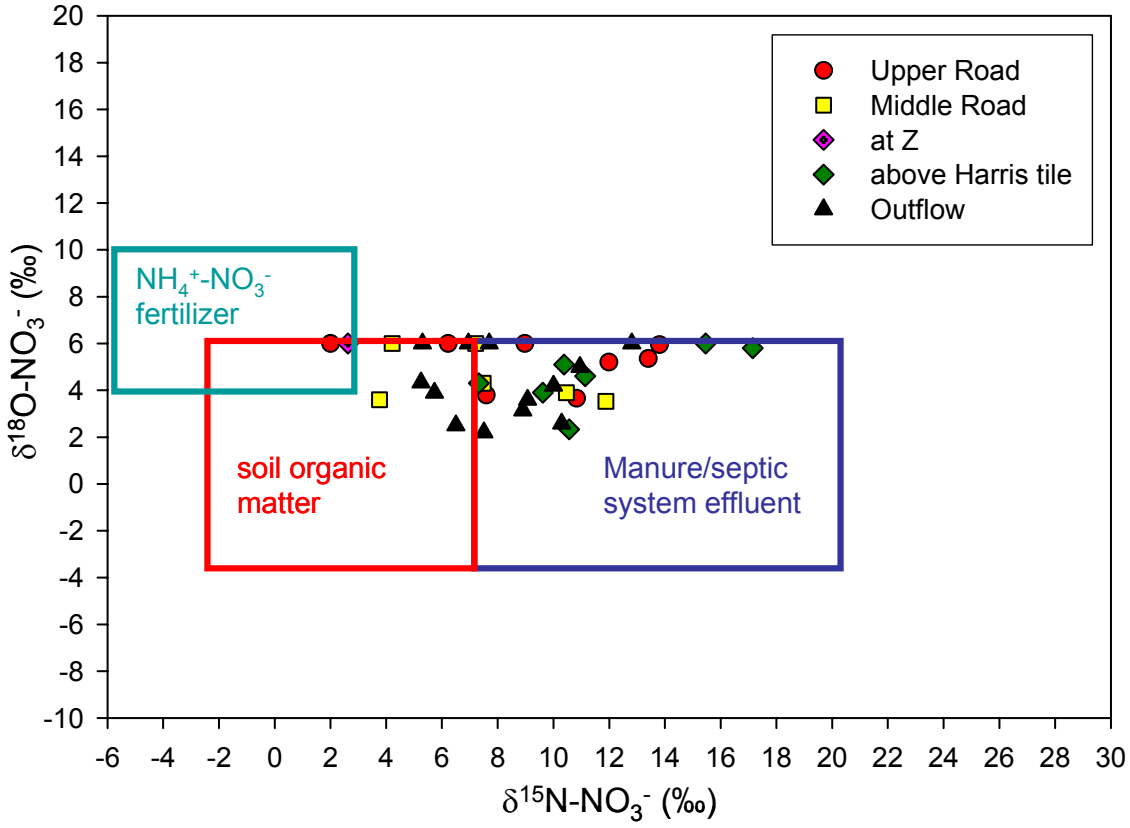

Figure 2-13: $\delta^{15}N$ and $\delta^{18}O$ of NO_3^- of streams corrected to the maximum expected $\delta^{18}O$ value of +6‰.

2.6 Conclusions

Average NO_3^- concentrations were highest at Bend, AMR (2000), BMR, and Harris tile. Variability in concentration between tiles is linked to hydrology, season, drainage, and land-use. High concentrations at Bend tile are associated with high discharge events whereas low concentrations at Shantz tile are associated with low discharge. Harris and BMR tiles show consistently high NO_3^- concentrations over a wide range of discharge and

through the seasons. Fertilizer application, consistent drainage and nutrient retention strategies of the Strawberry crop likely influence concentrations at the Harris tile. Although inorganic fertilizer is used on the field drained by the Harris tile a consistent signal from soil organic matter is measured. High NO_3^- concentrations at BMR and AMR tiles (2000) are linked to manure sources (chicken) whereas low NO_3^- concentrations from AMR tile (1999) are from soil organic matter sources. However, the annual difference in NO_3^- concentration at AMR tile is also linked to discharge and likely relate to how different NO_3^- sources are flushed from the soil. Low NO_3^- concentrations at the Forest and Fencerow tiles were measured in the summer when plant uptake would have been high meaning little NO_3^- would be flushed from the system despite adequate drainage conditions. The effects of partial denitrification were observed in some tile water samples and were corrected to expected source $\delta^{18}O$ values.

Variability in stream NO_3^- concentrations and isotopes is a product of variable inputs from tiles and diffuse groundwater. High NO_3^- concentrations from tiles are associated with high basin discharge (~40L/s) whereas low NO_3^- concentrations from groundwater inputs are associated with low basin discharge (≤2.5L/s). Low NO_3^- concentrations were associated with enriched $\delta^{15}N\text{-}NO_3^-$ (spring, summer and fall) and $^{18}O\text{-}NO_3^-$ values (summer, fall, and winter) which is indicative of groundwater denitrification. Enriched stream $^{15}N\text{-}NO_3^-$ isotopes are similar to those measured in groundwater by Mengis et al. (1999), which was a product of partial denitrification. Isotope values affected by denitrification were corrected to expected source $\delta^{18}O$ values. Stream NO_3^- isotopes generally reflected the catchment sources as identified at tile drain outlets.

Chapter 3: Stable Isotopes of NO_3^- and N_2O during two major melt events at the Strawberry Creek catchment, near Waterloo, ON

Overview

Dissolved NO_3^- and N_2O dynamics during the 2007 Springmelt and 2008 mid-winter thaw events were explored using NO_3^- and N_2O isotopes at the Strawberry Creek Catchment near Waterloo, Ontario, Canada. Tiles are a source of NO_3^- to the stream during both events and concentrations at the outflow are above the 10 mg N/L drinking water limit during the 2008 mid-winter thaw. Tiles are also a source of N_2O to the stream that, in turn, was a source of N_2O to the atmosphere during both events. NO_3^- isotopes from the 2007 Springmelt reveal that nitrification of soil organic matter and manure are the main source of NO_3^- in the catchment though evidence of NO_3^- from atmospheric deposition is also apparent. NO_3^- isotopes from all sites show evidence of denitrification from a common NO_3^- endmember during the 2008 mid-winter thaw. This denitrification occurred during the long drought that preceded the 2008 mid-winter thaw. $\delta^{15}N$ and $\delta^{18}O$ of N_2O reveal that N_2O is produced from denitrification during both events. Isotopic shifts ($\Delta_{N2O\text{-}NO3\text{-}}$) of -6 to -31 for ^{15}N and +14 to +35‰ for ^{18}O from the 2007 Springmelt are similar to enrichment factors for denitrification reported in the literature. Isotopic shifts ($\Delta_{N2O\text{-}NO3\text{-}}$) for ^{15}N (-13 to -38‰) and ^{18}O (+33 to +47‰) from the 2008 mid-winter thaw are also similar to those reported in the literature. $\delta^{18}O$:$\delta^{15}N$ slopes in N_2O data is due to the influence of several processes including substrate consumption and gas exchange. Following production, gas exchange influences the isotopic composition of N_2O in stream waters. Isotopic composition of N_2O endmembers at the outflow are representative of average source N_2O for the 2008 mid-winter thaw but not for the 2007 Springmelt event. The isotopic signature of N_2O flux to the atmosphere at the outflow is -12 to -18‰ for ^{15}N and +32 to +42‰ for ^{18}O.

3.1 Introduction

There is a markedly similar timing in the rise of industrial activity and increases in the atmospheric mixing ratio of N_2O (Kaiser, 2002; Prinn et al., 1990). Agricultural activities are among the major sources of anthropogenic N_2O in the global N_2O budget (Stein and Yung, 2003). A major cause of agricultural N_2O production is the extensive use of organic and inorganic nitrogen (N) fertilizers where increased N availability enhances transformations of N in the soil. Agriculturally produced N_2O has primarily been measured as direct flux from fields, though the importance of emissions from secondary N_2O sources such as agricultural drainage water, has been recognized and is receiving more attention (Mosier et al., 1998).

The occurrence of increased export of dissolved gaseous and soluble N species in groundwater, drainage tiles, and streams from small agricultural catchments following periods of major precipitation or snowmelt events has been demonstrated (Macrae et al., 2007; Thuss et al; 2008a, Reay et al., 2004; Harrison and Matson, 2003). In small first-order catchments these events are often short-lived (often 2 to 7 days) but can contribute a significant portion of the annual stream N_2O flux. For example, 37% of the annual N_2O flux was released from the Strawberry Creek during March 2006 largely because of the snowmelt event (Thuss et al., 2008a). Because of their importance in the annual N_2O flux budgets these events need to be better understood if the agricultural industry wishes to manage its GHG emissions.

The stable isotopes of N_2O are one of the most powerful tools used to delineate the sources and processes responsible for N_2O production. Incubation and field studies of nitrification have provided ^{15}N enrichment factors of -45 to -68‰ ($\varepsilon_{NH4\text{-}N2O}$) while those for denitrification are in the range of -13.5 to -35‰ ($\varepsilon_{NO3\text{-}N2O}$) (Yoshida, 1988; Ueda et al., 1999; Barford et al., 1999; Perez et al., 2006; Blackmer and Bremner; 1977). Direct measurement of ^{18}O fractionation during nitrification has evaded researchers, though the $\delta^{18}O\text{-}N_2O$ produced is near that of atmospheric oxygen (+23.5‰ VSMOW) (Perez et al., 2001; Whalen and Yoshinari, 1985). ^{18}O enrichment factors during denitrification are

generally constrained between -10 and +35‰ ($\varepsilon_{NO3\text{-}N2O}$). Additionally, oxygen exchange with water during both nitrification and denitrification are known to effect the ^{18}O composition of N_2O (Casciotti et al., 2002; Ye et al., 1991; Shearer and Kohl, 1988; Kool et al., 2007; Snider et al., 2008).

Despite the growing body of research, there have been virtually no isotope studies on secondary sources of agricultural N_2O. N_2O isotopes studies in aquatic systems have generally focused on oceanic N_2O contributions and biochemical processes (Dore et al., 1998; Naqvi et al., 1998; Ostrum et al., 2000). Bootanaan et al. (2000) provide some of the only river data, though this study was done in Thailand and is likely not representative of temperate environments. Some of the only measurements of dissolved N_2O in temperate agricultural watersheds are from groundwater studies. However, processes in agricultural groundwater are likely different than those in tile drains or open channels (Well et al., 2005; Wada and Ueda, 1996; Ueda et al., 1999).

There are four main objectives of this chapter: (1) To spatially and temporally characterize concentrations and isotopes of NO_3^- and N_2O streams, groundwaters and tiles during two melt events (Springmelt 2007, January thaw 2008) that were intensely sampled; (2) To determine if there are differences between these two major events and, if so, why those differences may have occurred; (3) and to determine the sources and processes responsible for the measured N_2O isotopes.

3.2 Study Site

As described in Section 1.2.

3.3 Methods

Various tile drains and stream locations at the Strawberry Creek Catchment were periodically sampled from March 9, 2007 to March 27, 2007 for the spring melt of that year. Groundwater was sampled from the Harris transect and Cabrera (A-A') transect on March 13, 2007. The sampling period of January 5, 2008 to January 19, 2008 characterized the January 2008 melt event. Groundwater was also collected on January 27

and 28, 2008. Samples were collected for N_2O and NO_3^- isotopes and concentrations of N_2O, and major anions (Cl^-, Br^-, NO_3^-, PO_4^{3-}, SO_4^{2-}). Waters for N_2O isotopes were collected in duplicate in 160mL glass serum bottles, without creating a headspace. Saturated $HgCl_2$ solution (0.3mL) was used for preservation.

Waters for major anion chemistry were collected in 125mL plastic screw-top bottles and were filtered with Whatman 0.45 μm syringe-tip filters within 24 hours of collection. For analysis of major anions, 0.5 mL sample aliquots were used on a Dionex ICS-90 ion chromatograph, equipped with an IonPac AS14A column and AS40 automated sampler. Samples were corrected to a calibration curve made from Dionex brand standards.

Duplicate 60mL serum bottles for N_2O concentration were stoppered with butyl blue stoppers (Belco Glass) and preserved with 0.15mL $HgCl_2$. N_2O was equilibrated in a 5mL headspace and injected manually onto a Varian CP-3800 gas chromatograph. Trace gases were separated by a Poroplat Q column and N_2O was analyzed by an ECD detector. The analytical error of this analysis is approximately +/- 5% at 8.5 nmol/L and the detection limit is approximately 6.5 nmol/L.

N_2O was extracted from water using a modified CO_2 extraction technique (EIL method) developed by the Environmental Geochemistry Group (Thuss et al., 2008b). In brief, the 160mL sample is bubbled for 10 minutes with a helium line that is attached to a 20mL capped serum vial sitting in liquid nitrogen to cryogenically trap the N_2O gas. The bottom and top of the vial is filled with glass beads and has silica glass wool in the middle to increase the surface area on which the gas may be trapped. After sample purging is complete the vial is pressurized with a known quantity (20mL) of Helium. Ideal injection size of the sample was calculated based on peak height of standard injection. Samples were analyzed for N_2O isotopes by injecting 10 to 15 nmol of N_2O on a Micromass Trace Gas Analyzer connected to a Micromass continuous flow mass spectrometer (TG-CFMS). Ideal injection size of the sample was calculated based on peak height of standard injection. Samples were corrected to EGL 5 N_2O standard ($\delta^{15}N$-N_2O = 2.03, $\delta^{18}O$-N_2O = 38.44) for instrumental drift, linearity, and isotopologue contamination. Results are

reported in delta (δ) notation in units of per mil (‰) relative to to N_2 (air) for $\delta^{15}N$ and VSMOW for $\delta^{18}O$. Analytical errors for $\delta^{15}N$ and $\delta^{18}O$ is ±0.13‰ and ±0.31‰. The instrument was calibrated to tropospheric N_2O.

The method used for NO_3^- isotope analysis was originally developed by McIlven and Altabet (2005) but is presented here with modifications by Spoelstra (unpublished, 2007). After collection, 30mL of water is filtered (0.45μm) into plastic screw-top bottles and frozen for storage. When ready to analyze for nitrate isotope ratios, a volume of water containing 0.6μg N is freeze dried. The sample is redissolved with 0.75M NaCl and 1mL of 0.08M Imidazole is added to aid the cadmium reduction reaction. The sample is then placed in a column with copperized cadmium and slowly shaken for 2 hours to reduce NO_3^- to NO_2^-. The sample is then syringe filtered into a stoppered 20mL serum vial. N_2O is subsequently produced by addition of a 2mL sodium azide and acetic acid buffer solution for 10 minutes. 1mL of 6M NaOH is added to stop the reaction. The vial is pressurized with 10mL of Helium and placed on a shaker to equilibrate for 10 minutes. The sample is then run on the TG-IRMS as above for dissolved N_2O. Analytical error calculated for this method was ±1.1 for $\delta^{15}N$-NO_3^- and ±3.0 for $\delta^{18}O$-N_2O.

3.4 Results

3.4.1 2007 Springmelt

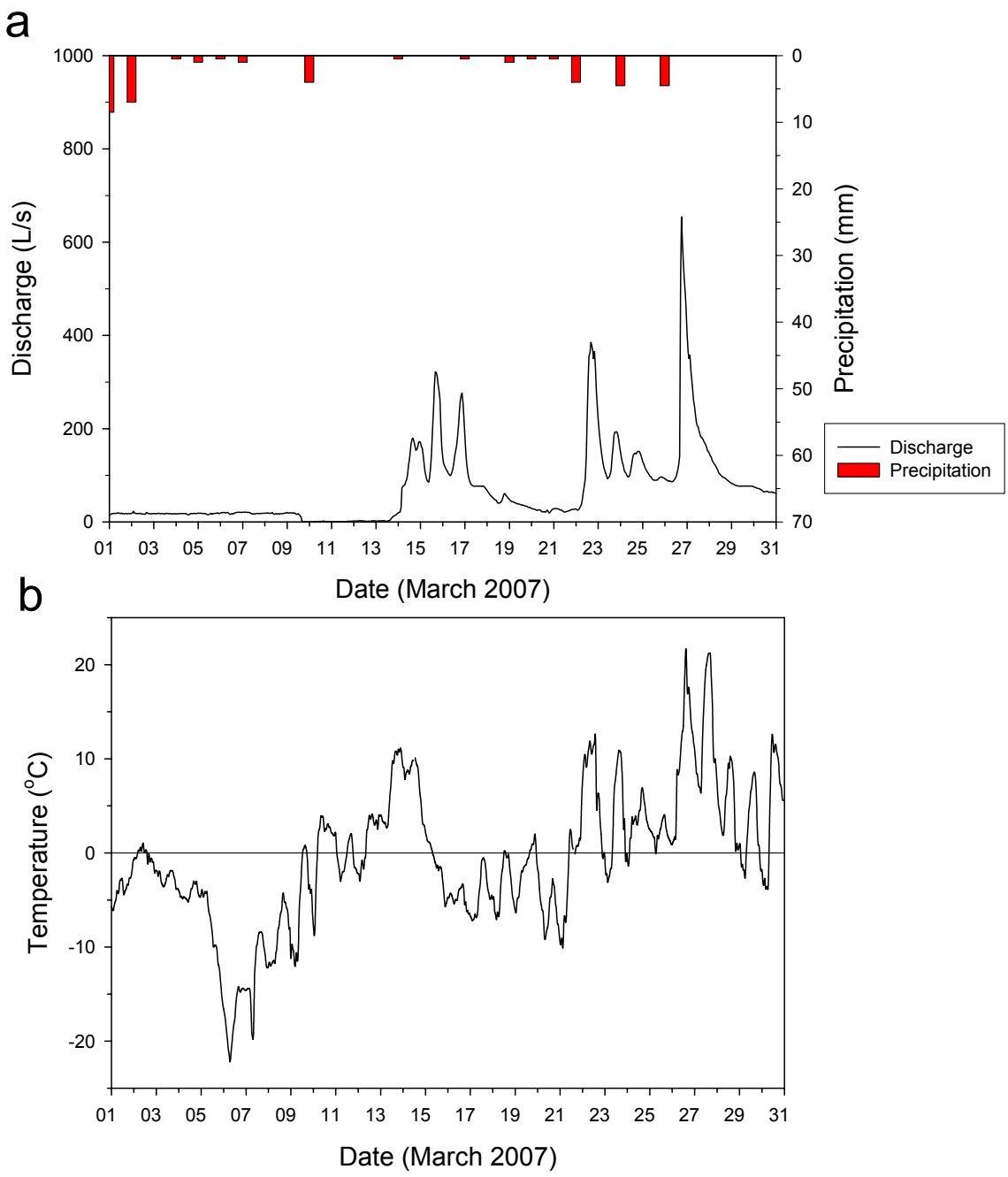

Figure 3-1: (a) Outlet discharge, precipitation, and (b) temperature for the 2007 Springmelt The effect of diurnal temperature variation on melting can be seen in discharge.

3.4.1.1 Event Hydrology

The 2007 Springmelt event was largely driven by the thaw of a significant snowpack that accumulated previous to the event. During the beginning of March, 22cm of snow fell in Breslau, ON (Waterloo-Wellington 2) which translate into the 40mm of precipitation seen in Figure 3-2. From March 10 to 13 daily temperatures rise to 4°C and then over 10°C on March 14 and 15 which initializes the first portion of the event (Figure 3-1). Snow accumulation at Breslau, ON drops from 28 to 0cm between March 9 and 14, 2007. High daily temperatures (up to 20°C) on March 22 to 25 and March 27 in combination with modest precipitation and run-off of standing water from the first portion of the event, drives the second portion of the event.

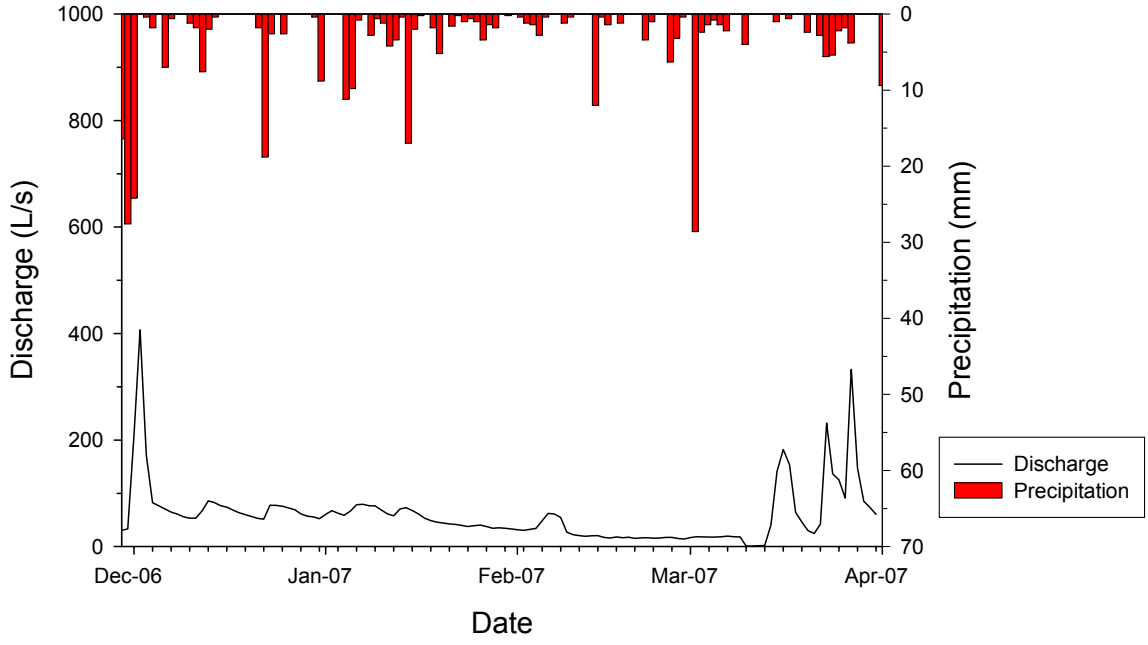

Figure 3-2: Discharge and precipitation data from December 2006 to the end of March 2007 shows that moderate precipitation fell on the catchment. Except for a major event in December 2006 baseline conditions and smaller events characterize catchment hydrology previous to the 2007 Springmelt event.

3.4.1.2 NO_3^- and N_2O concentrations

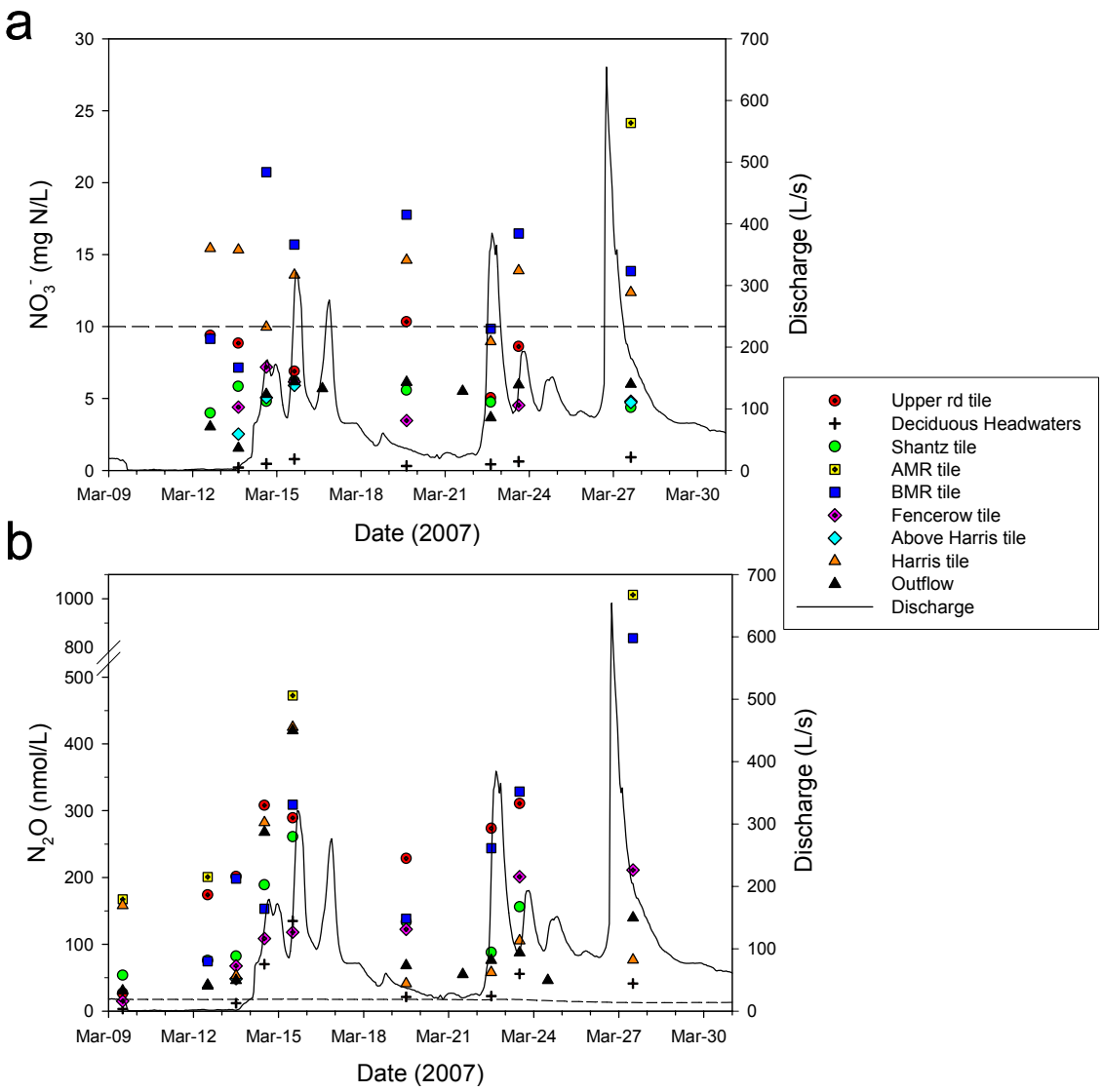

Figure 3-3: (a) NO_3^- concentrations with the 10 mg N/L drinking water limit (dashed line) and (b) N_2O concentrations with the stream concentration at 100% saturation (dashed line) through the 2007 Springmelt event. Analytical errors for NO_3^- and N_2O concentration are +/- 0.03 mg N/L and +/- 0.43 nmol/L (at 8.5 nmol/L), respectively.

NO_3^- and N_2O concentrations for the 2007 Springmelt event are shown along with basin discharge in Figure 3-3. NO_3^- measured at BMR and Harris tiles are consistently above the drinking water limit while other tiles remain below throughout the event. NO_3^-

concentrations at BMR and Harris tile show the same trend after March 15 despite having different concentrations from March 12 until this date. Stream NO_3^- concentrations at the Deciduous Headwaters are consistently lower (≤1mg N/L) than at the Outflow and above Harris tile (~5 mg N/L) throughout the event. The NO_3^- concentrations at Shantz tile are also similar to those of stream samples (Outflow and above Harris tile) throughout the event. Groundwater inputs from the Harris 3 and Cabrera A-A' transects were less than 2.25 mg N/L during this event. Despite small variability, NO_3^- concentrations at individual tiles and stream locations are relatively consistent through the event though different from each other.

Comparison of average pre-event NO_3^- concentration to the average NO_3^- concentration during the event reveals that between the two time periods pre-event NO_3^- concentration is greater for tiles (Upper road, Shantz, BMR, and Harris)(Table 3-1). However, for stream samples (above Harris tile and Outflow) the average event NO_3^- concentration is slightly greater (Table 3-1). Concentrations measured in 2007 before the event were used for the pre-event average and were found to be fairly consistent at individual sites. The deciduous headwaters and Fencerow tile were not measured in the pre-event period, so are not included in this comparison. AMR tile was sampled during this period but only once during the 2007 Springmelt which would not provide a representative event average. These results suggest that although tile NO_3^- contributions were less during the event period, overall NO_3^- concentrations to the stream were not masked by dilution. This likely means that NO_3^- concentrations in the stream were maintained by groundwater inputs during this period.

N_2O concentrations for all tiles and stream locations are above atmospheric saturation of the stream throughout the event. All sampling locations show increasing N_2O concentrations from March 9 to March 15. N_2O concentrations are again lower on March 19 before increasing to March 27 except for in the stream above Harris tile and at Harris tile. Regression analysis between tile discharge and tile N_2O concentrations are insignificant. Generally, N_2O concentration increases with NO_3^- concentration for the 2007 Springmelt (Figure 3-4) but the relationships are not strong.

Table 3-1: Comparison of pre-event NO_3^- concentration with average NO_3^- from the 2007 Springmelt

Site	Average Pre-event NO_3^- (mg N/L)	Average Event NO_3^- (mg N/L)
Upper road tile	10.3	8.2
Shantz tile	5.9	5.1
BMR tile	15.9	13.8
Harris tile	17.8	13.0
above Harris tile	4.1	4.7
Outflow	4.1	4.8

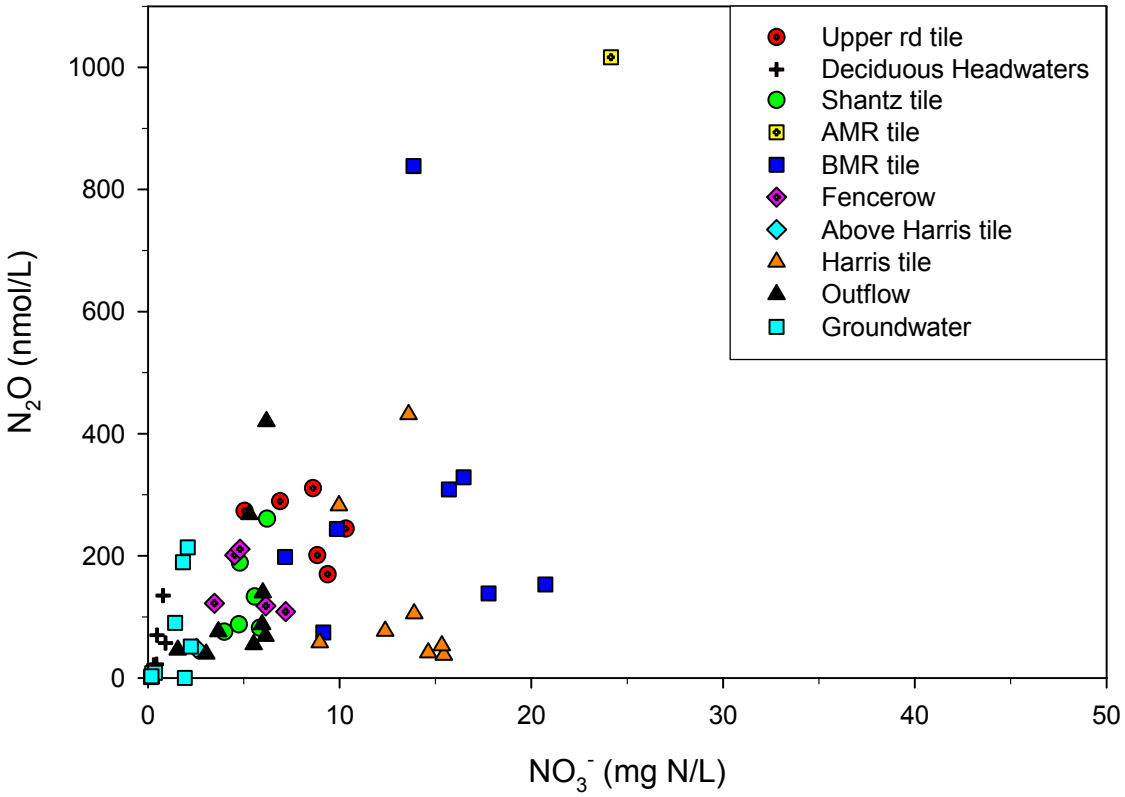

Figure 3-4: The relationship between NO_3^- concentration and N_2O concentration for the 2007 Springmelt.

3.4.1.3 $\delta^{15}N$ and $\delta^{18}O$ of NO_3^-

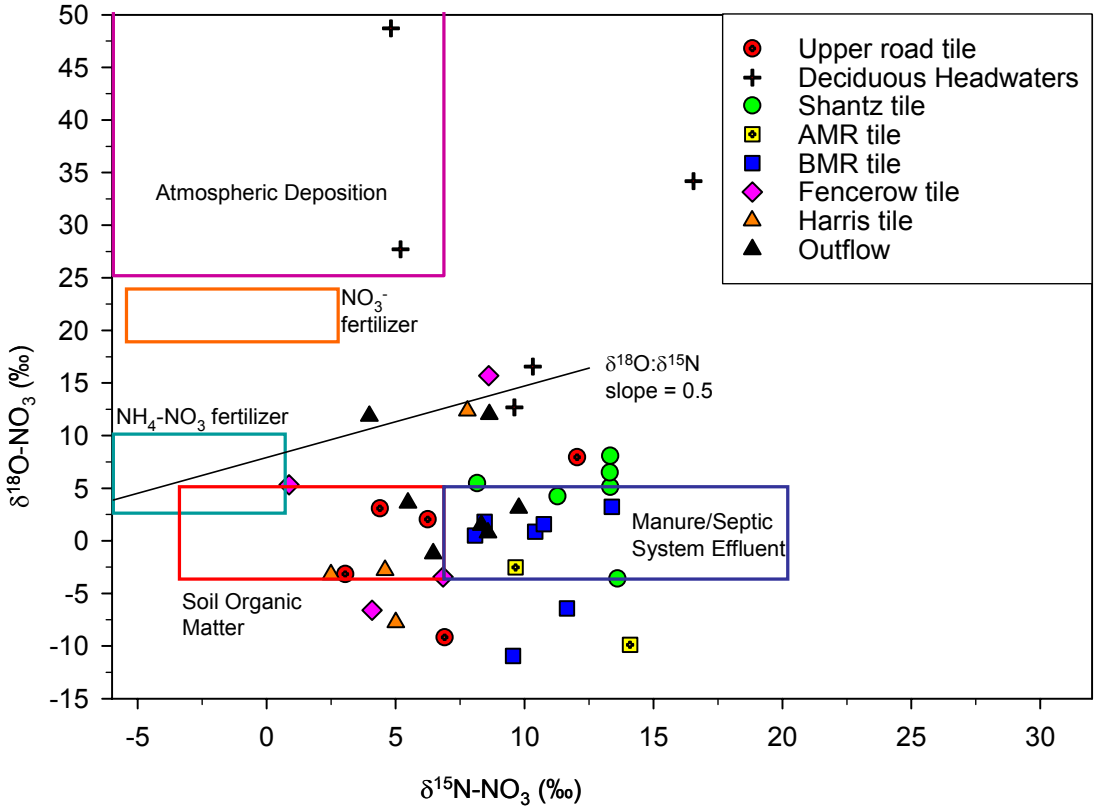

Figure 3-5: $\delta^{15}N$ and $\delta^{18}O$ of NO_3^- from the 2007 Springmelt

$\delta^{15}N$–NO_3^- values range from +0.9 to +16.6‰ for all measurements (Table 3-1). Shantz, AMR, and BMR tiles have similar $\delta^{15}N$-NO_3^- ranges where all measurements are between +8.1‰ and +14.1‰. Minimum $\delta^{15}N$-NO_3^- values for Upper road tile, Harris tile, and outflow are all between +2.5‰ and +4.0‰ while maximum values are +12.0, +7.8‰, and +9.8‰, respectively. There are two groups with similar average $\delta^{15}N$-NO_3^- values: +5.0 to +7.3‰ for Upper road tile, Fencerow tile, Harris tile, and Outflow; and +10.3 to 12.2‰ for Deciduous Headwaters, Shantz tile, AMR tile, and BMR tiles.

$\delta^{18}O\text{-}NO_3^-$ values from the 2007 Springmelt range between -10.95‰ (BMR tile) and +48.71‰ (Deciduous Headwaters) (Table 3-2). Minimum $\delta^{18}O\text{-}NO_3^-$ values for Upper road, AMR, BMR, Fencerow, and Harris tiles are between +6.6 and +10.9‰. Upper road (+7.9‰) and Shantz tile (+8.1‰) have similar maximum $\delta^{18}O\text{-}NO_3^-$ values as does the Fencerow tile (+15.7‰), Harris tile (+12.4‰), and Outflow (+12.0‰). These are near the minimum $\delta^{18}O$ measured for the Deciduous Headwaters (+12.7‰).

The combination of high $\delta^{18}O\text{-}NO_3^-$ values and low NO_3^- concentrations at the Deciduous Headwaters is suggests that NO_3^- is from atmospheric deposition. Several samples with high $\delta^{18}O\text{-}NO_3^-$ values also have higher $\delta^{15}N$ values, likely due to a mixture of sources. The $\delta^{18}O$:$\delta^{15}N$ trend at the Upper Road tile is suggestive of denitrification which is supported by strong relationships between the natural log of NO_3^- concentration and $\delta^{15}N\text{-}NO_3^-$ ($R^2 = 0.96$, $p = 0.02$) and $\delta^{18}O\text{-}NO_3^-$ ($R^2 = 0.46$, $p = 0.31$)(Figure 3-6). Fencerow tile also has a strong relationship between the natural log of NO_3^- concentration and $\delta^{15}N\text{-}NO_3^-$ ($R^2 = 0.77$, $p = 0.17$) which would play a role in the $\delta^{15}N$ trend seen for this data.

$\delta^{15}N\text{-}NO_3^-$ is indicative that most NO_3^- is derived from soil organic matter and manure/septic system sources. To a certain extent $\delta^{18}O\text{-}NO_3^-$ data supports this but also has values that are both higher and lower than the expected ranges reported in the literature for these sources.

Table 3-2: Average, Standard Deviation, and Range of $\delta^{15}N\text{-}NO_3^-$ and $\delta^{18}O\text{-}NO_3^-$ during the 2007 Springmelt.

Site	Number of samples	$\delta^{15}N\text{-}NO_3^-$				$\delta^{18}O\text{-}NO_3^-$			
		Average	Standard Deviation	range		Average	Standard Deviation	range	
				Min.	Max.			Min.	Max.
Upper road tile	5	6.5	3.4	3.0	12.0	0.2	6.5	-9.2	7.9
Deciduous Headwaters	5	10.4	4.7	5.2	16.6	22.8	9.9	12.7	34.2
Shantz tile	6	12.2	2.1	8.2	13.6	4.3	4.1	-3.6	8.1
AMR tile	2	11.9	3.1	9.6	14.1	-6.2	5.2	-9.9	-2.5
BMR tile	7	10.3	1.8	8.1	13.4	-1.3	5.3	-10.9	3.2
Fencerow tile	4	5.1	3.4	0.9	8.6	2.8	10.0	-6.6	15.7
Harris tile	4	5.0	2.2	2.5	7.8	-0.4	8.8	-7.7	12.4
Outflow	7	7.3	2.1	4.0	9.8	4.5	5.3	-1.2	12.0

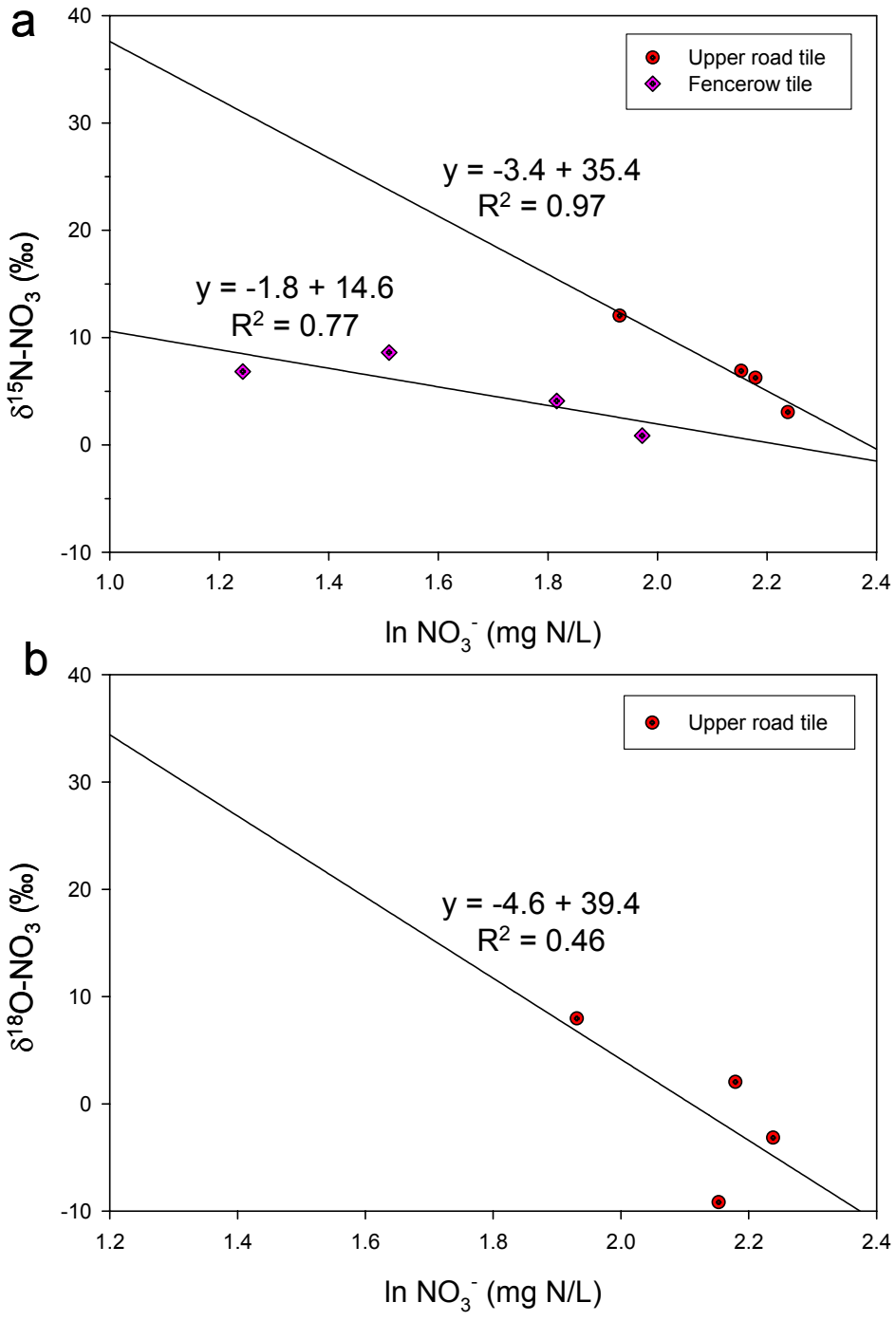

Figure 3-6: The relationship between the natural log of NO_3^- concentration and (a) $\delta^{15}N\text{-}NO_3^-$ and (b) $\delta^{18}O\text{-}NO_3^-$.

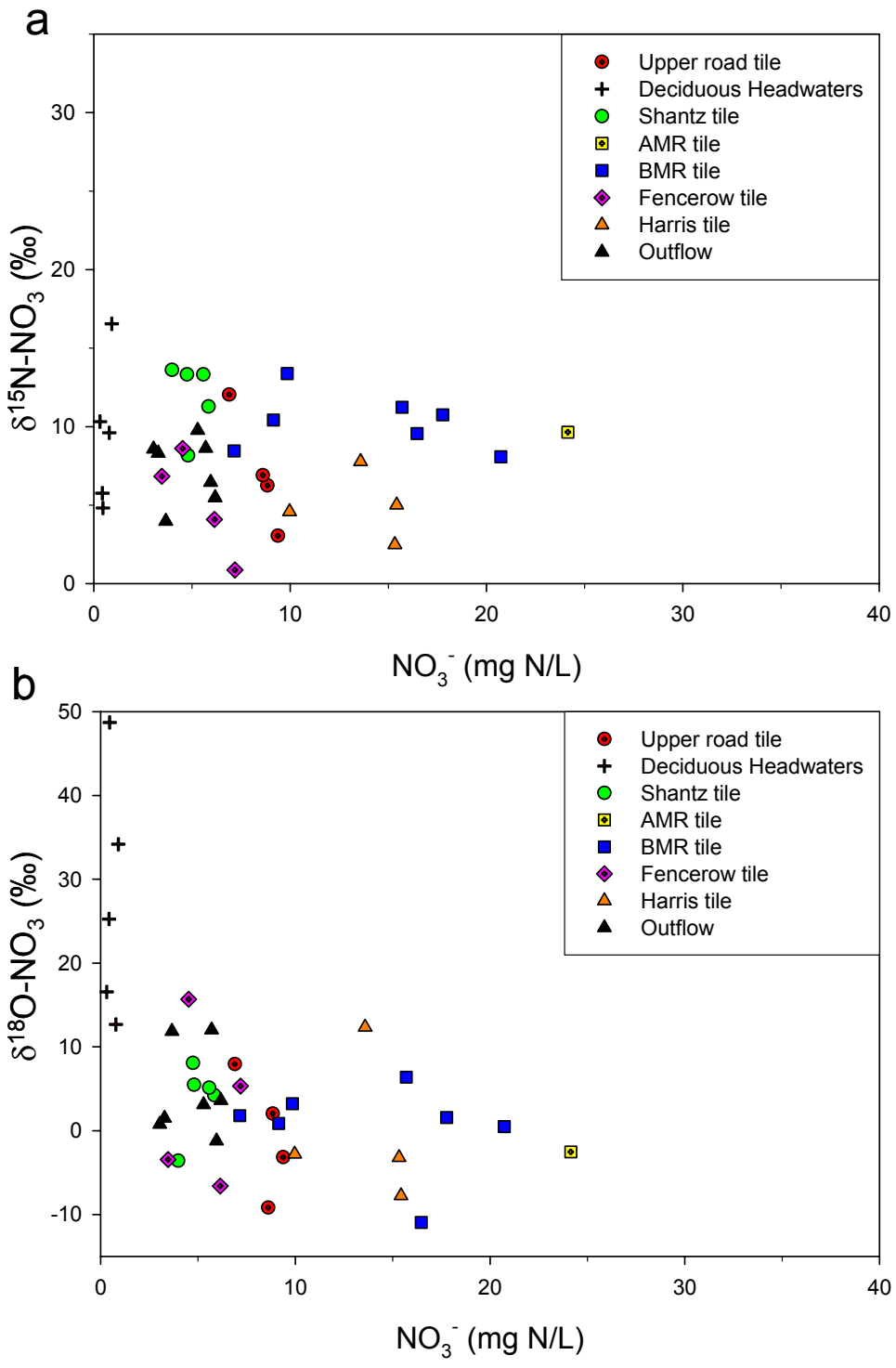

Figure 3-7: The relationship between NO_3^- concentration and (a) $\delta^{15}N\text{-}NO_3^-$ and (b) $\delta^{18}O\text{-}NO_3^-$ for the 2007 Springmelt

3.4.1.4 N_2O isotopes

$\delta^{15}N$-N_2O ranges from -21.9‰ to +2.0‰ during the 2007 Springmelt (Table 3-3). Minimum $\delta^{15}N$ values are similar at the Upper Road, Shantz, AMR, BMR, and Fencerow tiles, ranging between -21.9 and -18.5‰, while maximum $\delta^{15}N$ values are similar for Upper Road (-10.5‰), Shantz (-7.7‰), and Fencerow (-10.3‰) tiles. Maximum $\delta^{15}N$-N_2O is also similar for Harris tile (-9.8‰) but the minimum value (-14.4‰) produces a smaller range.

Minimum $\delta^{15}N$-N_2O for the Deciduous Headwaters and Outflow are -8.0‰ and -12.0‰, respectively, while maximums are +2.0‰ and -2.3‰, respectively. Average $\delta^{15}N$-N_2O for streams (-6.34‰) is larger than that of tiles (-15.2‰).

$\delta^{18}O$-N_2O ranges from +24.6‰ (AMR tile) to +52.8‰ (Deciduous Headwaters) during this event. Minimum $\delta^{18}O$ values are similar at Shantz tile, BMR tile, Fencerow tile, and Outflow with values between -31.4‰ and +32.9‰ whereas minimum values at Upper road (+27.9‰) and AMR (+24.6‰) tiles are lower. Maximum $\delta^{18}O$ values are similar (+39.0 to +42.3‰) between Shantz, BMR, Fencerow and Harris tiles. Average $\delta^{18}O$-N_2O values are greater for streams (+35.1‰) than they are for tiles (+41.7‰).

In addition to the general placement of N_2O isotopes, certain $\delta^{18}O$:$\delta^{15}N$ slopes are present in this dataset, though these are only significant for several sites. Fencerow has a moderate $\delta^{18}O$:$\delta^{15}N$ slope of 0.7 ($R^2 = 0.62$, $p = 0.21$) while Outflow has a $\delta^{18}O$:$\delta^{15}N$ slope of 1.4 ($R^2 = 0.82$, $p = 0.002$).

For the majority of tiles there are insignificant relationships between the natural log (ln) of N_2O concentration and N_2O isotopes. Decreasing $\ln N_2O$ concentrations and increasing N_2O isotope values can be indicative of a fractionating process (ie: substrate consumption, gas exchange, or N_2O consumption) that could, in turn, be the cause for the $\delta^{18}O$:$\delta^{15}N$ slopes observed. Only Upper road tile ($R^2 = 0.89$, $p = 0.005$) and outflow ($R^2 = 0.67$, $p = 0.02$) have significant relationships between $\ln N_2O$ concentration and $\delta^{15}N$-N_2O. For the

relationship between lnN_2O concentration and $\delta^{18}O\text{-}N_2O$, Fencerow tile ($R^2 = 0.79$, $p = 0.29$), and Outflow ($R^2 = 0.52$, $p = 0.07$) have significant negative relationships.

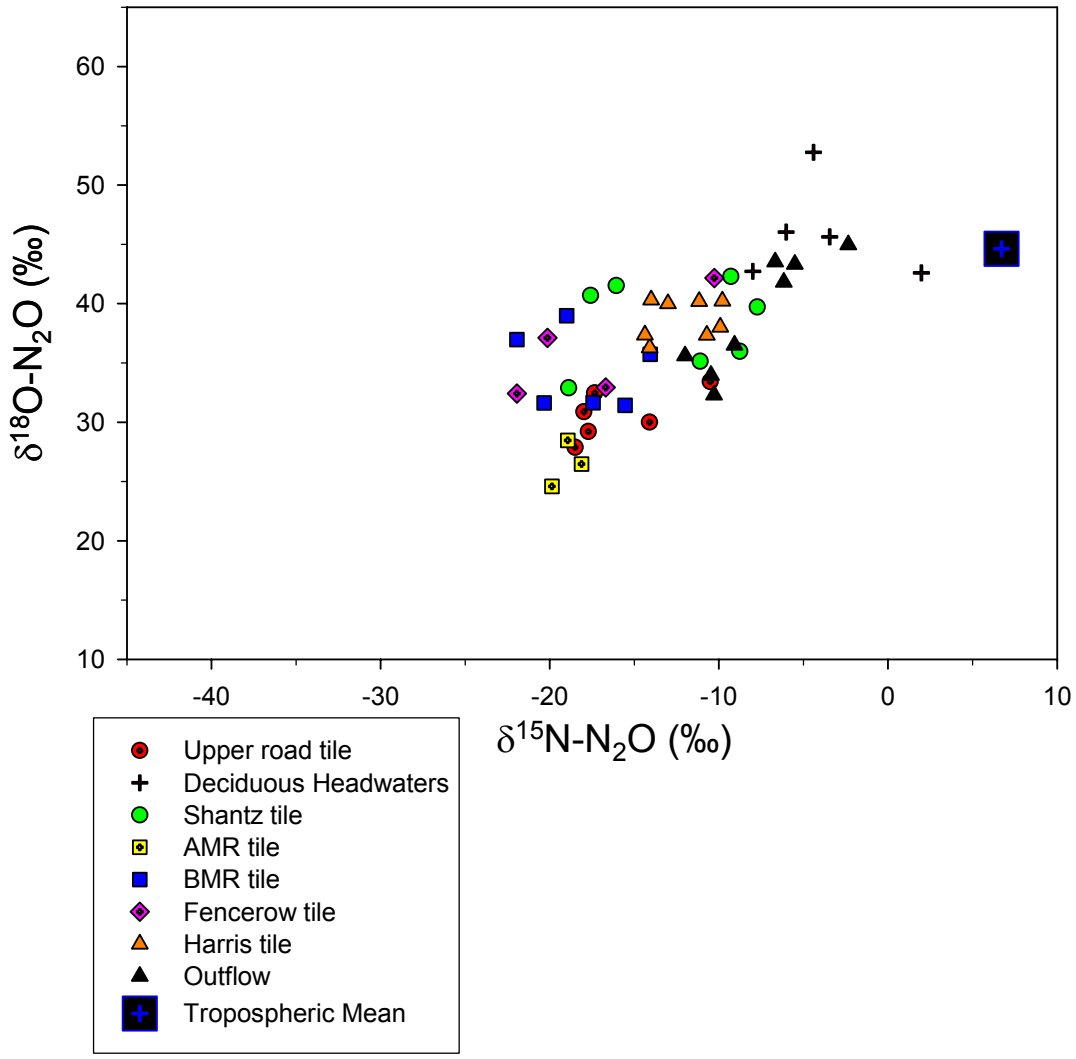

Figure 3-8: $\delta^{15}N$ and $\delta^{18}O$ of N_2O from the 2007 Springmelt

Table 3-3: Average, standard deviation, and range of $\delta^{15}N\text{-}N_2O$ and $\delta^{18}O\text{-}N_2O$ from individual sites for the 2007 Springmelt

Site	number of samples	Average		Standard Deviation		Range			
		$\delta^{15}N\text{-}N_2O$	$\delta^{18}O\text{-}N_2O$	$\delta^{15}N\text{-}N_2O$	$\delta^{18}O\text{-}N_2O$	$\delta^{15}N\text{-}N_2O$		$\delta^{18}O\text{-}N_2O$	
						Min.	Max.	Min.	Max.
Upper Road tile	6	-16.0	30.6	3.1	2.1	-18.5	-10.5	27.9	33.4
Deciduous Headwater	5	-4.0	46.0	3.7	4.1	-8.0	2.0	42.6	52.8
Shantz tile	7	-12.8	38.3	4.6	3.6	-18.9	-7.7	32.9	42.3
AMR tile	3	-19.0	26.5	0.9	1.9	-19.9	-18.1	24.6	28.5
BMR tile	6	-18.1	34.4	3.0	3.3	-21.9	-14.1	31.4	39.0
Fencerow tile	4	-17.3	36.2	5.1	4.5	-21.9	-10.3	32.4	42.2
Above Harris tile	1	-5.4	42.4						
Harris tile	8	-12.1	38.7	1.9	1.6	-14.4	-9.8	36.3	40.3
Outflow	8	-7.8	39.0	3.2	4.9	-12.0	-2.3	32.3	45.0
Tiles	34	-15.2	35.1	4.1	4.8	-21.9	-7.7	24.6	42.3
Streams	13	-6.3	41.7	3.8	5.7	-12.0	2.0	32.3	52.8

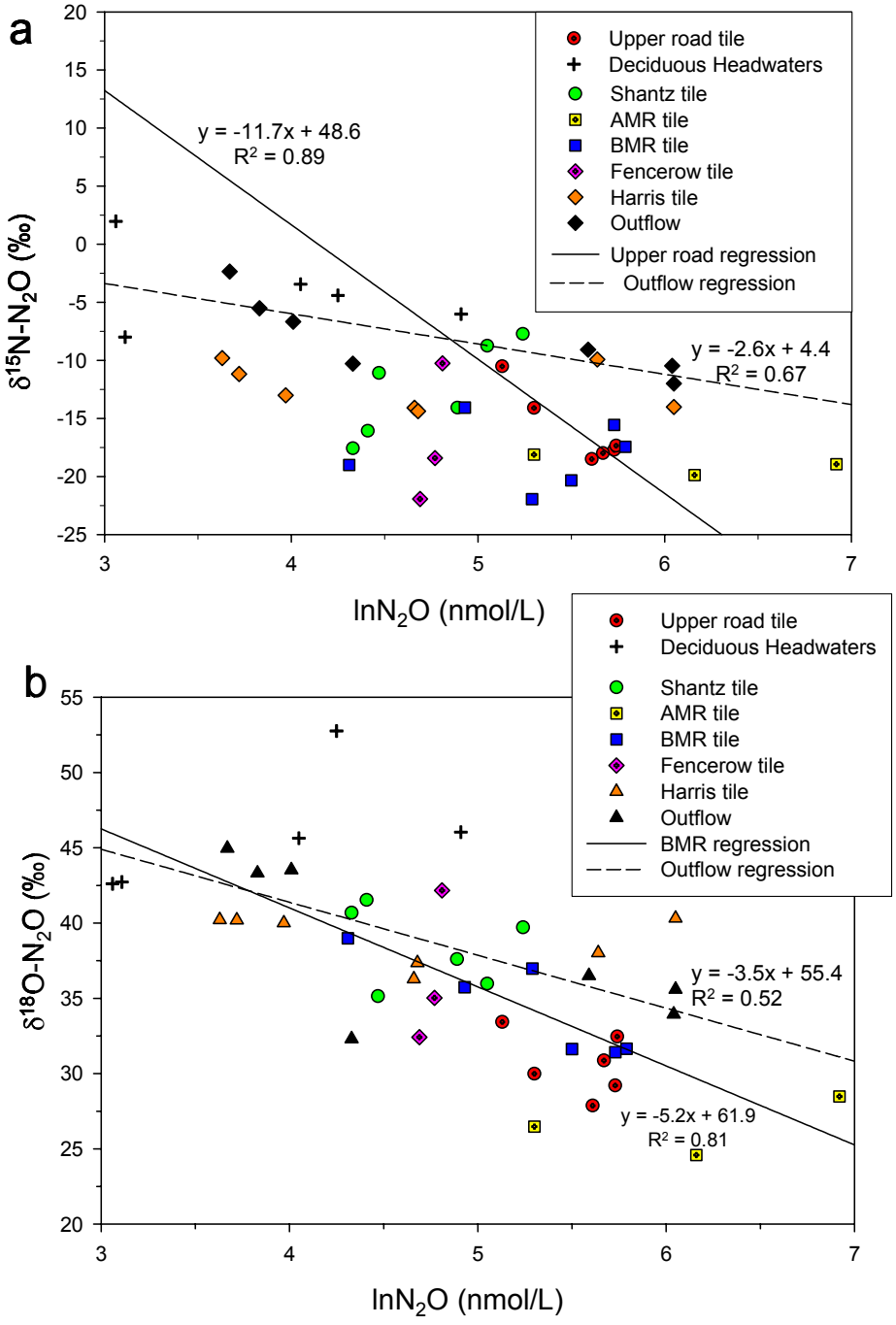

Figure 3-9: The relationship between the natural log (ln) of N_2O concentration and (a) $\delta^{15}N$-N_2O and (b) $\delta^{18}O$-N_2O from the 2007 Springmelt

3.4.2 2008 Mid-winter thaw

3.4.2.1 Event Hydrology

The 2008 mid-winter thaw is also driven by the melt of a significant snowpack in addition to significant precipitation on January 8 and 9. A significant amount of precipitation occurred between mid-November 2006 and the thaw event without change in base flow conditions which suggests that it occurred as snow (Figure 3-10a). Temperatures rise progressively from 0^{o}C on January 5 to almost 15^{o}C on January 9 which promoted thawing along with the precipitation (Figure 3-10b). From mid-June to mid-November 2007 there is minimal precipitation in the catchment and, consequently, no basin discharge (Figure 3-11). Discharge during the 2008 mid-winter thaw is much less than during the 2007 Springmelt.

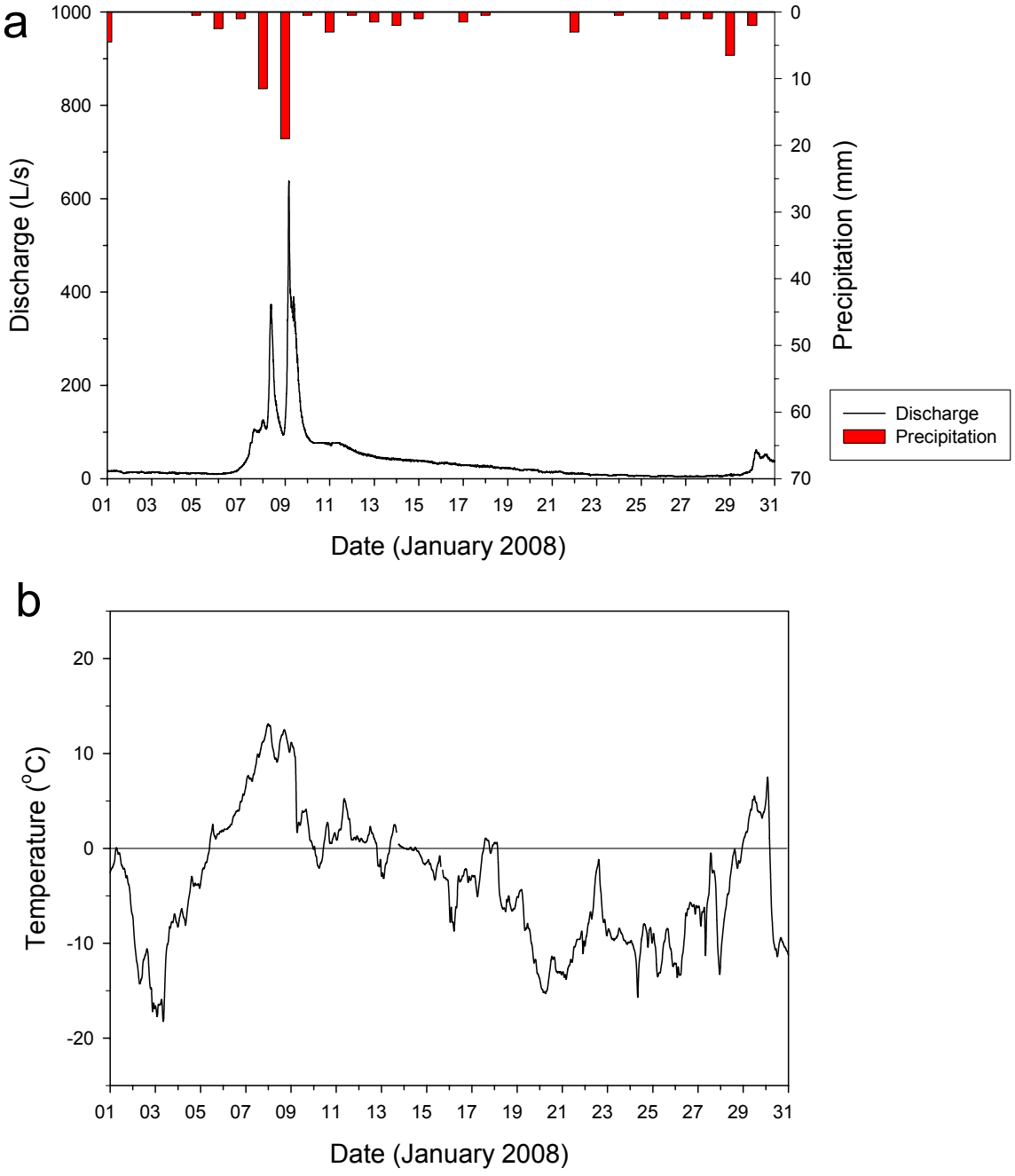

Figure 3-10: (a) Outlet discharge, precipitation, and (b) temperature for the January 2008 melt.

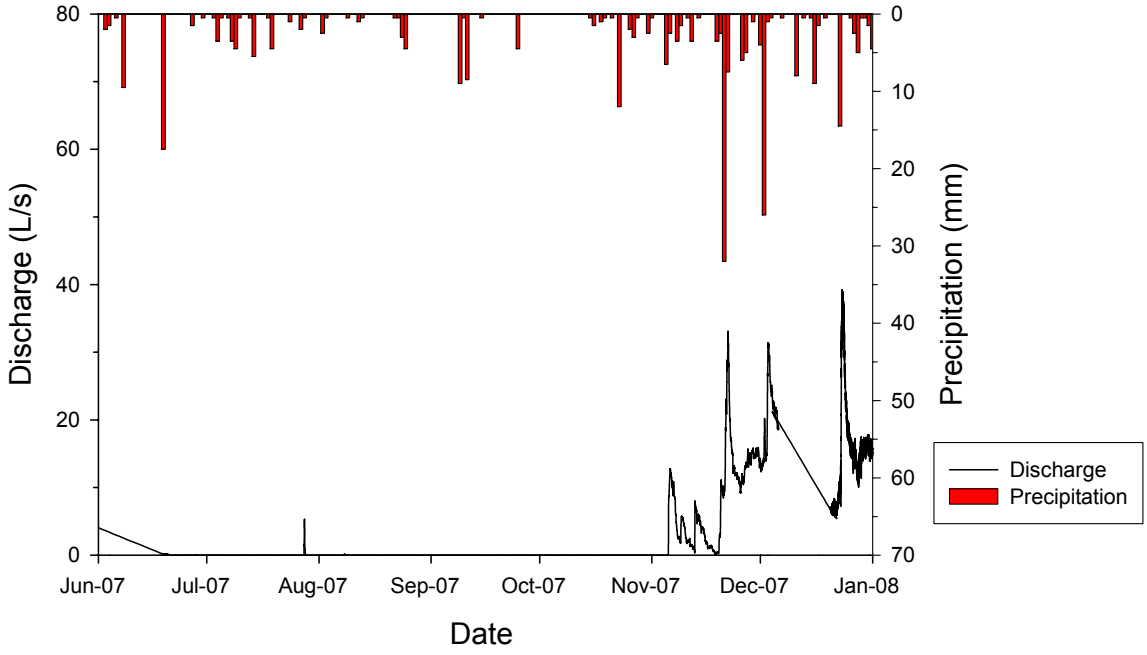

Figure 3-11: Discharge and precipitation from June 07 to the end of January 2008 indicates very dry conditions in the catchment for the seven months that precede the January 2008 melt event. A significant amount of precipitation fell on the catchment during December 2007 as snow leading to significant accumulation for the melt event.

3.4.2.2 NO_3^- and N_2O concentrations

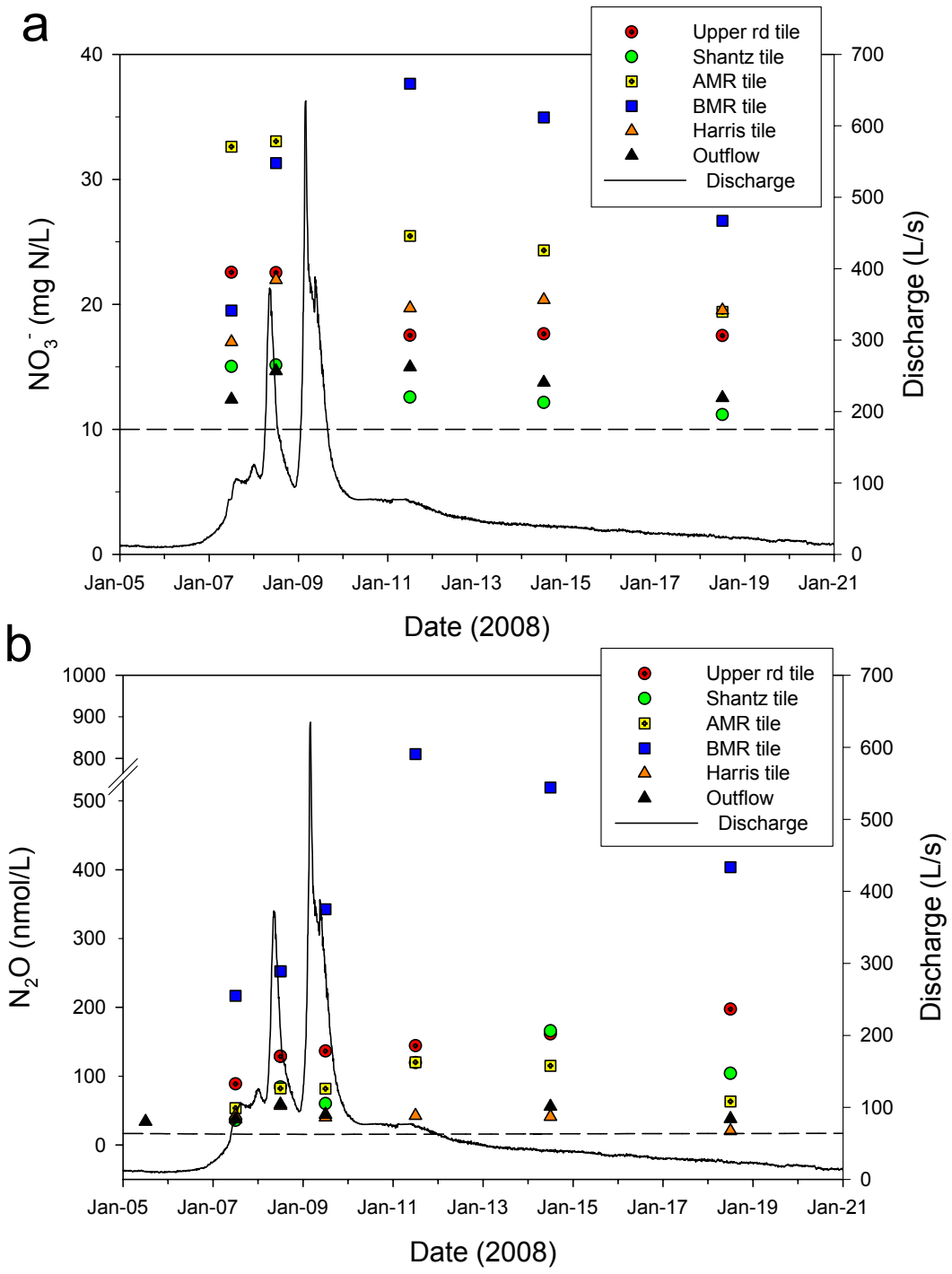

Figure 3-12: (a) NO_3^- and (b) N_2O concentration through the January 2008 mid-winter thaw shown with basin discharge

NO_3^- and N_2O concentrations for the 2008 January melt event are shown along with basin discharge (Figure 3-12). NO_3^- concentrations remain above the 10mg N/L drinking water limit and do not change dramatically through the event except for AMR and BMR tiles. NO_3^- concentrations from the other tiles generally decrease by less than 10 mg N/L over the duration of the event.

Comparison of pre-event NO_3^- concentrations to event NO_3^- concentrations shows that Shantz and Harris tiles had higher concentrations in the pre-event period whereas AMR tile and Outflow had higher concentrations during the event period. The pre-event period was an average of Fall 2007 data (Chapter 4). Shantz and AMR tiles may have flushed NO_3^- from the soil during the pre-event period so that when the event occurred there was less available. The reverse effect occurred at the AMR tile where low pre-event NO_3^- concentrations allowed for build-up in the soil that was "flushed" during the event at AMR. Groundwater NO_3^- concentration was 8.0 mg N/L on average for the event. Outflow concentrations suggest that the overall affect of tile and groundwater inputs is that they were higher in the event period, despite dilution effects.

For most locations, except for Harris tile and the outflow, which remain relatively constant, N_2O concentrations increase with the two peaks of stream discharge and are highest on the recession limb of the hydrograph. N_2O concentrations decrease after January 14th but remain above atmospheric saturation of the stream which is about 12 nmol/L.

Table 3-4: Comparison of pre-event average NO_3^- concentration (Fall 2007) with the average NO_3^- concentration for the 2008 mid-winter thaw.

Site	Pre-event (Fall 2007) average NO_3^- (mg N/L)	Average event NO_3^- (mg N/L)
Shantz tile	16.1	12.5
AMR tile	0.8	25.8
Harris tile	21.2	19.5
Outflow	4.0	13.1

3.4.2.3 $\delta^{15}N\text{-}NO_3^-$ and $\delta^{18}O\text{-}NO_3^-$

The relationship between NO_3^- concentration and $\delta^{15}N\text{-}NO_3^-$ produces several distinctive patterns for Strawberry Creek sampling locations (Figure 3-13). AMR and BMR tiles have consistent $\delta^{15}N$ values over a wide range of NO_3^- concentrations (20-40 mg N/L). At AMR tile the relationship between the natural log (ln) of NO_3^- concentration and $\delta^{15}N\text{-}NO_3^-$ is strong ($R^2 = 0.99$, $p = 0.0001$) which could be because of denitrification. However, this relationship assumes a constant starting NO_3^- concentration which would not be expected. Groundwater shows low NO_3^- concentrations (0-10 mg N/L) that range from +15 to +32‰ for $\delta^{15}N\text{-}NO_3^-$. The relationship between $lnNO_3^-$ concentration and $\delta^{15}N\text{-}NO_3^-$ for groundwater is moderate in strength ($R^2 = 0.53$) though it is insignificant ($p = 0.44$) which is not supportive evidence for denitrification. The other tiles and outflow are grouped between 10 and 25 mg N/L for NO_3^- and +3 to +12.5‰ for $\delta^{15}N\text{-}NO_3^-$. Shantz tile is within this group and shows a weak ($R^2 = 0.24$) but negative relationship between $lnNO_3^-$ concentration and $\delta^{15}N\text{-}NO_3^-$. Individual sites show little variation in $\delta^{15}N\text{-}NO_3^-$ (2 to 3.5‰) except for Shantz tile and groundwater. The average $\delta^{15}N$ values for these sites shows small but progressive increases through Harris tile, Upper road tile, Shantz tile, Outflow, AMR tile, BMR tile, and then a larger increase to the groundwater average (Table 3-5).

The relationship between $lnNO_3^-$ concentration and $\delta^{18}O\text{-}NO_3^-$ is weak for all locations. $\delta^{18}O\text{-}NO_3^-$ is consistently between -10 and 0‰ over a large range of NO_3^- concentrations (10-40 mg N/L) for all sites except groundwater. Groundwater has NO_3^- concentrations less than 10 mg N/L and $\delta^{18}O\text{-}NO_3^-$ is higher than that of tiles and the outflow (0 to +10‰). The weak negative relationship between $lnNO_3^-$ concentration and $\delta^{18}O\text{-}NO_3^-$ for groundwater is not supportive evidence of denitrification. The range of $\delta^{18}O\text{-}NO_3^-$ is small (1.2‰ to 4.6‰) for all sites except groundwater (59.8‰). The average $\delta^{18}O\text{-}NO_3^-$ from each site shows a progressive increase through Upper road tile, Outflow, Harris tile, Shantz tile, BMR tile, and AMR tile and then a larger increase to the groundwater average (Table 3-5).

While $\delta^{15}N\text{-}NO_3^-$ isotopes are fairly similar between the two events ($\delta^{15}N\text{-}NO_3^-$ = 2 to 15‰) those of $\delta^{18}O\text{-}NO_3^-$ are, on average, much lower (Figure 3-5 and Figure 3-14). The collective NO_3^- isotope dataset has a $\delta^{18}O{:}\delta^{15}N$ slope of 0.55 (Figure 3-14). Data from groundwater and Shantz tile fall along this slope and are indicative of denitrification. Other individual sites are grouped upon this slope.

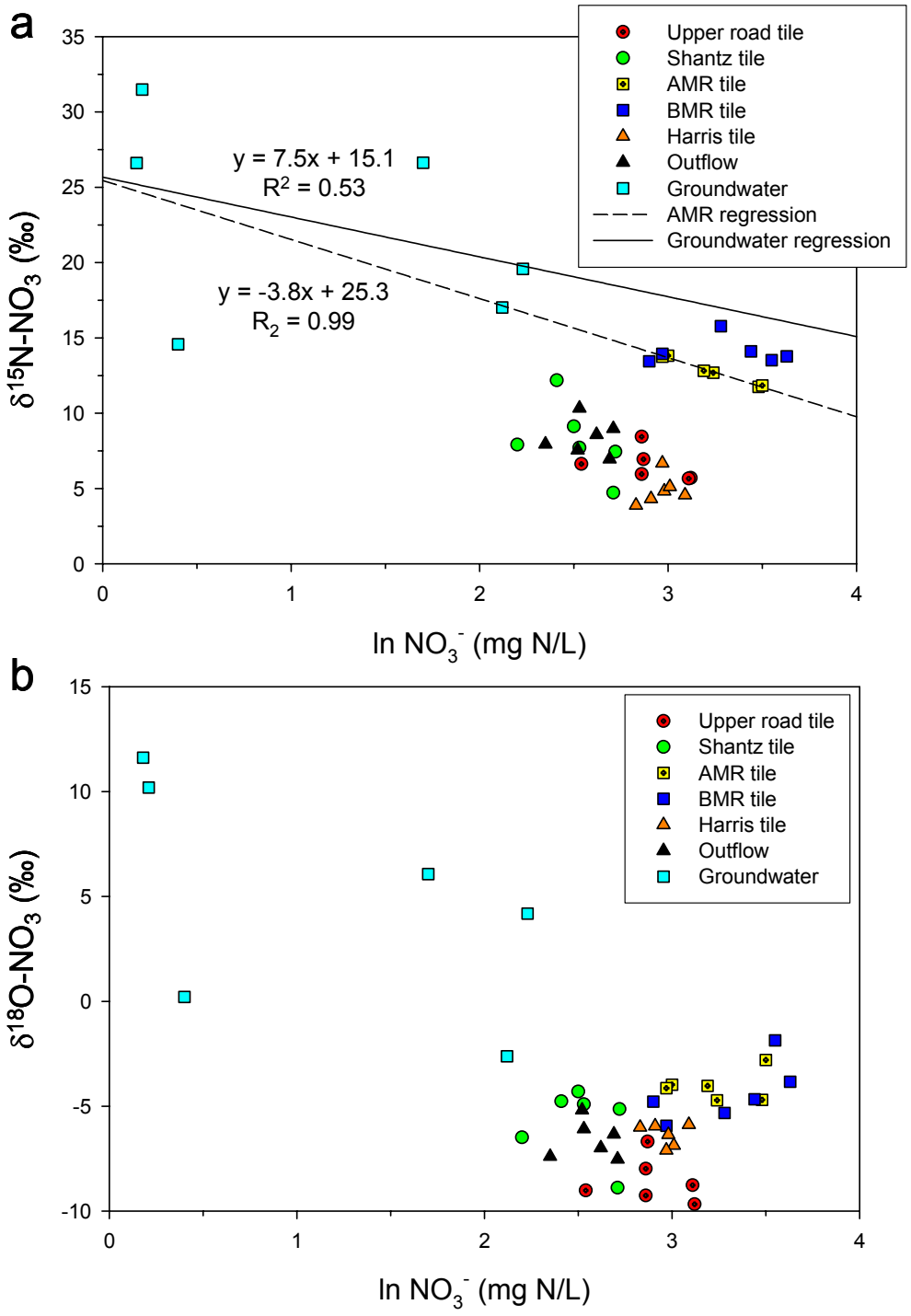

Figure 3-13: The relationship between the natural log (ln) of NO_3^- concentration and (a) $\delta^{15}N$-NO_3^- and (b) $\delta^{18}O$-NO_3^- for the 2008 mid-winter thaw. The best-fit equations for AMR tile and groundwater are provided for ^{15}N data.

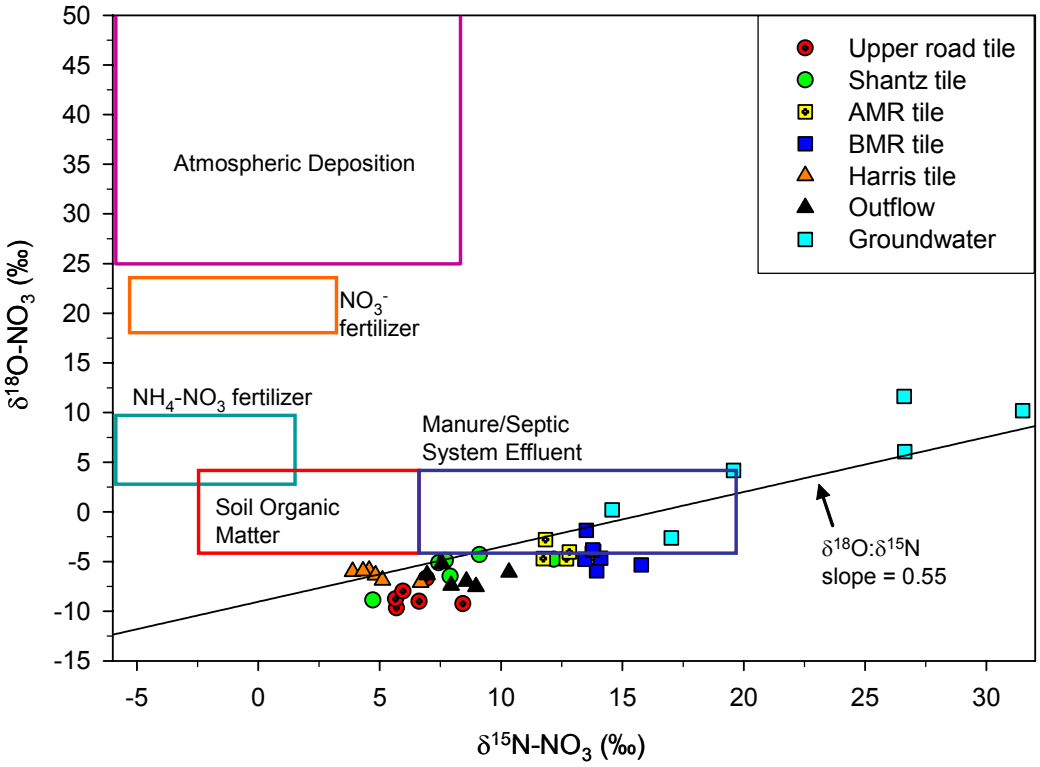

Figure 3-14: $\delta^{15}N$ and $\delta^{18}O$ of NO_3^- for the 2008 mid-winter thaw with the best-fit $\delta^{18}O$:$\delta^{15}N$ slope through the dataset.

Table 3-5: Average, Standard Deviation, and Range of $\delta^{15}N\text{-}NO_3^-$ and $\delta^{18}O\text{-}NO_3^-$ for the 2008 mid-winter thaw.

Site	Number of samples	$\delta^{15}N$				$\delta^{18}O$			
		Average	Standard Deviation	Range		Average	Standard Deviation	Range	
				Min.	Max.			Min.	Max.
Upper road tile	6	6.6	1.1	5.7	8.4	-8.6	1.1	-9.7	-6.7
Shantz tile	6	8.2	2.4	4.7	12.2	-5.8	1.7	-8.9	-4.3
AMR tile	6	12.8	0.9	11.7	13.8	-4.1	0.7	-4.7	-2.8
BMR tile	6	14.1	0.9	13.4	15.8	-4.4	1.4	-5.9	-1.9
Harris tile	6	4.9	1.0	3.9	6.7	-6.4	0.5	-7.1	-5.9
Outflow	6	8.4	1.2	7.0	10.3	-6.6	0.9	-7.5	-5.2
Groundwater	7	20.6	8.2	8.1	31.5	12.4	20.4	-2.6	57.2

3.4.3 $\delta^{15}N\text{-}N_2O$ and $\delta^{18}O\text{-}N_2O$

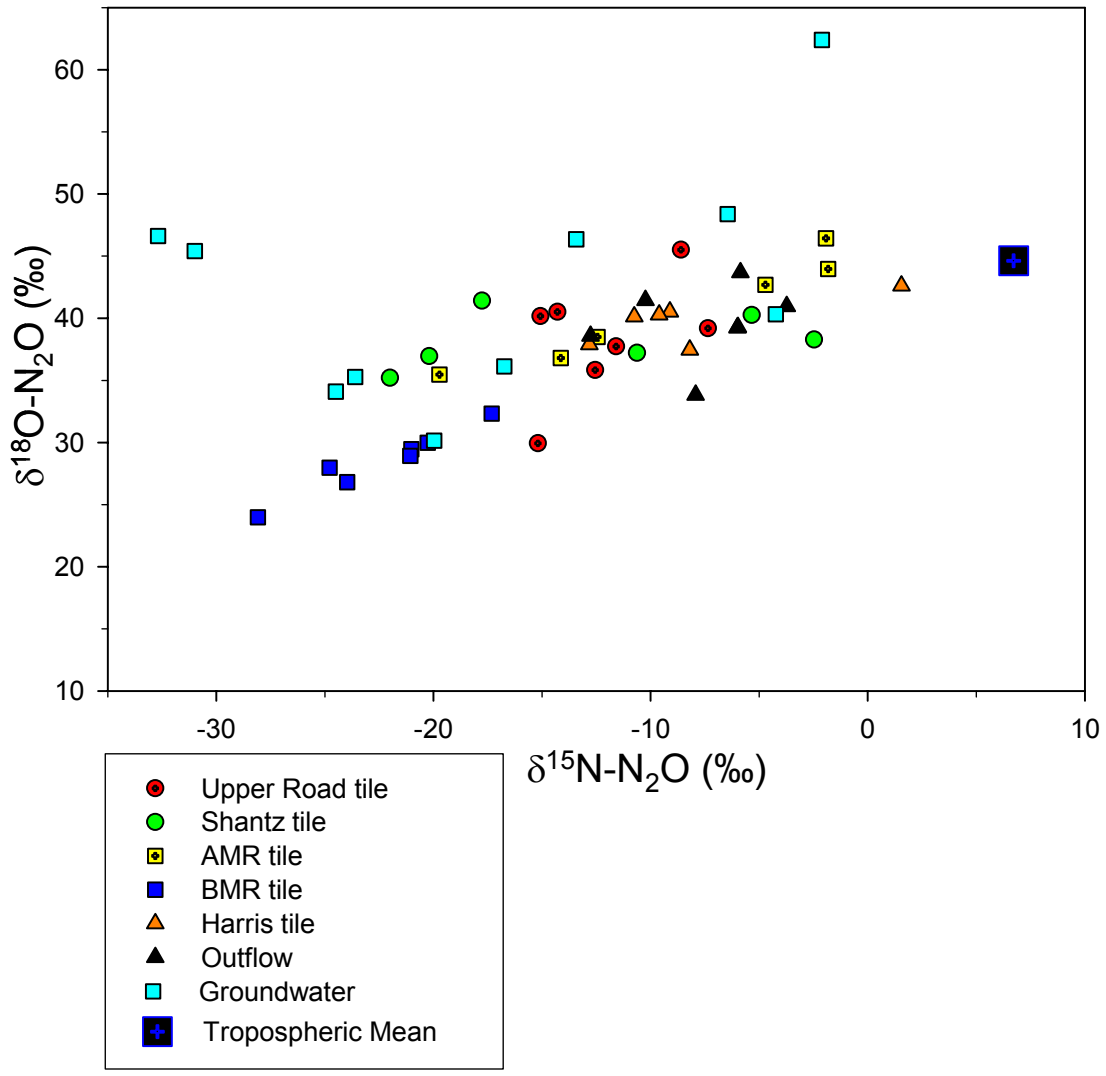

Figure 3-15: $\delta^{15}N\text{-}N_2O$ and $\delta^{18}O\text{-}N_2O$ during the 2008 mid-winter thaw

$\delta^{15}N\text{-}N_2O$ ranges from -32.7 (groundwater) to +1.6‰ (Harris tile) during the 2008 mid-winter thaw (Figure 3-15 and Table 3-6). Shantz and AMR tiles have a similar range in $\delta^{15}N$ values while outflow and groundwater have similar maximum values (-3.7‰ and -2.1‰, respectively). Upper road tile (-15.2‰), Harris tile (-12.8‰), and outflow (-

12.8‰) have similar minimum values. BMR tile has few similarities to other sites with a minimum of -28.1‰ and a maximum of -17.3‰.

Strong negative relationships between the natural log (ln) of N_2O concentration and $\delta^{15}N$-N_2O values are observed for Shantz tile ($R^2 = 0.92$, $p = 0.002$), Harris tile ($R^2 = 0.96$, $p = 0.0005$), Outflow ($R^2 = 0.90$, $p = 0.001$), and groundwater ($R^2 = 0.61$, $p = 0.008$). For these locations it is possible that a fractionating process is responsible for this relationship.

$\delta^{18}O$-N_2O values range from +24.0‰ (BMR tile) to +62.4‰ (groundwater) for the 2008 mid-winter thaw. Similar minimum $\delta^{18}O$-N_2O values between +33.8‰ and +37.5‰ were found for Shantz tile, AMR tile, Harris tile, and Outflow. Similar maximum $\delta^{18}O$-N_2O values between +42.6‰ and +46.4‰ were found for Upper road tile, AMR tile, Harris tile, and Outflow. BMR tile had few similarities to other tiles with a range between +24.0‰ and +32.3‰.

The relationship between the natural log (ln) of N_2O concentration and $\delta^{18}O$-N_2O is negative and strong for Upper road ($R^2 = 0.98$, $p = 0.0001$) and Harris tiles ($R^2 = 0.68$, $p = 0.04$) (Figure 3-16). This means that N_2O concentrations decrease while $\delta^{18}O$-N_2O values increase which is often indicative of an isotopic fractionating process.

$\delta^{18}O$:$\delta^{15}N$ slopes with strong relationships are measured at Shantz, AMR, BMR, and Harris tiles. "Moderate" slopes of 0.57 ($R^2 = 0.94$, $p = 0.001$) and 0.73 ($R^2 = 0.95$, $p = 0.0002$) were measured at AMR and BMR tiles, respectively (Figure 3-15). Shallow positive slopes of 0.17 ($R^2 = 0.67$, $p = 0.46$) and 0.27 ($R^2 = 0.51$, $p = 0.1$) were measured at Shantz and Harris tiles, respectively.

Table 3-6: Average, standard deviation, and range of $\delta^{15}N\text{-}N_2O$ and $\delta^{18}O\text{-}N_2O$ from individual sites for the January 2008 melt

Site	Number of samples	Average		Standard Deviation		Range			
		$\delta^{15}N\text{-}N_2O$	$\delta^{18}O\text{-}N_2O$	$\delta^{15}N\text{-}N_2O$	$\delta^{18}O\text{-}N_2O$	$\delta^{15}N\text{-}N_2O$		$\delta^{18}O\text{-}N_2O$	
						Min.	Max.	Min.	Max.
Upper road tile	7	-12.1	38.4	3.1	4.8	-15.2	-7.4	29.9	45.5
Shantz tile	6	-13.1	38.2	8.1	2.3	-22.0	-2.5	35.2	41.4
AMR tile	6	-9.1	40.6	7.4	4.4	-19.7	-1.8	35.5	46.4
BMR tile	7	-22.4	28.5	3.5	2.6	-28.1	-17.3	24.0	32.3
Harris tile	6	-8.2	39.8	5.0	1.9	-12.8	1.6	37.5	42.6
Outflow	8	-7.6	39.1	2.9	3.1	-12.8	-3.7	33.8	43.7
Groundwater	10	-17.5	42.5	10.8	9.4	-32.7	-2.1	30.2	62.4

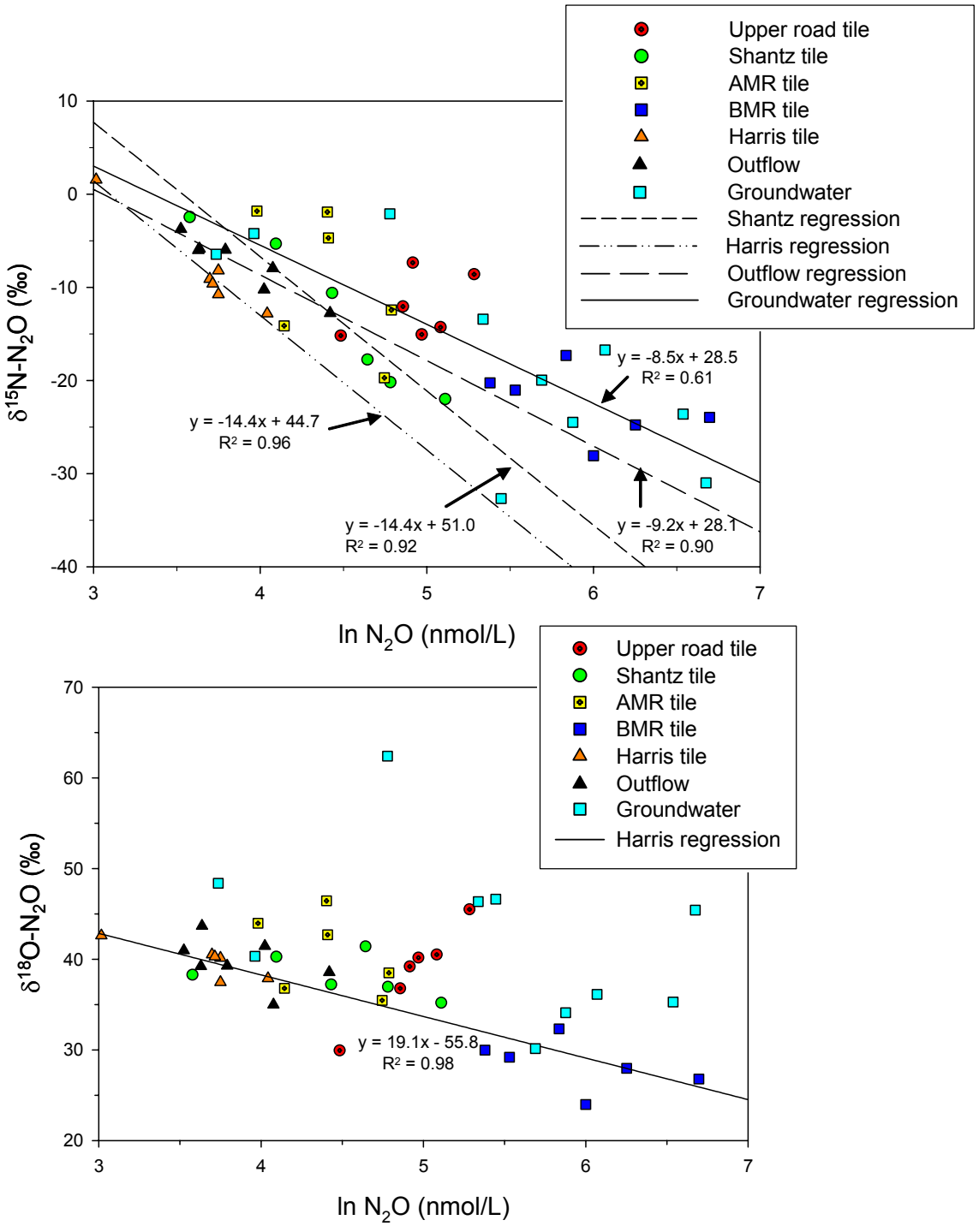

Figure 3-16: The relationship between the natural log (ln) of N_2O concentration and (a) $\delta^{15}N$-N_2O and (b) $\delta^{18}O$-N_2O for the 2008 mid-winter thaw. The best fit lines for Shantz tile, Harris tile, Outflow, and groundwater are shown in (a). The best fit line for Harris tile is shown in (b).

3.5 Discussion

3.5.1 Sources and Variability of NO_3^- at Strawberry Creek

Higher NO_3^- concentrations were measured at tiles and stream locations during the 2008 January melt event than for the 2007 Springmelt (Figure 3-3 and Figure 3-12). NO_3^- concentrations at only Harris tile and BMR tile were above the drinking water limit (10mg N/L) during the 2007 event, whereas concentrations at all sampling locations are greater than the drinking water limit during the 2008 event. This is likely the result of antecedent conditions of the watershed as a long drought had preceded the 2008 mid-winter thaw whereas several smaller storms occurred throughout the fall and winter preceding the 2007 Springmelt (Macrae, 2003). This would have resulted in significant accumulation of NO_3^- in the soil profile during the period preceeding the 2008 melt event. 2008 event NO_3^- concentrations were moderately lower than pre-event concentrations at Shantz and Harris tiles, though tile discharge was much higher suggesting dilution played a role (Table 3-4). Despite the potential effect of dilution event concentrations are much higher at the AMR tile. Due to low tile and groundwater discharge to the stream during the 2008 pre-event, less NO_3^- would have been removed from the soil. High groundwater NO_3^- concentrations (~100 mg N/L) from the Harris groundwater transect (Harris 1998) during the 2008 event would have increased stream concentrations (Table 3-7). Harris (1998) and Cabrera (2000) also found that NO_3^- in groundwater may not always be attenuated in the riparian zone during high flow events.

Table 3-7: NO_3^- concentrations taken from the Harris 3 transect (Harris, 1998) on January 27, 2008

Well	NO_3^- (mg N/L)
216-23	107.8
191-26	103.6
185-30	105.4
185.5-36.5	103.9
HTP1-J	100.0

While tile NO_3^- concentrations were higher during the event than pre-event period, stream concentrations were lower during the event period. Groundwater with low NO_3^- concentrations (<2.5 mg N/L) during 2007 shows that much less NO_3^- was in the soil profile and would have offset higher inputs from tiles through dilution. Low NO_3^- concentrations at the Deciduous Headwaters also show that this is an input of low NO_3^- concentrations to the stream.

NO_3^- isotopes measured at Strawberry Creek during the 2007 Springmelt and 2008 mid-winter thaw reflect differences in sources and processes as driven by hydrologic conditions in the catchment preceding and during the events. Evidence of NO_3^- from atmospheric deposition in the Deciduous Headwaters (2007 Springmelt) reveals a source that might otherwise be masked by high fertilizer use (Figure 3-5). The deciduous swamp also shows evidence of either mixing of NO_3^- from atmospheric deposition and manure sources or denitrification. If the two data points in question ($\delta^{15}N = 9.6$ and $\delta^{18}O = 12.7$; $\delta^{15}N = 10.3$ and $\delta^{18}O = 16.6$) are corrected for denitrification to a conservative $\delta^{18}O$ value of +6‰ (manure) using a $\delta^{18}O$:$\delta^{15}N$ ratio of 0.63 (Mengis et al., 1999), $\delta^{15}N$ values are -0.4‰ and -5.4‰, respectively. This is lower than what is normally measured for $\delta^{15}N$ of soil organic matter (+2 to +4‰) at Strawberry Creek. Source mixing is therefore the likely cause for these values.

Similar NO_3^- signatures from a possible combination of atmospheric and manure sources is also found at the Outflow during the 2007 Springmelt (Figure 3-5). This was unlikely to have come from the deciduous headwaters since NO_3^- concentrations here were less than 1 mg N/L while outflow concentrations were approximately 3 to 6 mg N/L. Fencerow and Harris tile also suggest mixing of atmospheric and manure/septic system sources which could have influenced sampling at the outflow. It is possible that NO_3^- from atmospheric deposition was present in the snow accumulated previous to the event though snow NO_3^- concentrations were also less than 1 mg N/L while concentrations at the Fencerow and Harris tiles were 4.5 and 13.6 mg N/L, respectively. This diminishes the potential influence of snow NO_3^- on tile NO_3^- sources. In addition, direct overland

inputs to the stream would have minimized the chance for snow infiltration to Fencerow and Harris tiles. As stated in the results variable $\delta^{18}O\text{-}NO_3^-$ could be the result of analytical errors associated with the chemical denitrification method for NO_3^- isotope analysis which is discussed further at the end of this section.

NO_3^- isotopes measured from the 2008 mid-winter thaw suggest that either specific sources or a specific process dominates NO_3^- dynamics during this period (Figure 3-14). As discussed in the results, NO_3^- isotopes from each sampling location show distinct groupings which could be indicative of distinct sources. Harris tile is a good example of this where $\delta^{15}N$ values are tightly grouped in the expected range of NO_3^- from soil organic matter as observed in Chapter 2. $\delta^{15}N$ values from BMR tile are also comparable between the two studies.

On the other hand, grouping of data along a $\delta^{18}O{:}\delta^{15}N$ slope of 0.55 could be indicative of denitrification if the NO_3^- source is the same for all sites (Mengis et al., 1999, Aravena and Robertson, 1998; Wassenaar, 1995). As such, a $\delta^{15}N$ value of +4‰ and a $\delta^{18}O$ value of -7.5‰ could represent a NO_3^- endmember source for all sites of this event. This is similar to the most depleted ^{15}N and ^{18}O isotope values from Shantz, Upper Road, and Harris tiles. It is possible that, from this endmember, NO_3^- became enriched to varying extents between individual sites though the extent was the same at individual sites. Hydrology in the catchment plays a major role for creating the conditions necessary for this scenario. Very minimal precipitation resulted in absence of basin discharge for the period of mid-June to November 2007 after which very little discharge occurred until the mid-winter thaw (Figure 3-1). As discussed above, NO_3^- produced at this time was not flushed from the system leaving it susceptible to denitrification in anaerobic microsites. A strong negative relationship between the natural log (ln) of NO_3^- concentration and $\delta^{15}N\text{-}NO_3^-$ observed groundwater and Shantz tile is indicative of denitrification though this is not observed for $\delta^{18}O$ (Figure 3-13). Strong relationships between ln of NO_3^- concentration and NO_3^- isotopes would not be expected for individual sites if they were subject to the same amount of denitrification. Strong relationships would be expected for

the collective dataset only if source NO_3^- concentrations of the sites were the same which hasn't been previously observed at Strawberry Creek (ie: Chapter 2).

Using the widely accepted theory that one third of nitrate oxygen is from atmospheric O_2 (+23.5‰) and two thirds are from water's oxygen would mean that water at Strawberry Creek would have to be -23.5‰ for ^{18}O (Andersson and Hooper, 1983; Kumar et al., 1983; Hollocher, 1984). This is much lower than the $\delta^{18}O\text{-}H_2O$ of -10‰ for average groundwater at Strawberry Creek (Mengis et al., 1999), though the mean monthly weighted average $\delta^{18}O\text{-}H_2O$ for December, January, and February is -13.1, -17.1, and -14.2, respectively. This issue is also apparent for 2007 Springmelt data but for Chapter 2 data which utilizes the more established silver nitrate method outlined by Spoelstra et al. (2004). Detectable errors (above ±0.5‰ uncertainty for NO_3^- analysis) in the chemical denitrification method for $\delta^{18}O\text{-}NO_3^-$ analysis can come from NO_2 if it is 2% of the total NO_3^- and NO_2 in a sample (Casciotti et al., 2007). However, NO_2 was measured in the samples prior to analysis and found to be less than this. Casciotti et al. (2007) also found that $\delta^{18}O\text{-}NO_2$ was altered during storage by freezing due to oxygen exchange with water. Assuming a NO_2 concentration of 2% (total NO_3^- and NO_2), an initial $\delta^{18}O\text{-}NO_3^-$ of 0‰ (low end of $\delta^{18}O\text{-}NO_3^-$ from Chapter 2), and a final $\delta^{18}O\text{-}NO_3^-$ of -10‰ produces a $\delta^{18}O\text{-}NO_2$ of -500‰ using a simple isotope mass balance. Since it is unlikely that $\delta^{18}O\text{-}NO_2$ would be this low and combined with low NO_2 concentration the possibility of NO_2 interference can be excluded.

Additionally, the theory that one third of nitrate oxygen is from atmospheric O_2 and two thirds are from water does not always hold true. For example, Snider et al. (2008) show that 80% of oxygen can come from water while the other 20% can come from atmospheric O_2. Using this ratio with the January mean monthly average of -17‰ produces a $\delta^{18}O\text{-}NO_3^-$ of -8.9‰, which approaches the minimum $\delta^{18}O\text{-}NO_3^-$ value of -10‰. Low $\delta^{18}O\text{-}NO_3^-$ values could reflect the changing ratio of oxygen contributed from either water or atmospheric O_2.

Although these results challenge the accuracy of $\delta^{18}O\text{-}NO_3^-$ data run by the chemical denitrifier method, they may also provide insight into certain reaction mechanisms in the N cycle. However, interpretation of these values should be with caution until these mechanisms are more fully illustrated and other analytical issues are resolved.

3.5.2 Sources and Variability of N_2O during two storm events

With N_2O concentrations above atmospheric saturation the stream is a consistent source of N_2O flux to the atmosphere during both events (Figure 3-3 and Figure 3-12). Elevated tile N_2O inputs (relative to the stream) are the source of stream N_2O as opposed to diffuse groundwaters which have low N_2O concentrations during both these events. Thuss et al. (2006) also measured N_2O from the Shantz and Harris tiles that was well above atmospheric saturation during a November (2005) storm. Other studies have shown that, at high percent saturation, significant degassing of N_2O from agricultural drainage ditches occurs downstream of tile drain discharge points (Reay et al., 2003, 2004; Harrison and Matson, 2003).

$\delta^{15}N\text{-}N_2O$ and $\delta^{18}O\text{-}N_2O$ values from Strawberry Creek suggest that N_2O is mostly produced by denitrification since the data points fit in the expected range (Figure 3-17). Calculated isotopic shifts (average) also support this proposition. For the 2007 Springmelt (Table 3-8) average values are -6.07‰ to -30.85‰ for ^{15}N ($\Delta_{N2O\text{-}NO3}$) and +14.38‰ to +34.48‰ for ^{18}O ($\Delta_{N2O\text{-}NO3}$). For the January 2008 melt average isotopic shifts were -13.05 and -37.70 for ^{15}N ($\Delta_{N2O\text{-}NO3}$) and +32.77 to +46.18‰ for ^{18}O ($\Delta_{N2O\text{-}NO3}$) (

Table 3-9). Denitrification incubation studies have calculated ^{15}N enrichment factors of -10 to -38‰ ($\varepsilon_{N2O\text{-}NO3}$) and ^{18}O enrichment factors of -10 to +30‰ ($\varepsilon_{N2O\text{-}NO3}$) (see Appendix 1, Chapter 1). These results differ in comparison to ^{15}N isotope effects for nitrification and nitrifier-denitrification where fractionations of -30 to -55‰ and -45 to -68.2‰ ($\varepsilon_{N2O\text{-}NH4}$), respectively, can be expected (see Appendix 1, Chapter 1). With an average $\delta^{15}N\text{-}NH_4^+$ value of +7.32 ± 0.87‰ for Strawberry Creek soils (Schiff et al., 2007, unpublished results), $\delta^{15}N\text{-}N_2O$ values of approximately -37 to -75‰ could be

produced from nitrifier-denitrification, though fractionation factors could be less negative if NH_4^+ concentration was limiting (Wada and Ueda; 1996, Ueda et al.; 1991) (Figure 3-17).

From direct field measurements, Perez et al. (2001) calculated instantaneous ^{15}N enrichment factors and interpreted those in the range of -13 to -38‰ to be a product denitrification. These samples were collected in the second week following irrigation even though water filled pore space (WFPS) at the surface was decreasing (≤60%). Strawberry Creek soils would have also been saturated during both major events. In another experiment, Bol et al. (2004) found that both non-flooded and flooded estuarine soils produced N_2O that was isotopically in the range of denitrification, despite the favorable conditions for nitrification during non-flooded conditions. This is because even in aerobic soils denitrification can produce N_2O in anaerobic microsites. Bol et al. (2004) and Wrage et al. (2004) also state that nitrification or other pathways may have produced N_2O though the isotopic signal can be masked by that of denitrification if more N_2O is produced by that pathway. This is a likely scenario as when N_2O production is high it is usually being produced by denitrification.

Data from 2007 Springmelt shows that, despite comparatively elevated $\delta^{18}O\text{-}NO_3^-$ values to the 2008 mid-winter thaw, $\delta^{18}O\text{-}N_2O$ is relatively similar between the two events (Table 3-3 and Table 3-6). This is particularly evident for the Deciduous Headwaters which shows only slightly higher $\delta^{18}O\text{-}N_2O$ values (+7‰ greater than next highest average) despite higher $\delta^{18}O\text{-}NO_3^-$ values (average is +18.3‰ greater than next highest average). This is suggestive that another process, beside the ^{18}O fractionation of N_2O formation, is responsible for the $\delta^{18}O\text{-}N_2O$ signatures observed. A possible candidate is oxygen exchange between water and NO_x which, with $\delta^{18}O\text{-}H_2O$ signatures of -10‰ at Strawberry Creek, would have the effect of lowering the $\delta^{18}O\text{-}N_2O$ values (Kool et al., 2007; Ye et al., 1991; Shearer and Kohl, 1988; Garber and Hollocher, 1982).

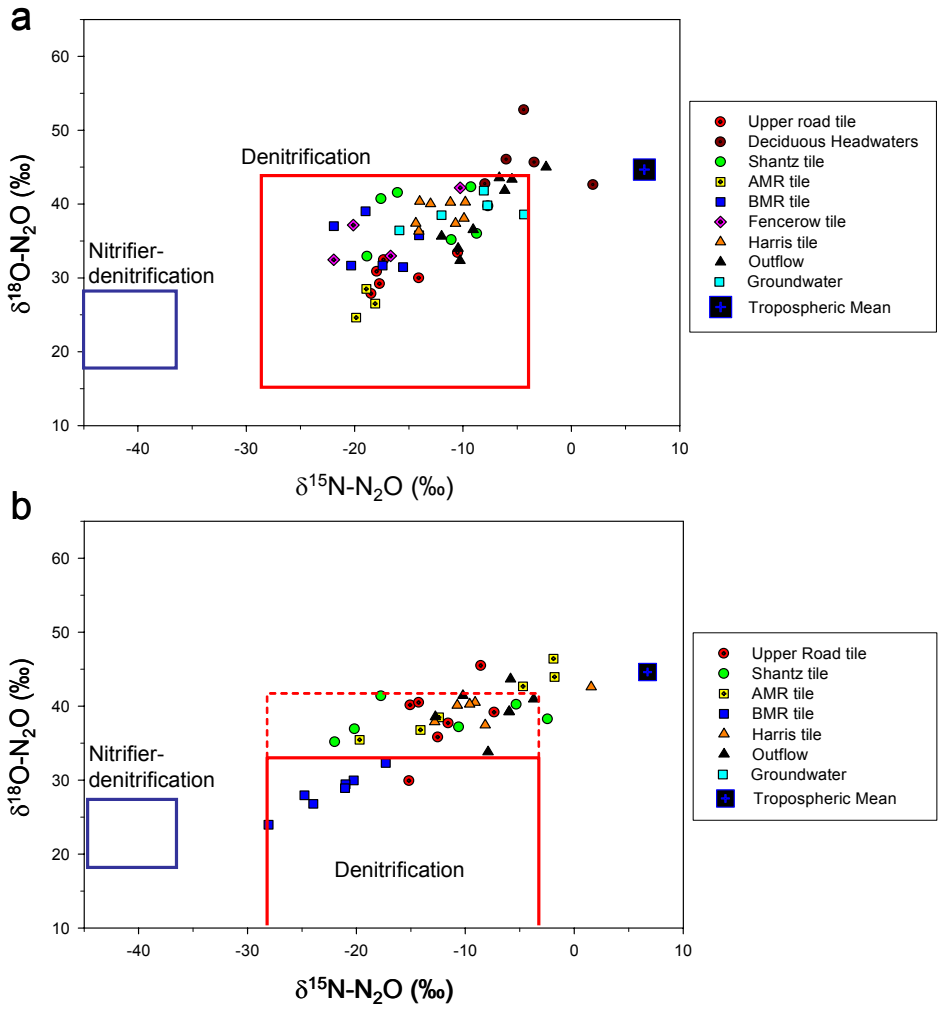

Figure 3-17: $\delta^{15}N$ and $\delta^{18}O$ of N_2O for the (a) 2007 Springmelt and the (b) 2008 mid-winter thaw. Expected ranges for denitrification were drawn by applying reported isotopic shifts on average NO_3^- values from each event. For the 2007 Springmelt an average $\delta^{15}N\text{-}NO_3^-$ of 8.5‰ and average $\delta^{18}O\text{-}NO_3^-$ of 3.32 was calculated. An $^{15}N\ \varepsilon_{N2O\text{-}NO3}^-$ range of -13 to -38‰ and a $^{18}O\ \varepsilon_{N2O\text{-}NO3}^-$ range of +10 to +40‰ was applied for denitrification. An average $\delta^{15}N\text{-}NO_3^-$ of 10‰ and average $\delta^{18}O\text{-}NO_3^-$ of -6‰ was calculated for the 2008 mid-winter thaw. The range for denitrification and nitrifier-denitrification was calculated as for the 2007 Springmelt. High $^{18}O\ \Delta_{N2O\text{-}NO3}^-$ of +48 calculated for the 2008 mid-winter thaw data, reflect the findings of Casciotti et al. (2002) where an $^{18}O\ \varepsilon_{N2O\text{-}NO3}^-$ of +50‰ was calculated. Based on this the range of denitrification could be extended by +10‰ for the 2008 mid-winter thaw. For nitrifier-denitrification an expected $^{15}NH_4^+$ of 7.00 from Strawberry Creek soils was assumed and a $^{15}N\ \Delta_{N2O\text{-}NH4}^+$ of -45 to -68 was applied which extends the box to -61‰ (^{15}N) (Perez et al., 2001; Snider et al., 2008; Yoshida, 1988; Ueda et al., 1999). $\delta^{18}O\text{-}N_2O$ values from nitrifier-denitrification have been reported as +23.5 ± 3‰ (Perez et al., 2001; Whalen and Yoshinari, 1985).

Table 3-8: Calculated range of isotopic shifts for denitrification ($\Delta_{N2O\text{-}NO3^-}$) for the 2007 Springmelt event. These were calculated as the difference between average N_2O and NO_3^- isotopes for the compiled dataset of each site.

	$\delta^{15}N$		$\delta^{18}O$	
Site	**Shift**	**sd**	**Shift**	**sd**
Upper road tile	-22.6	4.6	30.5	6.9
Deciduous Headwaters	-6.1	6.7	14.4	22.3
Shantz tile	-24.9	5.1	34.0	5.5
AMR tile	-30.8	3.3	32.7	5.6
BMR tile	-24.4	10.9	31.2	14.7
Fencerow tile	-22.4	6.2	33.4	11.0
Harris tile	-14.6	3.3	30.2	9.0
Outflow	-15.1	3.8	34.5	7.2

Table 3-9: Calculated range of isotopic shifts for denitrification ($\Delta_{N2O\text{-}NO3^-}$) for the 2008 January melt event. These were calculated as the difference between average N_2O and NO_3^- isotopes for the compiled dataset of each site.

	$\delta^{15}N$		$\delta^{18}O$	
Site	**Shift**	**sd**	**Shift**	**sd**
Upper road tile	-18.6	3.6	47.2	5.3
Shantz tile	-21.2	8.5	44.0	2.9
AMR tile	-21.9	7.4	44.7	4.4
BMR tile	-36.7	3.9	32.8	3.2
Harris tile	-13.1	5.1	46.2	2.0
Outflow	-16.5	3.1	46.1	3.0
Groundwater	-37.7	16.2	37.4	21.6

The distribution of N_2O isotopes is also characterized by different $\delta^{18}O$:$\delta^{15}N$ slopes. A $\delta^{18}O$:$\delta^{15}N$ slope around 0.5 could represent N_2O that is produced by changing NO_3^- isotope signature if the system is open. Following consumption by denitrification, the isotopes of residual NO_3^- become characteristically enriched at this ratio, though a range of 0.5 to 1.0 can be expected (Aravena and Robertson, 1998; Mengis et al., 1999; Green et al., 2008; Bottcher et al., 1990). With $\delta^{18}O$:$\delta^{15}N$ slopes of 0.42 ($R^2 = 0.41$, $p = 0.17$) and 0.69 ($R^2 = 0.62$, $p = 0.21$) for N_2O, the Upper Road and Fencerow tiles could represent this scenario during the 2007 Springmelt. NO_3^- isotopes at both sites do not show a $\delta^{18}O$:$\delta^{15}N$ slope between 0.5 and 1.0 which challenges the postulation that the trend in

N_2O isotopes is a product of substrate consumption, though Upper road tile has strong relationships between $lnNO_3^-$ and both $\delta^{15}N\text{-}NO_3^-$ ($R^2 = 0.97$, $p = 0.02$) and $\delta^{18}O\text{-}NO_3^-$ ($R^2 = 0.46$, $p = 0.31$) (Figure 3-6). Fencerow also has a strong relationship between $lnNO_3^-$ and $\delta^{15}N\text{-}NO_3^-$ ($R^2 = 0.77$, $p = 0.17$) (Figure 3-6a). However, an observable connection between the isotopes of the two N species may not necessarily be expected in samples from Strawberry Creek. N_2O can be produced in anaerobic microsites by only a small degree of denitrification. Although the residual NO_3^- following denitrification becomes enriched it is likely a small portion of NO_3^- measured at the tile outlet since this represents what is collected over the drainage network. The N_2O collected at the outlet also represents what is collected over the drainage network but is the product of denitrification of NO_3^- so it shows the $\delta^{18}O$:$\delta^{15}N$ slope of 0.5. Also, when NO_3^- is being consumed in anaerobic microsites its concentration decrease should result in less N_2O produced. The relationship between lnN_2O concentration and $\delta^{15}N\text{-}N_2O$ is negative and strong ($R^2 = 0.89$, $p = 0.005$) at Upper Road tile (2007 Springmelt) though it is not strong between lnN_2O concentration and $\delta^{18}O\text{-}N_2O$ (Figure 3-9). These relationships are positive at the Fencerow tile during this event, showing that the theory may not be reflected in the environment where many factors can influence these relationships. This theory should be tested under controlled laboratory conditions.

During the January 2008 melt event $\delta^{18}O$:$\delta^{15}N$ ratios of N_2O from BMR and AMR tiles have slopes of 0.57 ($R^2 = 0.95$, $p = 0.001$) and 0.73 ($R^2 = 0.94$, $p = 0.0002$), respectively (Figure 3-15). Both AMR and BMR tiles also have negative relationships between lnN_2O concentration and both isotopes though the relationships are weak ($R^2 \leq 0.35$) (Figure 3-16). Groundwater data also has a similar trend for N_2O isotopes with a $\delta^{18}O$:$\delta^{15}N$ slope of 0.36 though only the $\delta^{15}N$ of N_2O is moderately well correlated to lnN_2O concentration ($R^2 = 0.61$) (Figure 3-16a).

Shallow $\delta^{18}O$:$\delta^{15}N$ slopes with low regression coefficients (<0.50) also characterize the distribution of N_2O isotope data for some Strawberry Creek sites. Included in this classification are positive $\delta^{18}O$:$\delta^{15}N$ slopes less than 0.40 and negative slopes. $\delta^{18}O$:$\delta^{15}N$

slopes of 0.27 from measured N_2O can also be calculated from results in Perez et al. (2001) while negative ratios are found in Yoshida et al. (2005) due to the positive isotope effect on ^{18}O. More sites from the 2007 Springmelt are characterized this way than for the 2008 mid-winter thaw suggesting the former dataset is more randomly distributed. Although less of a trend is apparent the distribution is still important as it is likely the result of several combined processes. Evidence of NO_3^- consumption is not apparent for most 2007 Springmelt data though there could be some smaller effects that are not obvious. BMR tile is a good example of how variable NO_3^- isotope signatures could result in variable N_2O values though regression between NO_3^- and N_2O isotopes doesn't provide evidence of a direct influence (Figure 3-5). Variable fractionation factors are the most likely explanation for this observed effect.

Enrichment factors for denitrification would vary for several reasons. Denitrification is a sequential reduction series with different fractionation factors at each step. The combination of different fractionation factors and different ratios of the concentration of intermediates to N_2O concentration ($[NO_2] + [NO]/[N_2O]$) would produce different isotope effects for N_2O. Fractionation at each step could also be variable due to different reaction rates, environmental conditions, and the many genera of denitrifying bacteria completing the reactions (Menyailo and Hungate, 2006). Reduced NO_3^- availability, for example, would decrease ^{15}N enrichment factors (Menyailo and Hungate, 2006; Mandernack et al., 2002).

According to several incubation and field studies, $\delta^{18}O$:$\delta^{15}N$ slopes of 2.5 are expected for N_2O consumption (Mandernack et al., 2000; Schmidt and Voerkelius, 1989; Menyailo and Hungate, 2006; Vieten et al., 2007). Slopes of 1.15 (AMR tile) and 1.4 (Outflow) during the 2007 springmelt are the steepest measured from both events (Appendix C, Table C-2). Evidence of N_2O consumption at outflow is supported by enriching isotopes with decreasing concentration. However, given the high concentrations of N_2O in the stream this could also be the effect of gas exchange.

For the stream, the effect of gas exchange can be accounted for by assuming steady state conditions for isotopic composition and N_2O production rate. Under these conditions, the isotopic composition of N_2O flux can be calculated from dissolved N_2O concentration and dissolved N_2O isotopic using Equation 3-1.

$$\text{Flux Rate } {}^{15}\text{N}_2\text{O} = K\left[\alpha_{in}^{15} P(\text{N}_2\text{O})\text{K}_\text{h}\left(\frac{R_{gas}^{15}}{1+R_{gas}^{15}}\right) - \alpha_{ev}^{15}[\text{N}_2\text{O}]_{dissolved}\left(\frac{R_{dissolved}^{15}}{1+R_{dissolved}^{15}}\right)\right]$$

$$\text{Flux Rate N}_2{}^{18}\text{O} = K\left[\alpha_{in}^{18} P(\text{N}_2\text{O})\text{K}_\text{h}\left(\frac{R_{gas}^{18}}{1+R_{gas}^{18}}\right) - \alpha_{ev}^{18}[\text{N}_2\text{O}]_{dissolved}\left(\frac{R_{dissolved}^{18}}{1+R_{dissolved}^{18}}\right)\right] \quad \textbf{Equation 3-1}$$

Where the flux of ${}^{15}N_2O$ and $N_2{}^{18}O$ is measured in $mol \cdot m^{-2} \cdot h^{-1}$ and K is the gas exchange coefficient ($m \cdot h^{-1}$), $P(N_2O)$ is the partial pressure of N_2O (atm), K_h is Henry's constant for N_2O ($mol \cdot atm^{-1} \cdot m^{-3}$), and $[N_2O]_{dissolved}$ is the dissolved concentration of N_2O ($mol \cdot m^{-3}$). $\alpha^{15}{}_{in}$ and $\alpha^{18}{}_{in}$ are the fractionation factors for invasion of N_2O into the dissolved phase and $\alpha^{15}{}_{ev}$ and $\alpha^{18}{}_{ev}$ are the fractionation factors for N_2O evasion from the dissolved phase (Inoue and Mook, 1994). $R^{15}{}_{dissolved}$ and $R^{15}{}_{gas}$ is the ratio of ${}^{15}N/{}^{14}N$ isotopes of N_2O in dissolved and gas phases and $R^{18}{}_{dissolved}$ and $R^{18}{}_{gas}$ is the ratio of ${}^{18}O/{}^{16}O$ isotopes of N_2O in dissolved and gas phases.

According to Thuss and Schiff (2008) the isotopic composition of N_2O flux will equal that of the N_2O source at steady state. This analysis provides the isotopic composition of the source for every isotopic measurement of dissolved N_2O unlike N_2O endmember analysis which only provides one value for a data set. Results of this analysis show that the source isotopic composition of the 2008 mid-winter thaw is relatively constant and that the N_2O isotope endmember is an appropriate average of the source (Figure 3-18). The same analysis for the 2007 Springmelt shows similar source signatures for all except one of the data points but suggests that the N_2O endmember is not an appropriate average value for source composition. The $\delta^{18}O$-N_2O source value is likely closer to +40‰. Regardless, the endmember and flux values are relatively well constrained and allows the conclusion that the isotopic signature of N_2O flux to the atmosphere at the outflow is -12 to -18‰ for ${}^{15}N$ and +32 to +42‰ for ${}^{18}O$.

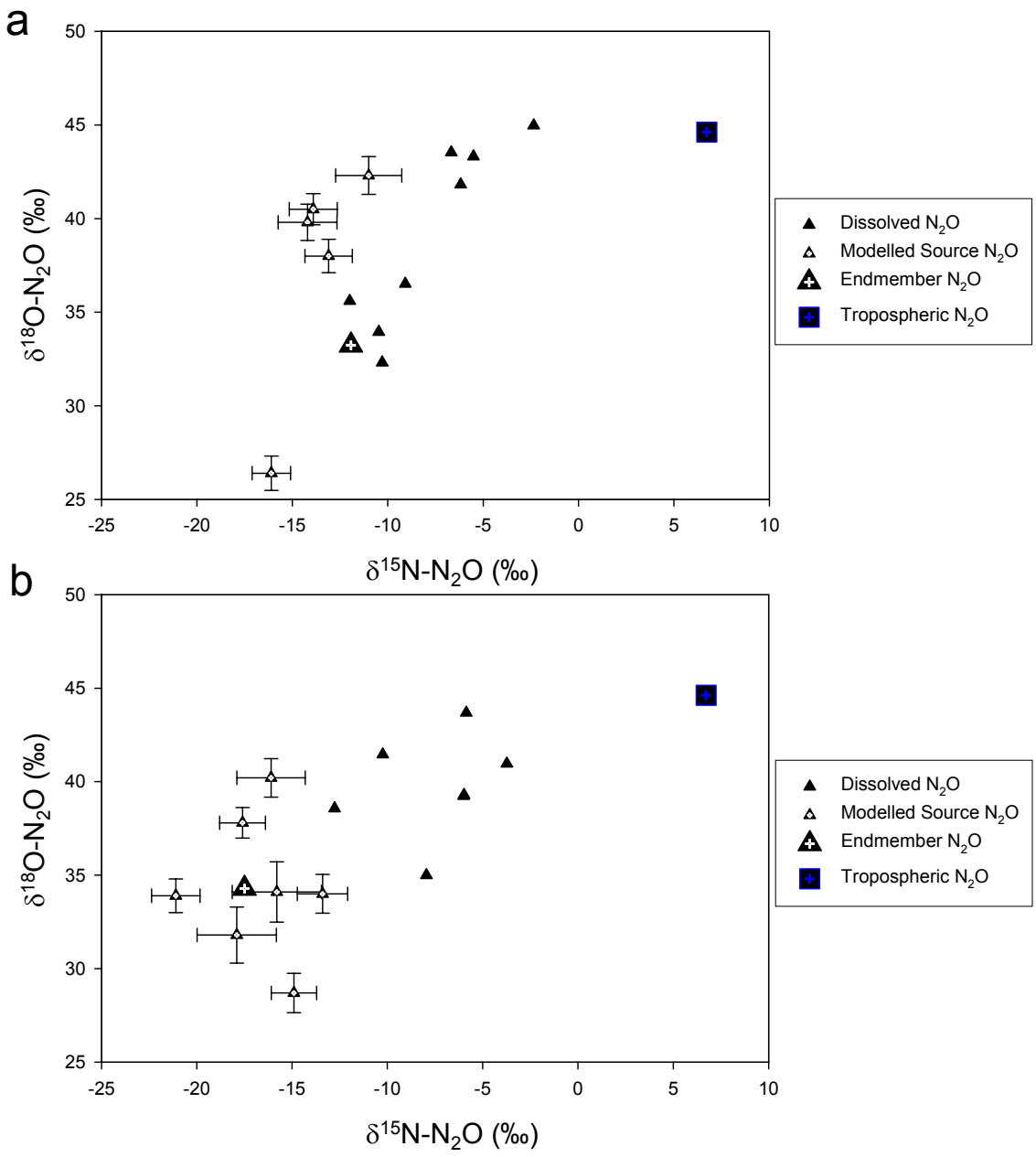

Figure 3-18: Modelled source N_2O at the outflow during (a) Springmelt 2007 and (b) the 2008 mid-winter thaw with calculated endmember N_2O.

Calculation of a N_2O endmember was performed by regression analysis of the inverse of N_2O concentration and the N_2O isotope species. This is known as a Keeling analysis for

determining the original source signature of a pool that has mixed with a background pool (Pataki et al., 2003). The y-intercept of this analysis is the original isotopic signature of the pool mixing with the background pool.

3.6 Conclusions and Recommendations

NO_3^- concentrations from BMR and Harris tiles was above the drinking water limit (10 mg N/L) during the 2007 Springmelt though concentrations at the Outflow are below this level. On the other hand NO_3^- concentrations during the 2008 mid-winter thaw are above the drinking water limit for all tiles and also at the outflow, which makes this a more critical event in terms of NO_3^- concentrations in the catchment. This is likely linked to the build up of NO_3^- during the long drought prior to the 2008 mid-winter event.

N_2O from tiles was a source to the stream during both events which, with consistent concentrations above atmospheric saturation, is a source of N_2O to the atmosphere.

NO_3^- isotopes suggest that sources were mainly soil organic matter and manure during the 2007 Springmelt. There is also evidence of NO_3^- from atmospheric deposition in the Deciduous Headwaters. NO_3^- isotopes from the 2008 mid-winter thaw shows tight grouping of data for specific sampling locations which could be indicative of slight variations from soil organic matter and manure sources. However, the groupings from individual tiles and the outflow fall along a $\delta^{18}O$:$\delta^{15}N$ NO_3^- line of 0.55 which is indicative of denitrification if the source is the same. For individual sites, groundwater and Shantz tile alone indicate progressive enrichment of NO_3^- isotopes. Denitrification of NO_3^- in Strawberry Creek tiles has not been previously observed but is directly linked to the drought conditions preceding the 2008 mid-winter thaw. Since little NO_3^- was flushed from the system over this long period denitrification was possible on a large scale.

N_2O measured during the 2007 Springmelt and the January 2008 melt was produced by denitrification. Calculated isotopic shifts ($\Delta_{N2O\text{-}NO3^-}$) for ^{15}N and ^{18}O are indicative of this in comparison with literature values of denitrification. High denitrification potential is also indicated by saturated environmental conditions during these events. The slope of $\delta^{18}O$:$\delta^{15}N$ for N_2O is indicative of processes influencing N_2O production. Moderate

slopes around 0.5 are observed for certain tiles pointing to the influence of NO_3^- consumption, particularly when the combination of increasing N_2O isotopes values with decreasing N_2O concentrations are congruent. Shallow negative or positive slopes reflect a combination of processes including NO_3^- consumption, N_2O consumption, and variable fractionation factors due to substrate availability, reaction rate, and microbial assemblages.

Gas exchange is the dominant process in the stream. The isotopic composition of the N_2O source can be calculated for each measured point using a steady-state flux model. This analysis suggests that the calculated N_2O endmember is not representative of the average isotopic composition of source N_2O during the 2007 Springmelt. However, the calculated N_2O endmember is representative of the average isotopic composition of source N_2O during the 2008 mid-winter thaw. The isotopic signature of N_2O flux to the atmosphere at the outflow is -12 to -18‰ for ^{15}N and +32 to +42‰ for ^{18}O.

Other studies of dissolved N_2O in agroecosystems should not neglect high magnitude events such as melt events as they can be significant portion of annual flux to the atmosphere. This study shows that N_2O isotopes are useful as a sensitive indicator of denitrification in aquatic systems including tile drain networks. N_2O isotopes are sensitive to both N_2O production and consumption and, thus, they should be used in conjunction with other geochemical tools for denitrification studies.

Chapter 4: NO_3^- and N_2O during non-melt conditions at Strawberry Creek: A stable isotope approach

Overview

N_2O is a powerful greenhouse gas that has a relatively long atmospheric residence time and contributes to ozone degradation. Recent increases in the atmospheric mixing ratio of N_2O have been associated with direct and indirect sources from agriculture amongst other anthropogenic sources. Stable isotope research has focused on direct N_2O emissions while research on indirect sources has lagged behind. In this study we report the $^{15}N/^{14}N$ and $^{18}O/^{16}O$ stable isotopes of N_2O in groundwater, tile drainage, and open streams during non-melt conditions at the Strawberry Creek catchment near Waterloo, Ontario, Canada. Two datasets; October 2006 to June 2007 and Fall 2007, are used to characterize these conditions. The isotope data suggests that N_2O is produced by denitrification. Furthermore, NO_3^- consumption or gas exchange is likely altering the original signature of the N_2O produced, particularly in tiles and streams. Isotopic distinction between soil gas N_2O and dissolved N_2O is suggestive of different production mechanisms between the unsaturated and saturated zones. Based on these results, and those of Chapter 3, a conceptual model of N_2O isotope dynamics in a small agricultural catchment is proposed, highlighting differences in what is measured between aquatic and non-aquatic systems. Compared to the variability in literature measurement of N_2O isotopes those from the Strawberry Creek catchment are relatively tight, thereby defining the isotopic signature of local secondary agricultural N_2O.

4.1 Introduction

N_2O is a major greenhouse gas (GHG) that evolves from agriculture environments. Globally, the largest source of N_2O is from land conversion for agriculture and heavy use of nitrogen (N) fertilizers (Stein and Yung, 2003) which is projected to increase in the future (Perez et al. 2001).

Direct N_2O flux from arable lands is an extensively documented type of N_2O emission but does not account for all emissions from agricultural sources (Mosier et al., 1998; Mosier, 1994; Bouwman, 1996). Mosier et al. (1998) estimated that indirect emissions from agriculture equal direct emissions at 2.1 Tg N-N_2O/yr. The 1994 IPCC reports on N_2O emissions did not consider secondary sources in the same detail as 1998 reporting which consequently accounted for missing portions in the total estimates of N_2O evolution

(Mosier et al., 1998). Volatilization and deposition of NH_3 and NO_x, N leaching and runoff, human consumption of agricultural crops and subsequent municipal wastewater treatment, N_2O formation from NH_3 in the atmosphere, and food processing are all considered indirect N sources (Mosier et al., 1998).

N_2O is produced by the microbially mediated processes of nitrification and denitrification. N_2O is a by-product of hydroxyl-amine oxidation in the nitrosification reaction series which proceeds under aerobic conditions. Nitrifying bacteria can also produce N_2O by reducing NO_2 when oxygen becomes limited. N_2O production by this process, known as nitrifier-denitrification, is believed to be more environmentally relevant than as a by-product of hydroxyl-amine oxidation. Under anaerobic conditions with a suitable electron donor source (often organic carbon) NO_3^- can be reduced through denitrification where N_2O is an obligatory intermediate. Consequent reduction of N_2O to N_2 completes the denitrification reaction series.

The most powerful tool in discriminating between the different pathways of N_2O production and consumption utilizes stable isotope ratios of $^{15}N/^{14}N$ and $^{18}O/^{16}O$ (Stein and Yung, 2003). As previously discussed N_2O produced in aerobic environments has been attributed to nitrification. Large isotopic shifts ($\Delta\delta^{15}N$ = -45 to -68‰) commonly cited for nitrification produce relatively depleted $\delta^{15}N$-N_2O values in aerobic aquifers and upper ocean columns (Ostrum et al., 2000). Relatively higher $\delta^{15}N$-N_2O values produced during anaerobic denitrification have been found in lakes, oceans, and emitted from soils (Boontanan et al., 2000; Wada and Ueda, 1996; Naqvi et al., 1998; Popp et al., 2002; Tilsner et al, 2003; Wrage et al,. 2004). For denitrification, ^{15}N fractionation ranging from -13 to -38‰ ($\varepsilon_{NO3\text{-}N2O}$) has commonly been reported. A wide range of oxygen-18 fractionation factors have also been reported for denitrification likely due to the complicating mechanisms of water exchange, N_2O consumption, and microbial assemblages. ^{18}O fractionation factors of -10 to +32‰ ($\varepsilon_{NO3\text{-}N2O}$) have commonly been reported for denitrification.

Defining isotopic signatures from temperate environments could be an important component in closing the global isotopic N_2O budget. More importantly, understanding the dynamics of the processes controlling emissions from temperate agricultural environments could lead to mitigation strategies. Though temperate zones studies of N_2O isotopes are becoming more common, few have focused on dissolved sources, particularly drainage tile inputs and streams. On the other hand, several groundwater N_2O isotope studies have made significant contributions (Bol et al., 2004; Well et al., 2005; Wada and Ueda, 1996; Ueda et al., 1999).

In this study we investigate the N_2O isotopes from indirect sources at the Strawberry Creek agricultural catchment, Ontario, Canada. Isotopic analysis was performed on dissolved N_2O collected from tile drain waters, streams, and groundwater for the period of October 2006 to January 2008. There are several objectives to this study. First, to characterize the N_2O isotopes during periods of baseflow and precipitation driven events (ie: periods other than melt events) and, secondly, to compare those collected from the various sampling locations including soil gas N_2O. The third objective is to answer whether differences in isotopic signatures are related to variability in pathway, fractionation factors, and substrates. The final objective is to define the isotopic signature of dissolved N_2O from secondary agricultural sources as defined at Strawberry Creek.

4.2 Site Description

A detailed description of the study site can be found in Section 1.2.

4.3 Methods

Tiles, and Streams at the Strawberry Creek were sampled from October 2006 to December 2007. Groundwater was periodically sampled from late September 2006 to December 2007 to characterize water chemistry on a seasonal basis and through a variety of hydraulic gradients. Samples were collected for N_2O and NO_3^- isotopes and concentrations of N_2O, and major anions (Cl^-, Br^-, NO_3^-, PO_4^{3-}, SO_4^{2-}). Waters for N_2O

isotopes were collected in duplicate in 160mL glass serum bottles, without creating a headspace. Saturated $HgCl_2$ solution (0.3mL) was used for preservation.

Waters for major anion chemistry were collected in 125mL plastic screw-top bottles and were filtered with Whatman 0.45 μm syringe-tip filters within 24 hours of collection. For analysis of major anions, 0.5 mL sample aliquots were used on a Dionex ICS-90 ion chromatograph, equipped with an IonPac AS14A column and AS40 automated sampler. Samples were corrected to a calibration curve made from Dionex brand standards. Analytical error for NO_3^- concentration is +/- 0.03 mg N/L.

Duplicate 60mL serum bottles for N_2O concentration were stoppered with butyl blue stoppers (Belco Glass) and preserved with 0.15mL $HgCl_2$. N_2O was equilibrated in a 5mL headspace and injected manually onto a Varian CP-3800 gas chromatograph. Trace gases were separated by a Poroplat Q column and N_2O was analyzed by an ECD detector. The analytical error of this analysis is approximately +/- 5% at 8.5 nmol/L and the detection limit is approximately 6.5 nmol/L.

N_2O was extracted from water using a modified CO_2 extraction technique (EIL method) developed by the Environmental Geochemistry Group (Thuss et al., 2008) In brief, the 160mL sample is bubbled for 10 minutes with a helium line that is attached to a 20mL capped serum vial sitting in liquid nitrogen to cryogenically trap the N_2O gas. The bottom and top of the vial is filled with glass beads and has silica glass wool in the middle to increase the surface area on which the gas may be trapped. After sample purging is complete the vial is pressurized with a known quantity (20mL) of Helium. Ideal injection size of the sample was calculated based on peak height of standard injection. Samples were analyzed for N_2O isotopes by injecting 10 to 15 nmol of N_2O on a Micromass Trace Gas Analyzer connected to a Micromass continuous flow mass spectrometer (TG-CFMS). Ideal injection size of the sample was calculated based on peak height of standard injection. Samples were corrected to EGL 5 N_2O standard ($\delta^{15}N$-N_2O = 2.03, $\delta^{18}O$-N_2O = 38.44) for instrumental drift, linearity, and isotopologue contamination. Results are reported in delta (δ) notation in units of per mil (‰) relative to to N_2 (air) for $\delta^{15}N$ and

VSMOW for $\delta^{18}O$. Analytical errors for $\delta^{15}N$ and $\delta^{18}O$ is ±0.13‰ and ±0.31‰. The instrument was calibrated to tropospheric N_2O.

The method used for NO_3^- isotope analysis was originally developed by McIlven and Altabet (2005) but is presented here with modifications by Spoelstra (unpublished, 2007). After collection, 30mL of water is filtered (0.45μm) into plastic screw-top bottles and frozen for storage. When ready to analyze for nitrate isotope ratios, a volume of water containing 0.6μg N is freeze dried. The sample is redissolved with 0.75M NaCl and 1mL of 0.08M Imidazole is added to aid the cadmium reduction reaction. The sample is then placed in a column with copperized cadmium and slowly shaken for 2 hours to reduce NO_3^- to NO_2^-. The sample is then syringe filtered into a stoppered 20mL serum vial. N_2O is subsequently produced by addition of a 2mL sodium azide and acetic acid buffer solution for 10 minutes. 1mL of 6M NaOH is added to stop the reaction. The vial is pressurized with 10mL of Helium and placed on a shaker to equilibrate for 10 minutes. The sample is then run on the TG-IRMS as above for dissolved N_2O. Analytical error calculated for this method was ±1.1 for $\delta^{15}N\text{-}NO_3^-$ and ±3.0 for $\delta^{18}O\text{-}N_2O$.

4.4 Results

4.4.1 Catchment Hydrology

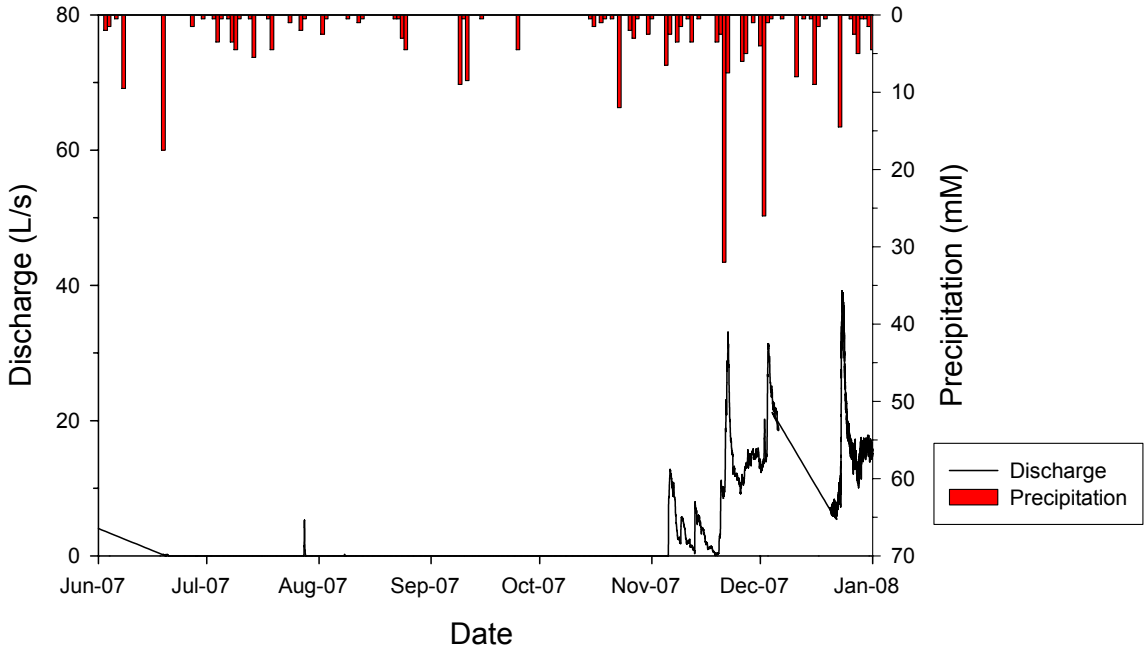

Figure 4-1: Catchment Discharge and Precipitation from June 2007 to December 2007. Dry conditions from mid June 2007 to the beginning of November 2007 prohibited tile and stream sampling. Sampling recommenced shortly after discharge began.

4.4.2 NO_3^- and N_2O concentrations

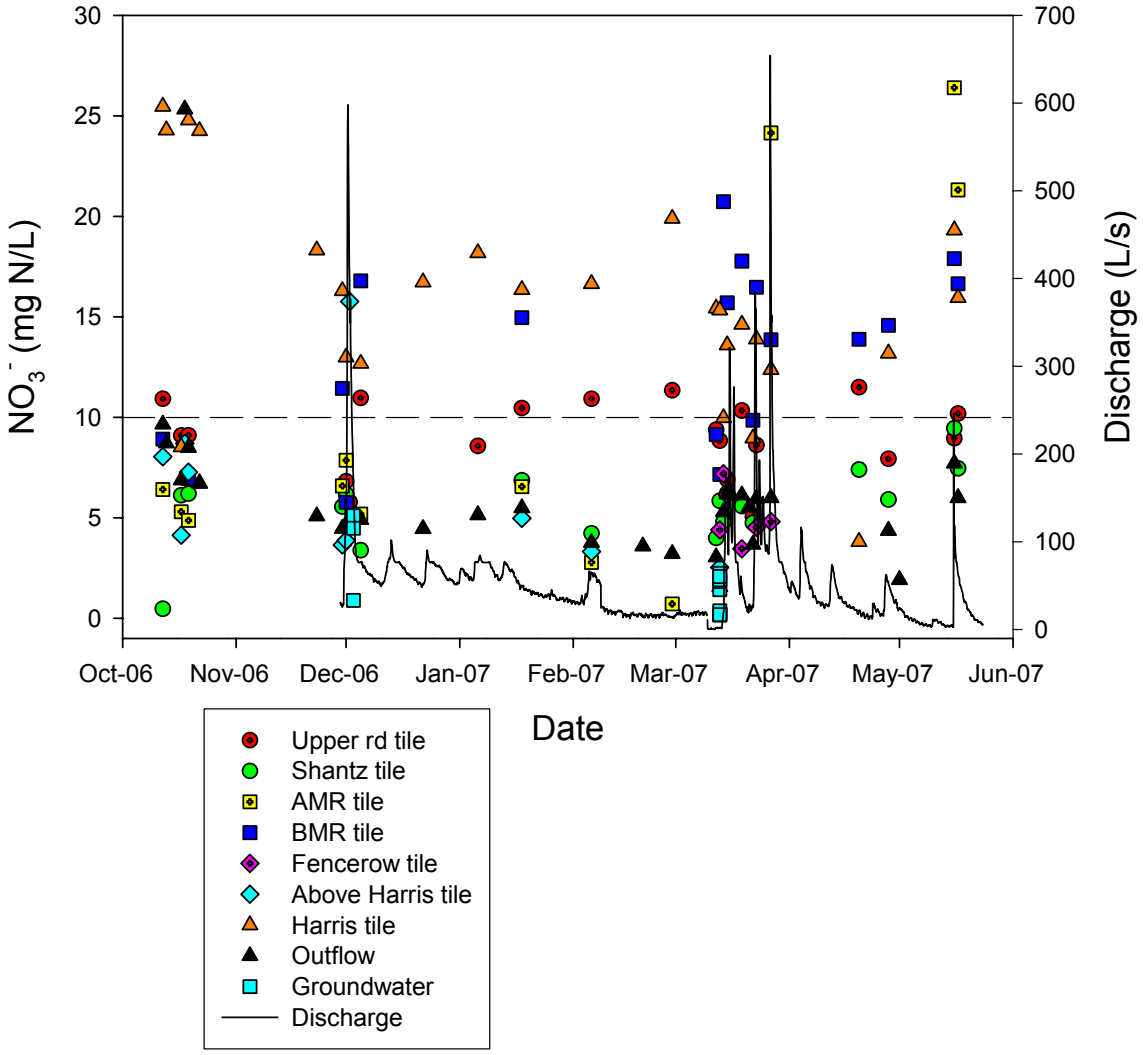

Figure 4-2: NO_3^- concentrations from October 2006 to June 2007 with the 10mg N/L NO_3^- drinking water limit (dashed line). Analytical error for NO_3^- concentration is approximately +/- 0.03 mg N/L.

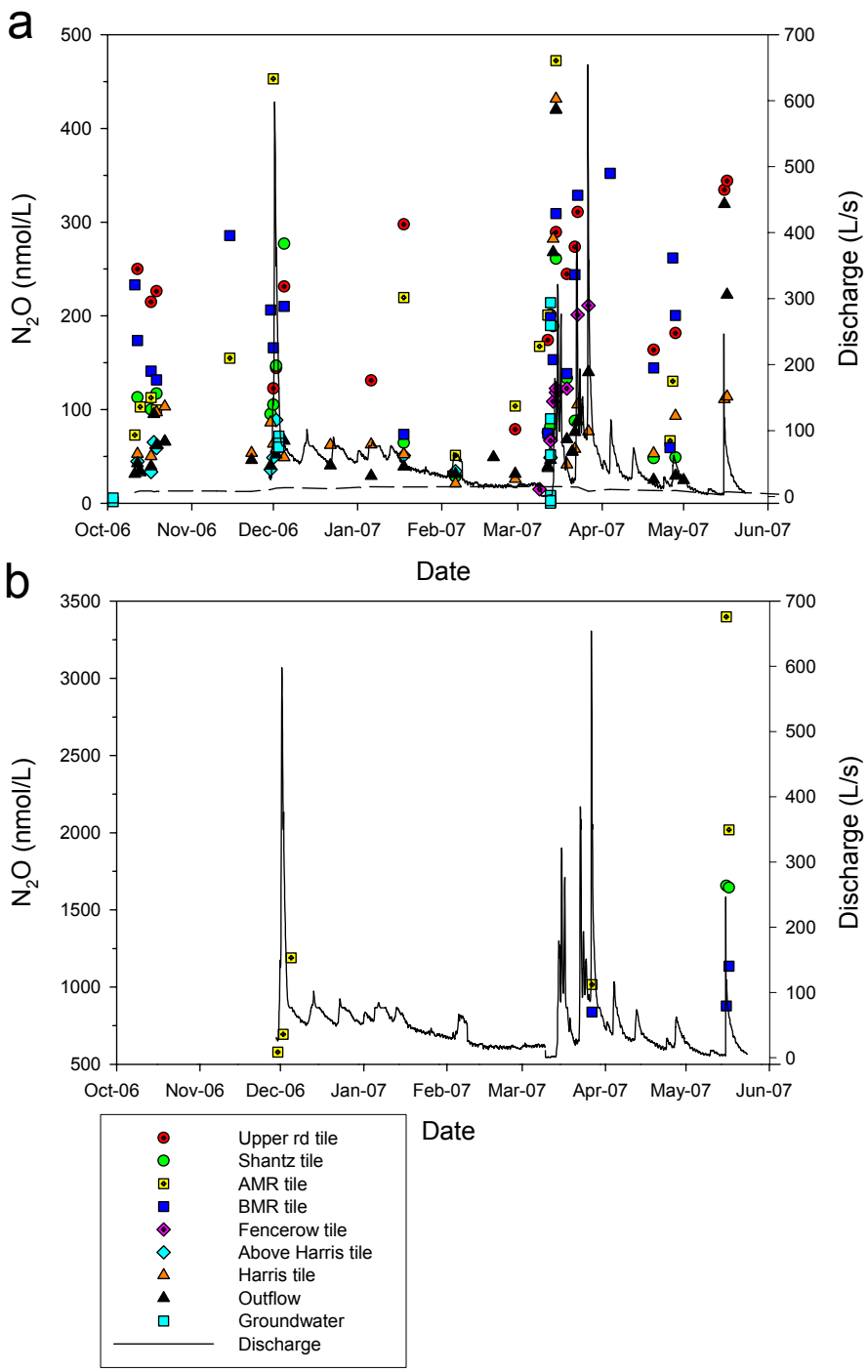

Figure 4-3: (a) N_2O concentrations less than 500 nmol/L and (b) N_2O concentrations greater than 500 nmol/L from October 2006 to June 2007. Stream N_2O concentration at 100% saturation (dashed line). Analytical error for N_2O concentration is approximately +/- 5% at 8.5 nmol/L.

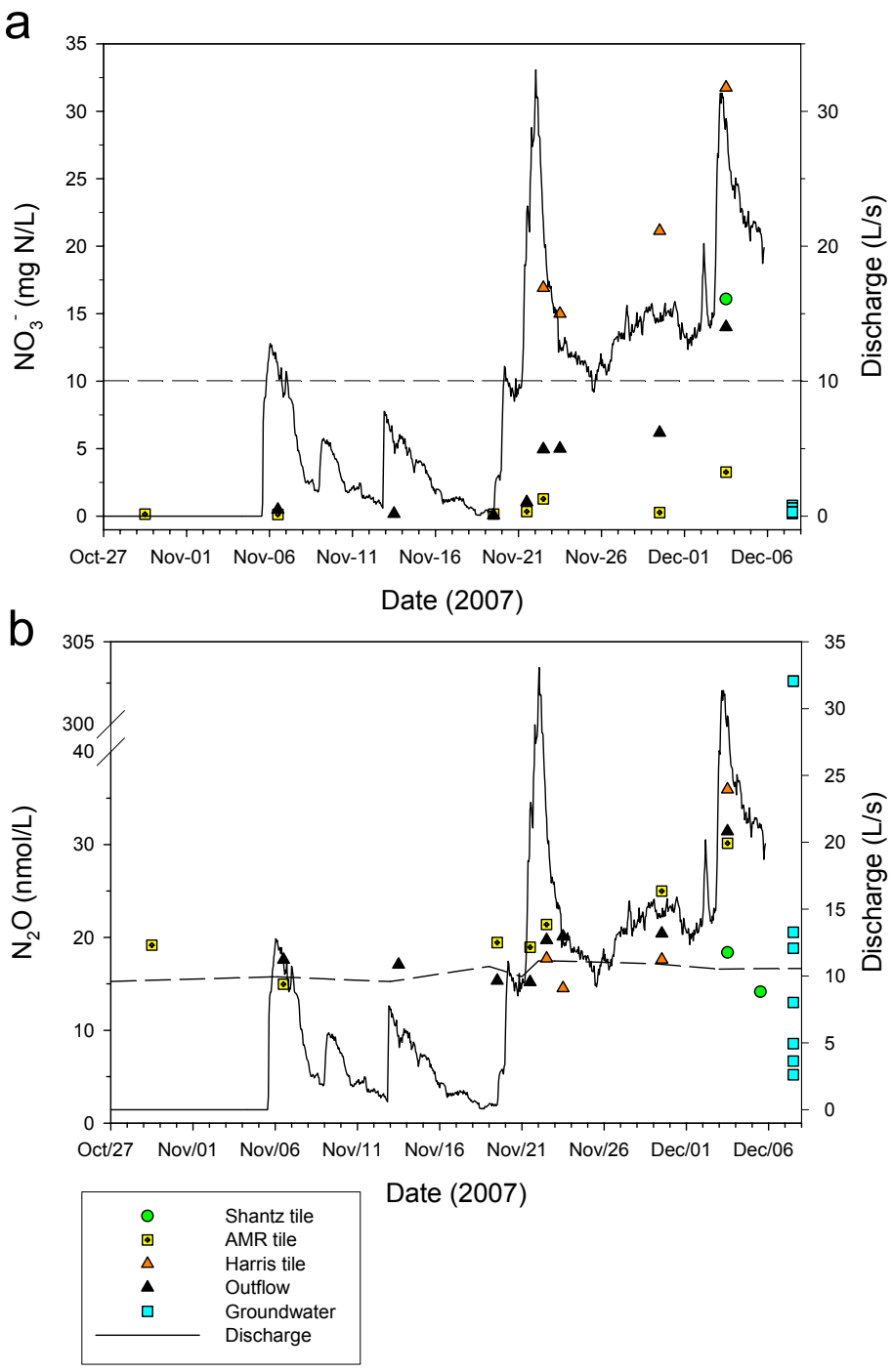

Figure 4-4: (a) NO_3^- concentrations from Fall 2007 with the 10 mg N/L NO_3^- drinking water limit (dashed line). (b) N_2O concentrations from Fall 2007 with N_2O at 100% saturation (dashed line).

A large range of hydrologic conditions exist in the catchment between October 2006 and June 2007 (Figure 4-2). Even excluding the 2007 Springmelt, outflow discharge ranges from 0 to 600 L/s during this period. Periods of increased discharge usually follow precipitation events which are frequent and often variable in magnitude. Stream discharge fed by groundwater inputs are considered baseflow conditions in this study and can be observed in comparison to high magnitude events such as in December 2006 and May 2007 (Figure 4-2). Even though it is arguable that these events should be analyzed separately they are included in the dataset since they are all driven by precipitation, not snowmelt, as in Chapter 3. A period of distinct hydrology is from July 2007 until November 2007 when no discharge occurred in the catchment. This long period of drought was followed by low discharge caused by several precipitation events in Fall 2007 that set up conditions for unique chemistry and isotopes. Due to the uniqueness of this dataset it was separated from the October 2006 to June 2007 data for analysis.

4.4.2.1 October 2006 to June 2007

4.4.2.1.1 NO_3^- concentrations

NO_3^- concentrations from Upper road, BMR, and Harris tiles are consistently above the 10 mg N/L drinking water limit throughout this period (Figure 4-2). These tiles have the highest average NO_3^- concentrations in addition to AMR tile presumably due to very high concentrations in December 2006 and May 2007 (Table 4-1). Excluding AMR tile, NO_3^- concentrations from these tiles are more significant during baseflow conditions, presumably due to dilution during major events, indicated by high outflow discharge. Although these tiles contribute high concentrations to the stream, NO_3^- concentrations at the outflow are usually not above the drinking water limit. An exception to this condition is in October 2006 where outflow NO_3^- concentrations are as high as they are at Harris tile, obviously reflecting the influence of the tile on this measurement (Figure 4-2 and Table 4-1). This likely means that groundwater, which is typically low in NO_3^- concentration (Table 4-1), is a large portion of stream inputs. Tiles such as Shantz and

others not measured in this study (ie: Forest and Bend tiles) may also contribute to dilution of higher NO_3^- concentrations.

Table 4-1: Average, Standard Deviation, and Range of NO_3^- concentrations from October 2006 to June 2007

Site	Number of samples	Average NO_3^- (mg N/L)	Standard Deviation of NO_3^- (mg N/L)	Min. NO_3^- (mg N/L)	Max. NO_3^- (mg N/L)
Upper Road tile	20	9.1	1.8	5.0	11.5
Shantz tile	19	5.5	1.9	0.5	9.5
AMR tile	12	9.8	8.8	0.7	26.4
BMR tile	18	13.3	4.4	5.8	20.7
Above Harris tile	9	6.6	4.0	3.3	15.8
Harris tile	27	15.4	5.6	3.8	25.5
Outflow	21	6.5	4.7	1.9	25.3
Groundwater	20	1.9	2.2	0.1	5.3

4.4.2.1.2 N_2O concentrations

Tiles and streams at Strawberry Creek are most often a source of N_2O to the atmosphere with concentrations above atmospheric saturation (Figure 4-3). High N_2O concentrations measured at tiles indicates they are a significant source of N_2O to the creek. Average N_2O concentrations at Upper Road, Shantz and BMR tiles are all consistently high (200-300 nmol/L) while the average at AMR tile is much higher (543nmol/L)(Table 4-2). Higher average N_2O concentrations at the outflow than at the stream above Harris tile exemplify the influence of tiles on streams. However, when basin discharge is less than 40L/s, tile discharge to the stream is often not significant which means that diffuse groundwater inputs make up stream flow during these periods. As groundwater N_2O concentrations are, on average, greater than those of the stream (above Harris tile and Outflow), they are likely a consistent source of N_2O to the stream during all hydrologic conditions. N_2O concentrations in both the stream and tiles appear to be consistently higher during storm events than they are during baseflow conditions.

Table 4-2: Average, Standard Deviation, and Range of N_2O concentrations from October 2006 to June 2007

Site	Number of samples	Average N_2O (nmol/L)	Standard Deviation of N_2O (nmol/L)	Min. N_2O (nmol/L)	Max. N_2O (nmol/L)
Upper Road tile	20	212.1	85.1	28.7	344.0
Shantz tile	19	277.5	488.0	28.6	1655.7
AMR tile	21	542.9	817.0	51.1	3398.8
BMR tile	24	289.0	270.9	59.4	1135.5
Above Harris tile	9	51.1	17.9	33.3	88.8
Harris tile	27	86.2	84.7	20.9	431.6
Outflow	23	64.4	68.9	24.6	319.3
Groundwater	21	90.2	171.1	1.3	590.9

4.4.2.2 Fall 2007

4.4.2.2.1 NO_3^- concentrations

NO_3^- concentrations in Harris tile are consistently above the 10 mg/L drinking water limit throughout this time period while other tiles (except Shantz) and the outflow remain below (Table 4-3). This is with the exception of NO_3^- concentrations on December 3, 2007 that are >12.5mg N/L for Shantz tile, Harris tile, and Outflow. This reflects the influence of tile NO_3^- concentrations on stream concentrations for this day.

Table 4-3: Average, standard deviation, and range of NO_3^- concentrations during Fall 2007

Site	Number of samples	Average NO_3^- (mg N/L)	Standard deviation of NO_3^- (mg N/L)	Min. NO_3^- (mg N/L)	Max. NO_3^- (mg N/L)
Shantz tile	1	16.1			
AMR tile	7	0.8	1.2	0.1	3.3
Harris tile	4	21.2	7.5	15.0	31.8
Outflow	8	4.0	4.8	0.1	14.0
Groundwater	7	0.4	0.2	0.2	0.8

4.4.2.2.2 N_2O concentrations

N_2O concentrations in the stream are above atmospheric saturation for most of this period including occasions (November 21-23, 2007) when concentrations from the Harris tile are

at or below atmospheric saturation. This suggests that diffuse groundwater inputs were more significant than tile inputs on these occasions, which is possible given that groundwater concentrations are the highest of all sampling locations measured during this period (Table 4-4). N_2O inputs from AMR tile would have been a source of N_2O to the stream those these would have likely degassed by the time they reached the outflow. Comparison of average N_2O concentration between the October 2006 to June 2007 dataset (Table 4-2) and the Fall 2007 dataset (Table 4-4) shows that concentrations are much higher in the former. This combined with differences observed in N_2O isotopes (section 4.4.4) constitute the reasoning for separate treatment of this data.

Table 4-4: Average, standard deviation, and range of N_2O concentrations during Fall 2007

Site	Number of samples	Average N_2O (nmol/L)	Standard deviation of N_2O (nmol/L)	Min. N_2O (nmol/L)	Max. N_2O (nmol/L)
Shantz tile	2	16.2	3.0	14.1	18.4
AMR tile	7	21.3	4.9	15.0	30.1
Harris tile	4	21.4	9.8	14.5	35.9
Outflow	8	19.6	5.2	15.2	31.4
Groundwater	8	84.8	134.6	5.2	302.6

4.4.2.2.3 NO_3^- and N_2O concentrations

Within the October 2006 to June 2007 dataset, only AMR tile ($R^2 = 0.88$, $p = 0.0001$) and above Harris tile ($R^2 = 0.84$, $p = 0.0005$) have strong, significant relationships (Figure 4-5). For Fall 2007 data, the relationship between NO_3^- and N_2O concentrations is strong and significant for AMR tile ($R^2 = 0.66$, $p = 0.03$), Harris tile ($R^2 = 0.93$, $p = 0.03$), and the outflow ($R^2 = 0.94$, $p = 0.0001$) (Figure 4-6). This is further support that the Fall 2007 dataset is unique and should be treated separately.

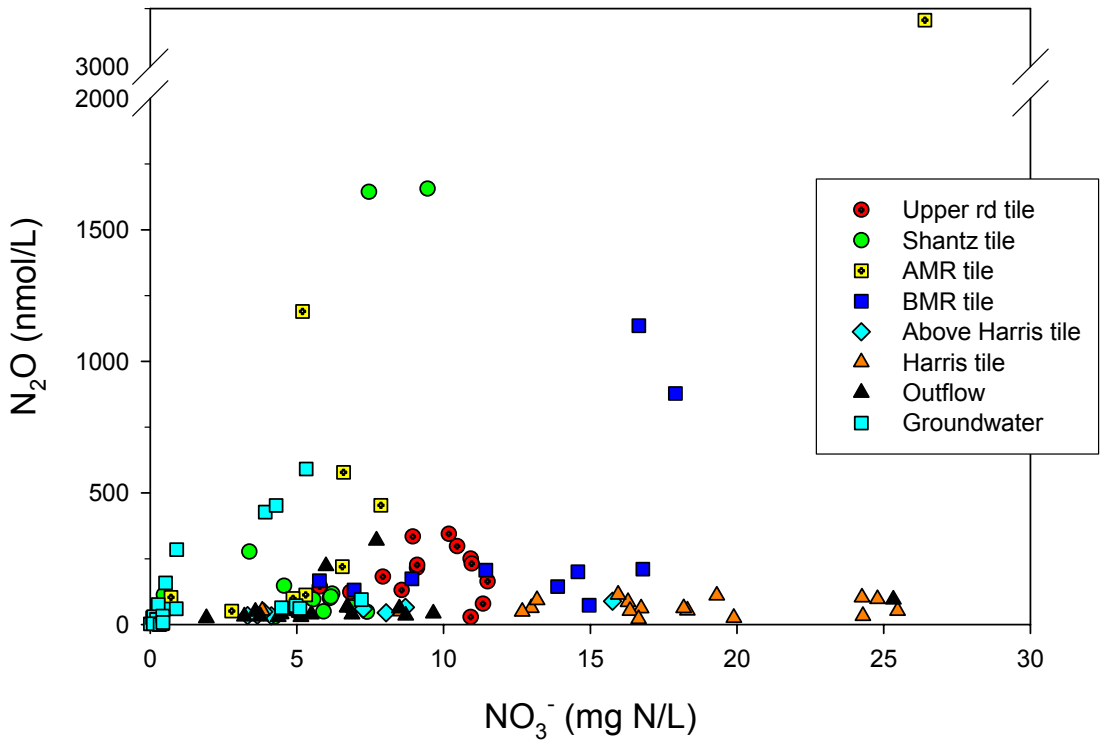

Figure 4-5: The relationship between NO_3^- and N_2O concentrations for October 2006 to June 2007.

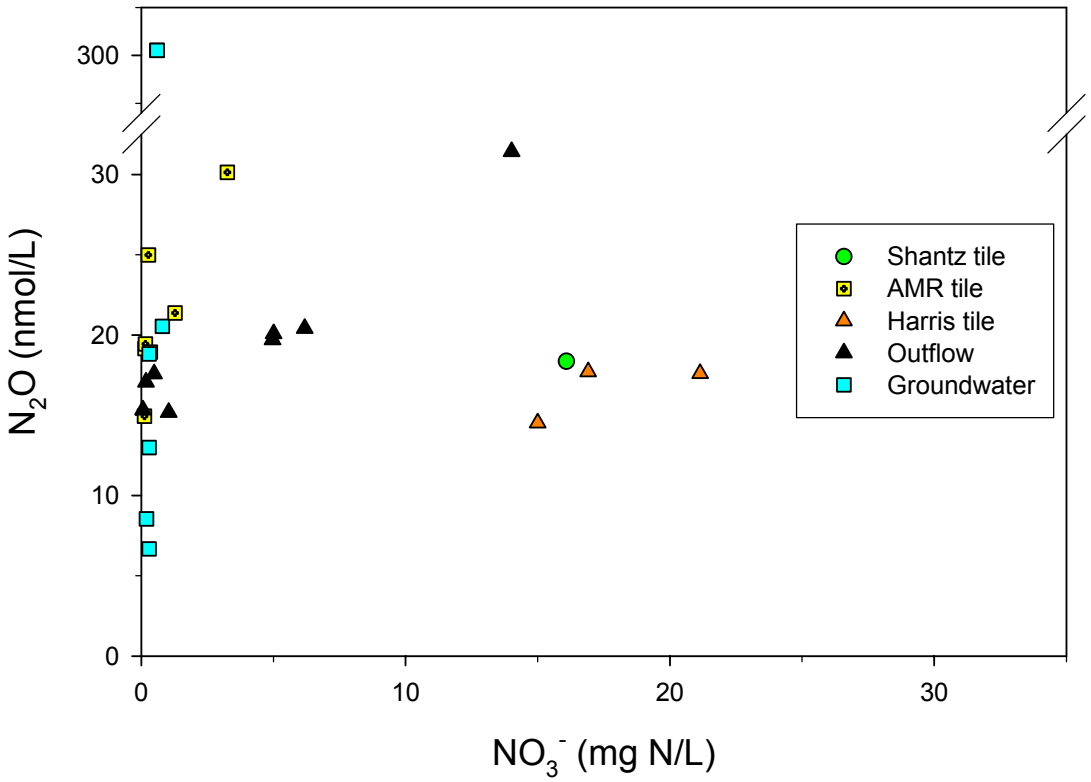

Figure 4-6: The relationship between NO_3^- and N_2O concentration for Fall 2007.

4.4.3 $\delta^{15}N$ and $\delta^{18}O$ of NO_3^-

With the majority of the $\delta^{15}N$-NO_3^- data between 6 and 15‰ and the $\delta^{18}O$-NO_3^- data between -10 and 6‰ it is apparent that most of the NO_3^- during these two periods is from manure/septic system effluent sources (Figure 4-7 and Figure 4-9). Some of the NO_3^- is also derived from soil organic matter.

4.4.3.1 October 2006 to June 2007

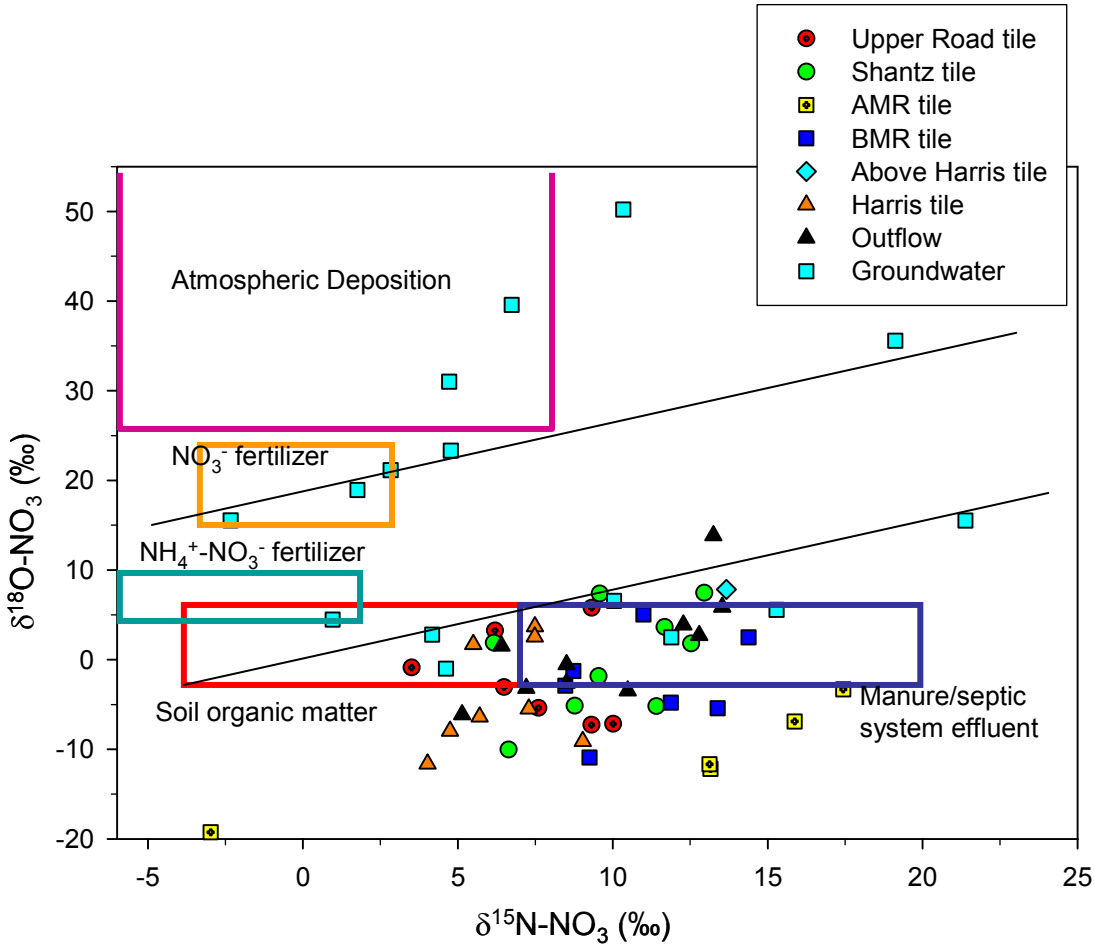

Figure 4-7: $\delta^{15}N$ and $\delta^{18}O$ of NO_3^- from October 2006 to June 2007. Expected $\delta^{15}N$ ranges of sources are adapted from Kendall (1998). $\delta^{15}N$ ranges are based on literature values reported in Aravena et al. (1993); Wassenaar (1995); Aravena and Robertson, (1998); Kendall (1998); and Spoelstra et al. (2001). $\delta^{18}O$ ranges for NO_3^- from atmospheric deposition, NO_3^- fertilizers, and NH_4^+-NO_3^- fertilizers are based on literature values reported in Kendall (1998); Mayer et al. (2001); Spoelstra et al. (2001); and Wassenaar (1995). The upper range for $\delta^{18}O$-NO_3^- from atmospheric deposition extends to +80‰. $\delta^{18}O$ ranges for NO_3^- from soil organic matter and manure/septic system effluent were calculated based on the range of mean monthly weighted average $\delta^{18}O$ of precipitation (IAEA, 2001) and the $\delta^{18}O$ of atmospheric O_2 (+23.5‰) (see Section 2.1, equation 2-1). Included on the graph are $\delta^{18}O$:$\delta^{15}N$ slopes of 0.5 which are a typical signal of denitrification.

In addition to NO_3^- from soil organic matter and manure/septic system effluent evidence of NO_3^- from atmospheric deposition and inorganic NO_3^- fertilizers is apparent in

groundwater in the October 2006 to June 2007 period (Figure 4-7). NO_3^- from the expected range for fertilizer also fall on the 0.5 $\delta^{18}O$:$\delta^{15}N$ slope for denitrification which connects to a data point near +20‰ and +35‰ for $\delta^{15}N$ and $\delta^{18}O$, respectively. The potential for denitrification of NO_3^- in groundwater is possible though the relationship between the natural log (ln) of NO_3^- concentration and isotopes doesn't provide evidence of denitrification (Figure 4-8). The only strong and significant relationship is at Harris tile, between ln NO_3^- and $\delta^{15}N$-NO_3^- ($R2 = 0.65$, $p = 0.05$) (Figure 4-8).

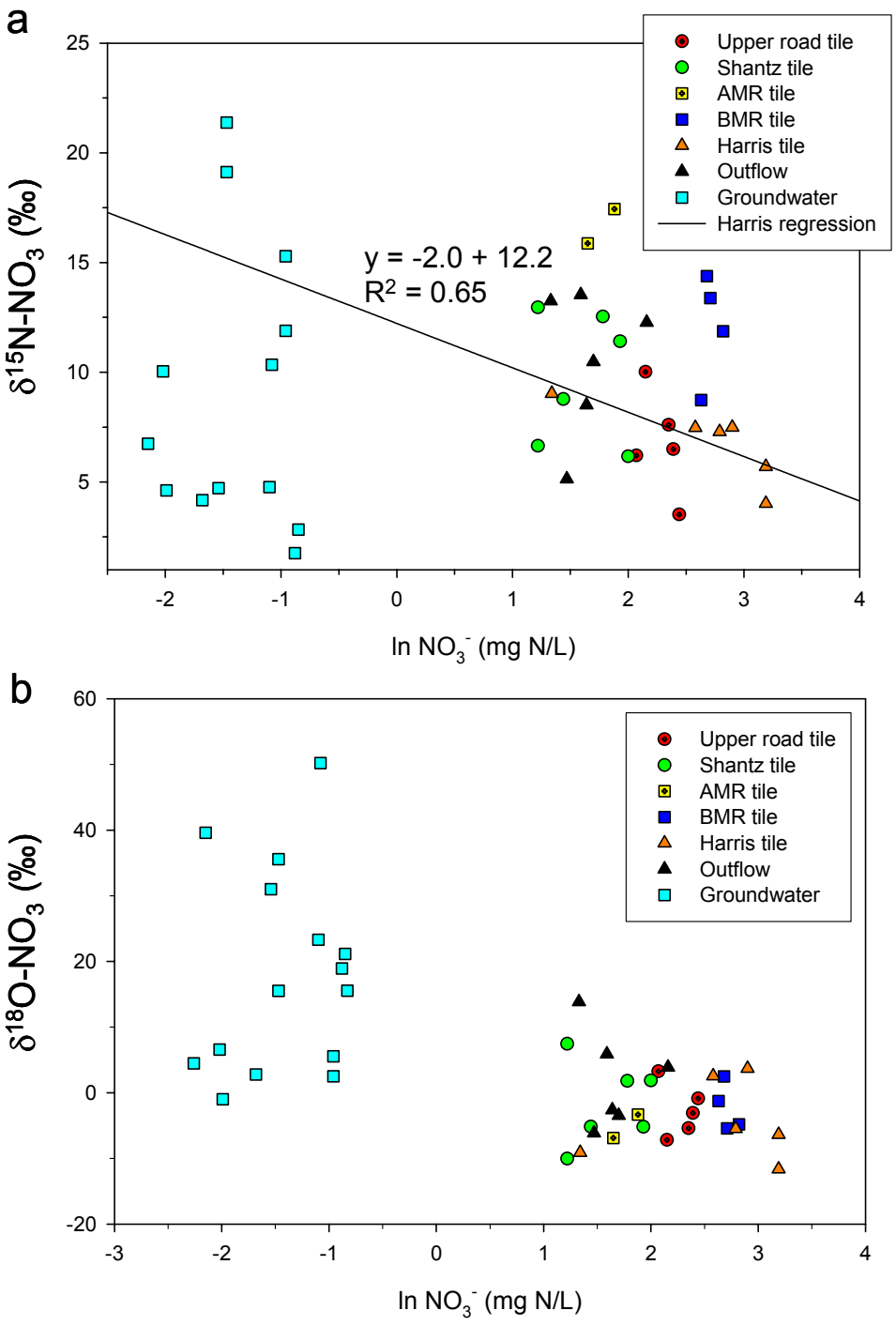

Figure 4-8: The relationship between the natural log (ln) of NO_3^- concentration and (a) $\delta^{15}N$-NO_3^- and (b) $\delta^{18}O$-NO_3^- for the October 2006 to June 2007 dataset.

4.4.3.2 Fall 2007

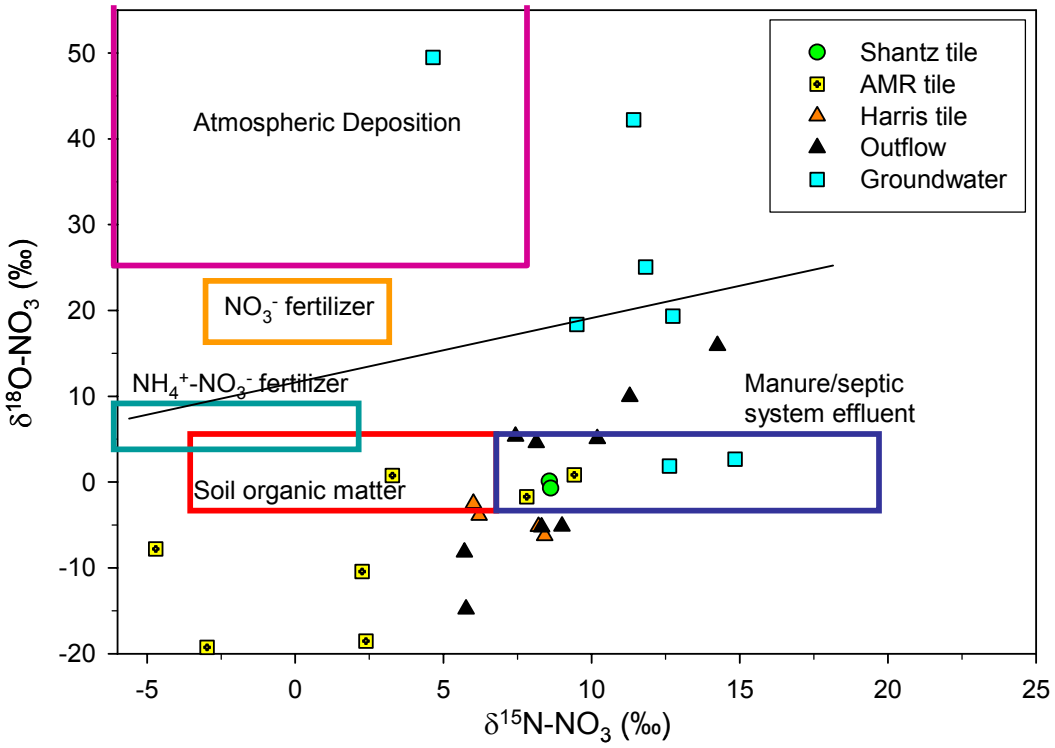

Figure 4-9: $\delta^{15}N$ and $\delta^{18}O$ of NO_3^- from Fall 2007. Expected ranges of sources were constructed as in Figure 4-7. Included on the graph is a $\delta^{18}O$:$\delta^{15}N$ slope of 0.5 which is a typical signal of denitrification.

Evidence of NO_3^- from atmospheric deposition is apparent in Fall 2007 (Figure 4-9). NO_3^- concentrations in groundwater are very low (<1 mg N/L) here and atmospheric sources would also be very low. High $\delta^{18}O$-NO_3^- values (around +20‰) could be due to mixing of atmospheric source with manure/septic system effluent sources or denitrification of NH_4^+-NO_3^- fertilizers. A strong relationship between the natural log (ln) of NO_3^- concentration and $\delta^{15}N$-NO_3^- ($R^2 = 0.78$, $p = 0.004$) (Figure 4-10a) and $\delta^{18}O$-NO_3^- ($R^2 = 0.93$, $p = 0.0001$) (Figure 4-10b) for outflow data could be also caused by denitrification. However, a $\delta^{18}O$:$\delta^{15}N$ slope of 3.0 for outflow NO_3^- is contradictory to this evidence (Figure 4-9). The strong and significant relationship between lnNO_3^- and

δ^{15}N-NO_3^- at the Harris tile (R^2 = 0.75, p = 0.13) and between lnNO_3^- and δ^{18}O-NO_3^- for groundwater (R^2 = 0.56, p = 0.09) could also be caused by denitrification.

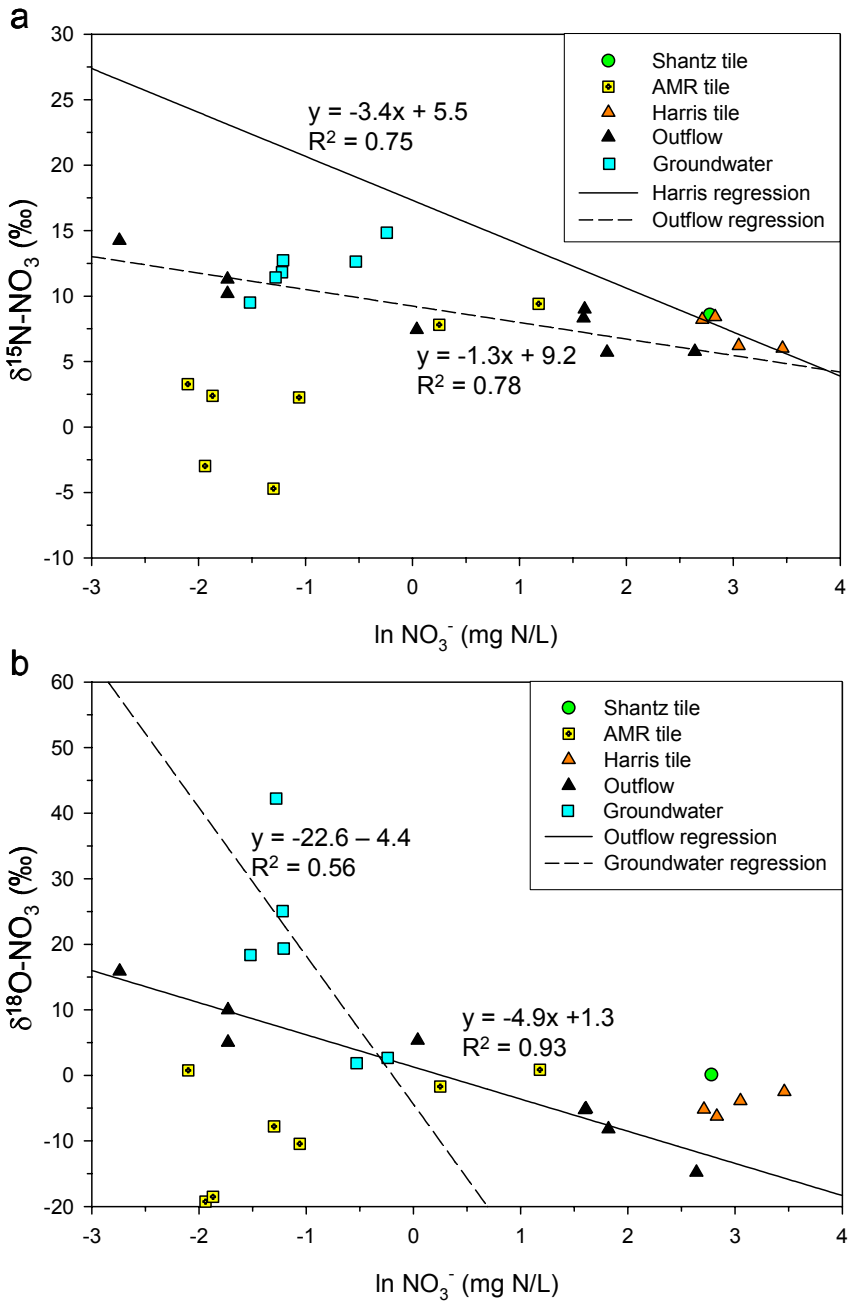

Figure 4-10: The relationship between the natural log (ln) of NO_3^- concentration and (a) δ^{15}N-NO_3^- and (b) δ^{18}O-NO_3^- for Fall 2007.

4.4.4 $\delta^{15}N$ and $\delta^{18}O$ of N_2O

4.4.4.1 October 2006 to June 2007

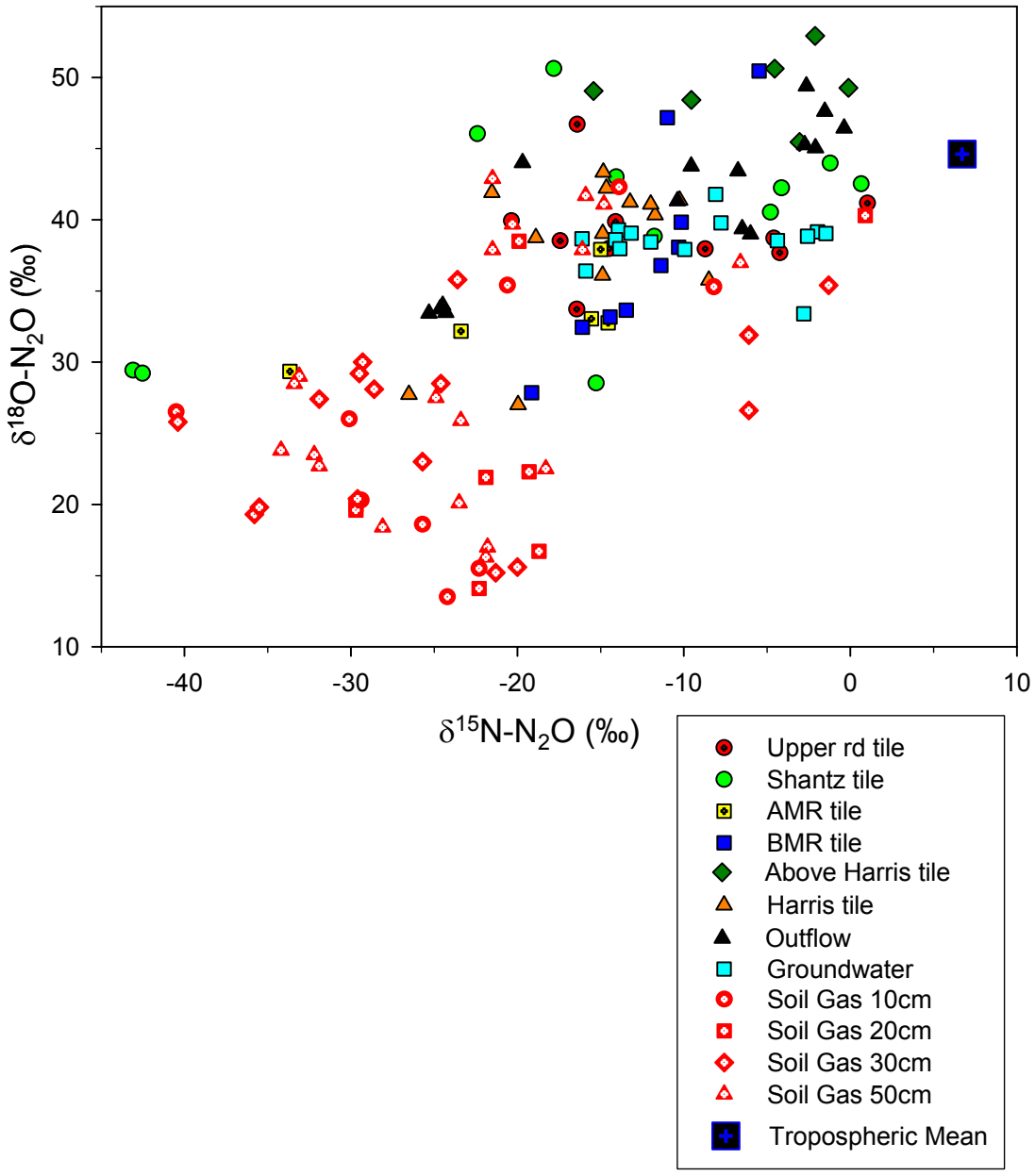

Figure 4-11: $\delta^{15}N$ and $\delta^{18}O$ of N_2O for October 2006 to June 2007. Soil gas N_2O data was provided by John Spoelstra (2007, unpublished data). The tropospheric mean value is +6.7‰ +/- 0.12 ($\delta^{15}N$) and +44.6‰ +/- 0.21 ($\delta^{18}O$) (Kaiser, 2002).

Table 4-5: Average, standard deviation, and range of N_2O isotopes for October 2006 to June 2007

Site	Number of samples	$\delta^{15}N\text{-}N_2O$				$\delta^{18}O\text{-}N_2O$			
		Average	Standard Deviation	Range		Average	Standard Deviation	Range	
				Min.	Max.			Min.	Max.
Upper Road tile	10	-11.6	7.0	-20.3	1.0	39.2	3.3	33.7	46.7
Shantz tile	10	-13.4	12.8	-42.8	0.6	40.6	6.9	28.5	50.6
AMR tile	6	-20.4	8.2	-33.7	-14.6	33.1	3.1	29.3	37.9
BMR tile	9	-12.4	3.9	-19.1	-5.5	37.7	7.2	27.9	50.5
Above Harris tile	6	-5.8	5.7	-15.4	-0.1	49.3	2.5	45.5	52.9
Harris tile	12	-16.6	5.5	-26.5	-10.3	38.3	5.5	27.0	43.3
Outflow	13	-9.0	8.6	-24.9	-0.4	42.5	4.9	33.6	49.4
Groundwater	15	-9.2	5.4	-16.1	-1.5	38.5	1.8	33.4	41.8

$\delta^{15}N\text{-}N_2O$ ranges from -42.8‰ to +1.0‰ while $\delta^{18}O$ ranges from +27.0‰ to +52.9‰ (Table 4-5). The average $\delta^{15}N\text{-}N_2O$ and $\delta^{18}O\text{-}N_2O$ values for groundwater are -9.2‰ and

38.5‰, respectively. The Harris tile average for $\delta^{18}O\text{-}N_2O$ (38.37‰) is very similar to ground water though there is a larger range for this site, largely a result of two depleted outliers (27.01‰ and 27.73‰) collected in April 2007. The average $\delta^{15}N\text{-}N_2O$ value for Harris tile (-16.6‰) is lower than that of groundwater (-9.2‰).

Average $\delta^{15}N\text{-}N_2O$ values for Upper Road, Shantz, and BMR tiles are similar at -13.24‰, -14.77‰, and -14.65‰, respectively while standard deviations are variable at 7.0‰, 12.8‰, and 3.9‰, respectively (Table 4-5). Average $\delta^{18}O\text{-}N_2O$ values for Upper rd, Shantz, and BMR tiles are 36.00‰, 39.06‰, and 36.39‰ while standard deviations are 3.3‰, 6.9‰, and 7.2‰, respectively.

The average $\delta^{15}N\text{-}NO_3^-$ value for AMR tile is -19.89‰ with a range of -33.7‰ to -14.6‰ while the average $\delta^{18}O\text{-}N_2O$ value is 30.6‰ with a range of +29.3‰ to +37.9‰(Table 4-5). N_2O isotopes from this site are distinctly lower from those of groundwater, other tiles, and stream locations (Figure 4-11). Generally speaking $\delta^{15}N$ and $\delta^{18}O$ values of N_2O from the stream samples collected at the Outflow and above Harris tile are higher than other N_2O isotopes measured in tiles and groundwater at Strawberry Creek. Average $\delta^{15}N\text{-}N_2O$ for Outflow and above Harris tile are -9.05 and -5.8‰, respectively. Average $\delta^{18}O\text{-}N_2O$ was +42.29 and +42.46 for Outflow and above Harris tile, respectively (Table 4-5).

$\delta^{18}O$:$\delta^{15}N$ slopes are indicative of trends within the data at individual sites. Upper road tile, above Harris tile, and groundwater all have very shallow negative or positive slopes (-0.067 to 0.096) with low regression coefficients. AMR tile, Harris tile, and Outflow have slopes of 0.28 ($R^2 = 0.56$, $p = 0.15$), 0.64 ($R^2 = 0.47$, $p = 0.06$), and 0.45 ($R^2 = 0.62$, $p = 0.0001$). The steepest slope (1.65) was measured at BMR tile ($R^2 = 0.81$, $p = 0.001$).

Soil Gas flux $^{18}O\text{-}N_2O$ isotopes collected by Spoelstra (2007, unpublished data) from February to June 2007 show a range of ~+10 to +45‰. One grouping of data points has $\delta^{15}N\text{-}N_2O$ values of -40 to -18‰ while $\delta^{18}O\text{-}N_2O$ values are less than +30‰. Another grouping of data has higher $\delta^{15}N$ and $\delta^{18}O$ values which places them in a range with values from the tiles. Most of the data points from this second grouping are from 50cm

depth, though other depths are also represented. This separation of two distinct groups likely shows the difference between N_2O produced in the unsaturated zone versus saturated zone production.

The relationship between the natural log (ln) of N_2O concentration and $\delta^{15}N\text{-}N_2O$ is strong and significant for all sites except Upper Road tile, Shantz tile, and groundwater in the October 2006 to June 2007 (Figure 4-12). The relationship between ln N_2O concentration and $\delta^{18}O\text{-}N_2O$ is strong and significant for Shantz tile ($R^2 = 0.52$, $p = 0.06$), AMR tile ($R^2 = 0.64$, $p = 0.1$), and Outflow ($R^2 = 0.56$, $p = 0.003$) (Figure 4-12).

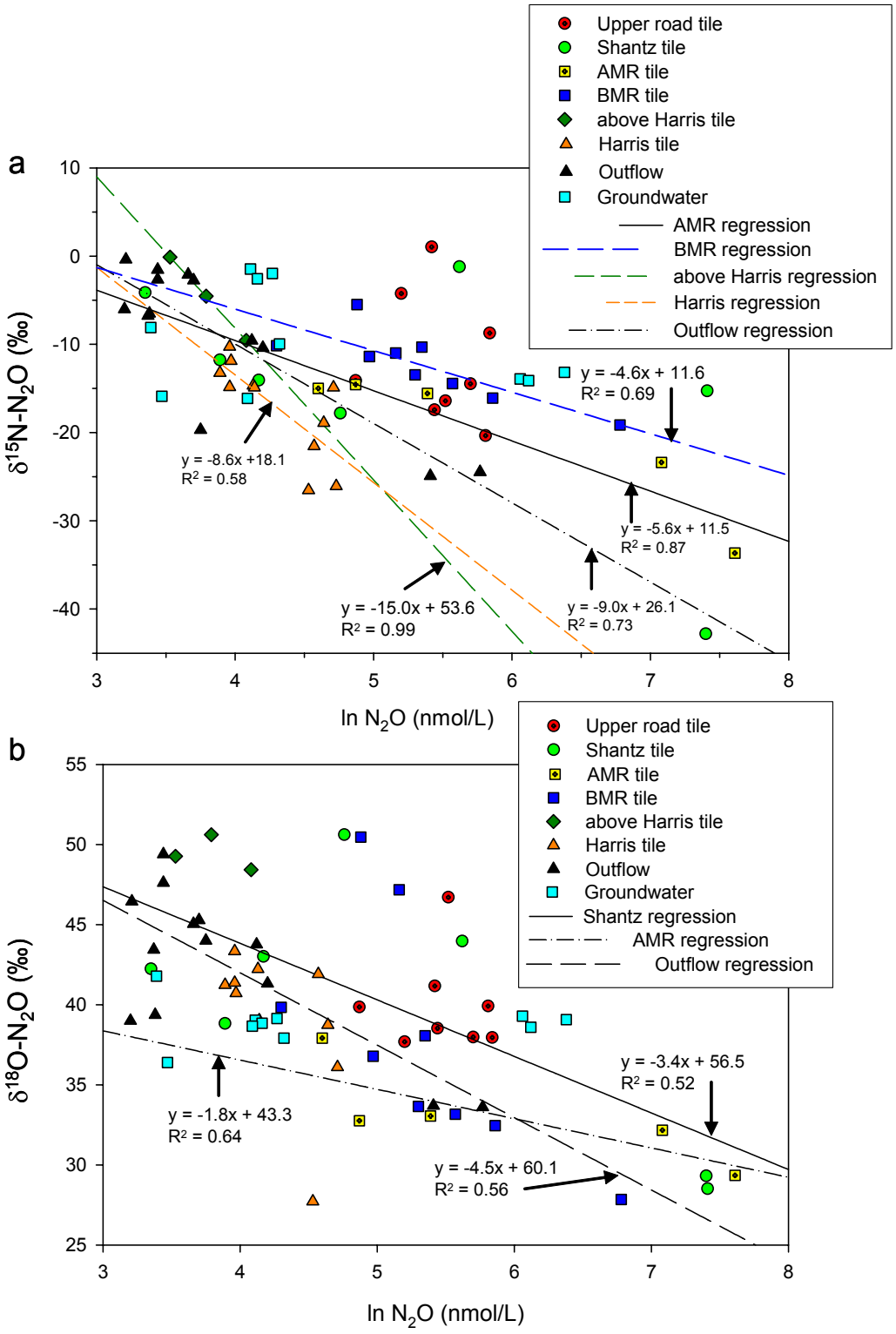

Figure 4-12: The relationship between the natural log (ln) of N_2O concentration and (a) $\delta^{15}N$-N_2O and (b) $\delta^{18}O$-N_2O for the October 2006 to June 2007 period.

4.4.4.2 Fall 2007

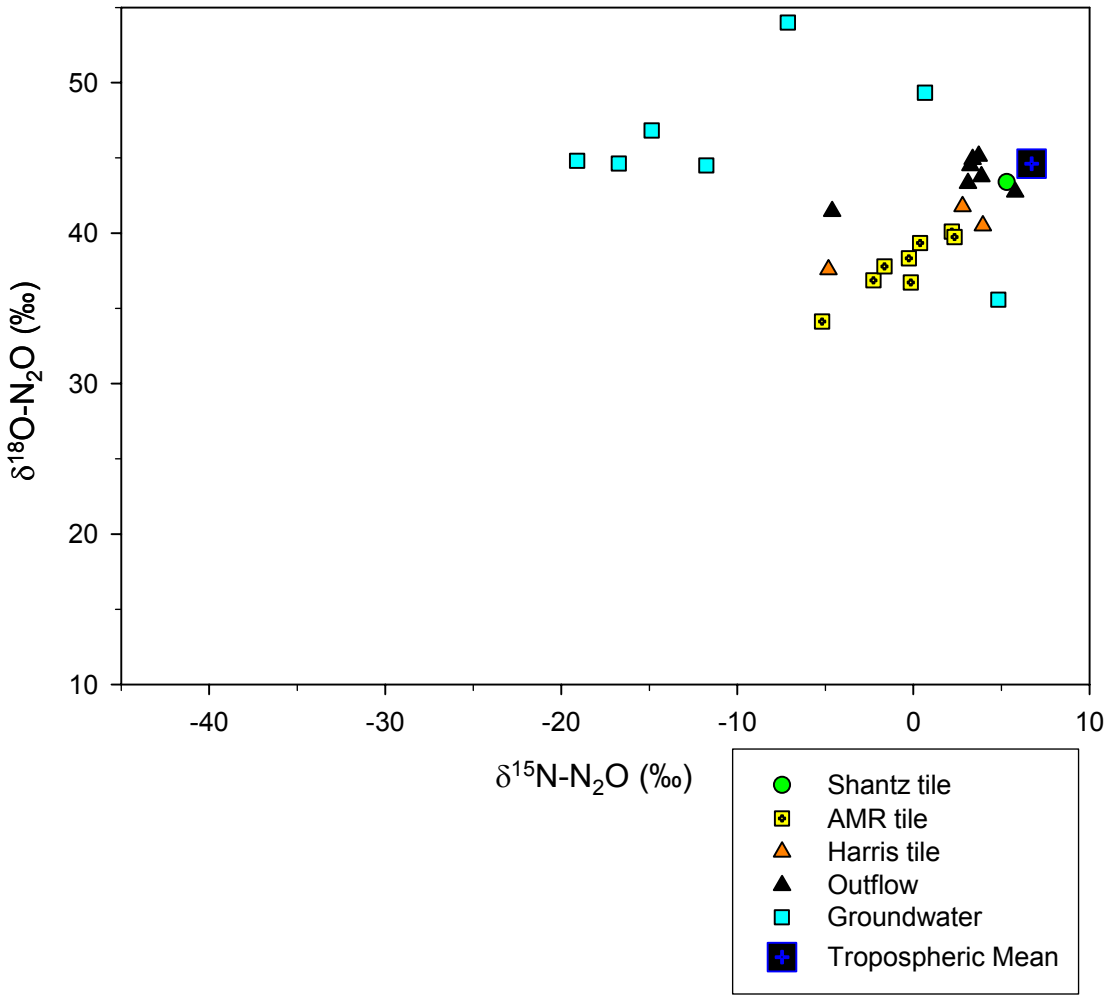

Figure 4-13: $\delta^{15}N$ and $\delta^{18}O$ of N_2O for Fall 2007.

Table 4-6: Average, standard deviation, and range of N_2O isotopes for Fall 2007

Site	Number of samples	$\delta^{15}N$-N_2O				$\delta^{18}O$-N_2O			
		Average	Standard Deviation	Range		Average	Standard Deviation	Range	
				Min.	Max.			Min.	Max.
Shantz tile	2	9.5	5.9	5.3	13.6	41.5	2.7	39.6	43.4
AMR tile	8	-0.6	2.5	-5.2	2.3	37.9	2.0	34.1	40.1
Harris tile	4	1.9	4.6	-4.8	5.6	40.0	2.2	37.6	41.8
Outflow	8	4.1	5.3	-4.6	14.7	43.5	1.3	41.4	45.1
Groundwater	7	-9.2	9.0	-19.1	4.8	45.7	5.6	35.6	54.0

Average $\delta^{15}N$ of N_2O during Fall 2007 ranges from -0.58 to 4.14‰ for tiles and the outflow and is -9.16 for groundwater (Figure 4-13). Average $\delta^{18}O$ of N_2O ranges from

+37.88 to +43.52‰ for tiles and outflow and is +45.67‰ for groundwater. This generally places the data closer to the tropospheric mean than for the October 2006 to June 2007 data (Figure 4-11).

Shallow positive and negative $\delta^{18}O$:$\delta^{15}N$ slopes (-0.45 to 0.01) come from Shantz tile, Outflow, and groundwater while medium slopes of 0.76 and 0.41 are found at AMR and Shantz tile, respectively.

The relationship between the natural log (ln) of N_2O concentration and $\delta^{15}N$-N_2O is strong and significant for Harris tile ($R^2 = 0.99$, $p = 0.005$), Outflow ($R^2 = 0.65$, $p = 0.02$), and groundwater ($R^2 = 0.63$, $p = 0.03$) in the Fall 2007 data set (Figure 4-14). Only Harris tile has a strong and significant relationship between ln N_2O concentration and $\delta^{18}O$-N_2O ($R^2 = 0.91$, $p = 0.19$) (Figure 4-14). The importance of decreasing lnN_2O concentrations with increasing N_2O isotopes is that this is often indicative of a fractionating process, in this instance associated with N_2O production, N_2O consumption, or gas exchange. As such these processes could be responsible for the trends observed in the N_2O isotope data (ie: $\delta^{18}O$:$\delta^{15}N$ slopes). The possible influence of these processes at the various sites will be discussed further.

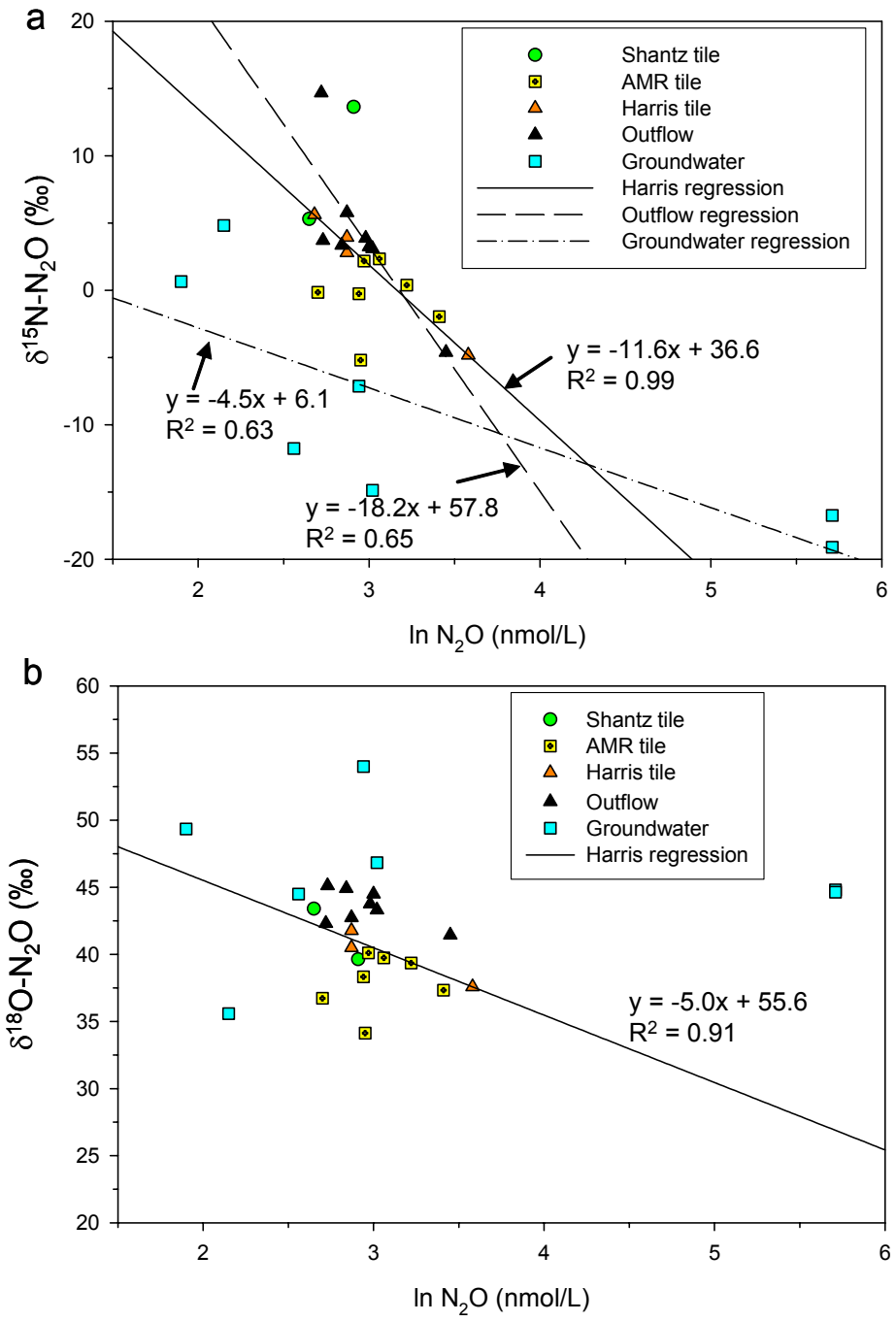

Figure 4-14: The relationship between the natural log (ln) of N_2O concentration and (a) $\delta^{15}N$-N_2O and (b) $\delta^{18}O$-N_2O for Fall 2007

4.4.5 Isotopic Shifts

For October 2006 to June 2007 data, $\Delta^{15}N\text{-}N_2O$ ranges from -17.0 (groundwater) to -24.2‰ (AMR tile) (Table 4-7). Shantz, AMR, BMR, and Harris tiles have similar $\Delta^{15}N$ (-24.2 to -23.0) though the standard deviation of Shantz and AMR tiles (13.0 and 12.2, respectively) is much greater than that of BMR and Harris tiles (4.6 and 5.7, respectively). For Fall 2007 data, $\Delta^{15}N\text{-}N_2O$ ranges from -20.25 (groundwater) to 0.87‰ (Shantz tile) while $\Delta^{15}N$ of -4.5, -5.3, and -4.8‰ is measured at AMR, Harris, and Outflow, respectively (Table 4-8). Standard deviation is between 4.8 and 5.9‰ except for groundwater which has a standard deviation of 9.6‰. Altogether $\Delta^{15}N$ is much less negative and less variable for the Fall 2007 dataset than for the October 2006 to June 2007 dataset.

$\Delta^{18}O\text{-}N_2O$ for the October 2006 to June 2007 period (Table 4-7) is between +38.1 and +44.3‰ with the exception of groundwater (20.35‰). Standard deviation for tiles and outflow are between 5.6 and 9.1‰ and 15.5‰ for groundwater. $\Delta^{18}O\text{-}N_2O$ for Fall 2007 is between 41.83 to 45.35‰, again with the exception of groundwater (22.95‰) (Table 4-8). Standard deviation is small for Shantz and Harris tiles (2.7‰), larger for AMR tile (8.6‰) and Outflow (9.8‰), and largest for groundwater (19.0‰). $\Delta^{18}O$ is similar between the two events for most sites, including the variation with these shifts.

Table 4-7: Calculated range of isotopic shifts for denitrification ($\Delta_{N2O\text{-}NO3^-}$) for the October 2006 to June 2007 period. These were calculated as the difference between average N_2O and NO_3^- isotopes for the compiled dataset of each site. Standard deviation reported is the square root of the sum of squares from NO_3^- and N_2O isotope datasets.

	$\delta^{15}N$		$\delta^{18}O$	
Site	**Shift**	**Standard Deviation**	**Shift**	**Standard Deviation**
Upper road tile	-20.7	6.6	38.1	7.2
Shantz tile	-23.3	13.0	40.6	9.1
AMR tile	-24.2	12.2	44.3	5.6
BMR tile	-23.4	4.6	40.3	9.0
Harris tile	-23.0	5.7	42.4	8.0
Outflow	-18.9	9.1	41.3	7.6
Groundwater	-17.0	8.7	20.4	15.5

Table 4-8: Calculated range of isotopic shifts for denitrification ($\Delta_{N2O\text{-}NO3^-}$) for Fall 2007. These were calculated as the difference between average N_2O and NO_3^- isotopes for the compiled dataset of each site. Standard deviation reported is the square root of the sum of squares from NO_3^- and N_2O isotope datasets.

	$\delta^{15}N$		$\delta^{18}O$	
Site	**Shift**	**Standard Deviation**	**Shift**	**Standard Deviation**
Shantz tile	0.9	5.9	41.8	2.7
AMR tile	-4.5	5.2	45.3	8.6
Harris tile	-5.3	4.8	44.4	2.7
Outflow	-4.8	5.9	42.7	9.8
Groundwater	-20.2	9.6	23.0	19.0

4.5 Discussion

4.5.1 NO_3^- and N_2O concentrations

During baseflow conditions NO_3^- concentrations at the outflow remain below the 10 mg N/L drinking water limit. Lower NO_3^- concentrations at Strawberry Creek during baseflow conditions are consistent with the findings of Macrae et al. (2007). However, NO_3^- concentrations above 10 mg N/L consistently measured from Upper Road, BMR, and Harris tiles (October 2006 to June 2007) continue to pose a threat to the health of aquatic organisms (Figure 4-2). Fall 2007 is a good example of NO_3^- concentration dynamics in tiles and streams during low flow conditions (Figure 4-4). Due to the long drought before the Fall 2007 period, NO_3^- would have built up in the soil, though a slow increase in the water table following several small precipitation events was not enough to flush it from the unsaturated zone. If a high magnitude event followed the long drought, higher concentrations of NO_3^- would be expected from tiles and in stream. For example, AMR tile and Outflow had higher average NO_3^- concentrations during the 2008 mid-winter thaw than in the Fall 2007 (Chapter 3, Section 3.4.2.2). High groundwater NO_3^- concentrations during the 2008 mid-winter thaw indicate that significant build-up of NO_3^- had occurred during the drought period. The extreme difference in hydrologic conditions between the Fall 2007 and 2008 mid-winter thaw exemplifies the difference in NO_3^-

concentration dynamics between periods of baseflow and high magnitude events at Strawberry Creek.

N_2O concentrations at the stream outflow, and probably along the entire course of the stream, remain a consistent source of flux to the atmosphere throughout the annual range of hydrologic conditions at Strawberry Creek (Figure 4-3 and Figure 4-4). However, higher stream concentrations during precipitation and snowmelt events show that these are periods of higher flux to the atmosphere. Tiles are a source of N_2O to the stream during baseflow conditions and with concentrations above atmospheric saturation rapid gas exchange downstream of tile inputs is expected (Reay et al. 2003). The influence of tile N_2O concentrations on the stream is exemplified with similar N_2O concentrations between Harris tile and the Outflow in October 2006 (Figure 4-3). Groundwater N_2O concentrations can also be above atmospheric saturation, and are a source of stream N_2O along its course. The role of groundwater N_2O inputs are exemplified on November 21-23, 2007 when concentrations from the Harris tile are lower than at the outflow.

Despite the long drought before the Fall 2007 period, high concentrations of NO_3^- and N_2O are not measured at sampling sites due to a slowly rising water table (Figure 4-4). This would have left NO_3^- within the unsaturated soil profile and would have allowed N_2O the time to escape to the atmosphere. High concentrations of N_2O in tiles and streams from January 2008 melt (Chapter 3) show that N_2O was accumulating during this period. As with NO_3^- concentrations, comparison of the Fall 2007 period with the 2008 mid-winter thaw provides insight into how N_2O concentrations are largely determined by hydrologic conditions within the catchment.

4.5.2 Sources and Processes of NO_3^-

Identification of NO_3^- sources using expected ranges from the literature and calculations for Strawberry Creek, reveals similar sources between the October 2006 to June 2007 and Fall 2007 periods. NO_3^- from mainly manure/septic system effluent and also soil organic matter is consistent with the results archived tile data (Chapter 2) and the 2007 Springmelt (Chapter 3). Also consistent with Chapter 3 data are many $\delta^{18}O$-NO_3^- values around -10

to 0‰ and some values as low as -20‰ from the AMR tile during both periods (Figure 4-7). As discussed in section 3.5 a $\delta^{18}O\text{-}NO_3^-$ value of -10 would require that $\delta^{18}O\text{-}H_2O$ is -26.9‰ assuming that $\delta^{18}O\text{-}O_2$ is +23.5‰. This also assumes that 1/3 of the NO_3^- oxygen is from atmospheric O_2 and 2/3 are from water (Andersson and Hooper, 1983; Kumar et al., 1983; Hollocher, 1984). The lowest monthly mean-weighted average $\delta^{18}O\text{-}H_2O$ values collected from Simcoe, Ontario are -13.1, -17.1, and -14.2‰ for December, January, and February, respectively. Other possibilities include analytical interference by NO_2 though Casciotti et al. (2007) state that if NO_2 concentration is less than 2% of total NO_2 and NO_3^-, which was confirmed in our samples, there would be no detectable effect (<0.5‰) using this method. Even if NO_2 was 2% of total NO_2 and NO_3^-, $\delta^{18}O\text{-}NO_2$ would have to be around -500‰, assuming an original $\delta^{18}O\text{-}NO_3^-$ of 0‰.

Additionally, the theory that one third of nitrate oxygen is from atmospheric O_2 and two thirds are from water does not always hold true. For example, Snider et al. (2008) show that 80% of oxygen can come from water while the other 20% can come from atmospheric O_2. Using this ratio with the January mean monthly average of -17‰ produces a $\delta^{18}O\text{-}NO_3^-$ of -8.9‰. Low $\delta^{18}O\text{-}NO_3^-$ values could reflect the changing ratio of oxygen contributed from either water or atmospheric O_2.

Evidence of NO_3^- from atmospheric deposition in groundwater is another unexpected observation considering previous measurements of groundwater NO_3^- isotopes at Strawberry Creek. Atmospheric source NO_3^- during the 2007 springmelt was considered reasonable since it was measured at low concentrations (<1 mg N/L) in the deciduous headwaters. All NO_3^- concentrations of the groundwater samples are also below 1 mg N/L for both October 2006 to June 2007 and Fall 2007 datasets. Consistent $\delta^{18}O\text{-}NO_3^-$ values are also measured at several peizometers between the two datasets. For example from the Cabrera A-A' transect peizometer "F15" measured $\delta^{18}O$ of +23.31‰ and +25.06‰ on April 19 and December 7 of 2007. "F18" of the same transect measured $\delta^{18}O\text{-}NO_3^-$ of +50.21‰ and +42.22‰ on April 19 and December 7 of 2007. Contamination from direct precipitation inputs is unlikely since wells were capped and also purged before

sampling. The groundwater from the October 2006 to June 2007 came from sampling on April 19, 2007 which means that NO_3^- from the snowpack of the 2007 Springmelt could have been in those waters. However, water from that event would have likely not been sampled in groundwater on December 7, 2007 (Figure 4-7b) since the aquifer was sampled after recharge from precipitation in Fall 2007. Although it is unexpected, consistent NO_3^- concentrations and isotopes in groundwater are suggestive of NO_3^- from atmospheric sources.

NO_3^- from inorganic fertilizer sources in groundwater measured during October 2006 to June 2007 is also unexpected. NO_3^- isotopes within this range may be influenced by denitrification since they fall along a $\delta^{18}O$:$\delta^{15}N$ slope of 0.5, which would be reasonable to measure in a riparian groundwater transect. Groundwater samples at +20±5‰ ($\delta^{18}O$) from Fall 2007 may also have a similar original source, that have been significantly altered by denitrification.

4.5.3 Sources and Processes of N_2O

N_2O in groundwater at Strawberry Creek is produced by denitrification (Figure 4-7 and Figure 4-9). $\delta^{15}N$ and $\delta^{18}O$ of N_2O is in the range of N_2O measured by Well et al. (2005) which they concluded was a product of denitrification. Additionally, the range of calculated isotopic shifts ($\Delta_{N2O\text{-}NO3}$) for $\delta^{15}N$ (-4.74 to -32.56‰) and $\delta^{18}O$ (-0.78 to +46.69‰) are within the bounds of isotopic shifts reported for denitrification from incubation studies (Chapter 1, Appendix 1). Perez et al. (2000) also suggest that if water filled pore space (WFPS) is greater than 60%, which would be the case in the saturated zone at Strawberry Creek, denitrification will be the dominant pathway. Dissolved oxygen concentrations in Strawberry groundwater have typically been measured at less than 1 mg/L which would also promote the anaerobic conditions for denitrification.

In aerobic aquifers Wada and Ueda (1996) and Ueda et al. (1999) also measured comparable $\delta^{15}N$ and $\delta^{18}O$ of N_2O values to those of Strawberry Creek and to those reported by Well et al. (2005) though N_2O was produced by nitrification (or nitrifier denitrification). Wada and Ueda (1996) explain that the small ^{15}N nitrification

fractionation factors (ε_{NH4^+-N2O} = -9 to -33‰) were caused by NH_4^+ limitation on nitrification, though they do not exclude the possibility microsite denitrification. Comparible enrichment factors between nitrification and denitrification suggest that they cannot be used for pathway determination without considering aquifer conditions, as above.

Calculated isotopic shifts ($\Delta_{N2O-NO3}$) for Strawberry Creek tiles during the October 2006 to June 2007 period range from -8.02 to -38.53‰ for ^{15}N and +27.68 to +53.77‰ for ^{18}O which are similar to values reported from denitrification incubation studies (Table 4-7). N_2O from AMR and Harris tiles have $\delta^{18}O$:$\delta^{15}N$ slopes of 0.28 (R^2 = 0.56, p = 0.15) and 0.64 (R^2 = 0.62, p = 0.0001), respectively, a range that was observed earlier in Chapter 3. As residual NO_3^- isotopes following denitrification are typically enriched at a $\delta^{18}O$:$\delta^{15}N$ ratio of 0.5 to 1.0, N_2O produced by this enriching substrate should also produce a similar $\delta^{18}O$:$\delta^{15}N$ slope, if the system is open system (Mengis et al., 1999, Aravena and Robertson, 1998; Wassenaar, 1995). However, this effect on N_2O isotopes still needs to be unequivocally proven through combined incubation and field sampling experiments.

It is reasonable to assume that if N_2O isotopes show a $\delta^{18}O$:$\delta^{15}N$ slope of 0.5 to 1.0 due to substrate enrichment, it would also be observed in the NO_3^- isotopes. As NO_3^- consumption would result in decreasing NO_3^- concentrations less N_2O may be produced because the NO_3^- pool would be smaller. With a $\delta^{18}O$:$\delta^{15}N$ slope of 0.28, the AMR tile (October 2006 to June 2007 dataset) is a good example of how this could occur (Figure 4-11). A strong positive relationship between regression of NO_3^- and N_2O concentration at AMR tile (R^2 = 0.88, p = 0.0001) (Figure 4-5) and there is also a strong relationship between lnN_2O concentration and both $\delta^{15}N$-N_2O (R^2 = 0.87, p = 0.02) and $\delta^{18}O$-N_2O (R^2 = 0.64, p = 0.1) (Figure 4-12). For the Fall 2007, Harris tile also had $\delta^{18}O$:$\delta^{15}N$ ratios of 0.41 (R^2 = 0.83, p = 0.27) (Figure 4-13) and a highly correlated (R^2 = 0.93, p = 0.03), positive relationship between NO_3^- and N_2O concentration (Figure 4-6). Negative relationships between lnN_2O concentration and $\delta^{15}N$-N_2O (R^2 = 0.99, p = 0.005) and $\delta^{18}O$-N_2O (R^2 = 0.91, p = 0.19) (Figure 4-14) were also strong and significant as were the

relationships between $\ln NO_3^-$ concentration and $\delta^{15}N\text{-}NO_3^-$ ($R^2 = 0.75$, $p = 0.13$) and $\delta^{18}O\text{-}NO_3^-$ ($R^2 = 0.81$, $p = 0.1$) (Figure 4-10). These patterns are all indicative of NO_3^- consumption. For the Fall 2007 N_2O from AMR tile also had $\delta^{18}O{:}\delta^{15}N$ ratios of 0.76 ($R^2 = 0.88$) (Figure 4-13) and strong relationship between NO_3^- and N_2O concentration ($R^2 = 0.93$, $p = 0.03$) (Figure 4-6). The relationships between $\ln N_2O$ concentration and $\delta^{15}N\text{-}N_2O$ ($R^2 = 0.87$, $p = 0.02$) and $\delta^{18}O\text{-}N_2O$ ($R^2 = 0.64$, $p = 0.1$) (Figure 4-14) are strong and significant, as is the relationship between $\ln NO_3^-$ and $\delta^{15}N\text{-}NO_3^-$ ($R^2 = 0.54$, $p = 0.06$) (Figure 4-10a).

However, it is also possible that $\delta^{18}O{:}\delta^{15}N$ slopes of 0.5 to 1.0 would not be observed for NO_3^- even if it was observed for N_2O due to substrate consumption. First of all, N_2O is a sensitive indicator of denitrification and can be produced by a small amount of NO_3^- in anaerobic microsites. Degradation of a small amount of NO_3^- at a microsite would likely not be measured in a collective NO_3^- pool measured at a tile outlet since this pool would also include non-degraded NO_3^- sources as we have seen in this and other chapters (Chapter 2 and Chapter 3). Similarly, significant changes in NO_3^- concentrations may also not be measured because of NO_3^- consumption at tile outlets since the amount consumed may be small. However, as N_2O is likely produced in anaerobic microsites, enriching N_2O isotopes with decreasing concentration should be observable as less N_2O would be produced from a smaller (more enriched) NO_3^- pool. For the October 2006 to June 2007 dataset, Harris tile could represent this scenario. For N_2O isotopes the $\delta^{18}O{:}\delta^{15}N$ slope is 0.64 with a fairly strong regression coefficient ($R^2 = 0.47$, $p = 0.06$) (Figure 4-11). However a relationship between NO_3^- and N_2O doesn't exist ($R^2 = 0.022$) and, despite negative relationships, correlation between $\ln N_2O$ concentration and $\delta^{18}O\text{-}N_2O$ ($R^2 = 0.30$, $p = 0.1$) (Figure 4-12a) and between $\ln NO_3^-$ concentration and $\delta^{18}O\text{-}NO_3^-$ ($R^2 = 0.01$, $p = 0.82$) (Figure 4-8a) are also weak.

For the October 2006 to June 2007 dataset, the outflow also has a well correlated ($R^2 = 0.62$) $\delta^{18}O{:}\delta^{15}N$ slope of 0.45 (Figure 4-11). There is also negative relationships and good correlation between $\ln N_2O$ concentration and $\delta^{15}N\text{-}N_2O$ ($R^2 = 0.73$, $p = 0.0002$) and $\delta^{18}O\text{-}$

N_2O ($R^2 = 0.56$, $p = 0.003$) (Figure 4-12). This could be indicative of NO_3^- consumption either as a stream process or as a signal from tile input, most likely from Harris tile. Gas exchange must also be considered as Reay et al. (2003) suggest that it will occur more rapidly than biological processes such as NO_3^- or N_2O consumption. Modeling of N_2O concentrations and isotopes, as in Section 3.5 (Equation 3-1), showed that the isotopic effects of gas exchange can be significant but that the original source signature of N_2O can be calculated (Thuss and Schiff, 2008). This analysis also showed that the calculated N_2O endmember can represent the average N_2O isotope values of the source.

As explained in Section 3-5, calculation of a N_2O endmember was performed by regression analysis of the inverse of N_2O concentration and the N_2O isotope species. This is known as a Keeling analysis for determining the original source signature of a pool that has mixed with a background pool (Pataki et al., 2003). The y-intercept of this analysis is the original isotopic signature of the pool mixing with, in our case, atmospheric N_2O. The results of this analysis show an original $\delta^{15}N\text{-}N_2O$ of -23.0‰ (October 2006 to June 2007) and -16.6‰ (Fall 2007) (Figure 4-15). The significance of these results is that original $\delta^{15}N\text{-}N_2O$ is more negative than what is normally measured in the stream. The implication of this is that isotopic shifts for denitrification ($\Delta_{N2O\text{-}NO3^-}$) could be greater than if calculated as in Table 4-7 and Table 4-8. Using the N_2O endmember results, the ^{15}N isotopic shift ($\Delta_{N2O\text{-}NO3^-}$) for the October 2006 to June 2007 dataset is -31.8‰ (a change of -12.9‰) and -25.5‰ (a change of -20.7‰) for the Fall 2007 dataset. These isotopic shifts are still within the range of what is expected for denitrification. The similarity in values between the two datasets implies a consistent $\delta^{15}N\text{-}N_2O$ value for the stream, which allows for characterization of that source signature. Weak and insignificant relationships were produced for the same analysis for $\delta^{18}O\text{-}N_2O$.

Other trends present in the N_2O data include a $\delta^{18}O{:}\delta^{15}N$ slope of 1.65 at BMR tile for the October 2006 to June 2007 dataset (Figure 4-12). Several incubation and field studies have found that a $\delta^{18}O{:}\delta^{15}N$ slope of 2.5 is most indicative of N_2O consumption though the ratio can be as low as 2 (Menyailo & Hungate 2006, Vieten et al 2007, Mandernack

2000). Negative relationships between N_2O concentration and $\delta^{15}N$ ($R^2 = 0.64$) and $\delta^{18}O$ ($R^2 = 0.42$) indicate isotopic enrichment with decreasing N_2O concentration. However, a $\delta^{18}O$:$\delta^{15}N$ slope this steep would likely not be seen for NO_3^- consumption so likely represents an upper limit for N_2O consumption.

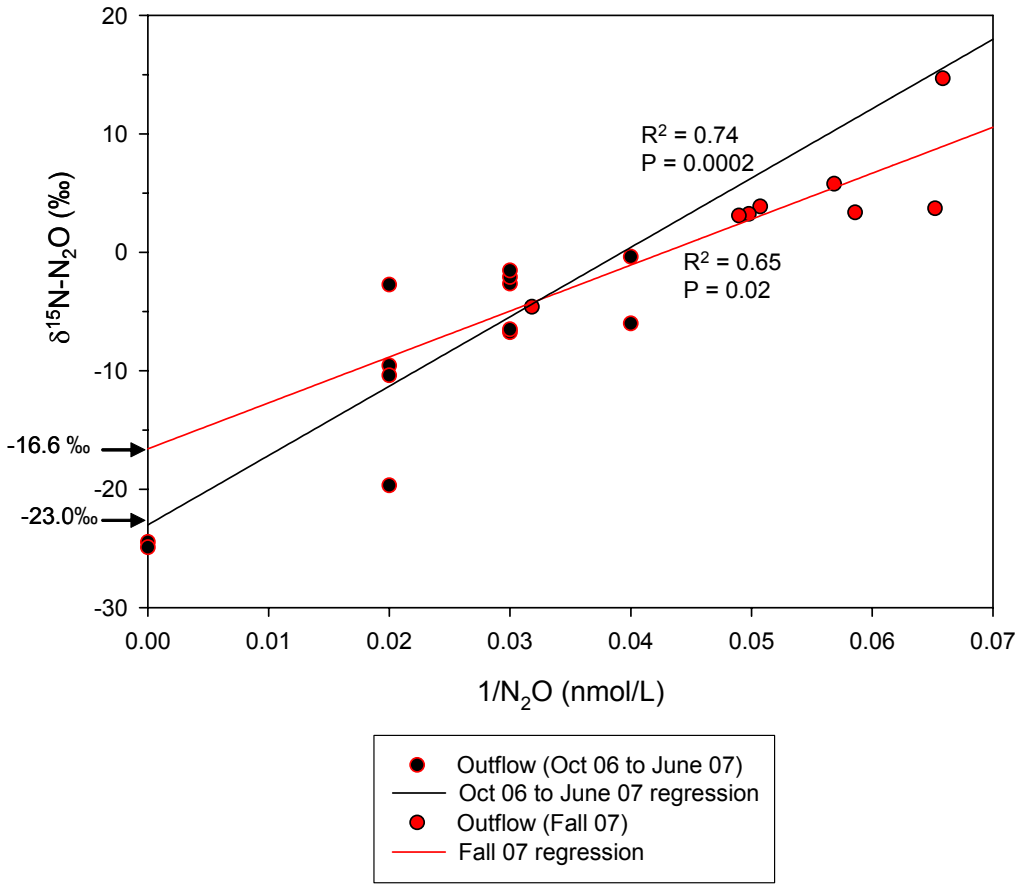

Figure 4-15: The results of $\delta^{15}N$-N_2O endmember analysis for October 2006 to June 2007 and Fall 2007 datasets

At all sites, some variability of N_2O isotopes may be due to variation of substrate isotopes and differences in denitrification fractionation factors created by reaction rate, substrate availability and microorganisms (Menyailo and Hungate, 2006; Mandernack et al., 2002). This is most evident in sites with shallow slopes and poor regression

coefficients (ie: $R^2 \leq 0.17$) as in the case of Upper road tile (October 2006 to June 2007) (Figure 4-11) which also has poor correlation between lnN_2O concentration and isotopes. Substrate variability could account for some of the product variation where the range of $\delta^{18}O\text{-}NO_3^-$ and $\delta^{18}O\text{-}N_2O$ is 15‰ while $\delta^{15}N\text{-}NO_3^-$ has a range of 8‰ and $\delta^{15}N\text{-}N_2O$ has a range of 20‰.

Larger $\delta^{15}N\text{-}N_2O$ values measured in Fall 2007 produce smaller ^{15}N isotopic shifts (average $\Delta_{N2O\text{-}NO3^-}$ = -5.32 to 0.87‰) while ^{18}O isotopic shifts remain comparable to the October 2006 to June 2007 period (Table 4-7 and Table 4-8). The difference in the ^{15}N isotope shifts is likely due to NO_3^- limitation which would reduce the ^{15}N fractionations of the various reactions. NO_3^- limitation on the other hand would not affect ^{18}O fractionation in the reaction series as preferential cleavage of ^{16}O is the cause of the fractionation. Low NO_3^- concentrations (< 3mg N/L) at AMR tile and Outflow are suggestive of NO_3^- limitation but high NO_3^- concentrations were measured at Harris tile which still shows higher $\delta^{15}N\text{-}N_2O$ values. Groundwater on the other hand had low NO_3^- concentrations yet $\delta^{15}N\text{-}N_2O$ values are also lower.

Differences between unsaturated and saturated zone $\delta^{15}N\text{-}N_2O$ signatures could be due to variable fractionation factors within and between production pathways (Figure 4-11). While most saturated zone N_2O is in the ^{15}N range for denitrification, unsaturated zone N_2O production more closely approaches the ^{15}N range of nitrifier-denitrification and could be the result of mixing between N_2O produced from nitrifier-denitrification and denitrification. $\delta^{18}O\text{-}N_2O$ values are also directly in the range of those measured from other nitrifier-denitrification studies (Perez et al., 2001). This seems reasonable since the unsaturated zone would be more aerobic than the saturated zone thereby promoting nitrifier-denitrification.

Variable fractionation within denitrification could also explain the observed differences between these zones of N_2O production. Unlimited substrate (NO_3^-) for denitrification would increase the ^{15}N fractionation factors and produce lower $\delta^{15}N\text{-}N_2O$ values. Unsaturated soils would have greater accessibility to NO_3^- by reduced distance of travel

for microbes to this substrate in comparison with saturated soils. Reduced reaction rates, through cooler temperatures for example, would also increase fractionation factors in unsaturated soils.

It is possible that N_2O from the unsaturated zone is produced by denitrification and subject to the same ^{18}O fractionation as in groundwater and tiles. However, larger amounts of oxygen exchange with water in the unsaturated zone could lower $\delta^{18}O\text{-}N_2O$ values to where they are observed. Results of a simple isotope mixing model show that 60% water exchange would result in $\delta^{18}O\text{-}N_2O$ values of +10.8‰ which is the lowest value observed for soil gas N_2O (Table 4-9). This model assumes a denitrification ^{18}O enrichment factor ($\varepsilon_{N2O\text{-}NO3\text{-}}$) of +40‰ and that $\delta^{18}O\text{-}H_2O$ is -10‰ (Mengis et al., 1999). Varying amounts of water exchange have been shown to occur between microbial species containing the same key enzymes (cytochrome cd_1 or copper-containing nitrite reductase) and between the enzymes themselves (Ye et al., 1991; Shearer and Kohl, 1988; Garber and Hollocher, 1982). It is likely that this effect would extend to the microbial community if differences were found in the saturated and unsaturated zone assemblages

Table 4-9: Results of an isotope mixing model accounting for the influence of water exchange

Water exchange (%)	$\delta^{18}O\text{-}N_2O$ produced
0	42
10	36.8
20	31.6
30	26.4
40	21.2
50	16
60	10.8
70	5.6

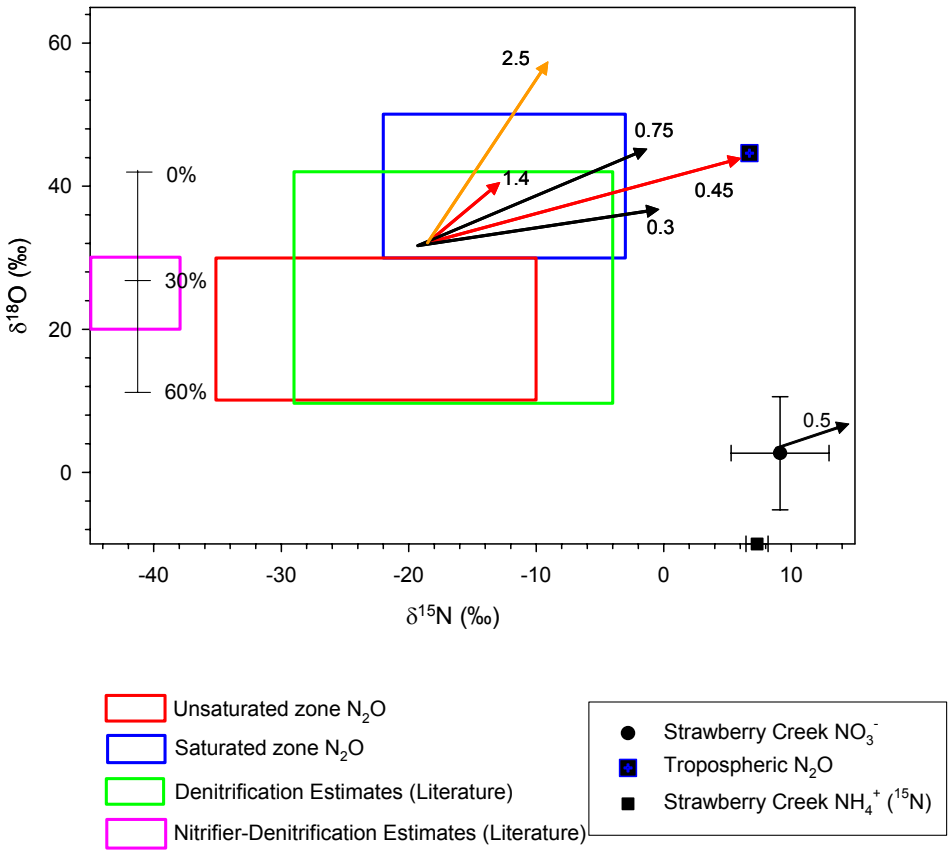

Figure 4-16: Conceptual Model of N_2O dynamics at the Strawberry Creek agriculture catchment. The range of values expected for saturated zone N_2O from denitrification were calculated using an average for isotopic shifts and standard deviation from the mean NO_3^- value measured in this study. The range of expected values for unsaturated zone N_2O production were taken directly from soil gas N_2O values measured by John Spoelstra (2007, unpublished results). The range of values expected for nitrifier-denitrification and denitrification were calculated using literature estimates of fractionation factors from Strawberry Creek endmembers. The range of $\delta^{15}N$-N_2O produced by nitrifier-denitrification extends to -63‰. The area in between $\delta^{18}O$:$\delta^{15}N$ slopes of 0.3 and 0.75 represents the trajectory of N_2O isotopes affected by NO_3^- consumption. The area in between $\delta^{18}O$:$\delta^{15}N$ slopes of 0.45 and 1.4 represents the trajectory of N_2O isotopes affected by gas exchange, which ultimately trend toward the tropospheric mean. The $\delta^{18}O$:$\delta^{15}N$ slope of 2.5 represents the trajectory of N_2O isotopes affected by N_2O consumption reported in the literature (Menyailo & Hungate 2006, Vieten et al 2007, Mandernack 2000). The $\delta^{18}O$:$\delta^{15}N$ slope (0.5) for residual NO_3^- following denitrification is also included. Calculations for the influence of oxygen exchange with water assumed an isotopic shift ($\Delta_{N2O\text{-}NO3^-}$) of +40‰ (Casciotti et al., 2002) from the mean $\delta^{18}O$-NO_3^- value (+2.63‰) with 0% exchange. A simple isotopic mixing model was used to calculate $\delta^{18}O$-N_2O at various exchange rates where $\delta^{18}O$-H_2O was -10‰ (Mengis et al., 1999).

Figure 4-16 represents a summary of what is observed for Strawberry Creek N_2O isotopes along with the expected range of N_2O isotopes from enrichment factors reported in the literature. The isotopic shifts ($\Delta_{N2O\text{-}NO3}$) used to create the range for saturated zone N_2O production at Strawberry Creek assumes no N_2O alteration (ie: by NO_3^- consumption, N_2O consumption, or gas exchange). The range of $\delta^{18}O$:$\delta^{15}N$ trajectories for NO_3^- consumption and gas exchange are those observed in this study and in Chapter 3. The range of $\delta^{18}O$:$\delta^{15}N$ trajectories for NO_3^- consumption is likely representative of that process since NO_3^- isotopes have a similar range of alteration due to denitrification. The $\delta^{18}O$:$\delta^{15}N$ trajectory for N_2O consumption is 2.5 (Menyailo & Hungate 2006, Vieten et al 2007, Mandernack 2000).

Unsaturated zone N_2O has larger negative $\delta^{15}N$ isotopic shifts for denitrification ($\Delta_{N2O\text{-}NO3}$ = -45 to -20) while $\delta^{18}O$ enrichment factors are smaller than those of the saturated zone ($\varepsilon_{N2O\text{-}NO3}$ = +10 to +30‰). Oxygen exchange is likely greater in the unsaturated zone and has the effect of reducing $\delta^{18}O$ isotopic shifts for denitrification.

Literature estimates of fractionation factors for denitrification from incubations produce a range of N_2O that is similar to what is observed in both unsaturated and saturated zones at Strawberry Creek. However, unsaturated zone N_2O is also within the range of $\delta^{18}O$ expected for nitrifier-denitrification and near to that expected for $\delta^{15}N$. This may be expected from unsaturated zone N_2O since conditions here would be more aerobic.

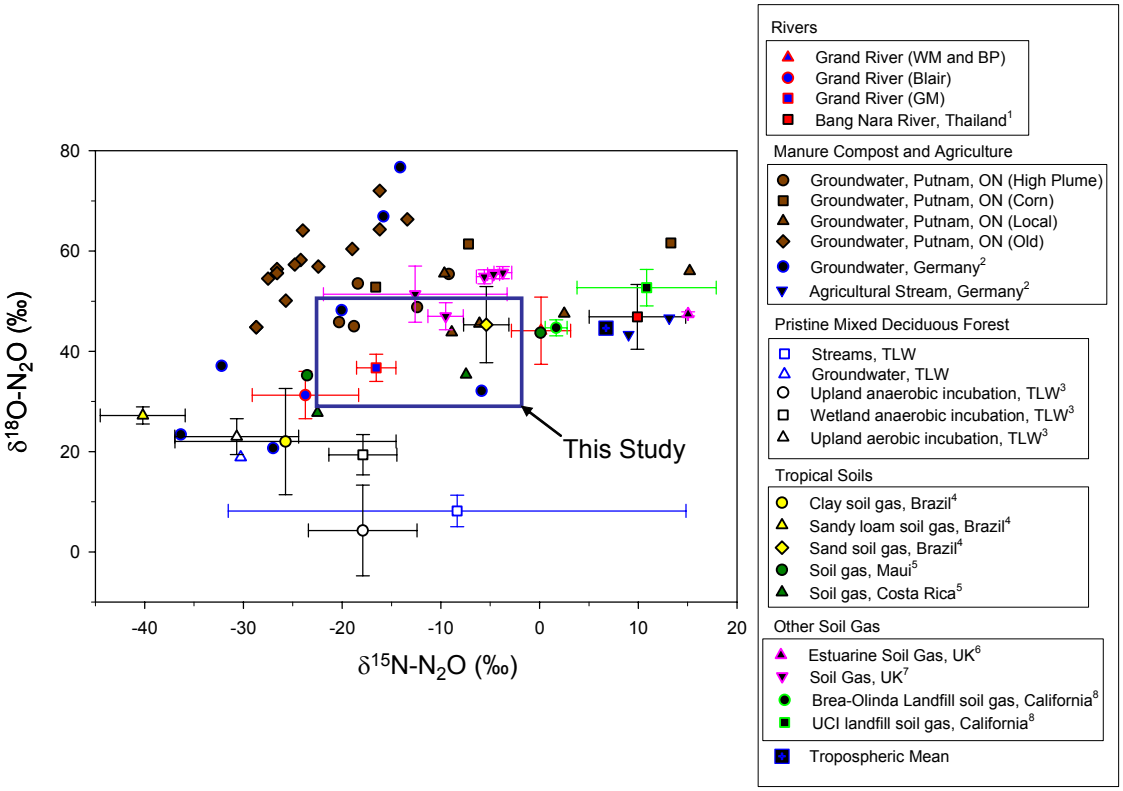

Figure 4-17: $\delta^{15}N$-N_2O and $\delta^{18}O$-N_2O from Strawberry Creek (dissolved N_2O) and from various field and incubation studies: 1) Bootanaan et al., 2000; 2) Well et al., 2005; 3) Snider et al., 2008, unpublished results; 4) Perez et al., 2006; 5) Kim and Craig, 1993 6) Bol et al., 2004; 7) Bol et al., 2003; 8) Mandernack et al., 2000. N_2O values were normalized to end member data where made available by each study.

Figure 4-17 shows $\delta^{15}N$ and $d^{18}O$ of N_2O from the Grand River, Putnam ground water, and a variety of reported values from field and incubation studies in the literature. This plot shows that the spread of N_2O isotope data currently available is very large. Considering the large range shown here, dissolved N_2O isotopes from Strawberry Creek data is relatively well constrained. Values within this range define the signal of dissolved N_2O isotopes from Strawberry Creek and they also possibly define the signal of regional agroecosystems. This is important since the isotopic signal from secondary agricultural sources has not previously been defined in this manner. This range may also define the signal from other secondary agricultural sources from similar environments in North

America and Europe. Future N_2O isotope studies in these environments should seek to better define both the signal and the processes that determine the measured signal.

Groundwater data from Bol et al. (2004) suggest upper limits for $\delta^{18}O$-N_2O measured in groundwater may be near +80‰. Bol et al. (2004) report that $\delta^{15}N$ and $\delta^{18}O$ isotopes of N_2O increase as a function of residence time in anaerobic aquifers due to N_2O consumption. "Old" groundwater from the Putnam site (Figure 4-17) show similar $\delta^{15}N$ and $\delta^{18}O$ values as those from the Bol et al. (2004) and may also be a product of N_2O consumption. The $\delta^{18}O$:$\delta^{15}N$ trajectory from old groundwater at the Putnam site is approximately 1.5 which means the trajectory of 1.65 measured at BMR tile (October 2006 to June 2007) may also be from N_2O consumption as previously proposed.

4.5.4 Conclusions

During baseflow conditions of October 2006 to June 2007 and Fall 2007, Strawberry Creek stream NO_3^- concentrations remained below 10 mg N/L. Tile NO_3^- concentrations from the Upper Road, BMR, and Harris tiles remained consistently above this threshold and continued to pose a threat to aquatic life from October 2006 to June 2007. N_2O concentrations in the tiles and streams remain above atmospheric saturation and, thus, are a source of N_2O to the atmosphere.

NO_3^- isotopes show that the main sources of tile NO_3^- during baseflow conditions are soil organic matter and manure/septic system effluent. There is also evidence of NO_3^- from atmospheric deposition in Strawberry Creek groundwater during both time periods.

Strawberry Creek N_2O isotopes suggest that production during baseflow conditions is by denitrification. Calculated isotopic shifts for denitrification are comparable with those reported in the literature. Moderate $\delta^{18}O$:$\delta^{15}N$ slopes for N_2O around 0.5 are caused by substrate (NO_3^-) consumption particularly when strong and significant relationships of increasing isotopes values and decreasing (ln) concentrations are also observed. Shallow negative or positive slopes reflect a combination of processes including NO_3^-

consumption, N_2O consumption, and variable fractionation factors due to substrate availability, reaction rate, and microbial assemblages.

The isotopic effects of gas exchange in the stream are significant but the original source signature of stream N_2O can be calculated using Keeling plot analysis. The results show that $\delta^{15}N\text{-}N_2O$ produced is more negative than that measured in the creek and that isotopic shifts are greater than if the measured N_2O isotopes are used for the calculation. The consistent $\delta^{15}N\text{-}N_2O$ values produced from the October 2006 to June 2007 and Fall 2007 datasets suggest that there is a specific signal of N_2O produced in the stream.

Divergent N_2O signatures between soil gas and dissolved samples suggest different production pathways between unsaturated and saturated zones at Strawberry Creek. A simple model of oxygen exchange with water explains differences in $\delta^{18}O$. N_2O produced in the unsaturated zone could be the result of 60% exchange, leading to lower $\delta^{18}O\text{-}N_2O$ values, whereas N_2O from the saturated zone could be the result of 0 to 30% exchange. Potential causal mechanisms are different production pathway where more unsaturated N_2O could be produced by nitrifier-denitrification or differences in fractionation for denitrification.

Based on the data of this study a conceptual model of N_2O isotope dynamics in a small agriculture catchment is proposed highlighting the differences between unsaturated and saturated zone production. Given the variability of N_2O isotopes reported in the literature, those of the Strawberry Creek catchment are relatively tight. This implies that the range observed can be used to define the N_2O isotope signal from local secondary agricultural sources.

Bibliography

Andersson K.K., S.B. Philson, and A.B. Hooper. (1982). ^{18}O isotope shift in ^{15}N NMR analysis of biological N-oxidations: H_2O-NO_2 exchange in the ammonia-oxidizing bacterium Nitrosomonas. Proceedings of the National Academy of Science, USA 79: 5871-5875.

Andersson, K.K., and A.B. Hooper. (1983). O_2 and H_2O are each the source of one O in NO_2 produced from NH_3 by Nitrosomonas: ^{15}N evidence. Federation of European Biochemical Societies Letters 164: 236-240.

Aravena, R., Evans, M.L., and Cherry, J.A. (1993). Stable isotopes of oxygen and nitrogen in source identification of nitrate from septic systems. Ground Water 31: 180-186.

Aravena, R., and W.D. Robertson. (1998). Use of multiple isotope tracers to evaluate denitrification in ground water: Study of nitrate from a large-flux septic system plume. Ground Water 36 (6): 975-982.

Averill, B.A. (1996). Dissimilatory nitrite and nitric oxide reductases. Chemical Reviews 96: 2951-2964.

Barford, C.C., J.P. Montoya, M.A. Altabet and R. Mitchell. (1999). Steady-state nitrogen isotope effects of N_2 and N_2O production in Paracoccus denitrificans. Applied and Environmental Microbiology 65(3): 989-994.

Baumgärtner, M., and Conrad, R. (1992). Role of nitrate and nitrite for production and consumption of nitric oxide during denitrification in soil. FEMS Microbiology Ecology 101:59-65.

Bernhardt, E.S. and Likens, G.E. (2002). Dissolved organic carbon enrichment alters nitrogen dynamics in a forest stream. Ecology 83: 1689-1700.

Blackmer, A.M. and J.M. Bremner. (1977). Nitrogen isotope discrimination in denitrification of nitrate in soils. Soil Biology and Biochemistry 9: 73-77.

Bol, R., T. Rockmann, M. Blackwell and S. Yamulki. (2004). Influence of flooding on delta N-15, delta O-18, (1)delta N-15 and (2)delta N-15 signatures of N_2O released from estuarine soils - a laboratory experiment using tidal flooding chambers. Rapid Communications in Mass Spectrometry 18: 1561-1568.

Bol, R., Toyoda, S., Yamulki, S., Hawkins, J., Cardenas, L., Yoshida, N., (2003) Dual isotope and isotopomer ratios of N_2O emitted from a temperate grassland soil after fertilizer application Rapid Communications in Mass Spectrometry 17:2550-2556.

Boontanon, N., S. Ueda, P. Kanatharana and E. Wada. (2000). Intramolecular stable isotope ratios of N2O in the tropical swamp forest in Thailand. Naturwissenschaften 87: 188-192.

Bouwman, A.F. (1996). Direct emissions of nitrous oxide from agricultural soil. Nutrient cycling in agroecosystems 46: 53-70.

Bottcher, J., Strebel, O., Voerkelius, S., and Schmidt, H.L. (1990). Using isotope fractionation of nitrate-nitrogen and nitrate-oxygen for evaluation microbial denitrification in a sandy aquifer. Journal of Hydrology 114: 413-424

Bremner, J.M. (1997). Sources of nitrous oxide in soils. Nutrient cycling in agroecosystems 49: 7-16.

Broadbent, F.E., and Stevenson, F.J. (1966). Organic matter interactions. *In* Agricultural Anhydrous Ammonia. M.H. McVickar, W.P. Martin, I.E. Miles, and H.H. Tucker (Eds.), pp. 169-187. Memphis and American Society of Agronomy, Madison, Wisconsin, U.S.A.

Cabrera, F.J. (2000). Nitrate attenuation in a first-order stream and associated riparian zone in an agricultural watershed in Southern Ontario. MSc thesis. University of Waterloo, Waterloo, ON, Canada.

Carpenter, S.R., Caraco, N.F., Correll, D.L., Howarth, R.W., Sharpley, A.N., and Smith, V.H. (1998). Nonpoint pollution of surface waters with phosphorus and nitrogen. Ecological Applications 8: 559-568.

Casciotti, K.L., Bohlke, J.K., McIlvin, M.R., Mroczkowski, S.J., and Hannon, J.E. (2007). Oxygen Isotopes in Nitrite: Analysis, Calibration, and Equilibration. Analytical Chemistry 79: 2427-2436.

Casciotti, K.L., D.M. Sigman, M. Galanter Hasting, J.K. Bohlke, and A. Hilkert. (2002). Measurement of the oxygen isotopic composition of nitrate in seawater and freshwater using the denitrifier method. Analytical Chemistry 74: 4905-4912.

Cey, E.E., Rudolph, D.L., Parkin, G.W., and Aravena, R. (1998). Quantifying groundwater discharge to a small perennial stream in southern Ontario, Canada. Journal of Hydrology 210: 21-37.

Cornwell J. C., Kemp W. M., and Kana T. M. (1999). Denitrification in coastal ecosystems: methods, environmental controls, and ecosystem level controls, a review. Aquatic Ecology 33: 41–54.

Cleland, W.W., O'Leary, M.H., Northrop D.B., Eds. (1977). Isotope Effects on Enzyme-Catalyzed Reactions: Proceedings of the Sixth Annual Harry Steenbock Symposium. University Park Press, Baltimore, MD, U.S.A.

Coplen, T.B., Bohlke, J.K., De Bievre, P., Ding, T., Holden, N.E., Hopple, J.A., Krouse, H.R., Lamberty, A., Peiser, H.S., Revesz, K., Rieder, S.E., Rosman, KJ.R., Roth, E., Taylor, P.D.P., Vocke, R.D., and Xiao, Y.K. (2002). Isotope-abundance variations of selected elements - (IUPAC Technical Report). Pure and Applied Chemistry 74: 1987-2017.

Delwiche, C.C. (1981). The nitrogen cycle and nitrous oxide. *In* Denitrification, nitrification, and atmospheric nitrous oxide. C.C. Delwiche (Ed.). John Wiley and Sons, Toronto, ON, pp. 1-16.

Deutsch, B., Liskow, I., Kahle, P., and Voss, M. (2005). Variations in the $\delta^{15}N$ and $\delta^{18}O$ values of nitrate in drainage wate of two fertilized fields in Mecklenburg-Vorpommern (Germany). Aquatic Science 67: 156-165.

Dinnes, D.L., Karlen, D.L., Jaynes, D.B., Kaspar, T.C., Hatfield, J.L., Colvin, T.S., and Cambardella, C.A. (2002). Nitrogen management strategies to reduce nitrate leaching in tile-drained Midwestern soils. Agronomy Journal 94:153-174.

Dore, J.E., Popp, B.N., Karl, D.M., and Sansone, F.J. (1998). A large source of atmospheric nitrous oxide from subtropical North Pacific surface water. Nature 396: 63-66.

Dowdell, R.J., Burford, J.R., and Crees, R. (1979). Losses of nitrous oxide dissolved in drainage water from agriculture land. Nature 278: 342-343.

Food and Agriculture Organization (FAO), (1999). FAOSTAT statistical database, available at http://apps.fao.or/c/s.dll/nph-db.pl

Fenn, L.B., Taylor, R.M., and Matocha, J.E. (1981). Ammonia losses from surface applied nitrogen fertilizer as controlled by soluble calcium and magnesium: general theory. Soil Science Society of America Journal 45: 777-781.

Fogel, M.L. and L.A. Cifuentes. (1993). Isotope fractionation during primary production. *In*: M.H. Engel and S.A. Macko (Eds). Organic Geochemistry. Plenum Press, New York, USA, pp. 73-98.

Fisher, D.C., and Oppenheimer, M. (1991). Atmospheric nitrogen deposition and the Chesapeake Bay estuary. Ambio 20: 102-108.

Firestone, M. K., and E. A. Davidson. (1989). Microbiological basis of NO and N_2O production and consumption in soil. *In* Exchange of Trace Gases between Terrestrial Ecosystems and the Atmosphere. M. O. Andreae and D. S. Schimel (Eds.). John Wiley & Sons Ltd, Chichester, UK, pp. 7-21

Freney, J.R., Simpson, J.R., and Denmead, O.T. (1983). Volatilization of Ammonia. *In* Gaseous Loss of Nitrogen from Plant-Soil Systems. J.R. Freney and J.R. Simpson (Eds.). Martinus Nijhoff/Dr. W. Junk Publishers, The Hague, Netherlands, pp. 1-32.

Galloway, J.N., Schlesinger, W.H., Levy II, H., Micheals, A., and Schnoor, J.L. (1995). Nitrogen fixation: Anthropogenic enhancement-environmental response. Global Biogeochemical Cycles 9: 235-252.

Garber, E.A.E., and Hollocher, T.C. (1982). ^{15}N, ^{18}O Tracer studies on the activation of nitrite by denitrifying bacteria. The Journal of Biological Chemistry 257: 8091-8097.

Gentry, L.E., David, M.B., Smith-Starks, K., and Kovacic D.A. (2000). Nitrogen Fertilizer and Herbicide Transport from Tile Drained Fields. Journal of Environmental Quality, 29: 232-240.

Gianessi, L.P., Peskin, H.M., Crosson, P., and Puffer, C. (1986). Non-point source pollution: are cropland controls the answer? U.S. Department of Agriculture and U.S. Environmental Protection Agency, Washington, D.C., U.S.A.

Hales, J.M., and Drewes, D.R. (1979). Solubility of ammonia in water at low concentrations. Atmospheric Environment 13: 1133-1147.

Harris, M. (1998). Nitrate attenuation by a narrow riparian buffer at Strawberry Creek, Ontario, Canada. MES Thesis. Wilfred Laurier University, Waterloo, ON, Canada.

Harrison, J. and Matson, P. (2003). Patterns and controls of nitrous oxide emissions from waters draining a subtropical agricultural valley. Global Biogeochemical Cycles 17: Article 1080.

Havens, K.E., and Steinman A.D. (1995). Aquatic systems. *In* Soil amendments: impacts on biotic systems. J.E. Rechcigl (Ed.). Lewis, Boca Raton, Florida, U.S.A. pp. 121-151

Herbert R. A. (1999) Nitrogen cycling in coastal marine ecosystems. FEMS Microbiology Review 23: 563–590.

Hochstein, L.I., and Tomlinson, G.A. (1988). The enzymes associated with denitrification. Annual Review of Microbiology 42: 231-261.

Högberg, P. (1997). ^{15}N natural abundance in soil-plant systems. New Phytologist 137: 179-203.

Hollocher, T.C. (1984). Source of the oxygen atoms of nitrate in the oxidation of nitrite by Nitrobacter agilis and evidence against a P-O-N anhydride mechanism in oxidative phosphorylation. Archives of Biochemistry and Biophysics 233: 721-727.

Hollocher, T.C., M.E. Tate and D.J.D. Nicholas. (1981). Oxidation of Ammonia by Nitrosomonas europaea: Definitive ^{18}O-Tracer evidence that hydroxylamine formation involves a monooxygenase. The Journal of Biological Chemistry 256: 10834-10836.

Howarth, R.W., Billen, G., Swaney, D., Townsend, A., Jaworski, N., Lajtha, K., Downing, J.A., Elmgren, R., Caraco, N., Jordan, T., Berendse, F., Freney, J., Kudeyarov, V., Murdoch, P., Zhao-liang, Z. (1996). Regional nitrogen budgets and riverine N & P fluxes for the drainages to the North Atlantic Ocean: Natural and human influences. Biogeochemistry 35: 181-226.

Hubner, H. (1986). Isotope effects of nitrogen in the soil and biosphere. *In* P. Fritz and J.C. Fontes (Eds.). Handbook of Environmental Isotope Geochemistry, vol. 2b, The Terrestrial Environment, Elsevier, pp. 361-425.

IAEA (2001). GNIP Maps and Animations, International Atomic Energy Agency, Vienna.Accessible at http://isohis.iaea.org

Inoue, H.Y. and W.G. Mook. (1994). Equilibrium and kinetic nitrogen and oxygen isotope fractionations between dissolved and gaseous N2O. Chemical Geology (Isotope Geoscience Section) 113: 135-148.

Jenkinson, D.S. (2001). The impact of humans on the nitrogen cycle, with focus on temperature arable agriculture. Plant and Soil 228: 3-15.

Kaiser, J. (2002). Stable isotope investigations of atmospheric nitrous oxide. PhD Thesis, Max Planck Institute for Chemistry/University of Mainz.

Karamanos, R.E., Voroney, R.P., and Rennie, D.A. (1981). Variation in Natural N-15 Abundance of Central Saskatchewan Soils**.** Soil Science Society of America Journal 45: 826–828.

Kates, R.W., Turner, B.L., and Clark, W.C. (1990). The great transformations. *In* The Earth as Transformed by Human Action. B.L. Turner, W.C. Clark, R.W. Kates, J.F. Richards, J.T. Matthews, and Meyer, W.B. (Eds.). Cambridge University Press, Cambridge, England, pp. 1-17.

Kellman L. and Hillaire-Marcel, C. (1998). Nitrate cycling in streams: using natural abundances of NO_3^-–$\delta^{15}N$ to measure in-situ denitrification. Biogeochemistry 43: 273-292.

Kellman, L.M. (2005). A study of tile drain nitrate – $\delta^{15}N$ values as a tool for assessing nitrate sources in an agricultural region. Nutrient Cycling in Agroecosystems 71: 131-137.

Kellman L.M. and Hillaire-Marcel, C. (2003). Evaluation of nitrogen isotopes as indicators of nitrate contamination sources in an agricultural watershed. Agriculture, Ecosystems, and Environment 95: 87-102.

Kemp, M.J. and Dodds W.K. (2002). The influence of ammonium, nitrate, and dissolved oxygen concentrations on uptake,nitrification, and denitrification rates associated with prairie stream substrata. Limnology and Oceanography 47:1380-1393.

Kendall C. (1998). Tracing Nitrogen Sources and Cycling in Catchments. *In* Isotope Tracers in Catchment Hydrology. C. Kendall and J.J. McDonnell (Eds). Elsevier, Amsterdam, pp. 51-86.

Kendall C. and Caldwell, E.A. (1998). Fundamentals of Isotope Geochemistry. *In* Isotope Tracers in Catchment Hydrology. Kendall C and McDonnell J.J. (Eds). Elsevier, Amsterdam, pp. 521-576.

Kim, C.H., and Hollocher, T.C. (1984). Catalysis of nitrosyl transfer reactions by a dissimilatory nitrite reductase (cytochrome c, d1). Journal of Biological Chemistry 259: 2092-2099.

Kim, K.R., and Craig, H. (1993). Nitrogen-15 and Oxygen-18 Characteristics of Nitrous Oxide: A Global Perspective. Science 262: 1855-1857.

Kirshenbaum I., Smith, J.S., Crowell, T., Graff, J., and McKee, R. (1947). Separation of the nitrogen isotopes by the exchange reaction between ammonium and solutions of ammonium nitrate. Journal of Chemical Physics 15: 440-446.

Kool, D.M., Wrage, N., Oenema, O., Dolfing, J., and van Groenigan, J.W. (2007). Oxygen exchange between (de)nitrification intermediates and H_2O and its implications for source determination of NO_3 and N_2O: a review. Rapid Communications in Mass Spectrometry 21: 3569-3578.

Krul, J.M. (1976). Dissimilatory nitrate and nitrite reduction under aerobic conditions by an aerobically and anaerobically grown *Alcaligenes* sp. and by activation sludge. Journal of Applied Bacteriology 40: 245-260.

Krul, J.M., and Veeningen, R. (1977). The synthesis of dissimilatory nitrate reductase under aerobic conditions in a number of denitrifying bacteria, isolated from activated sludge and drinking water. Water Resources 11: 39-43.

Kumar, S., D.J.D. Nicholas, and E.H. Williams. (1983). Definitive ^{15}N NMR evidence that water serves as a source of 'O' during nitrite oxidation by Nitrobacter agilis. Federation of European Biochemical Societies Letters 152: 71-74.

Lemon, E., and Van Houtte, R. (1980). Ammonia exchange at the land surface. Agronomy Journal 72: 876-883.

Lortie, S.L. (1999). An evaluation of the origin and fate of NO_3^- at Strawberry Creek using the stable isotopes ^{15}N and ^{18}O. BSc Thesis. University of Waterloo, Waterloo, ON, Canada.

Macrae, M.L., English, M.C., Schiff, S.L., and Stone, M. (2007). Capturing temporal variability for estimates of annual hydrochemical export from a first-order agricultural catchment in southern Ontario, Canada. Hydrological processes 21: 1651-1663.

Macrae, M.L., English, M.C., Schiff, S.L. and Stone, M. (2007). Intra-annual Variability in the Contribution of Tile Drains to Basin Discharge and Phosphorus Export in a First-Order Agricultural Catchment. Agricultural Water Management 92: 171-182.

Macrae, M. (2003). Temporal variability in nutrient transport in a first-order agricultural basin in Southern Ontario. PhD thesis. Wilfred Laurier University, Waterloo, ON, Canada

Mandernack, K.W., T. Rahn, C. Kinney, M. Wahlen. (2000). The biogeochemical controls of the δ15N and δ18O of N_2O produced in landfill cover soils. Journal of Geophysical Research. 105 (D14): 17,709-17,720.

Mariotti, A., Landreau, A., and Simon, B. (1988). ^{15}N isotope biogeochemistry and natural denitrification process in groundwater: Application to the chalk aquifer of northern France. Geochimica et Cosmochimica Acta 52: 1869-1878.

Mariotti, A., J.C. Germon, P. Hubert, P. Kaiser, R. Letolle, R. Tardieux, and P. Tardieux. (1981). Experimental determination of nitrogen kinetic isotope fractionation: some principles; illustration for the denitrification and nitrification processes. Plant and Soil 62: 413-430.

Mayer, B., Boyer, E.W., Goodale, C., Jaworski, N.A., Van Breeman, N., Howarth, R.W., Seitzinger, S., Billen, G., Lajtha, K., Nadelhoffer, K., Van Dam, D., Hetling, L.J., Nosal, M,. and Paustian, K. (2002). Sources of nitrate in rivers draining sixteen watersheds in the northeastern U.S.: Isotopic constraints. Biogeochemistry 57/58: 171-197.

Mayer, B., S.M. Bollwerk, T. Mansfeldt, B. Hütter, and J. Veizer. (2001). The oxygen isotope composition of nitrate generated by nitrification in acid forest floors. Geochimica et Cosmochimica Acta 65(16): 2743-2756.

McIlvin, M.R., and Altabet, M.A. (2005). Chemical Conversion of Nitrate and Nitrite to Nitrous Oxide for Nitrogen and Oxygen Isotopic Analysis in Freshwater and Seawater. Analytical Chemistry 77: 5589-5595.

Mengis, M., S.L. Schiff, M. Harris, M.C. English, R. Aravena, R.J. Elgood, and A. MacLean. (1999). Multiple geochemical and isotopic approaches for assessing ground water NO_3^- elimination in a riparian zone. Ground Water 37 (3): 448-457.

Menyailo, O. V., and B. A. Hungate. (2006). Stable isotope discrimination during soil denitrification: Production and consumption of nitrous oxide. Global Biogeochemical Cycles 20. doi: 10.1029/200GB002527.

Mortland, M.M. (1966). Ammonia interactions with soil minerals. *In* Agricultural Anhydrous Ammonia. M.H. McVickar, W.P. Martin, I.E. Miles, and H.H. Tucker (Eds.). Memphis and American Society of Agronomy, Madison, Wisconsin, U.S.A, pp. 188-197.

Mosier, A.R., Kroeze, C., Nevison, C.D., Oenema, O., Seitzinger, S., and van Cleemput, O. (1998). Closing the global N_2O budget: nitrous oxide emissions through the agricultural nitrogen cycle OECD/IPCC/IEA phase II development of IPCC guidelines for national greenhouse gas inventory methodology. Nutrient Cycling in Agroecosystems 52: 225-248.

Mosier, A.R. (1994). Nitrous oxide emissions from agricultural soils. Fertilizer Research 37: 191-200.

Naqvi, S.W.A., Yoshinari, T., Jayakumar, D.A., Altabet, M.A., Narvekar, P.V., Devol, A.H., Brandes, and Codispoti, J.A. (1998). Budgetary and biogeochemical implications of N_2O isotope signatures in the Arabian Sea. Nature 394:462-464.

Olivier, J.G.J., Bouwman, A.F., van der Hoek, K.W., and Berdowski, J.J.M. (1998). Global air emission inventories for anthropogenic sources of NO_x, NH_3, and N_2O in 1990. Environmental Pollution 102:135-148.

Ostrom NO, Russ ME, Popp B, Rust TM, Karl DM. (2000). Mechanisms of nitrous oxide production in the subtropical North Pacific based on determinations of the isotopic abundances of nitrous oxide and di-oxygen. Chemosphere Global Change Science 2: 281-290.

Payne, W.J. (1973). Reduction of nitrogenous oxide by microorganisms. Bacteriology Review 37: 409-452.

Payne, W.J. (1976). Denitrification. Trends in Biochemical Science 1: 220-222.

Perez, T., Garcia-Montiel, D., Trumbore, S., Tyler, S., de Camargo, P., Moriera, M., Piccolo, M., and Cerri, C. (2006). Nitrous oxide nitrification and denitrification ^{15}N enrichment factors from Amazon forest soils. Ecological Applications 16: 2153-2167.

Perez, T., Trumbore, S.E., Tyler, S.C., Matson, P.A., Ortiz-Monasterio, I., Rahn, T., and Griffith, D.W.T. (2001). Identifying the agricultural imprint on the global budget using stable isotope. Journal of Geophysical Research 106: 9869-9878.

Perez, T., S.E. Trumbore, S.C. Tyler, E.A. Davidson, M. Keller, and P.B. de Camargo. (2000). Isotopic variability of N_2O emissions from tropical forest soils. Global Biogeochemical Cycles 14 (2): 525-535.

Popp, BN, Westley, MB, Toyoda, S, Miwa, T, Dore, JE, Yoshida, N, Rust, TM, Sansone, FJ, Russ, ME, Ostrom, NE, Ostrom, PH. (2002). Nitrogen and oxygen isotopomeric constraints on the origins and sea-to-air flux of N_2O in the oligotrophic subtropical North Pacific gyre. Global Biogeochemical Cycles 16: 1064.

Postgate, J. (1987). Nitrogen fixation. Edward Arnold, Baltimore, Maryland, U.S.A. 73 pp.

Poth M. and Focht D. D. (1985) ^{15}N kinetic analysis of N_2O production by Nitrosomonas europaea: an examination of nitrifier denitrification. Applied Environmental Microbiology 49: 1134–1141.

Poth, M. (1986). Dinitrogen production from nitrite by a nitrosomonas isolate. Applied and Environmental Microbiology 52: 957-959.

Presant, R.C. and Wicklund, R.E. (1971). The soils of Waterloo County: Report 44 of the Ontario Soil Survey.

Prinn, R., Cunnold, D., Rasmussen, R., Simmonds, P., Alyca, F., Crawford, A., Fraser, P., and Rosen, R. (1990). Atmospheric emissions and trends of nitrous oxide deduced from 10 years of ALE-GAGE data. Journal of Geophysical Research 95: 18,369-18,385.

Rahn, T., and Whalen M. (1997). Stable isotopic enrichment in stratospheric nitrous oxide. Science 278: 1776-1778.

Rahn, T., and Wahlen, M. (2000). A reassessment of the global isotopic budget of atmospheric nitrous oxide. Global Biogeochemical Cycles 14: 537-543.

Randall, G.W., and Gross, M.J. (2001). Nitrate losses to surface water through subsurface tile drainage. In Nitrogen in the environment: Sources, problems, and management. Eds. R. Follett and J. Hatfield Elsevier Science Publ., Amsterdam. p. 95-122.

Reay, D.S., Edwards, A.C., Smith, K.A. (2004). Determinations of nitrous oxide emissions from agricultural drainage waters. Water, Air, and Soil Pollution: Focus 4: 107-115.

Reay, D.S., Smith, K.A., Edwards, A.C. (2004). Nitrous oxide in agricultural drainage waters following field fertilisation. Water, Air, and Soil Pollution: Focus 4: 437-451.

Reay, D.S., Smith, K.A., Edwards, A.C. (2003). Nitrous oxide emissions from agricultural drainage waters. Global Change Biology 9:195-203.

Robertson, G.P., Paul, E.A., and Harwood, R.R. (2000). Greenhouse gases in intensive agriculture: contributions of individual gases to radiative forcing of the atmosphere. Science 289: 1922-1925

Robertson, G.P. (1989). Nitrification and denitrification in humid tropical ecosystems: potential controls on nitrogen retention. In: Mineral Nutrients in Tropical Forest and Savanna Ecosystems. J Procter (Ed.). Blackford Scientific Publications, Oxford, England, pp. 55-69.

Robertson, G.P. and Tiedge, J.M. (1987). Nitrous oxide sources in aerobic soil: nitrification, denitrification, and other biological processes. Soil Biology and Biochemistry 19: 187-193.

Robertson, W.D., and Schiff, S.L. (2008). Persistent elevated nitrate in a riparian zone aquifer. Journal of Environmental Quality 37: 669-679.

Rockmann, T., Kaiser, J., Brennenkmeijer, C.A.M., Crowley, J.N., Borchers, R., Brand, W.A., and Crutzen P.J. (2001). The isotopic enrichment of nitrous oxide ($^{15}N^{14}NO$,

$^{14}N^{15}NO$, $^{14}N^{14}N^{18}O$) in the stratosphere and laboratory. Journal of Geophysical Research 106: 10403-10410.

Sander, R. (1999). Compilation of Henry's Law Constants for Inorganic and Organic Species of Potential Importance in Environmental Chemistry. Air chemistry department. Max-Planck Institute of Chemistry. http://www.mpch-mainz.mpg.de/~sander/res/henry.html

Santoro, A.E., Boehm, A.B., Francis, C.A. (2006). Denitrifier community composition along a nitrate and salinity gradient in a coastal aquifer. Applied and Environmental Microbiology 72: 2101-2109.

Schlesinger, W.H., and Hartley, A.E. (1992). A global budget for atmospheric NH_3. Biogeochemistry 15: 191-211.

Schmidt, H.L., R.A. Werner, N. Yoshida and R. Well. (2004). Is the isotopic composition of nitrous oxide an indicator for its origin from nitrification or denitrification? A theoretical approach from referred data and microbiological and enzyme kinetic aspects. Rapid Communications in Mass Spectrometry. 18: 2036-2040.

Schmidt, H.L., and Voerkelius, S. (1989). Origin and isotopic effects of oxygen in compounds of the nitrogen cycle. Isotopes in Nature. 5th Working Meeting Proceedings, Leipzig.

Seitzinger S. P. (1988) Denitrification in freshwater and coastal marine ecosystems: ecological and geochemical significance. Limnology and Oceanography 33: 702–724.

Shearer, G. and D.H. Kohl. (1988). Nitrogen isotopic fractionation and ^{18}O exchange in relation to the mechanism of denitrification of nitrite by Pseudomonas stutzeri. The Journal of Biological Chemistry 263(26): 13231-13245.

Shearer, G.B., and D. Kohl. (1986). N_2-fixation in field settings: estimations based on natural ^{15}N abundance. Australian Journal of Plant Physiology 13: 699-756.

Shearer, G.B., D.H. Kohl, and S.-H. Chien. (1978). The nitrogen-15 abundance in a wide variety of soils. Soil Science Society of America Journal 42: 899-902.

Snider, D.M., Schiff, S.L., Spoelstra, J., (2008). $^{15}N/^{14}N$ and $^{18}O/^{16}O$ stable isotope ratios of N_2O produced during denitrification in temperate forest soils. Geochimica et Cosmochimica Acta, in submission

Spoeltra, J., Schiff, S.L., Hazlett, P.W., Jeffries, D.S., and Semkin, R.G. (2007). The isotopic composition of nitrate produced from nitrification in a hardwood forest floor. Geochimica et Cosmochimica Acta 71: 3757-3771.

Spoelstra, J., Schiff, S. L., Jeffries, D. S. and Semkin, R. G. (2004). Effect of storage on the isotopic composition of nitrate in bulk precipitation. Environmental Science and Technology 38: 4723–4727.

Spoelstra, J., Schiff, S.L., Elgood, R.J., Semkin, R.G., and Jeffries, D.S. (2001). Tracing the sources of exported nitrate in the Turkey Lakes Watershed using $^{15}N/^{14}N$ and $^{18}O/^{16}O$ isotopic ratios. Ecosystems 4: 536-544.

Stein, L.Y., and Yung, Y.L. (2003). Production, isotopic composition, and atmospheric fate of biologically produced nitrous oxide. Annual Review of Earth Planet Sciences 31: 329-356.

Strauss, E.A., Mitchell, N.L., and Lamberti, G.A. (2002). Factors regulating nitrification in aquatic sediments: effects of organic carbon, nitrogen availability, and pH. Canadian Journal of Fisheries and Aquatic Sciences 59: 554-563.

Sutka, R.L., Ostrom, N.E., Ostrom, P.H., Gandhi, H., Breznak, J.A. (2003). Nitrogen isotopomer site preference of N_2O produced by Nitrosomonas europaea and Methylococcus capsulatus Bath. Rapid Communications in Mass Spectrometry 17: 738.745.

Tiedje, J.M. (1988). Ecology of denitrification and dissimilatory nitrate reduction to ammonium. *In* Biology of Anaerobic Microorganisms. J.B. Zehnder (Ed.). Wiley, New York, pp. 179-244.

Tilsner, J., N. Wrage, J. Lauf and G. Gebauer. (2003). Emissions of gaseous nitrogen oxides from an extensively managed grassland in NE Bavaria, Germany II. Stable isotope natural abundance of N2O. Biogeochemistry. 63: 249-267.

Thuss S.J., Elgood R.J., and Schiff S.L. (2008) A Simple "Purge and Trap" Method for the Isolation of Dissolved Nitrous Oxide for Stable Isotope Analysis. Rapid Communications in Mass Spectrometry, in submission.

Thuss, S.J., Rempel, M.J., Schiff, S.L., Rosamond, M., and Elgood, R.J. (2008). Emission of N_2O from drainage waters of a small agricultural basin in Southern Ontario. In preparation.

Thuss, S.J. and Schiff, S.L. (2008). A Dynamic Model to determine the $\delta^{15}N$ and $\delta^{18}O$ of Source, Dissolved, and Emitted Nitrous Oxide in Aquatic Ecosystems. In preparation.

Thuss, S.J. (2006). Temporal variability of dissolved nitrous oxide in drainage waters from a first-order agricultural basin. BSc Thesis. University of Waterloo, Waterloo, ON, Canada.

Tomer, M.D., Meek, D.W., Jaynes, D.B., Hatfield, J.L. (2003). Evaluation of Nitrate Nitrogen Fluxes from a Tile-Drained watershed in central Iowa. Journal of Environmental Quality 32: 642-653.

Toyoda, S., H. Mutobe, H. Yamagishi, N. Yoshida and Y. Tanji. 2005. Fractionation of N2O isotopomers during production by denitrifier. Soil Biology & Biochemistry 37: 1535-1545.

Ueda, S., Go, C.-S., Suwa, Y., Matsui, Y., Yamaguchi, F., Shoji, T., Noko, K., Sumino, T., Tanaka, A., and Matsufuji, Y. (1999). Stable isotope fingerprint of N_2O produced by ammonium oxidation under laboratory and field conditions. *In* Journal of the National Institute for Agronomy and Environmental Science. International workshop on the atmospheric N_2O budget: An analysis of the state of our understanding of sources and sinks of atmospheric N_2O, Tsukuba, Japan.

Vieten, B., Blunier, T., Neftel, A., Alewell, C., Conen, F. (2007). Fractionation factors for stable isotopes of N and O during N_2O reduction in soil depend on reaction rate constant. Rapid Communications in Mass Spectrometry 21: 846-850.

Vitousek, P.M., Aber, J.D., Howarth, R.W., Likens, G.E., Matson, P.A., Schindler, D.W., Schlesinger, W.H., and Tilman D.G. (1997). Human Alteration of the Global Nitrogen Cycle: Sources and Consequences. Ecological Applications 7: 737-750.

Vitousek, P.M., and Matson, P.A., (1993). Agriculture, the global nitrogen cycle, and trace gas flux. *In* The biogeochemistry of global change: radiative trace gases. R.S. Oremland (Ed.). Chapman and Hall, New York, U.S.A., pp. 193-208.

Wada and Ueda. (1996). Carbon, nitrogen and oxygen isotope ratios of CH_4 and N_2O on soil ecosystems, in: Mass Spectrometry of Soils, edited by T.W. Boutton and S.I. Yamaski, pp. 177-204, Marcel Dekker, New York, 1996.

Wahlen, M., Yoshinari, T. (1985). Oxygen isotope ratios in N_2O from nitrification at a wastewater treatment facility. Nature 317: 349-350.

Wassenaar, L.I. (1995). Evaluation of the origin and fate of nitrate in the Abbotsford aquifer using the isotopes of ^{15}N and ^{18}O in nitrate. Applied Geochemistry 10: 391-405.

Well, R., Kurganov, I., Lopes de Gerenyu, V., and Flessa, H. (2006). Isotopomer signatures of soil-emitted N_2O under different moisture conditions: A microcosm study with arable loess soil. Soil Biology and Biochemistry 38: 2923-2933.

Well, R., Flessa, H., Jaradat, F., Toyoda, S., and Yoshida, N. (2005). Measurement of isotopomer signatures of N_2O in groundwater. Journal of Geophysical Research 110, G02006, doi:10.1029/2005JG000044.

Wolf, I., and Russow, R. (2000). Different pathways of formation of N_2O, N_2, and NO in black earth soil. Soil biology and biochemistry 32: 229-239.

Wrage, N., van Groenigan, J.W., Oenema, O., Baggs, E.M. (2005). A novel dual-isotope labelling method for distinguishing between soil sources of N_2O. Rapid Communications in Mass Spectrometry 19: 3298-3306.

Wrage, N., Lauf, J., del Prado, A., Pinto, M., Pietrzak, S., Yamulki, S., Oenema, O., Gebauer, G., (2004) Distinguishing sources of N_2O in European grasslands by stable isotope analysis. Rapid Communications in Mass Spectrometry 18(11): 1201-1207.

Ye, R.W., I. Toro-Suarez, J.M. Tiedje and B.A. Averill. (1991). $H_2{}^{18}O$ isotope exchange studies on the mechanism of reduction of nitric oxide and nitrite to nitrous oxide by denitrifying bacteria: Evidence for an electrophilic nitrosyl during reduction of nitric oxide. The Journal of Biological Chemistry 266(20): 12848-12851.

Yoshida, N. (1988). ^{15}N-depleted N_2O as a product of nitrification. Nature 335: 528-529.

Yoshinari, T. and M. Wahlen. (1985). Oxygen isotope ratios in N_2O from nitrification at a wastewater treatment facility. Nature 317: 349-350.

Young, J.L. (1964). Ammonia and ammonium reactions with some Pacific Northwest soils. Soil Science of America Proceedings 28: 339-345.

Appendix

Appendix A: Summary tables of enrichment factors for nitrogen cycle processes

Table A-1: Nitrification enrichment factors reported in the literature

Reactant	Product	Organism	ε ^{15}N(‰)	ε ^{18}O(‰)	Reference
NH_4^+	N_2O	total community	-30 to -55		Perez et al., 2001
			-14.7 to -51.6		Snider et al., 2007 (submitted)
			-12 to -29		Shearer and Kohl, 1986; Kendall, 1998

Table A-2: Nitrifier-denitrification enrichment factors reported in the literature

Reactant	Product	Organism	ε ^{15}N(‰)	ε ^{18}O(‰)	Reference
NH_4^+	NO_2^-		-24.6 to –32.0		Yoshida, 1988
		Nitrosomonas europaea	-32 to -37		Mariotti et al., 1981
NH_4^+	N_2O		-45 to –68.2		Ueda et al., 1999; Yoshida, 1988
			-59.5 to -68.2		Yoshida, 1988
NH_2OH	N_2O	*Nitrosomonas europaea*	-20 to -32		Sutka et al., 2003 and 2004
		Nitrosomonas europaea	-3 to +7		Sutka et al., 2006
		Methylococcus capsulatus	0 to -3		Sutka et al., 2003 and 2004
		Methylosinus trichosporium	+4 to +8		Sutka et al., 2006
		Nitrosomonas multiformis	-1 to +5		Sutka et al., 2006
		methanotrophs	-55		Mandernack et al., 1998

Table A-3: Denitrification enrichment factors reported in the literature

Reactant	Product	Organism	ε ^{15}N(‰)	ε ^{18}O(‰)	Reference
NO_3^-	N_2O	*Paracoccus denitrificans*	-24.4 to -32.8		Barford et al., 1999
		Pseudomonas aureofacians		40	Casciotti et al., 2002
		Paracoccus fluorescens	-39 to –17	-1 to +23	Toyoda et al., 2005
		Paracoccus denitrificans	-22 to -10	+4 to +32	Toyoda et al., 2005; incubations
		Paracoccus fluorescens	-33 to –37		Yoshida, 1984
		Soil denitrifyers	-27		Wada et al., 1991
		Soil denitrifyers	-16	-8	Schmidt and Voerkelius, 1989
		Soil denitrifyers	-24 to -35		Mariotti et al., 1981 and 1982
		Pseudomonas aureofacians	-36.7		Sutka et al. 2006
		Pseudomonas chlororaphis	-12.7		Sutka et al. 2006
		Soil denitrifyers	-10.4 to -45.2		Perez et al., 2006
			-37.5		Tilsner et al, 2003
		overall bacterial community	10 to -30		Perez et al., 2001
		Soil denitrifyers	-24 to -29	-34 to -54	Menyailo and Hungate, 2006
		Soil denitrifyers		8	Wada and Ueda, 1996
		Soil denitrifyers	-38		Tilsner et al., 2003
		Soil denitrifyers	-14 to -23		Blackmer and Bremner, 1977
		Soil denitrifyers		-10	Wahlen and Yoshinari, 1985
		Pseudomonas chlororaphis	-13		Sutka et al., 2006

Table A-4: Denitrification enrichment factors reported in the literature (continued)

Reactant	Product	Organism	ε ^{15}N(‰)	ε ^{18}O(‰)	Reference
NO_3^-	N_2	Soil denitrifyers	-19.3 to -25.2	15.9 to 40.7	Snider et al., 2007
			-19 to -35		Perez et al., 2000
NO_2^-	N_2O	*Nitrosomonas europaea*	-35 to -36		Yoshida 1988
		Nitrosomonas europaea	-32 to -38		Sutka et al., 2003 and 2004
		Nitrosomonas multiformis	-24 to -25		Sutka et al., 2006
		Soil denitrifyers	-9 to -37		Mariotti et al., 1982
NO	N_2O	*Paracoccus denitrficans, Paracoccus fluorescens*	-10 to -39		Toyoda et al., 2005
N_2O	N_2	*Paracoccus denitrificans*	-7.1 to -18.7		Barford et al., 1999
		Paracoccus denitrificans	-27 to –1		Yoshida, 1984 (PhD Thesis)
		Soil denitrifyers	-2.4	-4.9	Mandernack et al., 2000
		Soil denitrifyers	-4	-11	Schmidt and Voerkelius, 1989
		Soil denitrifyers	-9	-26	Vieten et al., 2007
		Soil denitrifyers	-6 to -10	-13 to -25	Menyailo and Hungate, 2006
		Azotobacter vinelandii	-39		Yamazaki et al., 1987
		Pseudomonas aureofacians		-37 to -42	Wahlen and Yoshinari, 1985

Appendix B: NO_3^- concentrations and isotopes from 1998 to 2000 (Chapter 2)

Table B-1: NO_3^- concentrations and isotopes for Strawberry Creek tiles

Date	NO3- (mg/L)	δ^{15}N-NO3- (air)	δ^{18}O-NO3- (SMOW)
Shantz tile			
6/1/2000	6.9	6.1	5.5
6/9/2000	2.8	4.5	
8/16/2000	5.9	18.2	7.2
	Mean	9.6	6.4
	Min.	4.5	5.5
	Max.	18.2	7.2
	Range	13.7	1.7
Forest tile			
10/4/1999	6.5	8.1	1.9
2/26/2000	8.1	4.7	2.8
3/7/2000	4.1	7.5	4.6
3/28/2000	4.1	7.2	2.4
6/1/2000	9.9	5.4	3.9
8/16/2000	8.2	9.9	2.5
	Mean	7.1	3.0
	Min.	4.7	1.9
	Max.	9.9	4.6
	Range	5.1	2.7
Bend tile			
3/7/2000	33.2	5.7	2.0
3/28/2000	43.3	7.7	0.9
Halfway tile			
6/9/2000	9.0	11.1	4.9

Date	NO3- (mg/L)	δ^{15}N-NO3- (air)	δ^{18}O-NO3- (SMOW)
above Middle road (AMR) tile			
11/27/1998	0.1	3.3	
1/22/1999	0.4	1.1	
5/27/1999	0.3	4.8	
10/4/1999	1.0	6.5	4.7
12/8/1999	21.7	13.0	4.3
2/11/2000	0.4	0.9	6.5
3/7/2000	23.7	11.6	4.9
6/1/2000	12.9	12.7	5.8
8/16/2000	10.7	15.5	4.9
	Mean	7.7	5.2
	Min.	0.9	4.3
	Max.	15.5	6.5
	Range	14.6	2.3
below Middle road (BMR) tile			
1/26/1999	15.0	8.1	6.5
2/11/1999	13.2	10.4	1.2
12/8/1999	32.2	13.2	2.8
3/7/2000	17.5	9.1	3.5
3/28/2000	26.9	11.3	2.9
6/1/2000	27.1	10.9	2.6
	Mean	10.5	3.2
	Min.	8.1	1.2
	Max.	13.2	6.5
	Range	5.1	5.3

Figure B-1 continued: NO_3^- concentrations and isotopes for Strawberry Creek tiles

Date	NO3- (mg/L)	δ^{15}N-NO3- (air)	δ^{18}O-NO3- (SMOW)
Harris tile			
6/1/1997	10.7	4.7	0.3
8/10/1998	11.1	4.2	1.1
12/7/1998	16.5	5.4	-1.5
1/26/1999	22.0	5.2	1.3
2/12/1999	22.6	4.5	1.8
4/8/1999	17.1	4.2	1.3
5/14/1999	14.7	4.5	1.5
8/11/1999	6.6	5.4	1.2
10/4/1999	17.6	5.2	4.0
11/2/1999	15.2	5.4	0.9
12/8/1999	23.3	5.4	1.0
1/10/2000	20.3	3.5	1.3
2/11/2000	19.5	3.6	1.6
3/7/2000	22.8	3.6	1.6
6/1/2000	17.6	5.2	2.5
	Mean	4.7	1.3
	Min.	3.5	-1.5
	Max.	5.4	4.0
	Range	1.9	5.5
Complete Data Set			
	Mean	7.1	2.9
	Min.	0.9	-1.5
	Max.	18.2	7.2
	Range	17.3	8.7

Table B-4: NO_3^- concentrations and isotopes for Strawberry Creek stream locations

DATE	NO_3^- (mg N/L)	$\delta^{15}N$-NO_3^- (‰)	$\delta^{18}O$-NO_3^- (‰)
Upper road			
10/8/1997	7.92	9.80	8.39
5/14/1999	1.66	9.30	10.87
5/27/1999	1.29	9.12	16.30
6/22/1999	4.60	13.80	5.95
10/4/1999	1.91	13.40	5.36
12/8/1999	11.32	10.83	3.66
2/11/2000	2.38	7.09	
3/28/2000	2.97	9.72	6.50
6/1/2000	11.00	7.59	3.80
8/16/2000	11.37	11.99	5.20
	Mean	10.26	7.34
	Min.	7.09	3.66
	Max.	13.80	16.30
	Range	6.71	12.64
Middle road			
1/22/1999	0.47	2.67	13.66
2/5/1999	10.06	10.00	9.86
5/14/1999	0.10	8.60	22.74
10/4/1999	0.75	7.84	6.42
12/8/1999	18.54	11.88	3.53
2/11/2000	0.47	3.76	3.60
3/7/2000	12.64	7.48	4.30
3/28/2000	7.53	10.46	3.90
	Mean	7.84	8.50
	Min.	2.67	3.53
	Max.	11.88	22.74
	Range	9.21	19.21

DATE	NO_3^- (mg N/L)	$\delta^{15}N$-NO_3^- (‰)	$\delta^{18}O$-NO_3^- (‰)
at Z (Zinger's)			
1/22/1999	2.50	10.28	11.10
5/27/1999	1.13		12.61
	Mean	10.28	11.86
	Min.	10.28	11.10
	Max.	10.28	12.61
	Range	0.00	1.51
above Harris tile			
10/4/1999	2.04	16.60	6.76
12/8/1999	15.83	10.56	2.33
2/11/2000	3.18	11.14	4.60
3/7/2000	9.96	7.32	4.30
3/28/2000	8.73	9.62	3.90
6/1/2000	14.08	10.38	5.10
8/16/2000	5.12	17.15	5.80
	Mean	11.82	4.68
	Min.	7.32	2.33
	Max.	17.15	6.76
	Range	9.83	4.43

Table B-2 continued: NO_3^- concentrations and isotopes for Strawberry Creek stream locations

DATE	NO_3^- (mg N/L)	$\delta^{15}N$-NO_3^- (‰)	$\delta^{18}O$-NO_3^- (‰)
Outflow			
11/8/1997	2.78	14.62	7.21
7/28/1998	0.60		6.80
11/10/1998	2.30	13.82	
11/11/1998	3.00	13.70	10.50
11/25/1998	1.16		10.80
11/27/1998	2.50		14.39
12/7/1998	5.80	7.50	2.20
1/24/1999	15.02	5.25	4.34
1/25/1999	11.05		8.47
2/5/1999	7.27	8.50	8.14
4/8/1999	2.35	9.20	7.00
5/15/1999	0.39	14.50	21.79
7/22/1999	0.20		16.14
8/11/1999	0.21	15.20	
9/8/1999	1.80	8.90	3.14
10/4/1999	8.91	6.50	2.50
12/8/1999	15.27	10.30	2.58
2/11/2000	3.13	10.95	5.00
3/7/2000	11.17	5.73	3.90
3/28/2000	9.04	9.07	3.60
6/1/2000	15.29	10.00	4.20
	Mean	10.23	7.51
	Min.	5.25	2.20
	Max.	15.20	21.79
	Range	9.95	19.59
Complete Data Set			
	Mean	10.05	7.41
	Min.	2.67	2.20
	Max.	17.15	22.74
	Range	14.48	20.54

Appendix C: Results of Regression Analysis for the 2007 Springmelt and the 2008 mid-winter thaw (Chapter 3)

Table C-1: Results of linear regression analysis between the natural log (ln) of NO_3^- concentration and NO_3^- isotopes

	$\delta^{15}N$			$\delta^{18}O$		
Site	**linear equation**	**Regression Coefficient (R^2)**	**Level of signifi-cance (P)**	**linear equation**	**Regression Coefficient (R^2)**	**Level of signifi-cance (P)**
Upper road tile	y = -3.4x + 35.4	0.97	0.02	y = -4.7x + 39.4	0.46	0.31
Deciduous Headwaters	y = 12.4x + 2.2	0.46	0.31	y = 0.7x + 27.1	0.00	0.92
Shantz tile	y = -0.5x + 14.6	0.02	0.78	y = 3.3x - 12.3	0.31	0.28
BMR tile	y = -0.09x + 11.5	0.07	0.74	y = -0.2x - 10.4	0.12	0.63
Fencerow tile	y = -1.8x + 14.6	0.77	0.17	y = -0.2 + 3.9	0.00	0.99
Harris tile	y = -0.2x + 7.0	0.03	0.87	y = -0.5x + 6.5	0.02	0.90
Outflow	y = -0.1x + 7.8	0.00	0.89	y = 0.1x + 10.0	0.09	0.90

Table C-2: Results of regression analysis between $\delta^{15}N\text{-}N_2O$ and $\delta^{18}O\text{-}N_2O$ for 2007 Springmelt

Site	number of samples	linear regression equation	slope	Regression Coefficient (R^2)	Level of Significance (P)
Upper Road tile	6	y = 0.42x + 37.42	0.42	0.41	0.17
Deciduous Headwaters	5	y = -0.18x + 45.23	-0.18	0.03	0.79
Shantz tile	7	y = 0.14x + 40.04	0.14	0.03	0.71
AMR tile	3	y = 1.15x + 48.41	1.15	0.27	0.65
BMR tile	6	y = -0.27x + 29.51	-0.27	0.06	0.64
Fencerow tile	4	y = 0.69x + 48.09	0.69	0.62	0.21
Above Harris tile	1				
Harris tile	8	y = 0.19x + 41.06	0.19	0.05	0.58
Outflow	8	y = 1.4x + 49.91	1.40	0.82	0.002

Table C-3: Results of regression analysis between the natural log (ln) of N_2O concentration and N_2O isotopes for the 2007 Springmelt event.

	$\delta^{15}N$			$\delta^{18}O$		
Site	linear equation	Regression Coefficient (R^2)	Level of Signifi-cance (P)	linear equation	Regression Coefficient (R^2)	Level of Signifi-cance (P)
Upper road tile	y = -11.7x + 48.6	0.89	0.005	y = -3.3x + 49.1	0.17	0.43
Deciduous Headwaters	y = -1.6x + 2.2	0.11	0.58	y = 3.1x + 33.8	0.36	0.29
Shantz tile	y = 8.6x - 53.3	0.67	0.05	y = -1.8x + 47.1	0.07	0.61
AMR tile	y = -0.5x - 15.7	0.25	0.67	y = 1.2x + 19.4	0.24	0.68
BMR tile	y = 0.28x - 19.5	0	0.92	y = -5.2x + 61.9	0.81	0.02
Fencerow tile	y = 88.3x - 436.7	0.82	0.26	y = 73.0x - 310.7	0.79	0.29
Harris tile	y = -0.6x - 9.5	0.08	0.53	y = -0.4x + 40.9	0.06	0.6
Outflow	y = -2.6x + 4.4	0.67	0.02	y = -3.5x + 55.4	0.52	0.07

Table C-4: The results of regression analysis between the natural log of NO_3^- concentration and NO_3^- isotopes for the 2008 mid-winter thaw.

	$\delta^{15}N$			$\delta^{18}O$		
Site	**linear equation**	**Regression Coefficient (R^2)**	**Level of Signifi-cance (P)**	**linear equation**	**Regression Coefficient (R^2)**	**Level of Signifi-cance (P)**
Upper road tile	y = -2.1x + 12.5	0.17	0.41	y = -0.7x - 6.4	0.02	0.77
Shantz tile	y = -6.1x + 23.6	0.24	0.32	y = -1.9x - 0.96	0.05	0.68
AMR tile	y = -3.8x + 25.3	0.99	0.0001	y = 0.65x - 6.2	0.05	0.67
BMR tile	y = 0.07x + 13.9	0	0.97	y = 3.1x - 14.0	0.46	0.14
Harris tile	y = 3.8x - 6.4	0.12	0.51	y = -1.01x - 3.3	0.03	0.76
Outflow	y = 0.21x + 0.92	0	0.96	y = -0.4x - 5.6	0	0.92
Groundwater	y = 7.5x + 15.1	0.53	0.44	y = -3.2x + 8.62	0.32	0.24

Table C-5: The results of regression analysis between $\delta^{15}N$-N_2O and $\delta^{18}O$-N_2O for the 2008 mid-winter thaw

Site	**number of samples**	**linear regression equation**	**slope**	**Regression Coefficient (R^2)**	**Level of Significance (P)**
Upper rd tile	7	y = 0.78x + 47.89	0.78	0.26	0.24
Shantz tile	6	y = 0.17x + 39.70	0.17	0.67	0.46
AMR tile	6	y = 0.57x + 45.87	0.57	0.94	0.001
BMR tile	7	y = 0.73x + 44.73	0.73	0.95	0.0002
Harris tile	6	y = 0.27x + 42.02	0.27	0.51	0.1
Outflow	8	y = 0.26x + 41.14	0.26	0.06	0.61
Groundwater	10	y = 0.36x + 48.87	0.36	0.18	0.23
All data	50	y = 0.41x + 43.87	0.41	0.26	0.0001

Table C-6: The results of regression analysis between the natural log (ln) of N_2O concentration and N_2O isotopes for the 2008 mid-winter thaw.

	$\delta^{15}N$			$\delta^{18}O$		
Site	**linear equation**	**Regression coefficient (R^2)**	**Level of Signifi-cance (P)**	**linear equation**	**Regression coefficient (R^2)**	**Level of Signifi-cance (P)**
Upper road tile	y = 5.92x - 41.3	0.21	0.36	y = 19.1x - 55.8	0.98	0.0001
Shantz tile	y = -14.4x + 51.0	0.92	0.002	y = -1.7x + 46.0	0.17	0.42
AMR tile	y = -13.1x + 48.5	0.32	0.24	y = -5.8 + 66.6	0.18	0.40
BMR tile	y = -3.9x + 0.64	0.25	0.32	y = -2.77x + 44.8	0.22	0.35
Harris tile	y = -14.4x + 44.7	0.96	0.0005	y = -4.6x + 56.6	0.68	0.04
Outflow	y = -9.2x + 28.1	0.90	0.001	y = -4.2 + 56.0	0.24	0.26
Ground-water	y = -8.5x + 28.5	0.61	0.008	y = -4.0x + 64.0	0.18	0.22

Appendix D: Results of Regression Analysis for October 2006 to June 2007 and Fall 2007 (Chapter 4)

Table D-1: Results of regression analysis between NO_3^- and N_2O concentration for October 2006 to June 2007

Site	linear equation	Regression Coefficient (R^2)	Level of Significance (P)
Upper Rd Tile	y = 4.64x + 152.36	0.008	0.77
Shantz tile	y = 138.7x - 444.72	0.27	0.07
AMR tile	y = 122.5x - 218.57	0.88	0.0001
BMR tile	y = 45.19x - 245.89	0.29	0.11
Above Harris tile	y = 4.13x + 23.73	0.84	0.0005
Harris tile	y = 0.66x + 54.45	0.022	0.55
Outflow	y = 3.08x + 47.72	0.042	0.38
Groundwater	y = 39.48x + 34.95	0.31	0.002

Table D-2: Results of regression analysis between NO_3^- and N_2O concentration for Fall 2007

site	linear equation	Regression Coefficient (R^2)	Level of Significance (P)
AMR tile	y = 3.44x + 18.54	0.66	0.03
Harris tile	y = 1.26x - 5.26	0.93	0.03
Outflow	y = 1.06x + 15.40	0.94	0.0001
Groundwater	y = 329.6x - 47.23	0.25	0.25

Table D-3: The results of regression analysis between the natural log (ln) of NO_3^- concentration and NO_3^- isotopes for the October 2006 to June 2007 period.

	$\delta^{15}N$			$\delta^{18}O$		
Site	**Linear equation**	**Regression coefficient (R^2)**	**Level of Signifi-cance (P)**	**Linear equation**	**Regression coefficient (R^2)**	**Level of Signifi-cance (P)**
Upper road tile	y = -7.7x + 24.3	0.28	0.36	y = -5.9x + 10.8	0.05	0.71
Shantz tile	y = -0.4x + 10.4	0.00	0.92	y = 1.9x - 4.6	0.01	0.84
AMR tile	y = 6.8x + 4.6	1.00	0.00	y = 15.6x - 32.6	1.00	0.00
BMR tile	y = 9.1x - 12.5	0.09	0.70	y = -25.8x + 67.7	0.32	0.43
Harris tile	y = -2.0x +12.2	0.65	0.05	y = 1.1x - 7.3	0.01	0.82
Outflow	y = 2.1x + 7.1	0.03	0.73	y = -4.6x + 9.4	0.03	0.74
Ground-water	y = 0.1x + 7.8	0.00	0.99	y = 4.3x +24.2	0.02	0.61

Table D-4: The results of regression analysis between the natural log (ln) of NO_3^- concentration and NO_3^- isotopes for Fall 2007 data.

	$\delta^{15}N$			$\delta^{18}O$		
Site	**Linear equation**	**Regression coefficient (R^2)**	**Level of Signifi-cance (P)**	**Linear equation**	**Regression coefficient (R^2)**	**Level of Signifi-cance (P)**
AMR tile	y = 3.1x + 5.5	0.54	0.06	y = 4.0x - 4.1	0.34	0.17
Harris tile	y = -3.4x + 17.3	0.75	0.13	y = 4.4x - 17.8	0.81	0.1
Outflow	y = -1.3x + 9.2	0.78	0.004	y = -4.9x + 1.3	0.93	0.0001
Ground-water	y = 3.1x + 15.2	0.75	0.03	y = -22.6x - 4.4	0.56	0.09

Table D-5: Results of regression analysis between $\delta^{15}N\text{-}N_2O$ and $\delta^{18}O\text{-}N_2O$ for the period of October 2006 to June 2007.

Site	Linear Equation	Regression Coefficient (R2)	Level of Significance (P)
Upper road tile	y = -0.067x + 39.18	0.03	0.96
Shantz tile	y = 0.32x + 44.33	0.28	0.06
AMR tile	y = 0.28x + 38.79	0.56	0.15
BMR tile	y = 1.65x + 58.14	0.81	0.001
Above Harris tile	y = 0.096x + 49.89	0.17	0.79
Harris tile	y = 0.64x + 49.64	0.47	0.06
Outflow	y = 0.45x + 46.52	0.62	0.0001
Groundwater	y = -0.016x + 38.32	0.00	0.87

Table D-6: The results of regression analysis between $\delta^{15}N\text{-}N_2O$ and $\delta^{18}O\text{-}N_2O$ for Fall 2007 data

Site	linear equation	Regression Coefficient (R^2)	Level of Significance (P)
Shantz tile	y = -0.45x + 45.80	1.00	0.00
AMR tile	y = 0.76x +38.25	0.88	0.0007
Harris tile	y = 0.41x + 39.69	0.83	0.27
Outflow	y = 0.01x + 43.48	0.00	0.94
Groundwater	y = -0.15x + 44.27	0.06	0.59

Table D-7: The results of regression analysis between the natural log (ln) of N_2O concentration and N_2O isotopes

	$\delta^{15}N$			$\delta^{18}O$		
Site	**Linear equation**	**Regression coefficient (R^2)**	**Level of Signifi-cance (P)**	**Linear equation**	**Regression coefficient (R^2)**	**Level of Signifi-cance (P)**
Upper road tile	y = -2.2x - 0.59	0.05	0.59	y = -0.1x + 40.6	0	0.94
Shantz tile	y = -4.8x + 8.4	0.36	0.16	y = -3.4x + 56.5	0.52	0.06
AMR tile	y = -5.6x + 11.5	0.87	0.02	y = -1.8x + 43.3	0.64	0.1
BMR tile	y = -4.6x + 11.5	0.69	0.006	y = -6.8x + 73.6	0.46	0.05
above Harris tile	y = -15.0x + 53.6	0.99	0.002	y = -1.4x + 54.8	0.15	0.73
Harris tile	y = -8.6x + 18.1	0.58	0.007	y = -6.0x + 63.6	0.3	0.1
Outflow	y = -9.0x + 26.1	0.73	0.0002	y = -4.5x + 60.1	0.56	0.003
Ground-water	y = -0.95x - 6.3	0.18	0.13	y = 0.34x + 37.4	0.14	0.18

Table D-8: Results of regression analysis between the natural log (ln) of N_2O concentration and isotopes for Fall 2007

	$\delta^{15}N$			$\delta^{18}O$		
Site	**Linear equation**	**Regression coefficient (R^2)**	**Level of Signifi-cance (P)**	**Linear equation**	**Regression coefficient (R^2)**	**Level of Signifi-cance (P)**
Shantz tile	y = 32.0x - 79.6	1	0	y = -14.5x + 81.8	1	0
AMR tile	y = 0.75x + 1.9	0.004	0.89	y = 2.0x + 31.8	0.05	0.64
Harris tile	y = -11.6x + 36.6	0.99	0.005	y = -5.0x + 55.6	0.91	0.19
Outflow	y = -18.2x + 57.8	0.65	0.02	y = -3.1x + 52.6	0.3	0.16
Ground-water	y = -4.5x + 6.1	0.63	0.03	y = -0.04x + 45.8	0	0.98